



HAL
open science

Network Coding for Cooperative Wireless Sensor Networks based on Turbo Product Codes

Yizhi Yin

► **To cite this version:**

Yizhi Yin. Network Coding for Cooperative Wireless Sensor Networks based on Turbo Product Codes. Networking and Internet Architecture [cs.NI]. Télécom Bretagne, Université de Rennes 1, 2012. English. NNT: . tel-00777396

HAL Id: tel-00777396

<https://theses.hal.science/tel-00777396>

Submitted on 17 Jan 2013

HAL is a multi-disciplinary open access archive for the deposit and dissemination of scientific research documents, whether they are published or not. The documents may come from teaching and research institutions in France or abroad, or from public or private research centers.

L'archive ouverte pluridisciplinaire **HAL**, est destinée au dépôt et à la diffusion de documents scientifiques de niveau recherche, publiés ou non, émanant des établissements d'enseignement et de recherche français ou étrangers, des laboratoires publics ou privés.

Sous le sceau de l'Université européenne de Bretagne

Télécom Bretagne

En habilitation conjointe avec l'Université de Rennes 1

Ecole Doctorale – MATISSE

Network Coding in Cooperative Wireless Sensor Networks based on Turbo Product Codes

Thèse de Doctorat

Mention : Traitement du Signal et Télécommunications

Présentée par **Yizhi YIN**

Département : Signal & Communications

Laboratoire : Pôle CACS (Lab-STICC)

Directeur de thèse : Ramesh Pyndiah

Soutenue le 7 décembre 2012

Jury :

M. Raphaël Visoz, Ingénieur Expert, France Telecom – Orange Labs (Rapporteur)
M. Charly Poulliat, Professeur des Universités, INP de Toulouse – ENSEEIHT (Rapporteur)
M. Jacques Palicot, Professeur, Supélec – Campus de Rennes (Examineur)
Mme. Marie-Laure Boucheret, Professeur des Universités, INP de Toulouse – ENSEEIHT (Examineur)
M. Ramesh Pyndiah, Professeur, Télécom Bretagne (Directeur de thèse)
Mme. Karine Amis, Maître de Conférences, Télécom Bretagne (Encadrant)

Remerciements

Cette thèse a été réalisée sur trois années de recherche au sein du département Signal et Communications de Télécom Bretagne. Elle a été financée par la Région Bretagne et le PRACOM. Je tiens ici à remercier tous ceux qui y ont contribué.

Je tiens d'abord à remercier le Professeur Jacques Palicot de m'avoir fait l'honneur de présider le jury de ma thèse. Je remercie également les Professeurs Raphaël Visoz et Charly Poulliat pour l'attention qu'ils ont accordée à la lecture de ce mémoire ainsi que pour leurs remarques intéressantes.

Toute ma gratitude et mes remerciements vont à mon directeur de thèse, Ramesh Pyndiah, et mon encadrante, Karine Amis, avec qui, j'ai passé trois ans mémorables. Pendant ces années, ils m'ont bien orienté et ils m'ont donné beaucoup de conseils précieux aux niveaux professionnel et privé. Sans leurs aides et encadrement, il aurait été difficile de finir ce travail.

Je n'oublie pas non plus la secrétaire et le technicien de notre département, Monique Larsonneur et Jean-Marc Autret qui m'ont beaucoup aidé pour m'intégrer au sein du département Signal et Communications.

Je souhaite remercier aussi tous les membres du département Signal et Communications. Ils sont très aimables et grâce à eux, j'ai pu travailler dans un environnement très agréable.

Finalement, je tiens à remercier mes parents qui sont toujours à mes côtés pour me soutenir et me motiver. Je les aime de tout mon cœur.

Contents

| | |
|-----------------------------------------------------------------------|------------|
| Remerciements | i |
| Contents | vi |
| Abstract | vii |
| Résumé | ix |
| Résumé des chapitres | xi |
| Acronyms | xix |
| 1 Introduction | 1 |
| 1.1 Overview | 1 |
| 1.2 Introduction to Network Coding | 2 |
| 1.3 Algebraic linear Network Coding for wired transmissions | 4 |
| 1.3.1 Algebraic linear Network Coding model | 4 |
| 1.3.2 Construction of algebraic linear Network Coding | 5 |
| 1.3.2.1 Deterministic linear Network Coding | 5 |
| 1.3.2.2 Random linear Network Coding | 6 |
| 1.4 Network Coding for wireless cooperative communications | 6 |
| 1.4.1 Cooperative communications and Network Coding | 7 |
| 1.4.2 Noisy Network Coding and error propagation mitigation | 8 |
| 1.5 Thesis organization | 8 |
| 2 Elements in Digital Communications | 11 |
| 2.1 Wireless communication system model | 11 |
| 2.1.1 Wireless transmission chain | 12 |
| 2.1.2 Wireless channel models | 12 |

| | | |
|----------|-----------------------------------------------------------------------------|-----------|
| 2.1.2.1 | Additive white Gaussian noise | 13 |
| 2.1.2.2 | Propagation path-loss | 13 |
| 2.1.2.3 | Small-scale Rayleigh fading | 13 |
| 2.1.2.4 | AWGN and Rayleigh fading channels | 14 |
| 2.2 | Information theory and channel capacity | 15 |
| 2.2.1 | Channel classification | 15 |
| 2.2.2 | Entropy and mutual information | 16 |
| 2.2.3 | Channel capacity | 17 |
| 2.2.4 | Noisy channel coding theorem | 19 |
| 2.3 | Linear block FEC codes | 19 |
| 2.3.1 | Fundamentals of linear block codes | 19 |
| 2.3.2 | Bose-Chaudhuri-Hocquenghem codes | 21 |
| 2.3.3 | Product codes | 22 |
| 2.3.3.1 | Product code construction | 24 |
| 2.3.3.2 | Turbo decoding of product codes | 24 |
| 2.4 | Multiple-access methods | 27 |
| 2.4.1 | Major multiple-access techniques | 27 |
| 2.4.2 | Brief introduction to CDMA | 27 |
| 2.4.2.1 | Direct sequence spread spectrum principle | 27 |
| 2.4.2.2 | Synchronous CDMA channel model | 29 |
| 2.4.2.3 | Spreading sequences and correlation properties | 31 |
| 2.5 | Conclusion | 32 |
| 3 | Time-division multi-source relay cooperation using BCH product codes | 33 |
| 3.1 | Introduction | 34 |
| 3.2 | Cooperative network setup | 35 |
| 3.3 | Cooperation with a noisy source-relay channel | 40 |
| 3.3.1 | Relay detection strategies and error amplification | 40 |
| 3.3.2 | Theoretical network error probability bound | 42 |
| 3.3.3 | LLR limitation in the turbo decoding | 54 |
| 3.3.4 | LLR limiter for independent relay errors | 56 |
| 3.3.5 | Network error performance with different relay detection strategies | 58 |
| 3.3.5.1 | AWGN channel | 59 |
| 3.3.5.2 | Fast Rayleigh fading channel | 60 |
| 3.3.6 | Correlated relay errors and multi-relay cooperation | 62 |

| | | |
|----------|----------------------------------------------------------------------------------|-----------|
| 3.3.6.1 | Relay errors correlation | 62 |
| 3.3.6.2 | Error decorrelation using multiple relays | 62 |
| 3.3.6.3 | Performance of turbo Network Coding with multiple relays | 63 |
| 3.3.7 | Comparison of different cooperation strategies | 67 |
| 3.3.8 | Conclusions | 68 |
| 3.4 | Capacity of the cooperative network | 69 |
| 3.4.1 | Achievable rate using short-length FEC codes | 69 |
| 3.4.2 | Min-cut max-flow theorem and relay channel capacity bounds | 71 |
| 3.4.2.1 | Min-cut max-flow theorem | 71 |
| 3.4.2.2 | Relay channel capacity bounds | 72 |
| 3.4.2.3 | TDD relay channel capacity bounds | 72 |
| 3.4.3 | Achievable rate of the multi-source relay cooperative scheme | 75 |
| 3.4.3.1 | Time allocation factor and network transmission rate | 75 |
| 3.4.3.2 | Evaluation of network transmission rate | 77 |
| 3.5 | Conclusions | 82 |
| 4 | Superposed CDMA relay cooperation | 85 |
| 4.1 | Problem statement | 85 |
| 4.2 | CDMA-based relaying in the cooperative scheme | 86 |
| 4.2.1 | CDMA-based relay-destination model | 87 |
| 4.2.2 | Definition of the spreading sequences used at the relay | 88 |
| 4.2.3 | Maximum-likelihood multi-user detection | 89 |
| 4.3 | Iterative interference cancelation | 91 |
| 4.3.1 | Time-aligned transmission protocol | 92 |
| 4.3.2 | Turbo decoding with interference cancelation | 92 |
| 4.4 | Superposed TDMA-CDMA scheme | 93 |
| 4.4.1 | Network configuration | 93 |
| 4.4.2 | Block diagrams of the receiver | 94 |
| 4.4.3 | Relay-destination ML multi-user detection with TDMA interference | 97 |
| 4.4.4 | Energy scenarios | 98 |
| 4.4.5 | Simulation results | 100 |
| 4.4.5.1 | BER measured with E_b including the energy received from R-D channel | 100 |
| 4.4.5.2 | BER measured with the energy received from S-D channel | 102 |
| 4.4.5.3 | Data interleaving at the relay | 103 |

| | | |
|---------------------|------------------------------------------------------------------------|------------|
| 4.4.5.4 | Simulation results on the fast Rayleigh fading channel | 104 |
| 4.5 | Superposed FDMA-CDMA scheme | 107 |
| 4.5.1 | Network configuration | 107 |
| 4.5.2 | Block diagrams of the receiver | 108 |
| 4.5.3 | Relay-destination ML multi-user detection with FDMA interference | 110 |
| 4.5.4 | Discrete FDMA source detection model with CDMA interference | 112 |
| 4.5.5 | Energy scenarios | 112 |
| 4.5.6 | Simulation results | 113 |
| 4.5.6.1 | BER measured with E_b including the energy received from R-D channel | 114 |
| 4.5.6.2 | BER measured with the energy received from S-D channel | 114 |
| 4.5.7 | Comparison of TDMA-CDMA and FDMA-CDMA schemes | 115 |
| 4.6 | Conclusion and perspectives | 116 |
| Conclusion | | 119 |
| Appendix | | 123 |
| Appendix 3.A | | 123 |
| Appendix 3.B | | 126 |
| Appendix 4.A | | 127 |
| Appendix 4.B | | 127 |
| Appendix 4.C | | 128 |
| Appendix 4.D | | 135 |
| Appendix 4.E | | 136 |
| Bibliography | | 143 |

Abstract

This thesis studies the performance of the multi-source relay cooperative network where the linear algebraic Network Coding is applied at the relay. We work in the wireless sensor network context. We consider a cooperative coding scheme based on turbo product codes where a number of sensors transmit to a same destination with the help of a relay. In the proposed scheme, the relay applies algebraic systematic Network Coding (a systematic linear block code) to the detected source codewords and forwards only the additional redundancy to the destination where an overall product codeword is observed. Firstly, we focus on the time-division multiple-access (TDMA) cooperation scheme and we suppose a noisy source-relay channel. We analyze the theoretical error probabilities at the relay input and output for different relay strategies. We also establish a theoretical frame error probability bound for the proposed cooperative network in the case of soft decoding at the relay. Then we investigate the relay error mitigation at the destination using the log-likelihood ratio limitation. We evaluate the multi-relay cooperation to deal with the error correlation in the relay-generated redundancy. Different cooperation schemes (single or multi-relay cooperation using different relay strategies) are compared. We show that the source-relay link is the network bottleneck. Then we evaluate the network capacity in the short code-length regime. Lastly, we study the code-division multiple-access (CDMA) based relay cooperation where the relay signal is superposed with the source signals in the same radio-frequency band. To simplify the analysis, we suppose an error-free source-relay channel. In order to reduce the mutual interference, we propose a turbo decoding procedure with interference cancelation. We formulate two kinds of CDMA-based cooperation : TDMA-CDMA and FDMA-CDMA. The optimized energy allocation between the sources and relay is evaluated through simulations.

Résumé

Cette thèse étudie les performances d'un réseau de capteurs sans-fil coopératif, basé sur un codage réseau algébrique linéaire appliqué au relais. On considère un schéma coopératif basé sur le code produit en bloc où un grand nombre de sources transmettent des données indépendantes codées par un premier code en bloc vers un seul destinataire avec l'aide du relais. Dans ce schéma, le relais applique le codage réseau algébrique linéaire en utilisant un code correcteur d'erreur systématique linéaire en bloc sur les mots de code source détectés par le relais. Seule, la redondance générée par le relais est transférée vers le destinataire. Le destinataire observe un mot de code produit en bloc en combinant les observations des sources et du relais. Premièrement, on aborde la coopération en mode *time-division multiple-access* (TDMA) et on suppose un canal source-relais bruité. On analyse les probabilités d'erreurs théoriques à l'entrée et à la sortie du relais pour différentes stratégies de détection au relais. On établit aussi une borne théorique sur la probabilité d'erreur de trame pour le schéma coopératif proposé. Puis on évalue la coopération multi-relais afin de traiter la corrélation des erreurs dans la redondance générée par le relais. Différentes configurations de coopération (mono ou multi-relais avec différentes stratégies au relais) sont comparées. On montre que la liaison source-relais est le maillon faible du réseau. On évalue ensuite la capacité du réseau sous la condition de taille finie du code. Ensuite, on étudie la coopération basée sur la technique *code-division multiple-access* (CDMA) appliquée au relais de telle sorte que le signal du relais est avec ceux des sources dans la même bande de fréquence radio. Pour simplifier l'analyse, on suppose un canal source-relais sans erreur. On propose une procédure de décodage itératif avec la neutralisation de l'interférence. On formule deux cas de coopération basés sur CDMA : TDMA-CDMA avec répartition orthogonale dans le temps entre les sources et FDMA-CDMA avec allocation de sous-bandes de fréquences disjointes pour les sources. Le ratio d'allocation d'énergie entre les sources et le relais est évalué en utilisant les simulations.

Résumé des chapitres

Chapitre 1 : Introduction

Les communications sans-fil connaissent un développement très rapide depuis la mise en service de la deuxième génération (2G) pour la téléphonie mobile. Demain, avec la standardisation de la nouvelle 4G, les communications sans-fil supporteront le haut-débit, la haute fiabilité et une plus grande portée tout en respectant les contraintes sur la consommation d'énergie.

En parallèle des communications sans-fil individuelles, le réseau de capteurs sans-fil a également évolué d'une manière significative. Les capteurs sont des petits dispositifs de faible puissance et de faible coût. Ils sont souvent déployés en grand nombre dans l'environnement pour recueillir des informations utiles. La plupart des réseaux de capteurs sont autonomes et comptent sur l'énergie limitée de la batterie. Les capteurs transmettent un débit faible (10-100k bit/s) avec une portée courte (<100m) à cause de la contrainte sur la bande passante et sur la puissance d'émission. Le réseau de capteurs sans-fil a souvent une structure hiérarchique où quelques nœuds plus performants servent comme relais. Sur la base de cette structure et les contraintes (complexité, délai de transmission etc.), on s'intéresse aux techniques qui peuvent améliorer la performance du réseau.

L'idée des communications coopératives [CG79,NHH04] basée sur le relais est une solution prometteuse à la fois pour la nouvelle génération de communications personnelles et pour les applications de réseau de capteurs sans-fil. Les communications coopératives exploitent la nature de diffusion de la transmission radio. Les signaux transmis peuvent être entendus par les autres nœuds dans l'environnement sans-fil. Les nœuds du réseau sont ainsi en mesure de s'aider les uns les autres en relayant les informations reçues. La destination combine les signaux en provenance des différents canaux pour améliorer la performance d'erreurs du réseau et augmenter la capacité de transmission. Haut débit, haute fiabilité et plus grande portée deviennent réalisables. En plus, les communications coopératives sont organisées d'une manière distribuée, ce qui permet d'optimiser la répartition des tâches et des ressources entre les différents nœuds. Ce caractère rend la conception de réseaux sans-fil plus flexible, en particulier celle du réseau de capteurs, évitant de mettre toutes les fonctions dans les nœuds individuels dont la capacité est limitée.

Le codage réseau [ACLY00, KM03] est une technique spéciale qui peut être appliquée dans les communications coopératives sans-fil. Il a été initialement développé dans les réseaux filaires sans erreur de transmission. En utilisant le codage réseau, les données transmises sont codées dans les nœuds intermédiaires et le résultat de codage est transmis à la destination. [LYC03] a montré que le codage réseau permet d'obtenir un rendement de transmission optimal de *multicast* de la source vers les destinations dans un réseau *multi-hop* sans-erreur. On peut ainsi optimiser le rendement de transmission et économiser l'énergie. Les avantages du codage réseau ont attiré beaucoup d'attention en particulier dans les applications sans-fil. Lorsque nous utilisons le codage réseau sans-fil, l'un des principaux obstacles est la probabilité d'erreur élevée dans un environnement sans-fil, qui va provoquer la propagation des erreurs après le décodage du réseau à la destination. Ainsi, dans les communications coopératives, il n'est pas toujours avantageux d'appliquer le codage réseau au relais si le lien source-relais est médiocre.

Dans cette thèse, nous étudions la performance du codage réseau algébrique linéaire dans le réseau coopératif constitué de sources multiples, d'un ou plusieurs relais et un destinataire. C'est une configuration typique dans le réseau de capteurs. Notre étude est basée sur le schéma coopératif proposé dans [PGA10] où le relais applique le codage réseau algébrique linéaire sur les mots de code source détectés et seule la redondance générée par le relais est retransmise vers la destination. A la destination, les mots de code envoyés par les sources et la redondance envoyée par le relais sont décodés d'une façon itérative en utilisant le décodage turbo du code produit en bloc [RP98]. Nous examinons les erreurs résiduelles au relais en supposant un canal source-relais bruité. Nous évaluons et comparons la performance du réseau selon différentes stratégies de relais en fonction de la qualité du lien source-relais. Outre la coopération coordonnée par le mode *time-division multiple-access* (TDMA) sans interférence, l'utilisation de la technique *code-division multiple-access* (CDMA) est également étudiée pour la transmission du relais.

Dans ce premier chapitre, on introduit les notions de base du codage réseau. On commence par le codage réseau dans les réseaux filaires sans erreur de transmission. En prenant l'exemple du réseau Papillon [ACLY00], on montre que le codage réseau peut atteindre le rendement de *multicast* optimisé selon le théorème Coupe-Minimum Flux-Maximum (*Min-cut Max-flow*) [FF56, EFS56]. Et puis, on introduit le codage réseau algébrique linéaire basé sur le corps de Galois. On introduit aussi le modèle de codage réseau algébrique linéaire proposé dans [KM03]. Ensuite, on introduit la construction de codage réseau en utilisant la méthode déterministe ou aléatoire selon la topologie du réseau.

A la fin de ce chapitre, on présente l'application du codage réseau dans les communications coopératives sans-fil. Différentes solutions pour pallier la propagation des erreurs sont introduites, y compris celle basée sur un code correcteur d'erreur qui est étudiée au Chapitre 3 introduite dans [PGA10].

Chapitre 2 : Éléments de communications numériques

Avant d'aborder la coopération entre des sources multiples en utilisant le codage réseau au relais, on résume dans ce chapitre la plupart des notions de base concernées. On présente la chaîne de communications numériques, les modèles des canaux sans-fil, les mesures de l'information, la capacité du canal, le théorème de Shannon et le code correcteur d'erreur. On accorde une attention spéciale au code Bose-Chaudhuri-Hocquenghem (BCH) et le code produit, avec le décodage souple de Chase [Cha72] et le décodage turbo itératif du code produit [PGPJ94]. A la fin de ce chapitre, on introduit les différentes méthodes d'accès multiple comme TDMA, FDMA et CDMA, qui seront appliquées d'une façon hybride dans Chapitre 4.

Les rappels des notions de base de communications numériques effectuées dans ce chapitre et l'introduction du codage réseau au premier chapitre nous permettent d'aborder le sujet de cette thèse : le codage réseau dans le réseau de capteurs sans-fil coopératif basé sur le turbo code en bloc.

Chapitre 3 : Coopération entre des sources multiples basée sur un relais avec répartition dans le temps en utilisant un turbo code en bloc

Dans ce chapitre, nous étudions un schéma coopératif [PGA10] pour un réseau multi-capteurs sans-fil basé sur le turbo code en bloc, dans lequel un certain nombre de sources transmettent des données indépendantes vers une seule destination à l'aide d'un relais.

Dans le schéma étudié, le relais applique le codage réseau linéaire algébrique (en utilisant un code correcteur d'erreur linéaire systématique) sur les mots de code source détectés et transmet seulement la redondance supplémentaire vers la destination où un mot de code produit complet est observé. Comme le canal source-relais est affecté par le bruit et par des évanouissements, il y a des erreurs résiduelles dans les mots de code source détectés au relais, ce qui donne lieu à une propagation des erreurs après le codage réseau au relais. Le décodeur turbo à la destination prend en compte ces erreurs et utilise un log-rapport de vraisemblance (LLR) approprié pour limiter leur influence. On montre que les performances s'améliorent sur le canal gaussien et sur le canal de Rayleigh à évanouissements rapides.

Ensuite, on établit une borne théorique de la probabilité d'erreur du réseau dans le cas du décodage souple au relais. On montre que l'événement d'erreurs dominant à fort rapport signal à bruit (SNR) est provoqué par le motif d'erreurs au relais associé à une seule ligne erronée dans la matrice des mots de code source détecté. Différentes bornes sont dérivées en fonction de l'état du canal source-relais à la fois sur le canal gaussien et sur le canal de Rayleigh à évanouissements rapides. Les résultats théoriques ont été confirmés par des simulations et peuvent être utilisés pour prédire la performance d'erreurs du réseau sans utiliser les simulations qui prennent beaucoup de temps.

De plus, on analyse la corrélation d'erreurs dans la redondance générée par le relais et on étudie la performance de la coopération à plusieurs relais. Les probabilités d'erreurs théoriques à l'entrée et à la sortie du relais sont dérivées pour différentes stratégies de détection au relais, ce qui facilitera le calcul du limiteur du LLR. Différents types de coopération avec mono-relais ou multi-relais en utilisant différentes stratégies de détection sont comparés en termes de performance, de complexité et de consommation d'énergie. On montre que pour les applications pratiques, la coopération à mono-relais en utilisant la stratégie de décodage souple au relais nous donne un meilleur compromis entre probabilité d'erreurs et complexité.

Dans la dernière partie de ce chapitre, nous évaluons la capacité du réseau du schéma coopératif en utilisant le théorème *Min-cut Max-flow* [FF56,EFS56] et l'approximation du rendement de transmission du code de taille finie [PPV10].

On montre que le canal source-relais est le goulot d'étranglement du réseau coopératif. En tenant compte du fait que les sources utilisent un code en bloc de taille finie, nous devons évaluer la capacité du réseau dans le régime des codes de taille finie. En nous appuyant sur [PPV10], nous proposons une borne supérieure sur le rende-

ment de transmission sur le canal gaussien à entrée binaire et sortie continue sous contrainte de la taille de code. En utilisant cette borne et en suivant les méthodes utilisées dans [KSA03a, YGiA10], nous obtenons une borne supérieure sur le rendement du réseau coopératif étudié. Nous en déduisons la quantité optimale de la redondance générée au relais qui permet d'améliorer le rendement du réseau. Une référence est obtenue pour évaluer la redondance du relais optimale en fonction de la qualité des différents canaux. En comparant la borne du rendement de réseau et un point de fonctionnement de la coopération basé sur les codes produits BCH, nous montrons que la coopération proposée est quasi-optimale en termes de transmission des informations si le rendement du code utilisé au relais est optimal.

Chapitre 4 : Coopération avec un relais en mode accès multiple par répartition par code

Dans ce chapitre, nous considérons un scénario différent du chapitre 3. Nous supposons qu'un réseau de capteurs sans-fil a déjà été déployé dans une zone donnée. L'objectif est d'améliorer la qualité de transmission ou d'augmenter la portée du réseau sans modifier significativement la structure du réseau existant. Plus précisément, on ne peut pas se permettre de modifier les capteurs, car le nombre des capteurs est élevé et le coût total serait élevé. En plus, on ne peut pas élargir la bande radio-fréquentielle (RF) par rapport à la bande de réseau d'origine.

Comme solution, nous étudions un schéma de coopération basé sur le turbo code en bloc où la transmission du relais adopte le mode CDMA dans la même bande RF que le canal source-destination. Donc, il y a une perturbation limitée sur la liaison source-destination. Les sources peuvent utiliser le mode TDMA ou FDMA comme dans le réseau d'origine. On analyse l'interférence sur chaque liaison et on développe une procédure de décodage itérative, incluant une neutralisation des interférences. Après cela, nous évaluons la performance en termes de taux d'erreurs de deux types de réseaux coopératifs où le signal du relais (CDMA) est superposé avec la transmission des sources soit en mode TDMA soit en mode FDMA. Dans cette évaluation, on considère deux scénarios d'énergie au relais : selon que le relais est limité en l'énergie ou non. On essaie de trouver un ratio de l'allocation d'énergie entre les sources et le relais qui optimise la performance du réseau. On conclut que si le relais dispose de l'énergie en abondance, (e.g. panneau solaire etc.), la coopération proposée ici s'avère efficace avec un gain de codage d'environ 4dB au $TEB = 10^{-5}$, ce qui est similaire à la coopération étudiée dans le Chapitre 3 pour laquelle toutes les transmissions sont coordonnées en mode TDMA.

Contributions et perspectives

Les contributions de cette thèse sont les suivantes :

Sur la base de la coopération proposée dans [PGA10], nous avons analysé théoriquement la probabilité d'erreur à l'entrée et à la sortie du relais sur le canal de Rayleigh à évanouissements rapides. On a considéré trois stratégies de détection au relais : la détection ferme, le décodage ferme et le décodage souple. Nous avons prouvé que la probabilité d'erreur est amplifiée après l'encodage au relais quelle que soit la stratégie de détection. Le facteur d'amplification est indépendant de la stratégie de relais mais dépend du code appliqué au relais.

Nous avons également établi une borne théorique sur la probabilité d'erreur trame pour le schéma de coopération étudié dans le cas d'un décodage souple au relais. Nous avons montré que l'événement d'erreurs dominant à fort SNR est causé par le motif d'erreurs au relais associé à une seule ligne erronée dans la matrice des mots de code source détectés. Différentes bornes sont dérivées en fonction de l'état du canal source-relais à la fois sur le canal gaussien et sur le canal de Rayleigh à évanouissements rapides. Les résultats théoriques ont été confirmés par des simulations et peuvent être utilisés pour prédire le taux d'erreurs du réseau.

Nous avons aussi étudié la compensation des erreurs résiduelles au relais en utilisant la limitation du LLR dans le turbo décodage. Nous avons montré que, pour les trois stratégies de détection au relais, les erreurs générées au relais sont corrélées. Le taux d'erreurs du réseau présente un plancher de saturation. Pour réduire ce phénomène, nous avons étudié la coopération avec multi-relais. Deux méthodes de décorrélation sont proposées comme la division par lignes et la sélection pseudo-aléatoire de la redondance envoyée à la destination. Nous avons comparé différentes stratégies de coopération (relais simple ou multiple en utilisant différentes stratégies de détection au relais) en fonction de la qualité de la liaison source-relais. A l'aide de la coopération de multi-relais en mode sélection pseudo-aléatoire, le système est efficace en particulier pour un degré de corrélation élevé, ce qui correspond à une mauvaise qualité du canal source-relais. Les relais multiples impliquent plusieurs opérations de modulation / décodage des mots de code source, ce qui est plus complexe que la coopération avec mono-relais en utilisant le décodage souple au relais. Nous avons conclu que pour toutes les applications pratiques, la coopération avec un seul relais utilisant le décodage souple permet d'obtenir le meilleur compromis entre le taux d'erreurs binaires et de la complexité. Pour les très mauvaises conditions de la liaison source-relais, nous pouvons augmenter le nombre des motifs de test dans l'algorithme de décodage de Chase ou utiliser plusieurs relais pour la coopération. Dans le cas multi-relais, la sélection pseudo-aléatoire est privilégiée vis-à-vis de la division par lignes pour une meilleure décorrélation avec une complexité supplémentaire similaire.

En analysant le schéma de coopération proposé, nous avons constaté que le lien source-relais est en fait le goulot d'étranglement du réseau. Tenant compte du fait que les sources utilisent le code de taille finie, nous avons donc évalué la capacité du

réseau dans le régime de codes de taille finie. En exploitant les résultats de [PPV10], nous avons proposé une borne supérieure sur le rendement optimal du canal gaussien à entrée binaire sous la contrainte de la taille de code. En utilisant ce résultat, nous avons calculé une borne sur le rendement du réseau à partir des méthodes proposées dans [KSA03a, YGiA10]. En comparant cette borne et les points de fonctionnement du système coopératif basé sur les codes produits BCH, nous avons montré que le schéma proposé est quasi-optimal en termes de transmission de l'information.

Dans le schéma TDMA précédent, la transmission du relais n'interfère pas avec les transmissions des sources et consomme donc de la ressource supplémentaire. Nous avons également étudié des solutions de coopération qui permettent la superposition de la transmission du relais avec les transmissions des sources. Nous avons considéré que la transmission du relais occupe la même bande RF des transmissions que les sources. La redondance générée par le relais est transmise vers la destination avec une technique CDMA synchrone en utilisant un ensemble des séquences d'étalement quasi-orthogonales. Les sources peuvent utiliser le TDMA ou FDMA comme mode d'accès multiple. Les signaux des sources et du relais sont superposés à la destination et ils interfèrent mutuellement. Nous avons présenté une procédure de décodage turbo comprenant la neutralisation des interférences. Nous avons évalué le taux d'erreurs pour deux types de coopération superposée : le TDMA-CDMA et le FDMA-CDMA. Le ratio optimal de l'allocation d'énergie entre les sources et le relais a été trouvé par simulations. On montre que, en pratique, si l'énergie n'est pas limitée au relais, les deux solutions offrent un gain de codage similaire au schéma de coopération où toutes les transmissions sont coordonnées par le TDMA.

Voici les problèmes non résolus et quelques perspectives de notre étude :

Pour la coopération coordonnée par la technique TDMA :

- L'analyse de la capacité du réseau peut être étendue sur le canal de Rayleigh à évanouissements rapides si on peut trouver une borne sur le rendement de transmission dans le régime des codes de taille finie.

Pour la coopération avec superposition des transmissions des sources et du relais, il faudrait :

- Dériver le ratio optimal théorique de l'allocation d'énergie entre les sources et le relais ;
- Étendre les résultats théoriques et des simulations sur le canal de Rayleigh ;
- Envisager des multi-antennes à l'émission et à la réception au relais et à la destination.

Acronyms

| | |
|---------------|-----------------------------------------|
| AF | Amplify-and-Forward |
| AWGN | Additive White Gaussian Noise |
| BCH | Bose-Chaudhuri-Hocquenghem |
| BER | Bit Error Rate |
| BPSK | Binary Phase Shift Keying |
| BSC | Binary Symmetric Channel |
| CDMA | Code-division Multiple-access |
| CF | Compress-and-Forward |
| CRC | Cyclic Redundancy Check |
| DF | Decode-and-Forward |
| DSSS | Direct Sequence Spread Spectrum |
| FEC | Forward Error Correction |
| FEP | Frame Error Probability |
| FER | Frame Error Rate |
| FDMA | Frequency-division Multiple-access |
| FT | Fourier Transform |
| i.i.d. | Independent and Identically Distributed |
| ISI | Inter-symbol Interference |
| LDPC | Low-density Parity-check |
| LLR | Log-likelihood Ratio |
| LOS | Line Of Sight |
| MAI | Multiple Access Interference |
| ML | Maximum Likelihood |
| PDF | Probability Density Function |
| PG | Processing Gain |
| PN | Pseudo-random Noise |
| PR | Pseudo-random Selection |
| PSD | Power Spectral Density |

| | |
|-------------|-------------------------------|
| RF | Radio Frequency |
| SISO | Soft-input Soft-output |
| SNR | Signal-to-Noise Ratio |
| TEB | Taux d'erreurs binaire |
| TDD | Time-division Duplex |
| TDMA | Time-division Multiple-access |
| TPC | Turbo Product Code |
| WSN | Wireless Sensor Network |

1.1 Overview

Wireless communications begin with Marconi's long distance radio experiment in 1897. In 1990s, wireless communications become a worldwide standard with the second-generation (2G) digital wireless telephone service. The third generation (3G) wireless communications emerged since 2001 providing data services besides the traditional voice communication. At the time of our study, the commercial pre-4G network is being deployed in different countries and the 4G standardization is almost finished. In this evolution, one is no longer limited to voice or low-rate data services. Wireless techniques supporting high data rates, high reliability and long communication range with moderate energy consumptions are becoming a reality.

Besides the wireless personal communications, the wireless sensor network (WSN) has also developed rapidly with the advances of wireless and hardware technologies. Sensors are low-power, small-size and inexpensive devices and they are usually deployed in large numbers in the environment to collect useful information. Most WSNs are autonomous and rely on the limited battery energy. In WSN, sensors transmit at low data-rates (10-100kbit/s) for a short distance (<100m) due to bandwidth and power constraint [Kri05]. WSN usually has a hierarchical structure with some less-constrained nodes serving as relays. Based on this structure, the wireless link performance improvement subject to different constraints (complexity, transmission delay, etc.) has become a big concern of WSN engineering.

The concept of cooperative communications [CG79,NHH04] based on the relay node is a promising solution for both the new generation of personal communications and the WSN applications. Cooperative communications exploit the broadcast nature of the radio transmission. The transmitted signal can be overheard by other nodes in the wireless environment. The network nodes are thus enabled to help each other by relaying their received information. The destination combines the signals coming from the different channels to improve the network error performance and increases the network capacity. High data rate, high reliability and larger coverage become feasible. Besides that, the cooperative communication is accomplished in a distributed manner, which enables the efficient optimization of resources and task allocation among different network nodes. This character renders the design of wireless networks more flexible, especially for WSNs, without putting all the functions in the individual nodes with constrained resources.

Network Coding [ACLY00, KM03] is a special method that can be applied in wireless cooperative communications. It was initially developed in wired error-free networks. Using Network Coding, the transmitted data are encoded at intermediate nodes and the encoding result is forwarded to the destination. [LYC03] has proved that Network Coding achieves the optimal multicast rate from source to destinations in the multi-hop error-free networks. One can thus optimize the system throughput and economize the transmission energy. The advantages of Network Coding have drawn much attention and one is now interested in its performance in wireless applications. When we use the wireless Network Coding, one of the main obstacles is the high error probability in wireless environment, which will cause error propagation after the network decoding at the destination. So in cooperative communications, it is not always beneficial to apply the Network Coding at the relay node if the source-relay link is poor.

In this work, we will investigate the performance of linear algebraic Network Coding in the multi-source relay-cooperative network, which is a typical setup in WSNs. Our study is based on the cooperative scheme proposed in [PGA10] where the relay applies the algebraic linear Network Coding to the detected source codewords and forwards only the relay-generated redundancy to the destination. At the destination, the codewords from the sources and the redundancy from the relay are decoded iteratively using the turbo product code decoding [Pyn98]. We shall consider the residual errors at the relay supposing a noisy source-relay channel. We will evaluate the theoretical network performance according to different relay strategies as a function of the source-relay link quality. Besides the cooperation based on the interference-free time-division multiple-access (TDMA) mode, the use of code-division multiple-access (CDMA) technique is also investigated for the relay transmission superposed on the source signals in TDMA and FDMA mode.

In this chapter, we begin with the introduction of Network Coding including its potential benefits and known limitations in wireless cooperative communications. Non-familiar readers can thus have some background knowledge about Network Coding. The organization of the whole dissertation will be given at the end of this chapter.

1.2 Introduction to Network Coding

Store-and-Forward is the principle transmission mode in traditional networks. In this mode, the intermediate nodes forward the received data one hop after another until they arrive at the destination. Along the transmission path, the information is only replicated without further data processing. It is simple but sub-optimal with respect to the network capacity.

In 2000, Ahlswede, Cai, Li and Yeung introduced the concept of Network Coding which is referred to as coding at a node in a network [ACLY00]. In Network Coding, an intermediate node is not restricted to do the simple replication. It operates like an encoder that combines the incoming information and sends the result to the downstream nodes. Using the Network Coding, different data streams are merged at intermediate nodes. We can thus exploit the correlation between different data streams to promote their passage through network bottlenecks. In order to show the advantages of Net-

work Coding over Store-and-Forward, we consider a multicast example in the error-free butterfly network introduced in [ACLY00].

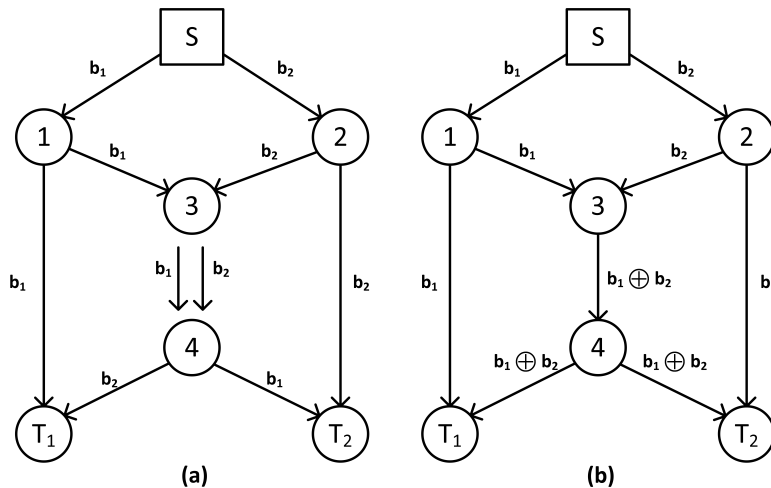


Figure 1.1 — Advantages of Network Coding in the butterfly network [ACLY00]

As illustrated in Fig. 1.1, the source \mathbf{S} wants to transmit two bits to two destinations \mathbf{T}_1 and \mathbf{T}_2 . The directed arc between two nodes represents an error-free channel through which we can transmit at most 1 bit per channel use. The intermediate nodes in Fig. 1.1(a) use the traditional Store-and-Forward. The network bottleneck occurs between nodes 3 and 4, where we need two arcs in parallel to deliver two bits to both destinations at the same time. If node 3 has only one output arc instead of two, then we need 2 network uses to multicast 3 bits to both sinks (1.5 bits/network use). In Fig. 1.1(b), node 3 applies the XOR operation on its received bits, which is the simplest form of Network Coding. The encoding result $b_1 \oplus b_2$ is forwarded to both destinations via node 4. After one network use, \mathbf{T}_1 can retrieve b_2 by a linear combination (XOR) of b_1 and $b_1 \oplus b_2$. In the same way, \mathbf{T}_2 can recover also both bits. Thus, we achieve a transmission rate of 2 bits/network use, which is the optimal transmission rate in the butterfly network.

It is clear that without Network Coding, an additional channel between node 3 and 4 is inevitable to guarantee the reception of both bits within the same transmission delay. Otherwise, we have to sacrifice the transmission rate. In this example, Network Coding optimizes the network rate and the network bandwidth usage.

An information-theoretical interpretation is also interesting. An introduction to information theory is provided in Chapter 2. From a rough approach, the capacity is the maximum rate achievable with arbitrarily small transmission error probability.

We can evaluate the network transmission rate by the min-cut max-flow theorem [FF56, EFS56]. A given network is modeled as a directed graph with nodes and directed edges. Each edge represents a point-to-point channel with a limited transmission capacity. A cut-set of a two-terminal network is a set of edges such that when deleted from the network, the network falls into two or more unconnected parts with the two terminals in different parts. The simple cut-set is a cut-set satisfying that if any edge is removed from the set, it is no longer a cut-set.

Theorem Min-cut max-flow theorem [FF56,EFS56] : the maximum possible flow, e.g., the transmission rate, from a source to a sink through a given network, is equal to the minimum capacity among all simple cut-sets.

The cut-set whose capacity is the minimum, is actually the most severe bottleneck of the network. In [ACLY00,LYC03], it has been proved that a source node can simultaneously multicast to all sinks at a rate r using Network Coding if r is achievable for each source-sink min-cut. Store-and-Forward is generally unable to achieve this rate in non-trivial networks.

In the following, we will detail the Network Coding based on the algebraic linear operations at intermediate nodes. The Network Coding applications will be extended from wired networks to wireless ones.

1.3 Algebraic linear Network Coding for wired transmissions

In [ACLY00], Network Coding is simply defined as coding at a node. The intermediate nodes can thus use any causal encoding functions. The linear network coding is introduced when the linear combination based on a finite (Galois) field is adopted at intermediate nodes. [LYC03] proved that it is sufficient to achieve the optimal multicast rate from source to sinks if Network Coding is restricted to be linear. In our study, we will focus on the linear Network Coding because of its performance and linear properties.

1.3.1 Algebraic linear Network Coding model

In 2003, Koetter and Médard [KM03] proposed an algebraic formulation for the linear Network Coding. Their work facilitates both theoretical studies and practical applications.

A communication network can be modeled as a finite and directed graph $G(\mathbf{V}, \mathbf{E})$ with nodes set \mathbf{V} and arcs set \mathbf{E} . A directed arc $a = (x, y)$ starts from node x and ends at node y . It represents a channel between two nodes. We analyze the acyclic networks where there is no directed circle in the graph. We do not model the data processing and the data propagation time, so all transmissions happen instantaneously and simultaneously. Furthermore, we suppose that all channels are error-free, which is reasonable in wired networks where the error rate is around 10^{-15} .

The linear coding is based on the finite field \mathbf{GF}_q whose size $q = 2^m$. The source data are grouped into symbol vectors in \mathbf{GF}_q . Each symbol is associated to m bits. For an intermediate node, it makes a linear combination of all the symbols received on its input arcs and the resulting symbol is forwarded to an output arc.

In Fig. 1.2, the linear coding at the intermediate node is given by :

$$Y_l = \sum_k a_{l,k} X_k, \quad (1.1)$$

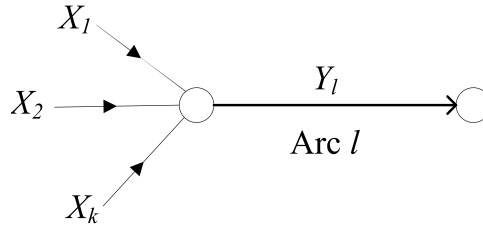


Figure 1.2 — Network Coding at an intermediate node

where $a_{l,k}$ is the local network coding coefficient chosen in \mathbf{GF}_q . X_k (resp. Y_l) is the input (resp. output) symbols of the intermediate node. Each intermediate node applies the linear Network Coding and the aggregate combination result on a particular arc l can be expressed as the linear combination of all the source symbols :

$$Y_l = \sum_{i=1}^K f_i S_i, \quad (1.2)$$

where K is the number of source vectors and S_i is the \mathbf{GF}_q symbol of the i -th source vector. f_i is the global network coding coefficient.

It is convenient to use a matrix representation to model the linear Network Coding. Let the row vectors $\vec{x}_1, \vec{x}_2, \dots, \vec{x}_K$ denote the K source vectors of length- N in \mathbf{GF}_q . \vec{x}_i is the i -th row of the source data matrix \mathbf{X} . According to Eq. 1.2, we get the following transfer equation :

$$\mathbf{Y} = \mathbf{F} \cdot \mathbf{X}, \quad (1.3)$$

where the transfer matrix \mathbf{F} is determined by the values of f_i .

The proper definition of matrix \mathbf{F} is crucial to the Network Coding problem. Its rank decides how many independent network-coded vectors can be received and whether the linear Network Coding is decodable, i.e. whether the sink can recover all the original data. If the rank of \mathbf{F} equals K , the network decoding is given by :

$$\hat{\mathbf{X}} = (\mathbf{F}^T \mathbf{F})^{-1} \mathbf{F}^T \mathbf{Y}. \quad (1.4)$$

1.3.2 Construction of algebraic linear Network Coding

The design of Network Coding is to find the right combination rule for all intermediate nodes satisfying that : 1. the final Network Coding transfer matrix \mathbf{F} is pseudo-invertible to guarantee the network decoding ; 2. the network transmission rate is optimal subject to the min-cut max-flow theorem. The solution is usually referred to as a network code. There are both deterministic and randomized code construction approaches.

1.3.2.1 Deterministic linear Network Coding

If the combination coefficients at intermediate nodes are deterministic for all network uses, then the transfer matrix \mathbf{F} is also a deterministic matrix. We can guarantee

the resolvability of the Network Coding at the code design phase. \mathbf{F} can be stored at the destination to facilitate the decoding. This approach is usually adopted in simple networks whose topology is static. In [JSC⁺05], the authors proposed a centralized polynomial-time algorithm to construct the linear network coding in multicast networks.

A special class of deterministic linear Network Coding is to use a linear block FEC code at the intermediate node. The received data at the intermediate node are treated as the message part of the Forward Error Correction (FEC) code. The combination rule of Network Coding imitates the encoding of a block FEC code. The resulting redundancy will be forwarded to the downstream nodes. This approach combines the Network Coding and the error correction, which is proved to be efficient in wireless networks. In [PGA10], the authors proposed a solution based on the turbo product codes. Good network error performance has been achieved. We will investigate this scheme in the following chapters and parts of the results have been published in [YPA11, YPA12].

1.3.2.2 Random linear Network Coding

In large or time-varying networks whose topology is hard to know, it is difficult to find a deterministic Network Coding solution. A randomized linear Network Coding approach is proposed in [HKM⁺03] and [HMK⁺06] such that “network nodes transmit on each outgoing link a linear combination of incoming signals, specified by independently and randomly chosen code coefficients from some finite field”. This randomized approach has been proved to achieve the optimized multicast rate with the probability approaching to one with the increase of the field cardinal [HMK⁺06].

In this approach, the Network Coding coefficients are random \mathbf{GF}_q values and vary for each network use. The corresponding transfer matrix \mathbf{F} has thus random entries. The destination needs the knowledge of \mathbf{F} to recover the source data. In order to convey this knowledge to the destination, an efficient way is to append a pilot vector in the header of each source packet. At the intermediate node, the same linear Network Coding combination is also applied on the pilot vectors of the incoming packets. The sink node can retrieve the knowledge of \mathbf{F} by examining the received pilot vectors. In networks using long packets, the bandwidth loss caused by pilot vectors becomes negligible. We have studied this approach through the random network codes concatenated with the Reed-Solomon codes. The corresponding result is published in [YPA10] and will not be addressed here.

1.4 Network Coding for wireless cooperative communications

Network Coding has been firstly studied in error-free networks, e.g. the wired networks where we consider only the packet loss caused by buffer overflow at intermediate nodes. Most studies focused on the construction algorithms of the Network Coding in order to optimize the network throughput. In recent years, the advantages of Network

Coding have made it a promising technology for wireless applications, especially in cooperative communications.

Compared to the wired error-free channels, the wireless transmission is affected by fading, noise and interference. The channel is no longer reliable and the received packets may contain errors.

In the following, we may alternatively use the terms ‘intermediate node’ and ‘relay’ because they refer to the same in the wireless Network Coding problem.

1.4.1 Cooperative communications and Network Coding

Cooperative communications have emerged as an extension of the relay network which is an old research domain dating from 1970s [dM71, CG79]. The three-node (source-relay-destination) relay network is the simplest form of cooperation. For general wireless cooperative communications, the transmission antennas are shared between different terminals in a wireless network. The terminals send their own information and also relay that of their partners. The destination combines the signals that have undergone independent fading to obtain the diversity gain.

There are three basic kinds of cooperation [CG79, NHH04] defining the relaying in the three-node relay network :

1. Amplify-and-Forward (AF) : The relay receives a noisy signal sent by its partner. It simply amplifies and forwards the signal to the destination node under some power constraint. Although the noise is also amplified at the relay, the destination gets two independent versions of the signal so the decision performance can be improved.
2. Decode-and-Forward (DF) : Each terminal detects / decodes the signal sent by its partner and then retransmits the re-encoded data to the destination. If the decoding at the relay is successful, the destination benefits from the diversity gain without noise amplification. But if the partner-relay channel is poor, the decoded data at the relay contain errors. After the re-encoding, these errors are usually amplified and will reduce the cooperation diversity gain.
3. Compress-and-Forward (CF) : The relay quantizes its received signal and compresses the information which will be forwarded to the destination.

The above three basic relay cooperation techniques can be easily extended to more general cooperative communications.

Wireless Network Coding is a special form of cooperative communications. Based on Decode-and-Forward, [HSOB05, CKL06, HD06] firstly studied the cooperation using Network Coding such that the relay nodes forward the linear combinations of decoded source packets to the destination.

In wireless applications, especially for relay networks, whose topology is known, the deterministic linear Network Coding construction is often adopted. The main concern is to resolve the error propagation problem.

1.4.2 Noisy Network Coding and error propagation mitigation

If we apply linear Network Coding at intermediate nodes based on erroneous packets, the result will also be contaminated. At the sink node, there will be more erroneous packets after the network decoding, which is known as the error propagation problem.

In order to mitigate the error propagation, researchers have proposed different solutions :

1. Network Coding can incorporate the Cyclic Redundancy Check (CRC) to verify the packet reception at the relay [JHHN04, XFKC07]. If the relay can't decode the incoming packet, it does not apply the Network Coding. Depending on the application, different treatments may be considered : discard the erroneous packet and notify the upper level of an erasure ; or apply the Automatic Repeat-reQuest (ARQ) mechanism at the relay, etc.

Another way to verify the packet reception is to measure the quality of the source-relay channel via its estimated SNR [SV06]. The relay applies the Network Coding only when the channel condition is stochastically good.

2. Instead of decoding the incoming packets or simply forwarding the signals to the destination, the relay calculates the packet soft information (LLR) and applies the Network Coding on these soft values [LVWD06, YK07, ZKBW08]. The resulting LLR of network coded bit is forwarded. This approach needs the quantification of analog signals. Each soft LLR value is quantified by at least 4-5 bits to guarantee the precision, which will burden the relay-destination channel.
3. Using error correcting codes to protect the wireless links. The link-by-link error correction is simple but may not be the optimal solution. Some powerful error correcting codes such as Low-Density Parity-Check codes [RY07, LAMY10, KO10], turbo product codes [OCC10, PGA10] are proposed. The error correcting code construction can be accomplished in a distributed manner at the sources and at the relay.
4. The Network Error Correction [YC06, CY06, Zha11] is a new research area. Its study is still in the theoretical phase. Its potential error correcting capability has been envisioned but we lack practical implementation algorithms.

In our study of wireless Network Coding, we adopt the solution proposed in [PGA10] based on the turbo product codes. In order to mitigate the errors involved in the relay Network Coding, a log-likelihood ratio (LLR) which takes into account errors at the relay is calculated at the destination. It is an efficient solution for reducing error propagation due to relay errors and we will detail it in Chapter 3.

1.5 Thesis organization

In this chapter, we have reviewed the basic notions about Network Coding and cooperative communications. A detailed introduction to Network Coding theory can be found in the textbook [HL08].

In Chapter 2, we will introduce the basic components of a digital communication system and the related principles of information theory. We will also give a brief introduction of the forward error correction (FEC) codes and the multiple-access methods. Special attention will be paid to the turbo product code (TPC) which is the basis of the cooperative scheme studied in chapters 3 and 4.

In Chapter 3, we investigate the wireless sensor networks (WSN) with the multi-source relay cooperation based on the linear Network Coding (the relay applies a linear FEC code). The cooperation is coordinated by the time-division multi-access (TDMA). The product code will be constructed through cooperation in a distributed manner. The turbo decoding at the destination will take the relay errors into consideration to mitigate the error propagation. We analyze the theoretical network error performance and the achievable network transmission rate. The simulation results will be given on both the Gaussian and the fast Rayleigh fading channels.

In Chapter 4, we extend the multi-source relay cooperation studied in Chapter 3. The whole cooperative network operates in the hybrid multiple-access mode. The relay transmission based on Network Coding is accomplished through the code-division multiple-access (CDMA), and it occupies the same radio-frequency (RF) band as the sources. An iterative turbo decoding procedure is proposed with interference cancellation. We will show different network error performance depending on different scenarios of the relay transmission energy.

Chapter 5 concludes the whole dissertation and gives the perspectives for future research.

Parts of this thesis have been published in [YPA11] and [YPA12].

Elements in Digital Communications

The framework of this PhD. thesis is wireless communications. Before focusing on its contributions, it is necessary to introduce basic concepts of digital communications for non-familiar readers and define the system model used in our work.

We start with the different functions that constitute a wireless digital system in the first section. So as to design and analyze original techniques, it is necessary to model the propagation medium or more generally the channel. This is the object of the second section.

The thesis addresses the problem of cooperation through coding. A brief introduction to fundamentals of forward error correcting codes is given in Section 2.3 with a special attention to Bose-Chaudhuri-Hocquenghem (BCH) codes used in our work.

Cooperation suggests multiple users accessing to the same resources. A short overview of the usual multiple-access techniques and a more detailed description of the code-division multiple-access (CDMA) are provided in Section 2.4.

2.1 Wireless communication system model

The purpose of digital communications is to transmit information generated by a source to the destination in the digital form [PS08]. In Fig. 2.1, we illustrate the principle elements in a basic digital communications system.

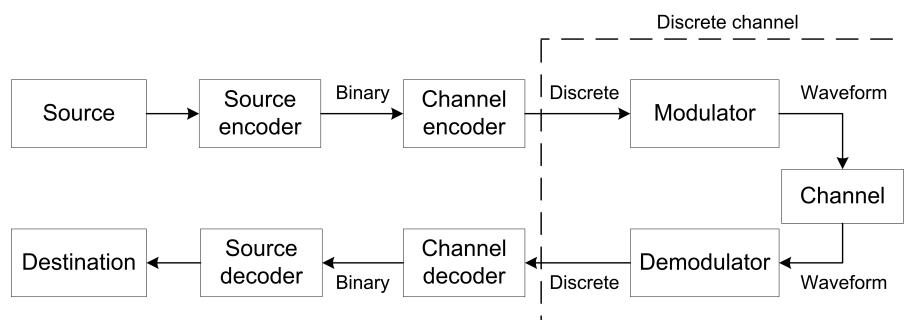


Figure 2.1 — Block diagram of the basic digital communication system

2.1.1 Wireless transmission chain

Source : its original output information can be either analog or digital (discrete) depending on the applications. This information is then digitalized and represented by a sequence of bits.

Source encoder : the source information is usually redundant in nature and the source encoder converts it into a bit sequence (message) such that the information is represented in a more concise and efficient way satisfying certain criteria. The source encoding is also known as the data compression. In our study we process directly the source messages at the output of the source encoder.

Channel encoder : it introduces the redundancy into the source message in a controlled manner to protect its transmission over the channel against the noise, distortions and interference. The corresponding binary sequence at the output of the channel encoder is called a codeword. At the receiver side, this redundancy can be exploited by the channel decoder to recover the original source message. The ratio of the source message length to the codeword length is defined as the code rate R . The technique used at the channel encoder / decoder to generate the redundancy and to correct the possible errors is known as the forward error correction (FEC). Our study is based on the linear systematic block code and also one of its concatenated form : the Turbo product code. We will introduce them in detail in the following sections.

Modulator : it is a digital-to-analog interface whose role is to map the binary codeword sequence at the output of the channel encoder into waveforms adapted to the channel properties and system constraints. In an M -ary modulation, every b codeword bits are transmitted by one of the $M = 2^b$ possible waveforms. In our study, we suppose $M = 2$ corresponding to the basic binary phase shift keying (BPSK) modulation.

The entities described above belong to the sender side of the transmission chain. Each of these entities has a counterpart at the receiver side accomplishing the inverse operations until the information is recovered at the destination. The quality of a digital transmission is usually evaluated by the binary error probability. In practice, we use the bit error rate (BER) defined as the ratio of the erroneous bit number and the total transmitted bit number to evaluate the binary error probability.

2.1.2 Wireless channel models

The channel represents the physical medium through which the information-carrying signal is transmitted. In this PhD. thesis, we consider a wireless environment where the signal is corrupted by the noise, the propagation path-loss and the fading. We will model the additive white Gaussian noise (AWGN) channel and the non-frequency selective (flat) Rayleigh fading channel used in our work. These two commonly-used channels are important in the error performance analysis.

2.1.2.1 Additive white Gaussian noise

The noise is one of the major impairments for the digital transmission. The external noise is often caused by the industry noise (difficult to model) and the interference of other signals in the transmission environment. The internal noise is usually associated with the electronic components (resistors, amplifiers and filters).

If the thermal noise caused by electronic components is dominant, then the noise can be modeled by a Gaussian process whose bilateral PSD is $\frac{N_0}{2}$ Watt/Hz. The noise is independent of the transmitted signal and corrupts the signal in an additive manner. We define this kind of noise as the additive white Gaussian noise (AWGN).

2.1.2.2 Propagation path-loss

The radio propagation path-loss belongs to the large-scale propagation model and is defined as the difference (in dB) between the transmitted power and the received power. It measures the signal attenuation over large distances (several hundred or thousand meters) separating the transmission and the receiving antennas.

According to the Friis free-space transmission equation [Fri46], the received power $P_r(d)$ is function of the transmitted power P_t and the distance d between the receiver and the transmitter :

$$P_r(d) = P_t \cdot G_t G_r \left(\frac{\lambda}{4\pi d} \right)^2, \quad (2.1)$$

where G_t is the transmitter antenna gain, G_r is the receiver antenna gain and λ is the signal wavelength in meters.

There are many analytical or empirical path-loss models depending on different setups of radio environment. We consider the simplified path-loss model based on the generalized Friis equation such that the received power $P_r(d)$ can be expressed as the received power $P_r(d_0)$ at the reference point d_0 providing that $d \geq d_0$:

$$P_r(d) = P_r(d_0) \cdot \left(\frac{d_0}{d} \right)^\rho, \quad (2.2)$$

where ρ is the path-loss coefficient whose typical values are given in In Table 2.1.

| Environment | Path-loss coefficient ρ |
|---------------------------|------------------------------|
| Free space | 2 |
| Urban area | 2.7 to 5 |
| Indoor with line-of-sight | 1.6 to 1.8 |

TABLE 2.1 — Path-loss coefficient values

2.1.2.3 Small-scale Rayleigh fading

In the wireless environment, there are various objects that co-exist with the transmitter and the receiver such as the buildings, trees, hills etc. The reflection, diffraction

and refraction from these structures yield the multi-path propagation. The resulting signals (multi-path components) will arrive at the receiver from different directions with different attenuations and delays. Their randomly-distributed time-varying amplitudes and phases may be either constructive or destructive at the reception. The fading corresponds to random fluctuations of the superposed signals at the receiver over a short duration or travel distance. It is a small-scale effect compared with the large-scale path-loss.

In our study, we are interested in the Rayleigh fading. Its physical propagation model is based on the observation that the multi-path components are well-scattered by a large number of reflecting objects. These components have negligible delay spread between them (only one resolvable path from the viewpoint of the receiver). Their contributions to the received signal power are in the same order without dominant line-of-sight (LOS) path. Based on these assumptions, the central limit theorem applies and we can deduce that the envelope of the channel response is Rayleigh distributed and its phase has a uniform distribution on $[0, 2\pi)$.

We will assume the frequency-nonselctive (flat) fading in our study, such that the channel gain and the phase shift are the same for the whole frequency band occupied by the signal. To satisfy this condition, the signal bandwidth should be much smaller than the channel coherence bandwidth.

2.1.2.4 AWGN and Rayleigh fading channels

Based on the above assumptions, we introduce two important channel models :

AWGN channel :

It is the simplest channel model that considers only the influence of the AWGN. It gives an upper bound on the system error performance without other channel impairments. The received signal $y(t)$ on the AWGN analog channel is given by :

$$y(t) = x(t) + n(t), \quad (2.3)$$

where $x(t)$ is the transmitted signal and $n(t)$ is the zero-mean AWGN noise process whose bilateral power spectral density (PSD) is $\frac{N_0}{2}$ Watt/Hz.

Using the Gram-Schmidt procedure [PS08, p.33], we can obtain a vector presentation of AWGN channel based on the N -dimensional orthogonal basis of the signal space :

$$y_i = x_i + n_i, \quad i = 1, 2, \dots, N, \quad (2.4)$$

which is equivalent to the waveform AWGN channel. $\{n_i\}$ are independent and identically distributed (i.i.d.) zero-mean Gaussian variables with variance $\sigma^2 = \frac{N_0}{2}$ and the probability density function (PDF) is :

$$p(n) = \frac{1}{\sqrt{2\pi\sigma^2}} e^{-\frac{n^2}{2\sigma^2}}. \quad (2.5)$$

The dimension N usually depends on the modulation scheme of the transmitted signal. For the BPSK modulation, $N = 1$. The detailed derivation is given in [PS08, p.167].

Frequency-nonselective Rayleigh fading channel :

Besides the AWGN noise, the frequency non-selective Rayleigh fading channel introduces a multiplicative distortion of the transmitted signal. The baseband-equivalent model of the received signal is given by :

$$y(t) = \alpha(t)e^{j\phi(t)} \cdot x(t) + n(t), \quad (2.6)$$

where the envelope $\alpha(t)$ is Rayleigh distributed for any given t .

We suppose that the fading channel varies slowly such that the multiplicative term reduces to a constant α during at least one symbol duration :

$$y(t) = \alpha e^{j\phi} \cdot x(t) + n(t). \quad (2.7)$$

Furthermore, we assume that the phase shift ϕ can be perfectly estimated and compensated at the receiver, thus the simplified transmission equation becomes :

$$y(t) = \alpha \cdot x(t) + n(t), \quad (2.8)$$

where the coefficient α is a Rayleigh random variable whose PDF is :

$$f(\alpha) = \begin{cases} \frac{\alpha}{\sigma^2} e^{-\frac{\alpha^2}{2\sigma^2}} & \text{if } \alpha > 0 \\ 0 & \text{otherwise} \end{cases} \quad (2.9)$$

Using the same Gram-Schmidt procedure as in the case of AWGN channel, we get the discrete transmission equation for the frequency non-selective Rayleigh fading channel :

$$y_i = \alpha \cdot x_i + n_i, \quad i = 1, 2, \dots, N. \quad (2.10)$$

2.2 Information theory and channel capacity

The information theory was initiated by Shannon's seminal work "A Mathematical Theory of Communication" in 1948 [Sha48]. It studies the theoretical performance of the information transmission over a noisy channel. Shannon proposed two important theorems : the Shannon's source coding theorem (first) about the efficient source data compression and the Shannon's noisy-channel coding theorem (second) about the channel capacity for the reliable transmissions. The source coding is out of the scope of our work and we will focus on the second Shannon theorem.

2.2.1 Channel classification

In the information theory framework, the physical channel properties are supposed to be known. The channel is statistically described by the channel input, output and the conditional probability (conditional PDF in the continuous case) relating the input sequence $\vec{\mathbf{x}} = (x_1, x_2, \dots, x_n)$ and the output sequence $\vec{\mathbf{y}} = (y_1, y_2, \dots, y_n)$. In our study,

we consider the memoryless channel such that the output at time index i depends only on the corresponding input at the same time, which leads to :

$$\Pr(\vec{y}|\vec{x}) = \prod_{i=1}^n \Pr(y_i|x_i). \quad (2.11)$$

We can classify the channel based on whether its input and output alphabets are discrete or continuous (in time and amplitude domains). The channel can be considered either discrete or continuous according to different viewpoints.

In digital communications, we usually consider the discrete-time channels whose input and output are both discrete in the time domain. The band-limited waveform channel can be transformed into an equivalent discrete-time channel by the signal expansion based on the complete set of orthogonal functions.

Based on Fig. 2.1, we can further classify the discrete-time channels in the amplitude domain :

Discrete-input discrete-output channel : if we consider the modulator and demodulator as part of the channel, the channel input and output are both discrete in amplitude. The discrete memoryless channel has both its input and output belonging to the finite alphabets. It is the most basic channel model used in the information theory.

Discrete-input continuous-output channel : the output of the channel detector is not quantized so that the channel output alphabet is the real number set. An important example is the M -ary AWGN channel.

Continuous input and output channel : both alphabets of the channel input and output are the real number set. This kind of channel is often used for theoretical analysis.

2.2.2 Entropy and mutual information

For a discrete scalar random variable X having M possible values, its **entropy** is defined as :

$$H(X) = \sum_{i=0}^{M-1} \Pr(x_i) \log \frac{1}{\Pr(x_i)}, \quad (2.12)$$

where $\Pr(x_i)$ is the probability of $X = x_i$. The entropy measures the total average uncertainty about an information source, i.e., the average information quantity delivered by the source. It also equals to the minimal number of bits that are required to encode a source symbol without information loss.

For two random variables X and Y , their **joint entropy** is defined as :

$$H(X, Y) = \sum_i \sum_j \Pr(x_i, y_j) \log \frac{1}{\Pr(x_i, y_j)}, \quad (2.13)$$

and the **conditional entropy** of X with respect to Y is :

$$H(X|Y) = - \sum_i \sum_j \Pr(x_i, y_j) \log \Pr(x_i|y_j), \quad (2.14)$$

which measures the average remaining uncertainty about X if Y is given.

The average **mutual information** between X and Y is defined as :

$$\begin{aligned} I(X; Y) &= \sum_i \sum_j \Pr(x_i, y_j) \log \frac{\Pr(x_i, y_j)}{\Pr(x_i) \Pr(y_j)} \\ &= H(X) - H(X|Y). \end{aligned} \quad (2.15)$$

It represents the reduction (in entropy) of the average uncertainty about X before and after the observation of Y . We can use it to measure the average information quantity transferred through a channel whose input (resp. output) are X (resp. Y).

2.2.3 Channel capacity

The channel capacity C is defined as the maximum mutual information between channel input X and output Y over all possible input distributions :

$$C = \max_{P_X(x)} I(X; Y) \text{ bits/channel use.} \quad (2.16)$$

It equals to the average information quantity that can be transferred through the channel with an arbitrarily low error rate. For the symmetric channels, it can be proved that the equiprobable input distribution can achieve C , which will facilitate the calculation because many channel models are symmetric in practice.

The channel input and output can be either continuous or discrete. For continuous variables, the probability used in the above definitions should be replaced by the corresponding PDF function and the summation is replaced by the integration.

In the following, we will detail the channel capacity on the unconstrained-input / binary-input AWGN channels :

Unconstrained-input AWGN channel

Consider the AWGN channel model in the discrete time domain :

$$y = x + n, \quad (2.17)$$

where x is a real-valued input variable and n is the sample of a real AWGN process. Since the channel input has not the constraint of a practical modulation, we denote it by unconstrained-input. The channel capacity can be achieved if the input is zero-mean Gaussian distributed :

$$C = \frac{1}{2} \log_2 (1 + SNR) \text{ bits/channel use,} \quad (2.18)$$

where SNR is the signal-to-noise power ratio. If the complex two-dimensional signaling is used, then the multiplicative coefficient $1/2$ will disappear in Eq. 2.18.

M -ary input AWGN channel

In this case, the input variable x belongs to an M -ary finite alphabet. According to the definition of the channel capacity and Eq. 2.16 :

$$\begin{aligned} C &= \max_{P_X(x)} I(X; Y) = \max_{P_X(x)} \sum_i \int_y p(x_i, y) \cdot \log_2 \frac{p(y|x_i)}{p(y)} dy \\ &= \log_2 M + \int_y \frac{1}{M} \sum_i p(y|X = x_i) \log_2 \frac{p(y|x_i)}{\sum_q p(y|X = x_q)} dy, \end{aligned} \quad (2.19)$$

where the maximization is achieved by using the equiprobable input distribution. In the above equation, the integration on y at the final step can be calculated numerically using the Monte-Carlo method [PTVF92, section 7.6].

In Fig. 2.2, we plot the capacity of the unconstrained / binary input AWGN channels (one-dimensional) as a function of SNR. The capacity of the general M -ary input AWGN channel (two-dimensional) is given in Fig. 2.3.

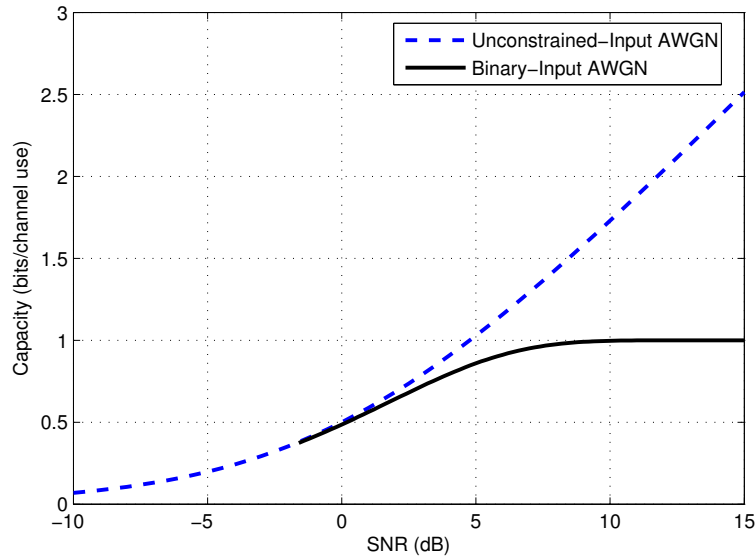


Figure 2.2 — Capacity of the unconstrained/binary input AWGN channel (one-dimensional)

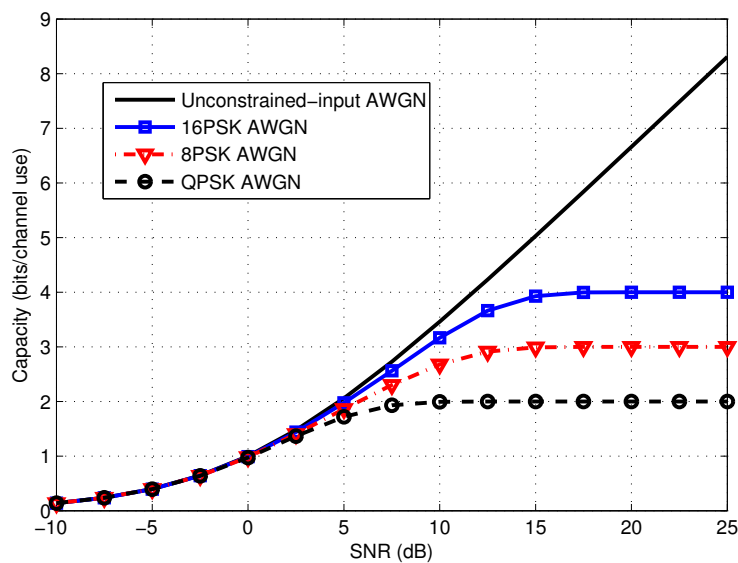


Figure 2.3 — Capacity of the unconstrained / M -ary input AWGN channel (two-dimensional)

We observe that in the low SNR regime, the capacity of BPSK transmission is almost equivalent to that of the unconstrained-input. So there is no benefit using large modulation set for low SNRs. When SNR increases, larger modulation set achieves better capacity approaching $\log_2 M$ bits/channel use.

2.2.4 Noisy channel coding theorem

Theorem Shannon's second theorem [Sha48] : Reliable communication over a discrete memoryless channel is possible if the communication rate R satisfies $R \leq C$. For any rate higher than capacity, reliable communication is impossible.

Consider a discrete memoryless channel with channel capacity of C bits/channel use. [Gal68, Theorem 5.6.2] shows that for the ensemble of block codes of length n and code rate R , the average codeword error probability using the Maximum-likelihood (ML) decoding is upper-bounded by :

$$P_e \leq 2^{-n \cdot E(R)}, \quad (2.20)$$

where $E(R)$ is a positive convex function for $0 < R \leq C$. According to Eq. 2.20, the codeword error probability tends to zero with the increase of code length n for $0 < R \leq C$.

In order to achieve the low target error probability, one has to use a long enough code. The corresponding encoding complexity will increase proportionally with the code length. Besides that, if the source information rate is low, the delay required to collect enough source message bits also increases in the long-code case. In practical applications especially for WSNs, we have some constraints on the energy consumption and the transmission delay. In the next chapter, we will study a cooperative scheme that benefits from the long code length and satisfy those constraints at the same time.

2.3 Linear block FEC codes

The forward error correcting (FEC) is the essential technique for achieving reliable digital transmissions. FEC adds some redundancy to the source message to correct at the receiver side the errors occurred during the transmission. There are two main families of FEC codes : block codes and convolutional codes. We concentrate on the binary linear block codes in our study, and more specifically on the Bose-Chaudhuri-Hocquenghem (BCH) codes and the turbo product codes (TPC), as they will be used in the proposed cooperative scheme.

2.3.1 Fundamentals of linear block codes

The encoding of block codes is a bijective mapping relating the source message sequence of length k and a codeword of length n . The code rate R is defined as the ratio of k out of n :

$$R = \frac{k}{n} \leq 1. \quad (2.21)$$

The linear block code satisfies that any linear combination of two codewords is also a codeword. Almost all the practical block codes are linear. If the source message part appears explicitly as a part of its corresponding codeword, it is a systematic code.

We denote d_{min} as the code minimum Hamming distance, which is the minimum distance between two distinct codewords. The linear block code is usually specified by three parameters (n, k, d_{min}) .

The linear block code can be defined by its generator matrix \mathbf{G} of dimension $(k \times n)$:

$$\vec{\mathbf{c}} = \vec{\mathbf{m}} \cdot \mathbf{G}, \quad (2.22)$$

where $\vec{\mathbf{m}} = (m_1, m_2, \dots, m_k)$ is the message vector and $\vec{\mathbf{c}} = (c_1, c_2, \dots, c_n)$ is the codeword vector. For every generator matrix, there is a corresponding parity-check matrix \mathbf{H} of dimension $((n - k) \times n)$ satisfying $\mathbf{G} \cdot \mathbf{H}^T = \mathbf{0}$. All the codewords verify that :

$$\vec{\mathbf{c}} \cdot \mathbf{H}^T = \mathbf{0}. \quad (2.23)$$

There are two error correction strategies for the linear block FEC codes : the hard decoding and the soft decoding.

Hard decoding :

Consider a binary symmetric channel (BSC). The received codeword $\vec{\mathbf{r}}$ at the input of channel decoder can be expressed as :

$$\vec{\mathbf{r}} = \vec{\mathbf{c}} \oplus \vec{\mathbf{e}}, \quad (2.24)$$

where $\vec{\mathbf{c}}$ is the transmitted codeword and $\vec{\mathbf{e}}$ is the error pattern. All vector elements belong to $\{0, 1\}$.

Based on the maximum-likelihood (ML) decoding which minimizes the probability of decoding errors, we obtain the following decision rule :

$$\vec{\mathbf{d}} = \vec{\mathbf{c}}_i = \arg \max_{1 \leq i \leq 2^k} \{\Pr(\vec{\mathbf{r}} | \vec{\mathbf{c}}_i)\} = \arg \min_{1 \leq i \leq 2^k} \{d_H(\vec{\mathbf{r}}, \vec{\mathbf{c}}_i)\}, \quad (2.25)$$

where $d_H(\vec{\mathbf{x}}, \vec{\mathbf{y}})$ calculates the Hamming distance between the two vectors. The ML hard decoding is optimal but its complexity grows exponentially with the codeword number. The practical hard decoding method is based on the code syndrome. The code syndrome is defined as :

$$\vec{\mathbf{s}} = \vec{\mathbf{r}} \cdot \mathbf{H}^T, \quad (2.26)$$

The syndrome $\vec{\mathbf{s}}$ has $(n - k)$ components so there are overall $2^{(n-k)}$ possible syndromes. Each one is associated with a special error pattern $\vec{\mathbf{e}}$, called the coset leader. The all-zero syndrome corresponds to the error-free case. We can establish a decoding table linking the syndromes $\vec{\mathbf{s}}$ and their corresponding coset leaders $\vec{\mathbf{e}}$. After calculating the syndrome using Eq. 2.26, we can look up the error $\vec{\mathbf{e}}$. The decoded codeword is the addition of $\vec{\mathbf{e}}$ and $\vec{\mathbf{r}}$. More details about the syndrome decoding are given in [Lin70, section 3.5].

A binary linear block code of minimum distance d_{min} can correct $t = \lfloor \frac{d_{min}-1}{2} \rfloor$ bits errors using the hard decoding, where $\lfloor \cdot \rfloor$ is the operation computing the greatest

integer less than or equal to the input. If the error number is higher than t , the decoder fails and adds supplementary errors in the decoding result.

Soft decoding :

Consider a binary-input AWGN channel. The channel output can be expressed as :

$$\vec{\mathbf{r}} = \vec{\mathbf{c}} + \vec{\mathbf{n}}, \quad (2.27)$$

where $\vec{\mathbf{r}}$ is the transmitted codeword and $\vec{\mathbf{n}}$ is the AWGN vector. The elements of $\vec{\mathbf{c}}$ belong to $\{\pm 1\}$.

The optimal ML decoding performs exhaustive search for the codeword at the minimum Euclidean distance to the observation $\vec{\mathbf{r}}$:

$$\vec{\mathbf{d}} = \vec{\mathbf{c}}_i = \arg \max_{1 \leq i \leq 2^k} \{p(\vec{\mathbf{r}}|\vec{\mathbf{c}}_i)\} = \arg \min_{1 \leq i \leq 2^k} \{d_E(\vec{\mathbf{r}}, \vec{\mathbf{c}}_i)\}, \quad (2.28)$$

where $d_E(\vec{\mathbf{x}}, \vec{\mathbf{y}})$ calculates the Euclidean distance between the two vectors. The ML soft decoding offers a coding gain of about 2.5dB versus the hard decoding at the high SNR regime.

In order to reduce the decoding complexity, we usually apply a sub-optimal soft decoding such as the Chase algorithm [Cha72]. The Chase decoding relies on a reduced subset of codewords. Its procedure is :

1. Hard detect the observed $\vec{\mathbf{r}}$: $\vec{\mathbf{y}} = \text{sgn}(\vec{\mathbf{r}})$.
2. Find the positions of the m least reliable bits in $\vec{\mathbf{y}}$, corresponding to the indices of components of $\vec{\mathbf{r}}$ whose absolute values are the smallest.
3. Generate 2^m test patterns considering all possible combinations of the binary values in the m least reliable positions found in step 2. Apply these test patterns to the hard-detected vector $\vec{\mathbf{y}}$ to obtain 2^m binary sequences.
4. Hard decode all the resulting binary sequences in step (3) to establish a subset of candidate codewords.
5. In the candidate codewords subset, find the codeword with the minimum Euclidean distance to the observation $\vec{\mathbf{r}}$. This codeword is the decided codeword.

The optimal ML soft decoding performance can be approached using the Chase method with a large enough m at the price of an increased complexity.

2.3.2 Bose-Chaudhuri-Hocquenghem codes

The cyclic codes satisfy that any cyclic shift of the codeword components is still a codeword. Bose-Chaudhuri-Hocquenghem (BCH) codes [Hoc59, BRC60] are binary cyclic linear block codes. Their definition is based on the finite (Galois) field theory. Thanks to their cyclic property and the polynomial representation, they can be efficiently encoded or decoded using shift registers of low complexity.

In this section, we will briefly introduce the primitive binary BCH codes. The background knowledge of the finite field and details about the BCH codes can be found in [Lin70, MS77].

The primitive binary BCH codes have the following parameters :

$$\begin{aligned}
\text{Block length :} & \quad n = 2^m - 1 \\
\text{Code dimension :} & \quad k \geq n - mt \\
\text{Minimum distance :} & \quad d_{\min} \geq 2t + 1
\end{aligned}$$

where m and t are positive integers satisfying $t < 2^{m-1}$.

The generator polynomial $g(x)$ of a primitive binary BCH code has $2t$ roots :

$$\alpha^1, \alpha^2, \alpha^3, \dots, \alpha^{2t}, \quad (2.29)$$

where α is the primitive element of the field. Using the generator polynomial, we can systematically encode the BCH code based on the shift registers and logical operations. The corresponding encoding equation is :

$$c(x) = m(x) \cdot g(x) = m(x) + v(x) \quad (2.30)$$

where $v(x)$ is the remainder of the Euclidean division of $x^{n-k} \cdot m(x)$ by $g(x)$.

In our study, we will use BCH codes with error correction capability $t \leq 2$. For the hard decoding of such BCH codes, we apply an algebraic algorithm such as that of Peterson [Pet60] or Berlekamp-Massey [Ber68, Mas69] :

1. Calculate the syndrome $\mathbf{s} = (S_1, S_2, \dots, S_{2t})$ from the received codeword vector.
2. Detect the number of errors and find the error location polynomial from the syndrome based on the method of Peterson [Pet60] or Berlekamp-Massey [Ber68, Mas69].
3. Correct the errors.

For the soft decoding of BCH codes, we apply the Chase algorithm as described in previous subsection.

In Fig. 2.4 and 2.5, we plot the BER performance of BCH (32, 26, 4) and BCH (64, 51, 6) codes on the AWGN channel. The first code has the error correction capability $t = 1$ and for the second one $t = 2$.

In the simulation, we use 16 test patterns in the Chase algorithm for the soft decoding for the sake of complexity reduction. Besides the BER curves of the hard / soft decoding, we also plot the theoretical error performance for the BPSK modulation. We can verify that the soft decoding offers a larger coding gain than the hard decoding for the same code.

2.3.3 Product codes

The code error correction capability increases with its minimum Hamming distance. According to the Gilbert-Varshamov bound [Gil52, Var57], the code length should be long in order to have a large code minimum Hamming distance. The large code length implies a high decoding complexity. We do not have efficient low-complexity decoding methods for long codes. To overcome this obstacle, long codes are usually constructed by concatenating several elementary short codes. The product codes are specific serial concatenation of linear block codes, which was introduced by Elias [Eli54]. In this subsection, we will introduce the binary product codes and their turbo decoding.

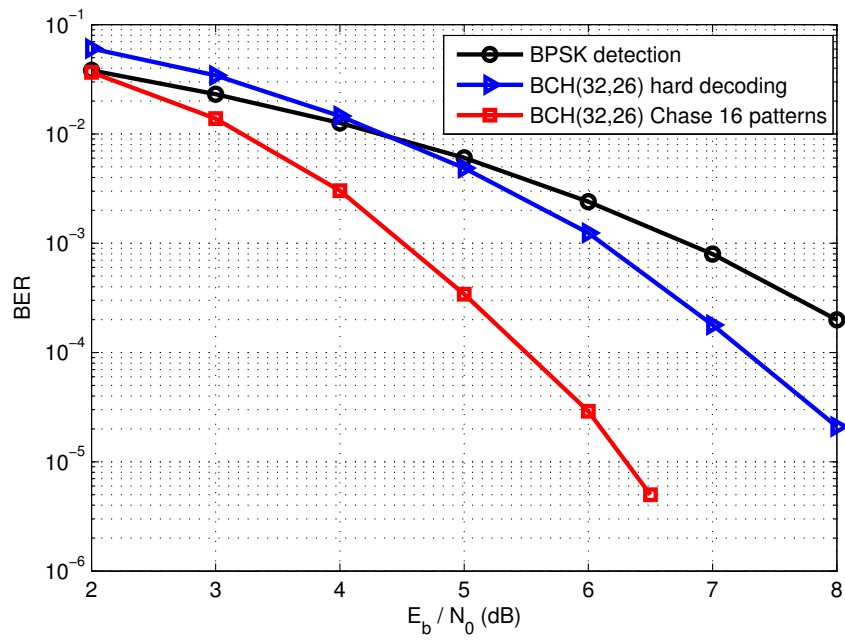


Figure 2.4 — BER performance of the hard / soft decoding of BCH (32, 26, 4) code on the AWGN channel

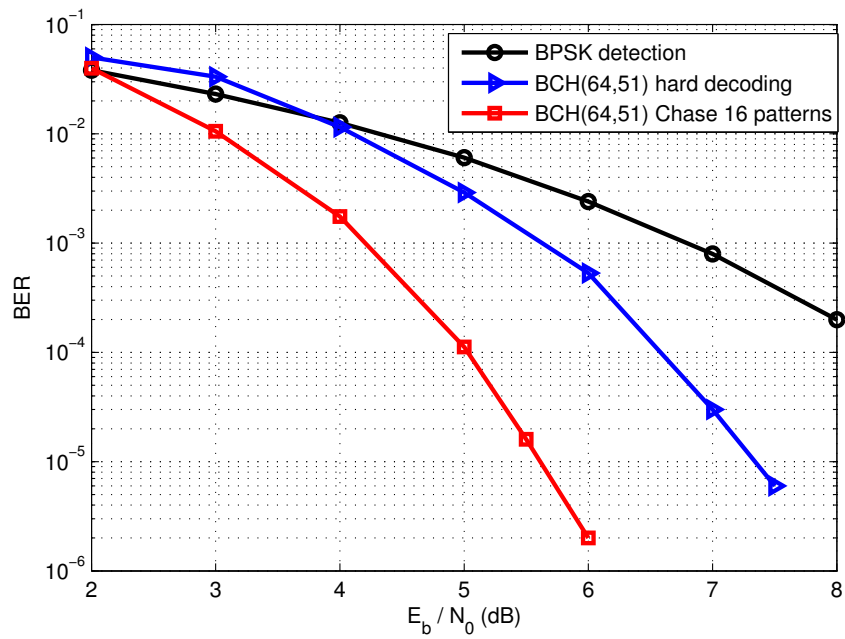


Figure 2.5 — BER performance of the hard / soft decoding of BCH (64, 51, 6) code on the AWGN channel

2.3.3.1 Product code construction

In Fig. 2.6, we illustrate the construction of the product code based on the serial concatenation of two systematic linear block codes.

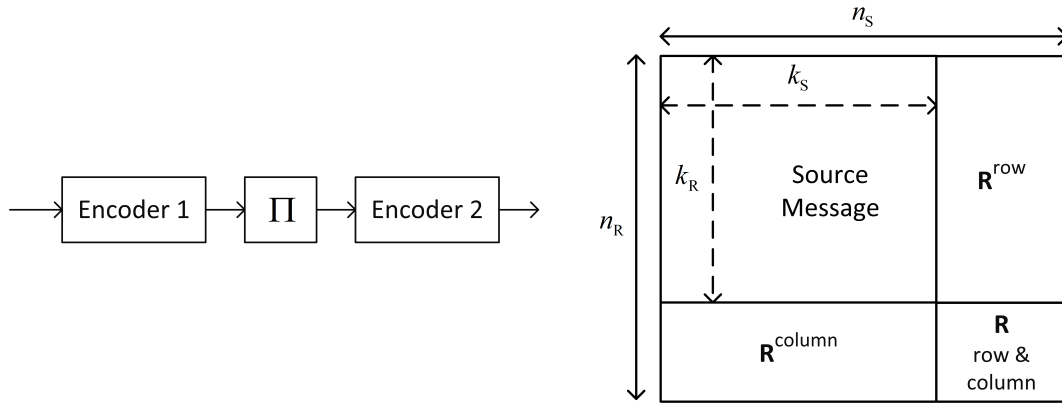


Figure 2.6 — Product code construction

The $(k_S \times k_R)$ message part is firstly encoded using the row elementary code $C^{Row}(n_S, k_S, \delta_S)$. The resulting matrix $(k_R \times n_S)$ is then encoded in the column-wise direction (a kind of interleaving) using the column elementary code $C^{Col}(n_R, k_R, \delta_R)$. The resulting matrix $(n_R \times n_S)$ is a product codeword. We can verify that each row (resp. column) of the product codeword is a valid codeword of C^{Row} (resp. C^{Col}) and the product code $C(n_P, k_P, \delta_P)$ has following parameters :

$$n_P = n_S n_R, \quad k_P = k_S k_R, \quad \delta_P = \delta_S \delta_R.$$

2.3.3.2 Turbo decoding of product codes

The turbo code was firstly introduced by C. Berrou et al. in [BGT93]. The authors defined an original parallel concatenation of convolutional codes separated by an interleaver and proposed a near-optimal iterative soft decoder. The decoder consists of the cascade of the two elementary decoders. The innovation is the definition of the extrinsic information delivered by one decoder to the other decoder. The extrinsic information collected at the output of a decoder is independent of its input. The corresponding error performance is very close to the Shannon limit [Sha48]. The turbo code has become a milestone in the information theory and is widely used in practice. It has paved the way for near-optimal low-complexity turbo-like receiver as turbo decoding of product codes [PGPJ94] and LDPC [Gal63], turbo detection [DJB⁺95] and turbo equalization [GLL97].

In our study, we will use the Chase-Pyndiah algorithm [PGPJ94] to decode the turbo product codes. This algorithm is based on a soft-input soft-output (SISO) decoder whose input and output are measurements of the reliability, which is usually given by the log-likelihood ratio (LLR).

1. SISO decoding for the component codes

The SISO decoding principle is the same for the row and column component codes, so we take the row-wise decoding as an example :

On the AWGN channel, we denote the i -th row of the product codeword as $\vec{\mathbf{c}}_i = (c_{i,1}, c_{i,2}, \dots, c_{i,n_S})$ where $i = 1, 2, \dots, n_R$. We use the BPSK modulation so that $c_{i,l} \in \{\pm 1\}$. The elements of the observation $\vec{\mathbf{r}}_i = (r_{i,1}, r_{i,2}, \dots, r_{i,n_S})$ at the destination can be expressed as :

$$r_{i,l} = c_{i,l} + n_{i,l}, \quad l = 1, 2, \dots, n_S, \quad (2.31)$$

where $n_{i,l}$ is the AWGN variable with zero mean and variance σ^2 . The LLR of the channel observation is defined by :

$$\lambda_{i,l}^{\text{in}} = \ln \frac{\Pr \{c_{i,l} = +1 | r_{i,l}\}}{\Pr \{c_{i,l} = -1 | r_{i,l}\}} = \frac{2}{\sigma^2} r_{i,l}. \quad (2.32)$$

It is the soft input of the SISO decoder. The soft output (LLR of $d_{i,l}$) of the SISO decoder can be calculated by :

$$\lambda_{i,l}^{\text{out}} = \ln \frac{\Pr \{c_{i,l} = +1 | \vec{\mathbf{r}}_i\}}{\Pr \{c_{i,l} = -1 | \vec{\mathbf{r}}_i\}}. \quad (2.33)$$

In [PGPJ94], it has been proved that for high SNR :

$$\lambda_{i,l}^{\text{out}} \approx \frac{1}{2\sigma^2} \left(\left\| \vec{\mathbf{r}}_i - \vec{\mathbf{c}}_i^{-1(l)} \right\|^2 - \left\| \vec{\mathbf{r}}_i - \vec{\mathbf{c}}_i^{+1(l)} \right\|^2 \right) = \frac{1}{\sigma^2} \left(\langle \vec{\mathbf{r}}_i, \vec{\mathbf{c}}_i^{+1(l)} \rangle - \langle \vec{\mathbf{r}}_i, \vec{\mathbf{c}}_i^{-1(l)} \rangle \right), \quad (2.34)$$

where $\vec{\mathbf{c}}_i^{-1(l)}$ (resp. $\vec{\mathbf{c}}_i^{+1(l)}$) is the codeword at the minimum Euclidean distance to $\vec{\mathbf{r}}_i$ satisfying that its l -th bit equals -1 (resp. +1). $\langle \vec{\mathbf{a}}, \vec{\mathbf{b}} \rangle$ denotes the inner product of two vectors.

In the Chase-Pyndiah algorithm, the sub-optimal SISO decoder applies the Chase algorithm described in subsection 2.3.1 to find the decision codeword $\vec{\mathbf{d}}_i$ for a given observation $\vec{\mathbf{r}}_i$. $\vec{\mathbf{d}}_i$ is the codeword with the minimum Euclidean distance to the observation $\vec{\mathbf{r}}_i$ within the subset of candidate codewords Ω . In order to calculate the soft output LLR of the l -th bit in the codeword, we search for a competing codeword $\vec{\mathbf{v}}_i$ in Ω satisfying that $v_{i,l} \neq d_{i,l}$.

After normalizing the input and the output LLR by $\sigma^2/2$, we can obtain that :

$$\lambda_{i,l}^{\text{in}} = r_{i,l}. \quad (2.35)$$

$$\begin{aligned} \lambda_{i,l}^{\text{out}} &\approx \frac{1}{2} \left(\langle \vec{\mathbf{r}}_i, \vec{\mathbf{c}}_i^{+1(l)} \rangle - \langle \vec{\mathbf{r}}_i, \vec{\mathbf{c}}_i^{-1(l)} \rangle \right) \\ &= \begin{cases} \frac{d_{i,l}}{2} \cdot \left(\langle \vec{\mathbf{r}}_i, \vec{\mathbf{d}}_i \rangle - \langle \vec{\mathbf{r}}_i, \vec{\mathbf{v}}_i \rangle \right), & \text{if competing codeword } \vec{\mathbf{v}}_i \text{ exists in } \Omega \\ \lambda_{i,l}^{\text{in}} + \beta d_{i,l}, & \text{otherwise} \end{cases} \end{aligned} \quad (2.36)$$

where β is a predefined positive value approximately proportional to $(-\ln P_{eb})$ and is obtained through simulation. in Eq. 2.36, $\vec{\mathbf{d}}_i$ can be either $\vec{\mathbf{c}}_i^{-1(l)}$ or $\vec{\mathbf{c}}_i^{+1(l)}$ and $\vec{\mathbf{v}}_i$ is called the competing codeword belonging to $\left\{ \vec{\mathbf{c}}_i^{-1(l)}, \vec{\mathbf{c}}_i^{+1(l)} \right\}$ satisfying that $v_{i,l} \neq d_{i,l}$.

Based on the normalized results in Eq. 2.35 and 2.36, the extrinsic information is calculated as :

$$w_{i,l} = \lambda_{i,l}^{\text{out}} - \lambda_{i,l}^{\text{in}}. \quad (2.37)$$

2. Iterative decoding procedure

The q -th half iteration of the turbo decoding is illustrated in Fig. 2.7. A complete iteration includes two half iterations : one is for the SISO decoding of all rows and the other one is for the SISO decoding of all columns.

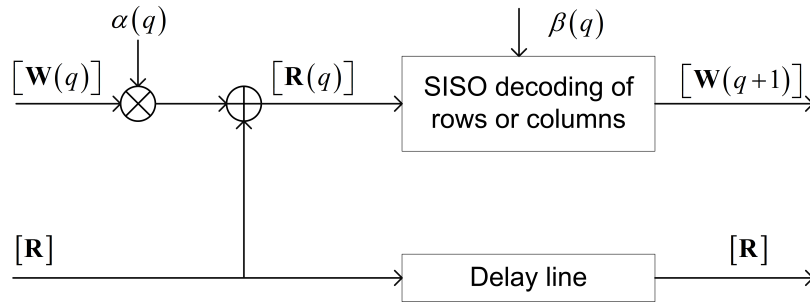


Figure 2.7 — Block diagram of the turbo product code decoder, for the q -th half iteration

At the initial step, the extrinsic information \mathbf{W} is set to zero. Once we observe the product codeword \mathbf{R} , the SISO decoding is applied on all the rows (or columns) of \mathbf{R} . Using Eq. 2.35-2.37, we can obtain the corresponding extrinsic information \mathbf{W} . For the q -th half iteration, the observation \mathbf{R} is updated by :

$$\mathbf{R}(q) = \mathbf{R} + \alpha(q) \cdot \mathbf{W}(q), \quad (2.38)$$

where $\alpha(q)$ is a scaling factor to adjust the influence of the extrinsic information. $\mathbf{W}(q)$ is the extrinsic information calculated by the previous half-iteration. The updated $\mathbf{R}(q)$ becomes the input of next half-iteration of SISO decoding in the column-wise (or row-wise) direction. The turbo decoding stops when a predefined number of iterations is reached or all syndromes of the decoded matrix along one dimension are null at the output of the component decoder corresponding to the other dimension.

In the Fig. 2.7, $\beta(q)$ is the β value given in Eq. 2.36 for the q -th half iteration. In our simulations, the maximum number of complete iterations is 10 and the values of $\alpha(q)$ and $\beta(q)$ are given by :

$$\alpha(q) = \min \{0.25 \cdot (q - 1), 0.5\}. \quad (2.39)$$

$$\beta(q) = \min \left\{ \sum_{j \in \Theta} |\lambda_{ij}^{\text{in}}|, \beta_{\max} \right\}, \quad (2.40)$$

where $\beta_{\max} = 10$ [Pyn98]. If we suppose that the Chase algorithm considers m least reliable bits (2^m test patterns). Θ is the subset of the positions of the m least reliable bits in the updated observation vector.

More details about turbo product codes can be found in [Pyn98].

2.4 Multiple-access methods

In a multiple-access system, different users share the same resources (time, frequency, etc.), which can generate interference. Without regulation, the receiver can consider the interference as noise, with the risk of high interference and incapacity of detecting its intended message. Usual techniques perform an orthogonal access to the resources either in time (TDMA), in frequency (FDMA) or with coding (CDMA). The counterpart is an asymptotic capacity per user proportional to the inverse of user number. As a consequence, the number of users accessing simultaneously to the same resources is limited.

In this section, we briefly introduce orthogonal multiple-access techniques as they are necessary to coordinate the transmissions in our cooperative network framework.

2.4.1 Major multiple-access techniques

FDMA divides the channel into non-overlapping frequency sub-channels. Each user is allocated with a sub-channel. All users transmit simultaneously on different carrier frequencies. It is often used in the wired communications and in the analog cellular systems.

TDMA orthogonally divides the channel in the time domain. The transmission time is divided into non-overlapping time slots. Each user is allocated with a predefined time slot. All users transmit one-after-another in a cyclical manner.

CDMA is based on the direct-sequence spread spectrum principle. Each user is allocated with a unique spreading sequence. The spreading sequences can be either orthogonal or near-orthogonal to each other. The spectrum of the transmitted signal is spread by multiplying the original signal with the spreading sequence. At the destination, different user flows can be separated by the cross correlation of the received signal with the locally-generated spreading sequence associated with the intended user. In CDMA transmission, all users occupy simultaneously the same frequency and time resources. The CDMA system capacity is limited by the spreading sequence alphabet cardinal.

In practice, the CDMA technique can be combined with either TDMA or FDMA for an enhanced exploitation of the resources.

2.4.2 Brief introduction to CDMA

2.4.2.1 Direct sequence spread spectrum principle

The CDMA uses the direct sequence spread spectrum (DSSS) principle. The block diagram of a binary DSSS system is shown in Fig. 2.8.

Let d_k be the BPSK modulated symbol to be transmitted on time interval $[kT_s, (k+1)T_s[$. We define the spreading sequence as a sequence of PG (also known as Processing Gain defined later) binary elements $\vec{s} = (s_0, s_1, \dots, s_{PG-1})^T$. The spreading

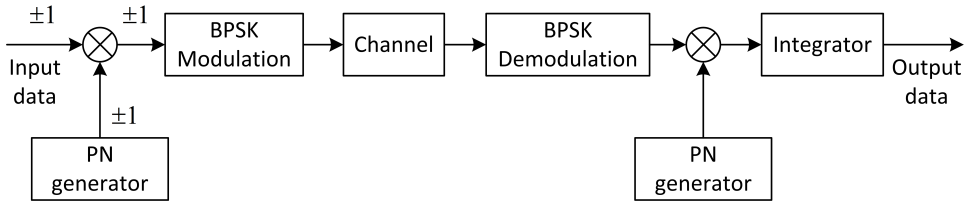


Figure 2.8 — Binary direct sequence spread spectrum (DSSS) communication block diagram

consists in defining a PG -length sequence $(c_{PG \cdot k+0}, c_{PG \cdot k+1}, \dots, c_{PG \cdot k+PG-1})^T$ as the multiplication of \vec{s} by d_k :

$$c_{PG \cdot k+n} = d_k \cdot s_{k,n}. \quad (2.41)$$

$c_{PG \cdot k+n}$ is called a chip. Its duration is denoted T_{chip} and satisfies $PG \cdot T_{chip} = T_s$. The equivalent baseband transmitted signal is given by :

$$x(t) = \sum_n c_n \cdot h(t - nT_{chip}). \quad (2.42)$$

The minimum bandwidth ensuring a transmission without inter symbol interference is equal to $B_{spread} = 1/T_{chip}$. For the non-spread transmission, $B_{non-spread} = 1/T_s = B_{spread}/PG$.

Since the spread and non-spread systems have the same average energy required to transmit a symbol d_k , it is necessary to normalize the spreading sequence component :

$$|s_m| = \frac{1}{\sqrt{PG}}. \quad (2.43)$$

To sum up, the spreading yields a decrease of the signal amplitude (justifying why spread spectrum techniques have been used in military communications) and a bandwidth expansion compared to a non-spread system.

At the receiver, the signal is first processed as a BPSK modulated symbol of rate $1/T_{chip}$. Then the information data are recovered by a simple scalar product between the samples at the demodulated output and the original spreading sequence. If z_i denotes the i -th sample output, the decision variable for d_k is given by :

$$\hat{d}_k = \sum_{m=0}^{PG-1} z_{k \cdot PG+m} \cdot s_m. \quad (2.44)$$

In presence of interference, the scalar product by the spreading sequence will yield a spreading of the interference followed by a band-pass filtering and hence an interference power decrease as shown in Fig. 2.9.

An important parameter of a spread spectrum system is the processing gain which is defined as the number of chips per data symbol. Here we will consider the short-code case where each data symbol has the same duration as the spreading sequence period,

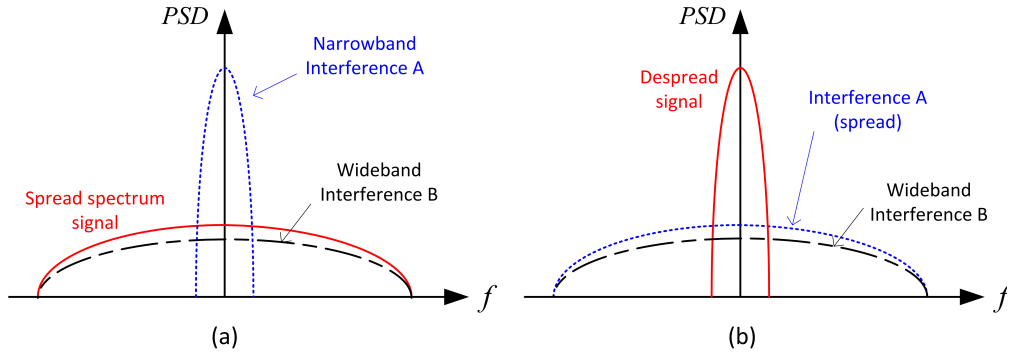


Figure 2.9 — Power spectral density of the spread spectrum signal in the presence of narrowband interference, (a) before despreading ; (b) after despreading

so we have $T_s = PG \cdot T_{chip}$. The processing gain is also the number of chips within one spreading sequence period :

$$PG = \frac{T_s}{T_{chip}} = \frac{R_{chip}}{R_s} = \frac{\text{Spread spectrum RF bandwidth}}{\text{Information bandwidth}}. \quad (2.45)$$

As shown in Fig.2.9, the use of spread spectrum technique offers a signal-to-interference improvement. The processing gain serves as an approximate measure of this advantage. A large processing gain yields a high interference rejection, which encourages the use of long spreading sequences. On the other hand, the processing gain cannot be arbitrarily large. For a fixed information rate, the bandwidth of the spread spectrum signal is proportional to the processing gain, which should respect the RF requirement and also the technology constraints imposed by the hardware.

2.4.2.2 Synchronous CDMA channel model

The CDMA consists in applying the spread spectrum techniques simultaneously to multiple users. Different spreading sequences are necessary to ensure the separation. They have the same processing gain and they are approximately or perfectly orthogonal to each other. After that, the spread spectrum signals are simultaneously transmitted in the same RF band. The destination can detect a given user by correlating the received signal with the user spreading sequence. Each unintended user contributes to the background noise (or as the wideband interference) affecting the target user but their influence is designed to be negligible within the system tolerance.

Let us consider a synchronous CDMA model as described in [Ver98] where the symbols of different user streams are aligned in time at the receiver.

Suppose there are K CDMA users. For the BPSK modulation on the AWGN channel, the baseband spread spectrum signal received on time interval $[0, T_s)$ is defined by :

$$r(t) = \sum_{i=0}^{K-1} A_i \cdot d_i \cdot s_i(t) + n(t), \quad (2.46)$$

where A_i , d_i and $s_i(t)$ are the received amplitude, the data symbol and the spreading waveform of the i -th CDMA user. $n(t)$ is a Gaussian noise. The spreading waveform

is normalized to have unit energy such that :

$$\int |s_i(t)|^2 dt = 1. \quad (2.47)$$

The normalized spreading sequence is denoted as $\vec{s}_i = (s_{i,0}, s_{i,1}, \dots, s_{i,PG-1})^T$ of length PG . $s_{i,1} \in \left\{ \pm 1 / \sqrt{PG} \right\}$ and satisfies the following condition :

$$\sum_{m=0}^{PG-1} s_{i,m}^2 = 1. \quad (2.48)$$

The CDMA performance depends on the correlation properties of the spreading waveforms whose cross-correlation is defined as :

$$\rho_{ij} = \langle \vec{s}_i, \vec{s}_j \rangle = \int s_i(t) s_j(t) dt. \quad (2.49)$$

At the receiver, the CDMA multi-user detector usually employs a matched filter bank to extract the discrete variables from the received spread spectrum signal $r(t)$, as shown in Fig. 2.10.

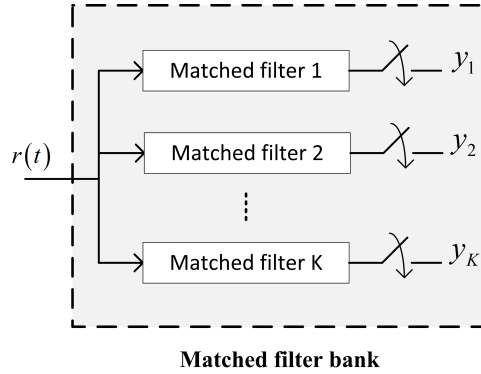


Figure 2.10 — The matched filter (correlator) bank of a CDMA detector

For a K -user system, there are K matched filters in the bank and each one is matched to a different spreading waveform. The soft output of the i -th matched filter can be expressed as :

$$\begin{aligned} y_i &= \int s_i(t) r(t) dt \\ &= A_i d_i \int s_i(t) s_i(t) dt + \sum_{j \neq i} A_j d_j \int s_i(t) s_j(t) dt + \int s_i(t) n(t) dt \\ &= A_i d_i + \sum_{j \neq i} A_j d_j \rho_{ij} + n_i, \end{aligned} \quad (2.50)$$

where the first term corresponds to the desired user contribution and the second term corresponds to the multiple access interference (MAI) coming from other CDMA users.

Based on Eq. 2.50, we can establish the discrete equivalent base band model of the synchronous CDMA transmission :

$$\vec{y} = \mathbf{C}\mathbf{A}\vec{d} + \vec{n}, \quad (2.51)$$

where $\mathbf{C} = \{\rho_{ij}\}$ is the normalized spreading waveform cross-correlation matrix. In the discrete equivalent transmission model, \mathbf{C} is the cross-correlation matrix of the spreading sequences. \mathbf{A} is a diagonal matrix containing the received amplitudes of all CDMA user signals. \vec{y} , \vec{d} and \vec{n} are K -dimensional column vectors and designate the outputs of the matched filters, the data symbols and the noise variables respectively.

2.4.2.3 Spreading sequences and correlation properties

The CDMA system performance depends mainly on the choice of the spreading sequences, especially on their length and correlation properties.

The design of the spreading sequences has usually three main constraints :

1. The antipodal elements in the sequence should have a balanced weight.
2. The auto-correlation should have a ‘Dirac’ form such that there is only one peak value at the 0-delay position while the other off-peak values are comparatively small. This property enables quick sequence detection to facilitate the system synchronization.
3. The cross-correlation should be small for all delays in order to reduce the multiple-access interference.

In the short-code system, we denote $\vec{s}_i = (s_{i,0}, s_{i,1}, \dots, s_{i,PG-1})^T$ as the i -th normalized spreading sequence of length PG . We will use the following correlation definitions in our analysis.

The full-period cross-correlation of the spreading sequences \vec{s}_i and \vec{s}_j is defined as :

$$\phi_{i,j}(n) = \sum_{p=0}^{PG-1} s_{i,p} s_{j,p+n}. \quad (2.52)$$

The aperiodic discrete auto-correlation of the normalized spreading sequence \vec{s}_i is defined as :

$$\phi^a(n) = \begin{cases} \sum_{p=0}^{PG-n} s_{i,p} s_{i,p+n}, & 0 \leq n \leq N-1 \\ \sum_{p=0}^{PG+n} s_{i,p} s_{i,p-n}, & -N+1 \leq n \leq 0 \\ 0, & \text{otherwise} \end{cases} \quad (2.53)$$

The cross-correlation given in Eq. 2.52 measures the resemblance between two spreading sequences with different cyclic chip shifts. In the case of 0-delay ($n=0$), $\phi_{i,j}(0)$ is actually the entries of the discrete cross-correlation matrix \mathbf{C} in the synchronous CDMA model. The auto-correlation given in Eq. 2.53 will be useful to evaluate the PSD of the spread spectrum signal in Chapter 4.

2.5 Conclusion

In this chapter, we have introduced the basic knowledge about the digital transmission chain, the information theory, the FEC codes and the multiple-access methods. Combing them with the Network Coding introduced in the previous chapter, we are ready to address the main subject of this thesis : Network Coding in the wireless relay cooperative networks.

In Chapter 3, we will introduce a cooperative scheme using the TDMA mode based on the product codes. The linear Network Coding is applied at the relay through the use of a systematic linear block FEC code. The hard detection, hard decoding and soft decoding strategies will be considered at the relay to detect the source FEC codewords. The theoretical error performance of turbo decoding will be investigated at the destination. Besides that, the network capacity introduced in this chapter will be extended to the finite code length regime.

In Chapter 4, the CDMA technique will be applied at the relay to help the cooperation. The source and relay transmissions will share the same RF band by using hybrid multiple-access methods. The relay transmission model is the synchronous CDMA introduced in this chapter and we will construct near-orthogonal spreading sequences with good correlation properties. We will study the interference introduced by the multiple-access and propose an iterative decoding procedure. The optimal energy allocation between sources and relay will be established through simulations.

Time-division multi-source relay cooperation using BCH product codes

In this chapter, we study a multi-source cooperative scheme based on the BCH product codes for wireless sensor networks (WSN), where a number of sources transmit to a single destination with the help of a relay.

In the proposed scheme, the relay applies algebraic systematic Network Coding to its detected source codewords and forwards only the additional redundancy to the destination where an overall product codeword is observed. Because the source-relay channel is affected by noise and fading, there are residual errors in the relay-detected source codewords, which give rise to error propagation after the relay encoding. The turbo decoder at the destination takes into account these errors and uses an appropriate log-likelihood ratio (LLR) to limit their influence. We will show the improved error performances on the Gaussian channel and on the fast Rayleigh fading channel. A theoretical bound of the error probability will be established in the case of soft decoding at the relay.

Besides that, we will analyze the error correlation in the relay-generated redundancy and investigate the performance of multi-relay cooperation. The theoretical error probabilities at the input and output of the relay encoder are investigated for different relay strategies, which will facilitate the calculation of the LLR limiter. Different cooperation schemes with single or multiple relays using different relay strategies are compared in terms of performance, complexity and energy consumption.

In the last part of this chapter, we evaluate the network capacity of the proposed cooperative scheme using the min-cut max-flow theorem and the channel rate approximation in the finite code-length regime. Special attention is paid to the source-relay link which is the bottleneck of the cooperative network.

3.1 Introduction

We consider a wireless sensor network (WSN) where a large number of sources transmit independent data to the same destination. These sources are sensors of low complexity and limited energy. Such cheap devices cannot afford too complicated algorithms or a high transmission power. The individual source data rate is low, which is the case of most WSN applications. We suppose that all sources use the same forward error correcting (FEC) code to protect their wireless transmissions. The sources are not inter-connected, so each one encodes independently its data.

For the data transmission, the information theory states that the arbitrary small error probability can only be achieved with long enough FEC codes. In practice, we should use turbo codes [BGT93, Pyn98] or low-density parity-check (LDPC) codes [Gal63] providing that the information block length is longer than 5000 bits [RL09, p.10]. The turbo-like encoding at each source under the long code constraint will introduce an additional transmission delay and complexity, which is often prohibitive for the low-rate cheap sensors. So we only consider the short FEC codes at the sources in our study.

In order to improve the transmission quality, a relay with enhanced processing ability and energy is placed close to the sources. The relay can eavesdrop on the source transmissions and help to forward the information to the destination after relay treatments. The sources and the relay will work cooperatively to accomplish the data transmission. In this chapter, we assume that all transmissions are scheduled using the time-division multiple-access (TDMA) mode so that there is no multiple-access interference at the reception. Besides that, we suppose perfect synchronization of time / frequency and there is no inter-symbol interference (ISI) at the reception.

Through the relay cooperation, we can construct more efficient systems based on different cooperative schemes [NHH04] such as the Amplify-and-Forward, the Decode-and-Forward and the Coded Cooperation. The Network Coding [ACLY00, KM03] is an emerging technique for the cooperative networks. By using the Network Coding, the transmitted blocks are combined at the relay node and the resulting blocks are forwarded to the destination. In wired error-free networks, one can optimize the system throughput and economize the transmission energy. When we use Network Coding in wireless networks, one of the main obstacles is the error propagation associated with the higher error probability in the wireless environment, which has been detailed in Chapter 1. Besides that, the wired networks have less constraint on the bandwidth than the wireless networks.

In our study, the algebraic Network Coding (through a linear systematic block FEC code) is applied at the relay. The corresponding relay cooperative scheme was proposed in [PGA10] based on the turbo product codes (TPC) whose encoding is accomplished in a distributed manner. In this scheme, all sources use the same systematic block code and broadcast the codewords to the relay and the destination. Instead of forwarding the received source codewords to the destination, the relay stores all detected source codewords in the rows of a matrix and encodes the columns using another systematic block code and forwards only the relay-generated redundancy to the destination. At the destination, the codewords from the sources and the redundancy from the relay are

decoded iteratively using the turbo decoding [Pyn98]. The advantages of such a scheme are numerous. The equivalent scheme without cooperation requires an additional device to connect the sources and implies transmission delays due to the source codewords storage and product code encoding. With the proposed scheme, the sources use short block codes and the relay connects them virtually to reduce the transmission delay.

Similar cooperative schemes based on turbo product codes have also been studied in other papers. For example, [XQYX09] investigates the multi-relay cooperation on the Gaussian channel. The error performance is analyzed with different relay positions, but the error propagation is not emphasized. [ABS10] considers the single relay case with an error-free source-relay channel. [OCC10] studies the multi-relay case with the product code based on the Bose-Chaudhuri-Hocquenghem (BCH) codes. In order to mitigate the error propagation, each relay applies a different cyclic interleaving on its detected source BCH codewords to generate different relay redundancy through column encoding. Each relay sends its whole redundancy to the destination. The error propagation is alleviated at the cost of a reduced code rate and a much higher complexity in the turbo decoding.

The rest of the chapter is organized as follows : Section 3.2 introduces the setup of the multi-source relay cooperation network and shows its error performance when source-relay transmission is error-free. In Section 3.3, we focus on the network error performance with the noisy source-relay channel. We will consider different relay detection strategies and will derive the theoretical error probabilities at the relay. Besides the LLR limiter proposed in [PGA10] to mitigate the influence of the residual errors at the relay, we will analyze the error correlation in the relay-generated redundancy and the solution of multi-relay cooperation. Different cooperation schemes (single or multi-relay cooperation with different relay strategies) are compared on the fast Rayleigh fading channel. Based on the analysis and simulation results, we show that the source-relay link is actually the bottleneck of the network and in Section 3.4, we will analyze the network capacity with the constraint of a finite length FEC code on the source-relay channel.

3.2 Cooperative network setup

The cooperative network setup is illustrated in Fig. 3.1. We suppose that K sources use the same systematic block code (n_S, k_S) of length- n_S and dimension- k_S . Each source broadcasts a codeword to the destination in the TDMA mode.

Since the source transmission is in the broadcast mode, the relay can receive and detect the source codewords. The K detected source codewords are stored in the first K rows of a matrix at the relay as illustrated in Fig. 3.2. Then, the relay encodes the columns of the matrix using a second systematic block code (n_R, k_R) with $k_R = K$ and forwards only the column redundancy, i.e., the last $(n_R - k_R)$ rows of the resulting matrix, to the destination.

As shown in Fig. 3.2, through the cooperation, the destination observes K source codewords via the direct source-destination channel and also the relay-generated redundancy via the relay-destination channel. The whole observation corresponds to a product codeword such that we can apply the turbo decoding [Pyn98] to recover the

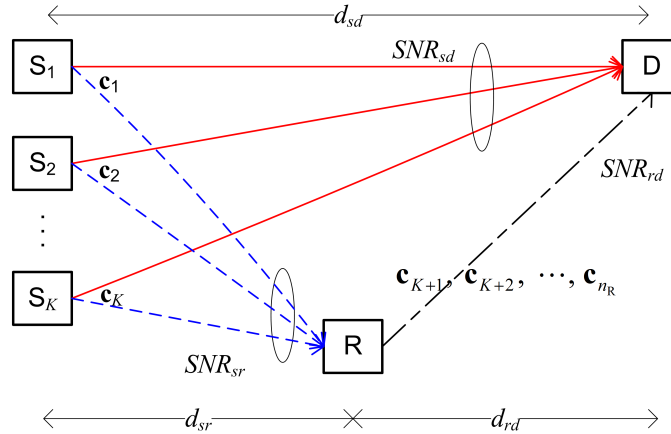


Figure 3.1 — Multi-source cooperative network setup

source information.

In this chapter, as in [PGA10], we suppose a noisy source-relay channel resulting in residual errors in the relay-detected source codewords. After the relay encoding, these errors propagate to the relay-generated redundancy, which will degrade the error correction efficiency at the destination.

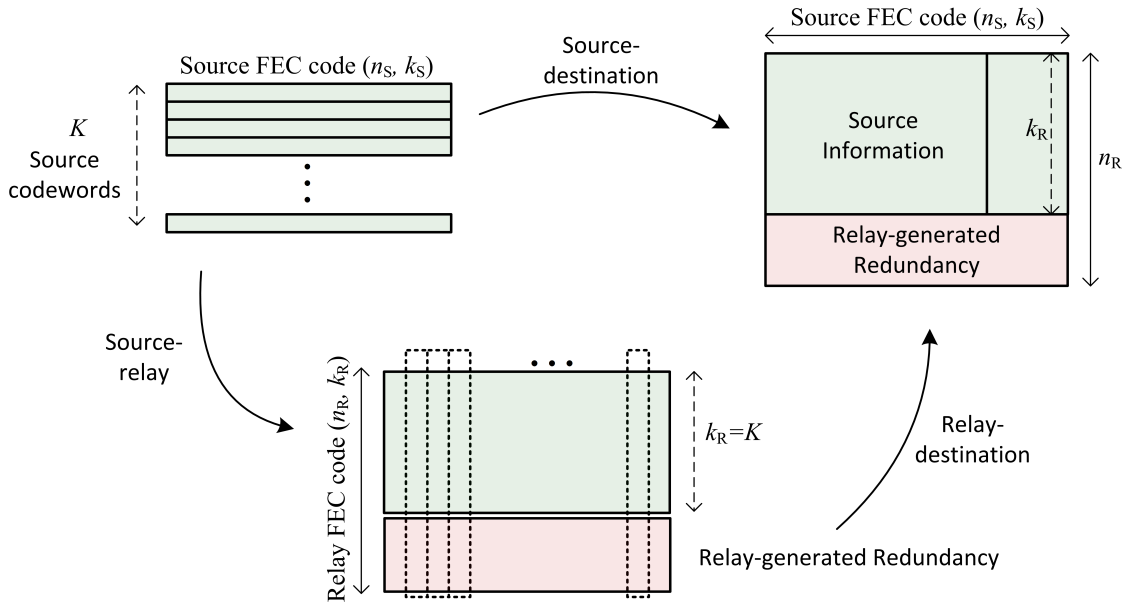


Figure 3.2 — Relay-aided distributed product code construction

We denote the average signal-to-noise ratio (SNR) of the source-destination (resp. source-relay and relay-destination) channels as SNR_{sd} (resp. SNR_{sr} and SNR_{rd}). We study the case where the source-relay distance d_{sr} is smaller than the source-destination distance d_{sd} . The relay is considered to be located at the same distance to the destination as the sources, so $d_{rd} = d_{sd}$ and $SNR_{rd} = SNR_{sd}$. We set that SNR_{sr} exceeds SNR_{sd} with a value of ΔSNR (dB) :

$$SNR_{sr} = SNR_{sd} + \Delta SNR, \quad (3.1)$$

where $\Delta SNR = 10\log_{10}(d_{sd}/d_{sr})^\alpha$ and α is the path-loss coefficient. For the free-space transmission (AWGN channel), α is equal to 2 and for the multipath fading transmission, it is between 3 and 4. Here, we set $\alpha = 3.5$ in the case of fast Rayleigh fading channel. In Table 3.1, different ΔSNR values are listed according to different distance ratios. For most practical WSN applications, the ratio d_{sd}/d_{sr} is usually greater than 4.

| d_{sd}/d_{sr} | AWGN | Rayleigh |
|-----------------|-------|----------|
| 1.3 | 2.3dB | 4dB |
| 1.7 | 4.6dB | 8dB |
| 2.7 | 8.6dB | 15dB |
| 4 | 12dB | 21dB |
| 10 | 20dB | 35dB |

TABLE 3.1 — SNR gap between S-R channel and S-D channel

At first, we consider the network error performance with a perfect source-relay link such that at the relay, the detected source codewords are error-free. In this case, once the destination observes all the source codewords and the relay-generated redundancy, it can decode them using the turbo-decoding algorithm described in the previous chapter.

The error performance is measured in terms of BER and FER as a function of E_b/N_0 . $N_0/2$ is the double-side noise power spectral density. E_b is the average received information bit energy at the destination, which includes the energy contributed by the relay-destination channel. In the described product code scheme, we have the following energy relation according to the encoding matrix in Fig. 3.2 :

$$(k_S \cdot k_R) E_b = (k_R \cdot n_S) E_{sd} + (n_R - k_R) n_S \cdot E_{rd}, \quad (3.2)$$

where E_{sd} is the average energy per codeword bit received on the source-destination channel. E_{rd} is the average energy per codeword bit received on the relay-destination channel. We denote the source code rate $R_S = k_S/n_S$ and the relay code rate $R_R = k_R/n_R$, then Eq. 3.2 can be reformulated as :

$$E_b = \frac{1}{R_S} \left[E_{sd} + \frac{1 - R_R}{R_R} E_{rd} \right]. \quad (3.3)$$

Furthermore, we consider that $SNR_{rd} = SNR_{sd}$, so we have $E_{rd} = E_{sd}$.

In simulations, we take an example where the sources use the BCH (64, 51, 6) code and the relay uses the BCH (32, 26, 4) code. In Fig. 3.3 to 3.6, we plot the simulated BER and FER of the proposed cooperative network in the case of no error at the relay. The corresponding curves are labeled with ‘TPC (error-free relay)’. In the same figures, we also plot the soft decoding BER and FER of the source BCH codes in the case of direct transmission without relay cooperation.

Compared to the direct transmission, the TPC-based cooperation with an error-free relay offers a coding gain of about 3dB (resp. 8.6dB) at a $BER = 10^{-5}$ on the AWGN (resp. fast Rayleigh fading) channel. This gain shows the potential of the proposed cooperation scheme. The error performance obtained with an error-free relay will serve as a lower bound in our following analysis of the noisy relay cooperation.

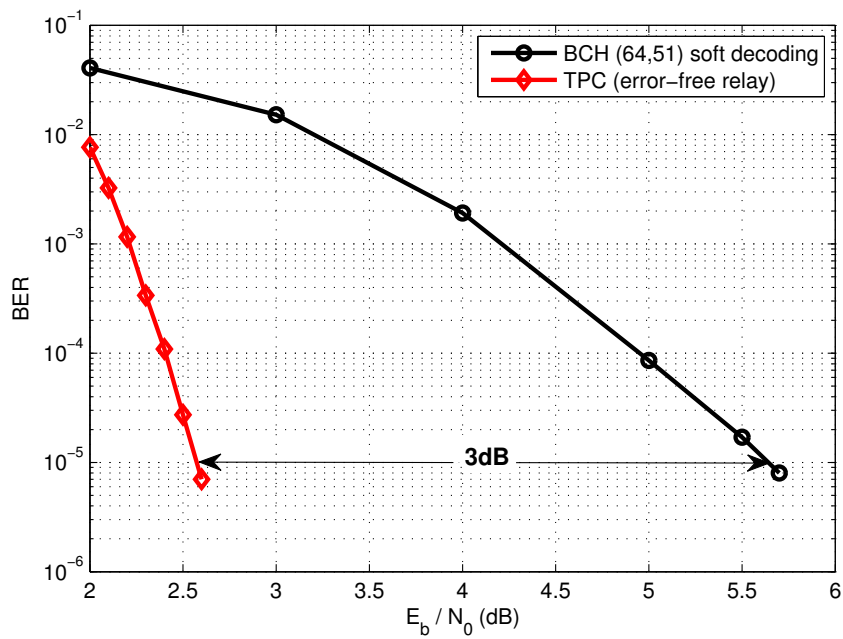


Figure 3.3 — BER of the cooperative network with an error-free relay on the AWGN channel, $SNR_{rd} = SNR_{sd}$, $(n_S, k_S, \delta_S) = (64, 51, 6)$, $(n_R, k_R, \delta_R) = (32, 26, 4)$.

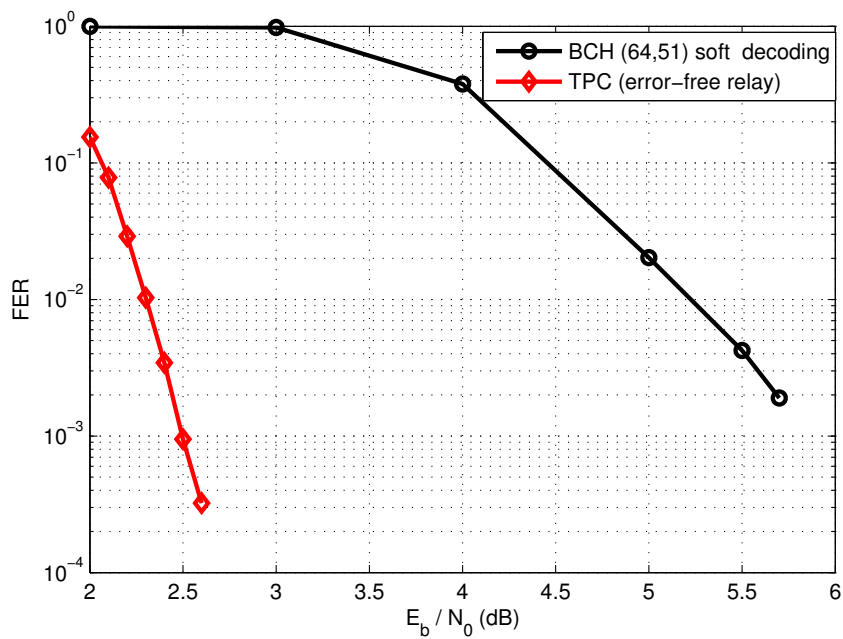


Figure 3.4 — FER of the cooperative network with an error-free relay on the AWGN channel, $SNR_{rd} = SNR_{sd}$, $(n_S, k_S, \delta_S) = (64, 51, 6)$, $(n_R, k_R, \delta_R) = (32, 26, 4)$.

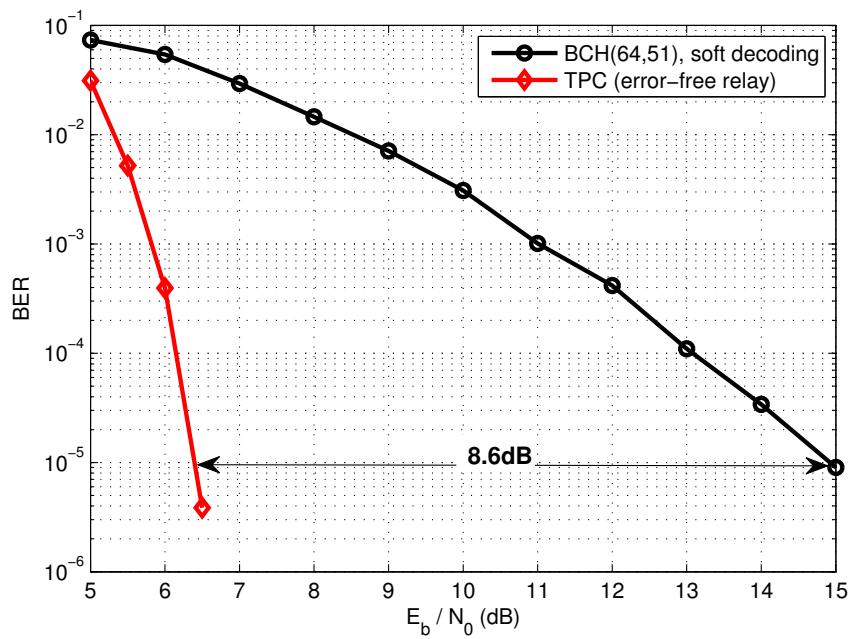


Figure 3.5 — BER of the cooperative network with an error-free relay on the fast Rayleigh fading channel, $SNR_{rd} = SNR_{sd}$, $(n_S, k_S, \delta_S) = (64, 51, 6)$, $(n_R, k_R, \delta_R) = (32, 26, 4)$.

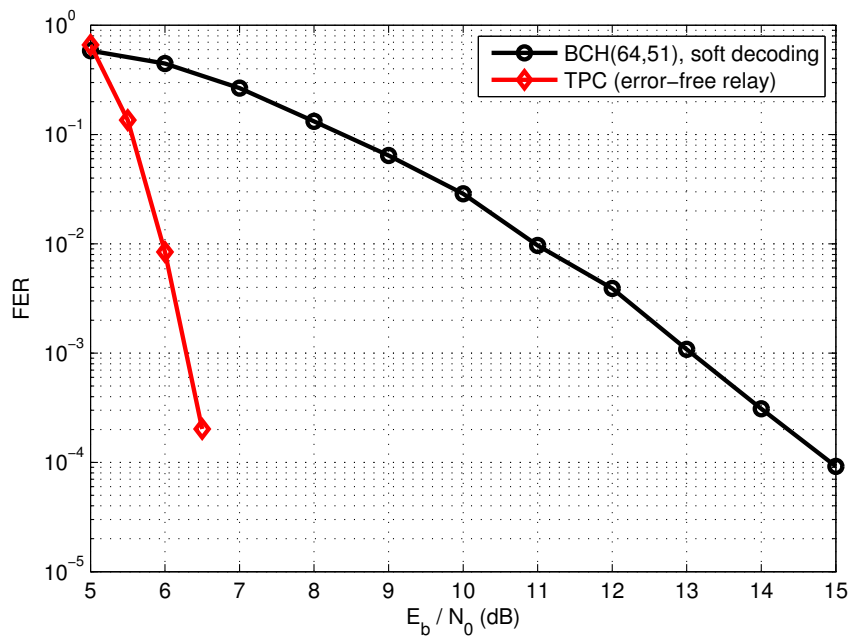


Figure 3.6 — FER of the cooperative network with an error-free relay on the fast Rayleigh fading channel, $SNR_{rd} = SNR_{sd}$, $(n_S, k_S, \delta_S) = (64, 51, 6)$, $(n_R, k_R, \delta_R) = (32, 26, 4)$.

3.3 Cooperation with a noisy source-relay channel

In most studies of the wireless cooperative networks, the source-relay channel is usually assumed error-free as in the previous section. This assumption simplifies the problem but is not always true in practice. In this chapter, we consider the cooperation with a noisy relay. In this case, there are residual errors at the output of the relay detector. These errors will degrade the network performance and need special treatments.

3.3.1 Relay detection strategies and error amplification

The relay can use different strategies to detect the source codewords such as the bit-by-bit hard detection, the hard decoding and the soft decoding. These detection strategies have different error performances under the same channel condition. The detected source codewords at the relay are encoded by a column-wise systematic linear block code as shown in Fig. 3.2. The residual errors contained in the column message part is then propagated to the relay-generated redundancy. In the following, we will prove that the errors are amplified at the output of relay encoder due to the error propagation resulting from the relay encoding.

Suppose that the sources use the systematic linear block code (n_S, k_S, δ_S) . We denote R_S the source code rate, δ_S the source minimum Hamming distance and t_S the source code error correction capability. After estimating the K source codewords, the relay uses the systematic linear block code (n_R, k_R, δ_R) to generate the relay redundancy where δ_R is the column code minimum Hamming distance. Each column of the product code matrix corresponds to a column codeword generated by the relay encoding. Let \mathbf{m} (resp. $\hat{\mathbf{m}}$) denote the column message part without (resp. with) errors. We denote \mathbf{c} (resp. $\hat{\mathbf{c}}$) the column codeword associated to the message \mathbf{m} (resp. $\hat{\mathbf{m}}$). The following considers one column of the matrix. We denote p_{in} the bit error probability at the input of relay encoder. For the fast Rayleigh fading channel, the p_{in} associated with the different relay strategies are given by :

Hard detection :

$$p_{in} = p_{eb}^* = \frac{1 - \mu}{2}, \quad (3.4)$$

Hard decoding :

$$p_{in} \leq \frac{2t_S + 1}{n} \sum_{m=t_S+1}^{n_S} \binom{n_S}{m} (p_{eb}^*)^m (1 - p_{eb}^*)^{n_S - m}, \quad (3.5)$$

Soft decoding [PS08, p.854] :

$$p_{in} \leq \sum_{d=\delta_S}^{n_S} \frac{d \cdot A_S(d)}{n_S} \left[\frac{1 - \mu}{2} \right]^d \cdot \sum_{m=0}^{d-1} \binom{d-1+m}{m} \left[\frac{1 + \mu}{2} \right]^m, \quad (3.6)$$

where $\mu = \sqrt{\frac{R_S \cdot (E_b/N_0)_{sr}}{1 + R_S \cdot (E_b/N_0)_{sr}}}$ and $A_S(d)$ is the weight distribution of the source codewords. The bit error probability at the output of relay encoder, i.e. relay-generated redundancy :

$$p_{out} = \sum_{d=\delta_R}^{n_R} \sum_{w=1}^{k_R} \frac{d-w}{n_R - k_R} \cdot \Pr(d_H(\mathbf{c}, \hat{\mathbf{c}}) = d). \quad (3.7)$$

where

$$\begin{aligned} \Pr(d_H(\mathbf{c}, \hat{\mathbf{c}}) = d) &\leq \sum_{w=1}^{k_R} \Pr(d_H(\mathbf{c}, \hat{\mathbf{c}}) = d | d_H(\mathbf{m}, \hat{\mathbf{m}}) = w) \\ &\leq \sum_{w=1}^{k_R} \frac{B_R(w, d)}{\sum_s B_R(w, s)} \cdot \left[\binom{k_R}{w} \cdot (p_{in})^w (1 - p_{in})^{k_R - w} \right]. \end{aligned} \quad (3.8)$$

where $B_R(w, d)$ is the number of column codewords of weight d with message part of weight w and $d_H(\mathbf{x}, \mathbf{y})$ is the Hamming distance between two vectors.

In our example, the sources use the BCH (64, 51, 6) code and the relay uses the BCH (32, 26, 4) code. In Fig. 3.7 and 3.8, we plot the theoretical bit error probabilities along with the simulated BER in the case of hard detection / decoding at the relay. The simulated BER coincide with the theoretical error probabilities in both cases.

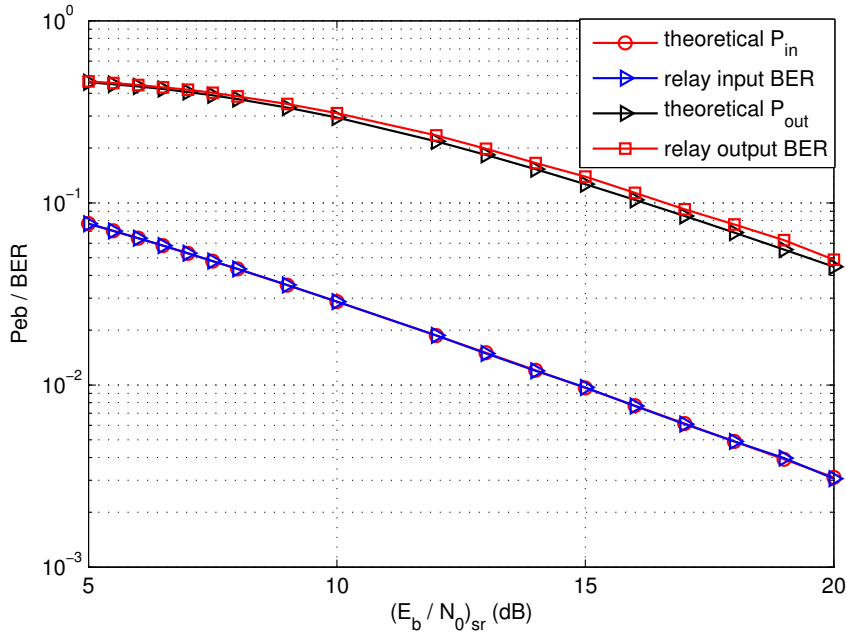


Figure 3.7 — Bit error probability at relay input/output, hard detection at the relay, fast Rayleigh fading channel, $SNR_{rd} = SNR_{sd}$, $(n_S, k_S, \delta_S) = (64, 51, 6)$, $(n_R, k_R, \delta_R) = (32, 26, 4)$.

In Fig. 3.9, we plot the theoretical bit error probability at the input / output of the relay encoder in the case of soft decoding at the relay. In BER simulations, we use the Chase algorithm [Cha72] with different test pattern numbers. With additional

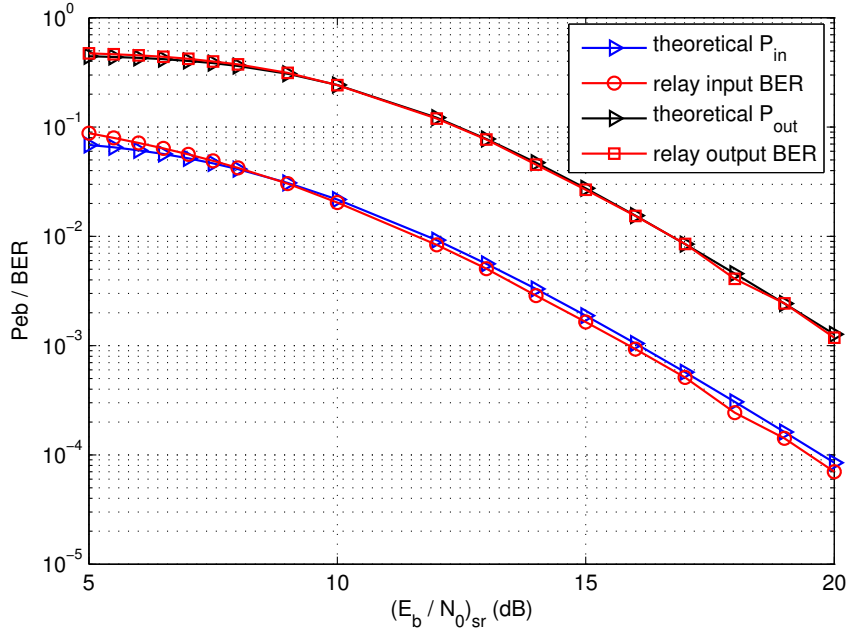


Figure 3.8 — Bit error probability at relay input/output, hard decoding at the relay, fast Rayleigh fading channel, $SNR_{rd} = SNR_{sd}$, $(n_S, k_S, \delta_S) = (64, 51, 6)$, $(n_R, k_R, \delta_R) = (32, 26, 4)$.

test patterns (from 16, 64 to 128 patterns), the Chase algorithm performs closer to the asymptotical upper bound at the price of an increased computation cost. In order to achieve the bit error probability bounds, which correspond to the ML optimal performance, we should use at least 128 test patterns in the Chase algorithm and the corresponding results are shown by the dashed curves in Fig. 3.9.

In Fig. 3.10, we plot all the theoretical results for the three relay strategies. The gap between the three strategies increases with the SNR. The soft decoding has the lowest error probability at both input and output of the relay encoder. We can observe the error amplification at the relay output for each relay strategy, which is due to the error propagation phenomenon during the column encoding at the relay. The amplification factor of p_{out} to p_{in} is about 10. It is determined by the relay code and independent of relay detection strategies.

3.3.2 Theoretical network error probability bound

In this subsection, we analyze the error probability of the proposed multi-source relay cooperation scheme. There are two benefits of such a theoretical analysis : firstly, the theoretical bound enables to verify the error performance obtained by simulations ; secondly, using the theoretical bound, we can directly evaluate the error performance corresponding to different SNR values without using the time-consuming simulations.

In the proposed cooperation, there are three possible relay strategies : the hard detection, the hard decoding and the soft decoding. At the first sight, the hard-detection strategy seems to be the easiest one since the detection errors are i.i.d.. However, it is

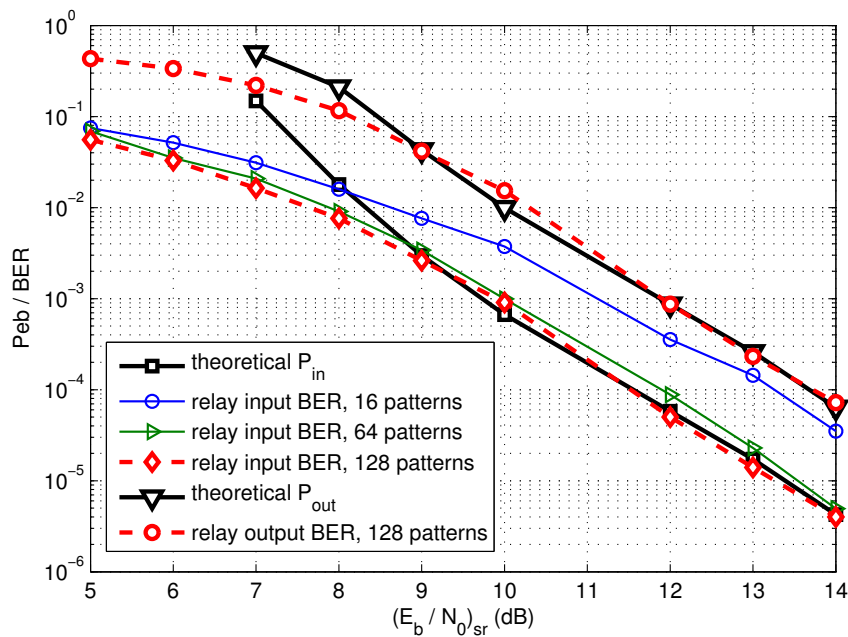


Figure 3.9 — Bit error probability at relay input / output, soft decoding at the relay, fast Rayleigh fading channel, $SNR_{rd} = SNR_{sd}$, $(n_S, k_S, \delta_S) = (64, 51, 6)$, $(n_R, k_R, \delta_R) = (32, 26, 4)$.

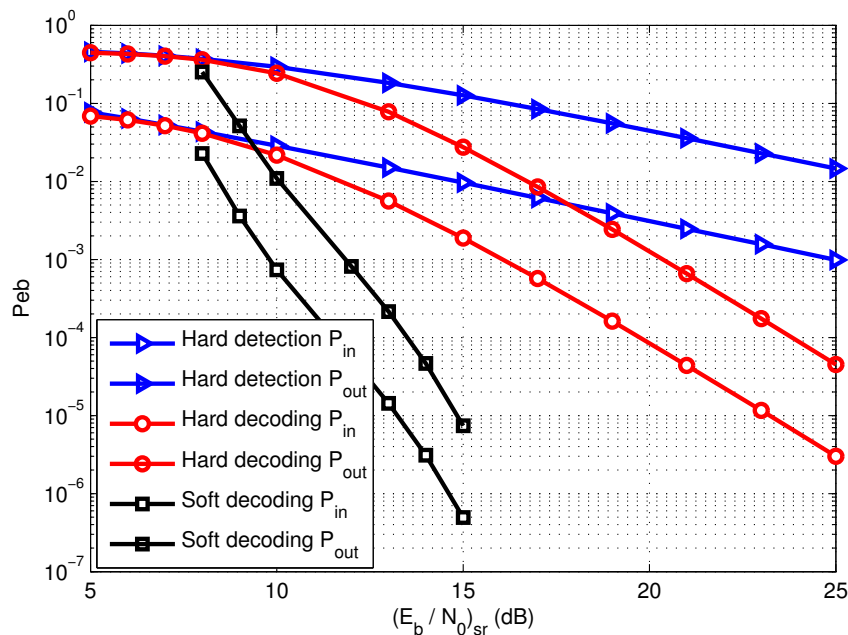


Figure 3.10 — Bit error probability at relay input / output for different relay strategies, fast Rayleigh fading channel, $SNR_{rd} = SNR_{sd}$, $(n_S, k_S, \delta_S) = (64, 51, 6)$, $(n_R, k_R, \delta_R) = (32, 26, 4)$.

more complicated to analyze both the hard-detection and the hard-decoding strategies than the soft-decoding one. At the relay, the soft decoding of the observed source codewords always produces a valid source codeword although it may contain decoding errors, i.e. the error pattern satisfies the source code parity check equations. Thus after the column encoding at the relay (appending relay-generated redundancy to the decoded source data), the resulting codeword associated with the error pattern is also a valid product codeword. This property facilitates the derivation of the whole network error probability based on the maximum-likelihood (ML) criterion. For the other two relay strategies, the detected source codewords at the relay are not always valid ones and there is no clear rule on the Hamming distance between the detection result and the original codewords, which makes the problem more difficult.

In the following, we will evaluate the theoretical error probability for the cooperation scheme using the soft-decoding relay strategy. A similar evaluation is presented in [GiAL10] for a two-source relay cooperative network using turbo-like code. At first, we introduce some notations :

Recall that all sources use the same systematic linear block code (n_S, k_S, δ_S) and the relay uses a systematic linear block code (n_R, k_R, δ_R) . The source code rate is denoted R_S . The destination observes a product codeword of $(n_S, k_S) \times (n_R, k_R)$ whose minimum Hamming distance $\delta_P = \delta_S \delta_R$ and its code rate is denoted R_P . At the destination, we observe a product codeword whose first k_R rows come from the direct source-destination transmission and the last $(n_R - k_R)$ rows correspond to the relay-generated redundancy forwarded by the relay.

At the relay, let \mathbf{C} denote the product codeword associated to the source information messages that would have been received if the relay was error-free. Generally, after the relay soft decoding, there can be decoding errors in the decoded $K = k_R$ source codewords. We denote by \mathbf{E} the corresponding error pattern. Let $\hat{\mathbf{C}}$ denote the product codeword generated at relay, which is associated with the error pattern \mathbf{E} .

Our purpose is to evaluate the network error probability :

$$P_e = \sum_{\mathbf{C}'} \Pr \{ \mathbf{C}' | \mathbf{C} \}, \quad (3.9)$$

where \mathbf{C}' is a valid product codeword of $(n_S, k_S) \times (n_R, k_R)$ which is different from \mathbf{C} . The pair-wise error probability $\Pr \{ \mathbf{C}' | \mathbf{C} \}$ in the above equation can be developed as :

$$\begin{aligned} \Pr \{ \mathbf{C}' | \mathbf{C} \} &= \sum_{\mathbf{E}} \Pr \{ \mathbf{C}', \mathbf{E} | \mathbf{C} \} \\ &= \sum_{\mathbf{E}} \Pr \{ \mathbf{C}' | \mathbf{E}, \mathbf{C} \} \Pr \{ \mathbf{E} | \mathbf{C} \} = \sum_{\mathbf{E}} \Pr \{ \mathbf{C}' | \mathbf{E}, \mathbf{C} \} \Pr \{ \mathbf{E} \} \\ &= \Pr \{ \mathbf{C}' | w_H(\mathbf{E}) = 0, \mathbf{C} \} \cdot \Pr \{ w_H(\mathbf{E}) = 0 \} \\ &\quad + \sum_{\mathbf{E}} \Pr \{ \mathbf{C}' | w_H(\mathbf{E}) \neq 0, \mathbf{C} \} \cdot \Pr \{ w_H(\mathbf{E}) \neq 0 \}, \end{aligned} \quad (3.10)$$

where $w_H(\mathbf{E})$ calculates the Hamming weight of the error pattern \mathbf{E} . In the following, we distinguish two cases depending on whether there are errors in the relay soft

decoding result :

Case 1 : The relay reception is error-free

In the case of soft decoding at the relay, the probability of decoding a source codeword at a Hamming distance d_1 from the transmitted one can be expressed as :

$$P_e^{Row}(d_1) = 0.5 \operatorname{erfc} \left(\sqrt{\frac{R_S d_1 (E_b)_{sr}}{N_0}} \right). \quad (3.11)$$

In the product code matrix at the relay, the first k_R rows correspond to the k_R source codewords. We denote P_e^{Row} the probability that the i -th row is not correctly decoded at the relay where $i = 1, 2, \dots, k_R$. It can be calculated as :

$$P_e^{Row} = \sum_{d_1=\delta_S}^{n_S} A_S(d_1) \cdot P_e^{Row}(d_1) = \sum_{d_1=\delta_S}^{n_S} A_S(d_1) \cdot 0.5 \operatorname{erfc} \left(\sqrt{\frac{R_S d_1 (E_b)_{sr}}{N_0}} \right), \quad (3.12)$$

where $A_S(d_1)$ represents the number of codewords with weight d_1 of the source code (n_S, k_S, δ_S) .

Then the probability that there is no error at the relay is given by :

$$\Pr \{w_H(\mathbf{E}) = 0\} = [1 - P_e^{Row}]^{k_R} \quad (3.13)$$

and according to the union bound of product code, $\Pr \{\mathbf{C}' | \mathbf{E}, \mathbf{C}\}$ can be calculated as :

$$\Pr \{\mathbf{C}' | w_H(\mathbf{E}) = 0, \mathbf{C}\} = 0.5 \operatorname{erfc} \left(\sqrt{\frac{R_P d \cdot E_b}{N_0}} \right), \quad (3.14)$$

where $d = d_H(\mathbf{C}, \mathbf{C}')$ is the Hamming distance between two product codewords \mathbf{C} and \mathbf{C}' .

Case 2 : There are residual soft decoding errors at the relay

We denote the error pattern in the column redundancy part of $\hat{\mathbf{C}}$ as \mathbf{E}^{Col} , which is associated with the error pattern \mathbf{E} in the first k_R rows of the product code matrix at the relay. The couple of $\{\mathbf{E}, \mathbf{E}^{Col}\}$ constitutes the whole error pattern in the product codeword $\hat{\mathbf{C}}$.

We define w as the weight of \mathbf{E}^{Col} and d as the Hamming distance between the product codewords \mathbf{C} and $\hat{\mathbf{C}}$. We have the following relation :

$$d = d_H(\mathbf{C}, \hat{\mathbf{C}}) = w_H(\mathbf{E}) + w_H(\mathbf{E}^{Col}) = w_H(\mathbf{E}) + w. \quad (3.15)$$

Based on the ML decoding principle, we can prove (see Appendix 3.A) that :

$$\Pr \{\hat{\mathbf{C}} | \mathbf{E}, \mathbf{C}\} = \begin{cases} 0.5 \cdot \operatorname{erfc} \left(\sqrt{\frac{(d-2w)^2}{d} \cdot \frac{R_P E_b}{N_0}} \right), & \text{if } d \geq 2w; \\ 1 - 0.5 \cdot \operatorname{erfc} \left(\sqrt{\frac{(d-2w)^2}{d} \cdot \frac{R_P E_b}{N_0}} \right), & \text{if } d < 2w. \end{cases} \quad (3.16)$$

At first, we consider that there is only one erroneous row among the k_R relay decoded source codewords. In general, a message part whose weight is 1 will generate a redundancy part having a weight between $\delta_R - 1$ and $n_R - k_R$. Suppose that we use the extended 1-error correction capacity code as the column code at the relay, i.e., BCH(32, 26, 4) in our example. According to its generator matrix, a column message part whose weight is 1 will generate a redundancy part whose weight is either $\delta_R - 1$ or $\delta_R + 1$. The error pattern \mathbf{E} in the k_R relay decoded source codewords will generate a multiple of $\delta_R - 1$ or $\delta_R + 1$ erroneous bits in the column redundancy part of the product code. Their relation is illustrated in Fig. 3.11.

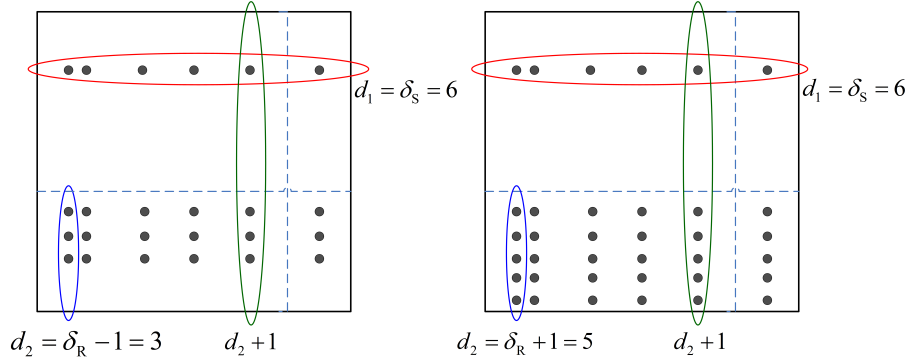


Figure 3.11 — Error pattern in the product codeword given that there is only one erroneous row among the k_R relay decoded source codewords, $(n_S, k_S, \delta_S) = (64, 51, 6)$, $(n_R, k_R, \delta_R) = (32, 26, 4)$.

We can verify that $d = d_1 (d_2 + 1)$, $w = d_1 d_2$ and the condition $d < 2w$ is satisfied in Eq. 3.16.

Combining the above results and substituting Eq. 3.10-3.16 into Eq. 3.9, we can express the network error probability P_e as :

$$\begin{aligned}
 P_e &= \sum_{\mathbf{C}'} \Pr \{ \mathbf{C}' | \mathbf{C} \} \\
 &\approx \sum_{\delta_P \leq d' \leq n_P} [1 - P_e^{Row}]^{k_R} \cdot \frac{A_P(d')}{2} \operatorname{erfc} \left(\sqrt{\frac{R_P d' \cdot E_b}{N_0}} \right) \\
 &+ \sum_{\substack{\delta_S \leq d_1 \leq n_S \\ d_2 = \delta_R - 1, \delta_R + 1}} \left\{ B_R(1, d_2 + 1) \cdot \left[1 - \frac{1}{2} \operatorname{erfc} \left(\sqrt{\frac{[d_1 (d_2 + 1) - 2d_1 d_2]^2}{d_1 (d_2 + 1)} \cdot \frac{R_P E_b}{N_0}} \right) \right] \right. \\
 &\quad \left. \cdot A_S(d_1) P_e^{Row}(d_1) [1 - P_e^{Row}]^{k_R - 1} \right\} \\
 &+ \dots
 \end{aligned} \tag{3.17}$$

where $A_P(d')$ is the number of product codewords that have a weight d' . $B_R(u, v)$ denotes the number of column codewords of weight v given the message part weight u . $B_R(u, v)$ of the BCH (32, 26) code is given in Appendix 3.B. d_1 in the second summation

term denotes the erroneous bits number in the only erroneous source codeword at the relay. d_2 corresponds to the error pattern weight in the column code redundancy part whose value is either $\delta_R - 1$ or $\delta_R + 1$ given that the column code message part has a weight of 1. Here, $[d_1(d_2 + 1)]$ (resp. $d_1 d_2$) corresponds to d (resp. w) in Eq. 3.16.

In Eq. 3.17, the first term corresponds to the product code union bound $\sum_{\delta_P \leq d' \leq N_P} \frac{A_P(d')}{2} \text{erfc} \left(\sqrt{\frac{R_P d' \cdot E_b}{N_0}} \right)$ under the condition of error-free relay. The second term is the error probability when there is only one erroneous row in the relay decoding result. In the high SNR regime, we can only consider $d' = \delta_P$ in the evaluation of product code union bound in the first term, which leads to :

$$\begin{aligned}
P_e &= \sum_{\mathbf{C}'} \Pr \{ \mathbf{C}' | \mathbf{C} \} \\
&\approx [1 - P_e^{Row}]^{k_R} \cdot \frac{A_P(\delta_P)}{2} \text{erfc} \left(\sqrt{\frac{R_P \delta_P \cdot E_b}{N_0}} \right) \\
&\quad + \sum_{\substack{\delta_S \leq d_1 \leq n_S \\ d_2 = \delta_R - 1, \delta_R + 1}} \left\{ B_R(1, d_2 + 1) \cdot \left[1 - \frac{1}{2} \text{erfc} \left(\sqrt{\frac{[d_1(d_2 + 1) - 2d_1 d_2]^2 \cdot R_P E_b}{d_1(d_2 + 1) \cdot N_0}} \right) \right] \right. \\
&\quad \left. \cdot A_S(d_1) P_e^{Row}(d_1) [1 - P_e^{Row}]^{k_R - 1} \right\} \\
&\quad + \dots
\end{aligned} \tag{3.18}$$

After that, we further consider the contribution to the error probability when there are two erroneous rows in the relay decoding result.

In the case that *all error bits in these two erroneous rows belong to different columns of the product codeword matrix*, i.e., non-overlapping error patterns, then the corresponding $\Pr \{ w_H(\mathbf{E}) \neq 0 \} = P_e^{Row}(d_1) P_e^{Row}(d'_1) [1 - P_e^{Row}]^{k_R - 2}$, where d_1 (resp. d'_1) is the error pattern weight of the first (resp. second) erroneous row. We can derive the following additional term in Eq. 3.18 :

$$\begin{aligned}
&\sum_{\substack{\delta_S \leq d_1, d'_1 \leq n_S \\ d_2, d'_2 = \delta_R - 1, \delta_R + 1}} \left\{ B_R(1, d_2 + 1) B_R(1, d'_2 + 1) \right. \\
&\quad \cdot \left[1 - \frac{1}{2} \text{erfc} \left(\sqrt{\frac{[d_1(d_2 + 1) + d'_1(d'_2 + 1) - 2(d_1 d_2 + d'_1 d'_2)]^2 \cdot R_P E_b}{d_1(d_2 + 1) + d'_1(d'_2 + 1) \cdot N_0}} \right) \right] \\
&\quad \left. \cdot A_S(d_1) A_S(d'_1) P_e^{Row}(d_1) P_e^{Row}(d'_1) [1 - P_e^{Row}]^{k_R - 2} \right\}.
\end{aligned} \tag{3.19}$$

In the case that *these two erroneous rows have identical error patterns occupying the same columns of the product codeword matrix*, then $d_1 = d'_1$ and the corresponding $\Pr \{\mathbf{w}_H(\mathbf{E}) \neq 0\} = P_e^{Row}(d_1) \cdot P_e^{Row}(d_1) \frac{1}{A_S(d_1)} \cdot [1 - P_e^{Row}]^{k_R-2}$. We can derive another additional term in Eq. 3.18 :

$$\sum_{\substack{\delta_S \leq d_1 \leq n_S \\ d_2 = \delta_R - 2, \delta_R, \delta_R + 2}} \left\{ B_R(2, d_2 + 2) \cdot \left[1 - \frac{1}{2} \operatorname{erfc} \left(\sqrt{\frac{[d_1(d_2 + 2) - 2d_1d_2]^2}{d_1(d_2 + 2)} \cdot \frac{R_P E_b}{N_0}} \right) \right] \cdot A_S(d_1) [P_e^{Row}(d_1)]^2 [1 - P_e^{Row}]^{k_R-2} \right\}. \quad (3.20)$$

We can verify that the term $[1 - 0.5\operatorname{erfc}(\cdot)]$ can be approximated by 1 in the above equations at high SNRs. Using $B_R(u, v)$ of BCH (32, 26) code given in Appendix 3.B, we can verify that the term in Eq. 3.20 is negligible in front of Eq. 3.19. The expression of P_e is thus reduced to :

$$\begin{aligned} P_e &= \sum_{\mathbf{C}'} \Pr \{\mathbf{C}' | \mathbf{C}\} \\ &\approx [1 - P_e^{Row}]^{k_R} \cdot \frac{A_P(\delta_P)}{2} \operatorname{erfc} \left(\sqrt{\frac{R_P \delta_P \cdot E_b}{N_0}} \right) \\ &\quad + \sum_{\substack{\delta_S \leq d_1 \leq n_S \\ d_2 = \delta_R - 1, \delta_R + 1}} B_R(1, d_2 + 1) \cdot A_S(d_1) P_e^{Row}(d_1) [1 - P_e^{Row}]^{k_R-1} \\ &\quad + \sum_{\substack{\delta_S \leq d_1, d'_1 \leq n_S \\ d_2, d'_2 = \delta_R - 1, \delta_R + 1}} \left\{ B_R(1, d_2 + 1) B_R(1, d'_2 + 1) \cdot A_S(d_1) A_S(d'_1) P_e^{Row}(d_1) P_e^{Row}(d'_1) [1 - P_e^{Row}]^{k_R-2} \right\} \\ &\quad + \dots \end{aligned} \quad (3.21)$$

We can further verify that, in the high SNR regime, the third term (Eq. 3.19) in the above equation becomes negligible if compared with the second term (Eq. 3.18). There are some intermediate situations such that *the only two erroneous rows have some error bits partially overlapping in the column-wise direction of the product codeword matrix*. We can also verify that their values are upper-bounded by Eq. 3.19 and thus negligible in high SNRs, which means that the contribution to the network error probability of two erroneous rows in the relay decoding result is negligible. It goes without saying that for three or more erroneous rows, the contributions are more and more small. So we conclude that **the dominant term in the network error probability P_e is due to the error patterns associated with only one erroneous row in the first k_R**

rows of the product code matrix. We can approximate P_e by :

$$\begin{aligned}
P_e &= \sum_{\mathbf{C}'} \Pr \{ \mathbf{C}' | \mathbf{C} \} \\
&\approx [1 - P_e^{Row}]^{k_R} \cdot \frac{A_P(\delta_P)}{2} \operatorname{erfc} \left(\sqrt{\frac{R_P \delta_P \cdot E_b}{N_0}} \right) \\
&\quad + \sum_{\substack{\delta_S \leq d_1 \leq n_S \\ d_2 = \delta_R - 1, \delta_R + 1}} B_R(1, d_2 + 1) \cdot A_S(d_1) P_e^{Row}(d_1) [1 - P_e^{Row}]^{k_R - 1}.
\end{aligned} \tag{3.22}$$

In Fig. 3.12, we show an example of the relation between the product codewords \mathbf{C} , $\hat{\mathbf{C}}$ and the observation at the destination in the Euclidean space. This relation corresponds to a particular situation in the high SNR regime such that there is only one erroneous row in the relay decoded source codewords. The relay-generated product codeword $\hat{\mathbf{C}}$ has a minimum Hamming distance δ_P to \mathbf{C} . In this case, the turbo decoder has two major competing competitors : \mathbf{C} and $\hat{\mathbf{C}}$ causing a degraded error performance.

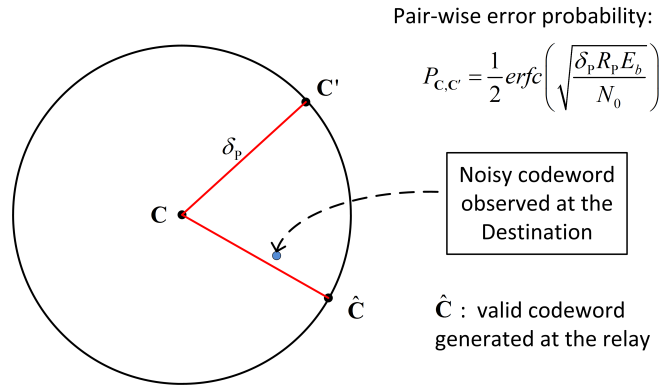


Figure 3.12 — Original / competitor product codewords in the Euclidean space for high SNR

In Eq. 3.22, we use the union bound of the product code $\frac{A_P(\delta_P)}{2} \operatorname{erfc} \left(\sqrt{\frac{R_P \delta_P \cdot E_b}{N_0}} \right)$ to evaluate the network frame error probability when there is no error at the relay. For long product codes, the union bound is asymptotically tight in the high SNR regime and becomes poor at low SNRs. In our example of BCH (64, 51) \times BCH (32, 26) code, the simulated FER of the turbo decoding (64 test patterns in Chase algorithm) and the union bound of product code on the AWGN channel are shown in Fig. 3.13. We can observe the big difference between them at low SNRs. Because we have the turbo product code performance at low SNR, we shall use the simulated FER of the TPC to improve the union bound in Eq. 3.22 for the low SNR region, as shown by the curve ‘Modified error bound’, which is reasonable and more accurate.

In Fig. 3.14 to 3.16, we show the theoretical approximations of the network frame error probability (FEP) with different values of $\Delta SNR = SNR_{sr} - SNR_{sd}$. The theoretical results are obtained using Eq. 3.22. The first term of Eq. 3.22 corresponds to the curve ‘ P_e given no error at relay’ and the second term corresponds to the curve ‘ P_e given one erroneous row at relay’. The curve ‘ P_e approximation’ shows their summation.

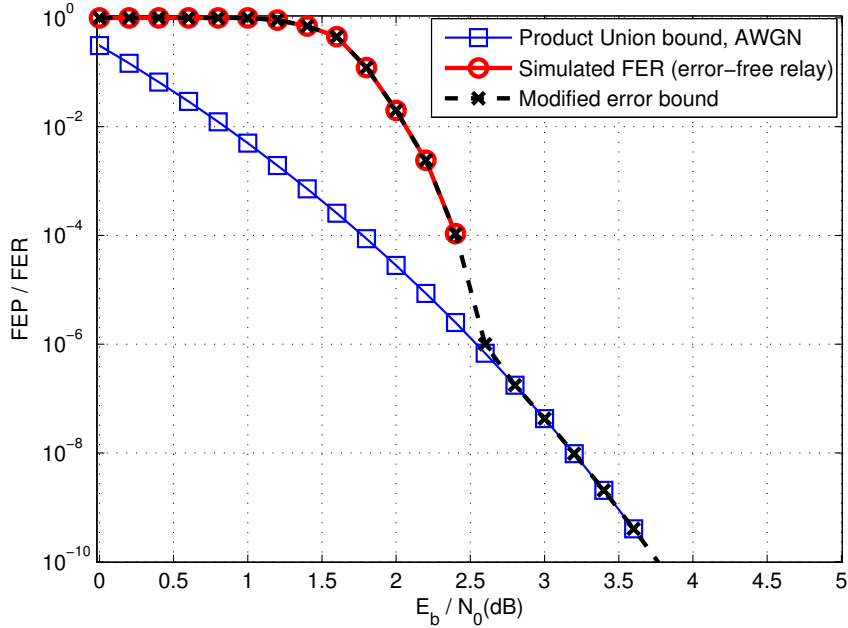


Figure 3.13 — Frame error probability (FEP) bound of BCH product code on the AWGN channel, $(n_S, k_S, \delta_S) = (64, 51, 6)$, $(n_R, k_R, \delta_R) = (32, 26, 4)$; ‘Simulated FER (error-free relay)’ is obtained with turbo decoding using Chase (6) at the destination.

In the cases of $\Delta SNR = 3\text{dB}$ and 4dB (Fig. 3.14 and Fig. 3.15), it is the error event caused by one erroneous row at relay that determines the FEP at high SNRs. In the case of $\Delta SNR = 5\text{dB}$ (Fig. 3.16), the contribution of the error event of one erroneous row at relay is negligible if compared with the error events on the relay-destination link given there is no error at the relay.

In Fig. 3.17, we compare different FEP approximations on the AWGN channel. The FEP approximation associated with an error-free relay is obtained by combining the FER of turbo decoding (using 64 test patterns for Chase algorithm) at low SNRs and the union bound of product code at high SNRs (see Fig. 3.13). **These approximations have been verified by simulations until a FER of about 10^{-4} .** In simulations, we use the Chase soft-decoding algorithm with 64 test patterns (6 least reliable bits) at the relay and at the turbo decoder to establish the theoretical results. In the case of low $\Delta SNR = SNR_{sr} - SNR_{sd}$, the error event caused by one erroneous row at the relay determines the network FEP, which means that the source-relay link is the bottleneck. We can thus use 64 test patterns for the relay soft decoding and only 16 test patterns for the destination turbo decoding to reach the corresponding theoretical FEP bound.

We observe that the FEP improves as we increase the ΔSNR up to $\Delta SNR = 5\text{dB}$. For $\Delta SNR \geq 5\text{dB}$, the corresponding FEP approximation is superposed with FEP approximation associated with an error-free relay. It means that when $\Delta SNR \geq 5\text{dB}$, the residual errors at the relay have a negligible impact on the network FEP in front of the error events on the relay-destination link. An example is already illustrated in Fig 3.16.

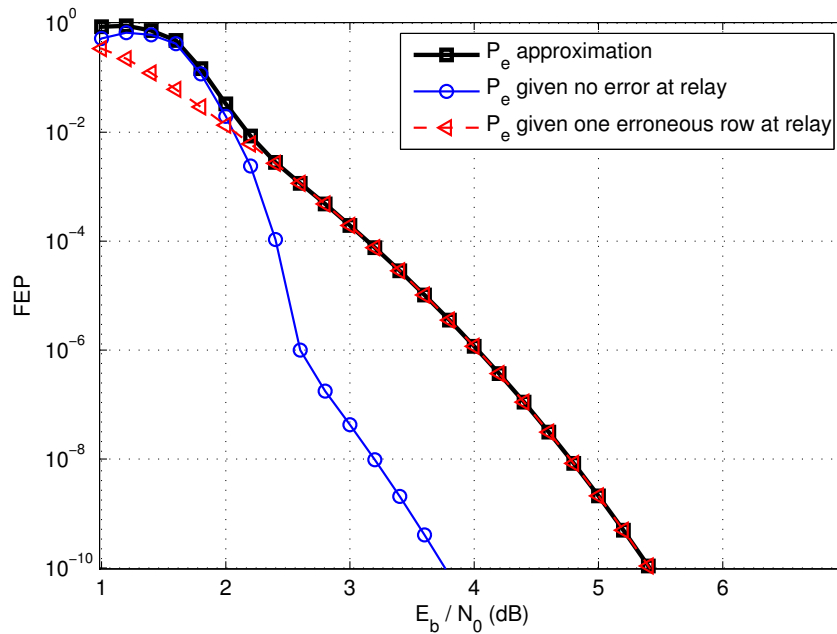


Figure 3.14 — Theoretical network frame error probability (FEP) on the AWGN channel in the case of soft decoding at the relay. $(n_S, k_S, \delta_S) = (64, 51, 6)$, $(n_R, k_R, \delta_R) = (32, 26, 4)$, $SNR_{rd} = SNR_{sd}$, $SNR_{sr} = SNR_{sd} + 3$ dB.

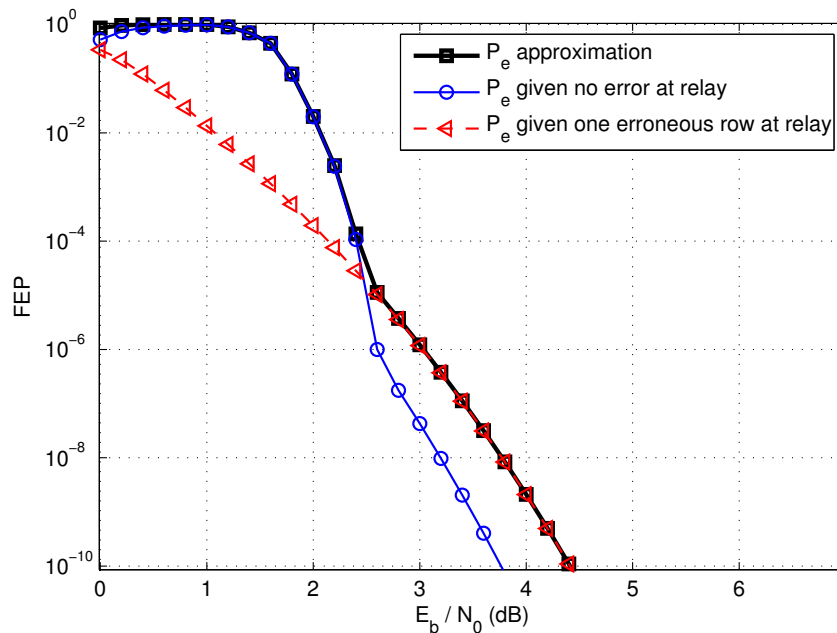


Figure 3.15 — Theoretical network frame error probability (FEP) on the AWGN channel in the case of soft decoding at the relay. $(n_S, k_S, \delta_S) = (64, 51, 6)$, $(n_R, k_R, \delta_R) = (32, 26, 4)$, $SNR_{rd} = SNR_{sd}$, $SNR_{sr} = SNR_{sd} + 4$ dB.

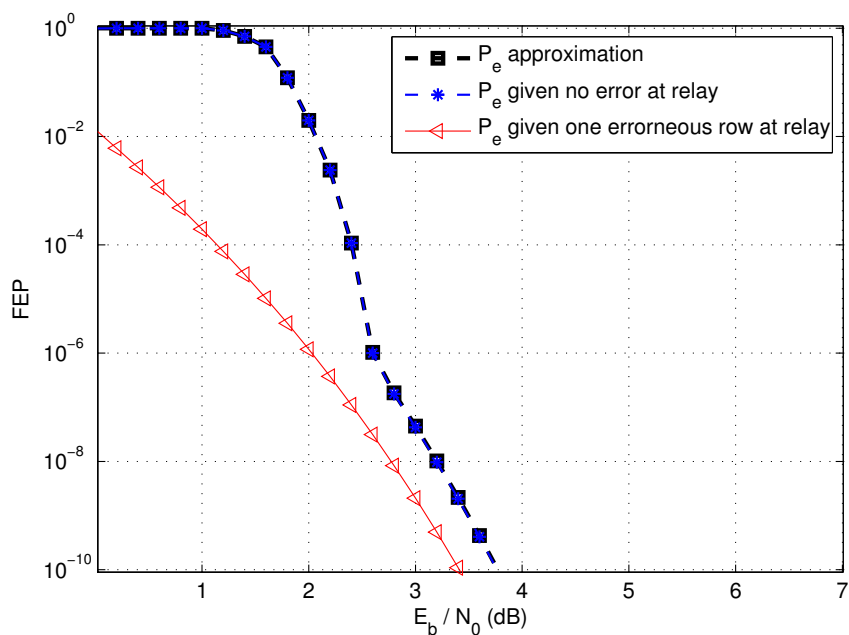


Figure 3.16 — Theoretical network frame error probability (FEP) on the AWGN channel in the case of soft decoding at the relay. $(n_S, k_S, \delta_S) = (64, 51, 6)$, $(n_R, k_R, \delta_R) = (32, 26, 4)$, $SNR_{rd} = SNR_{sd}$, $SNR_{sr} = SNR_{sd} + 5\text{dB}$.

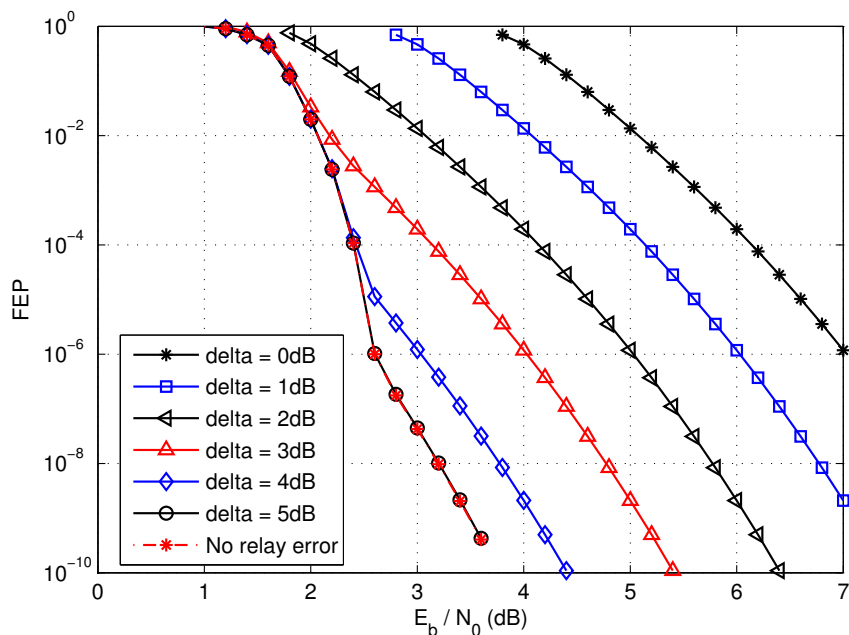


Figure 3.17 — Theoretical network frame error probability on the AWGN channel with the soft decoding at the relay. $(n_S, k_S, \delta_S) = (64, 51, 6)$, $(n_R, k_R, \delta_R) = (32, 26, 4)$, $SNR_{rd} = SNR_{sd}$, $SNR_{sr} = SNR_{sd} + \Delta SNR$.

On the fast Rayleigh fading channel, we show the simulated FER of turbo decoding (64 test patterns in Chase algorithm) and the union bound of product code in Fig. 3.18. Unlike the case on the AWGN channel, there is a big difference between them even at high SNRs considered in the figure. So we have to use the simulated FER associated with an error-free relay instead of the union bound in Eq. 3.20 to establish the theoretical FEP approximation.

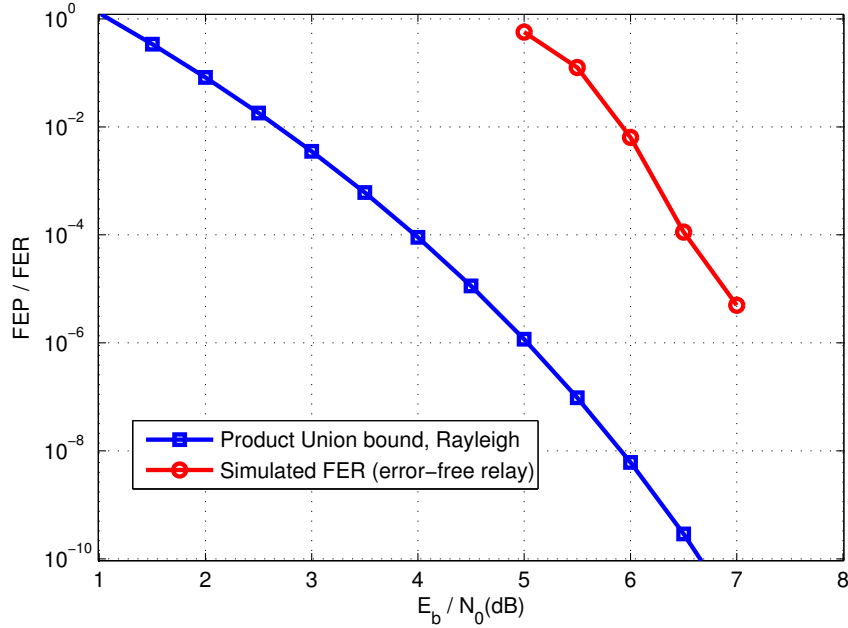


Figure 3.18 — FEP bound of BCH product code on the fast Rayleigh fading channel, $(n_S, k_S, \delta_S) = (64, 51, 6)$, $(n_R, k_R, \delta_R) = (32, 26, 4)$, ‘Simulated FER (error-free relay)’ is obtained with turbo decoding using Chase (6) at the destination.

The FEP approximation on the fast Rayleigh fading channel is given in Fig. 3.19. On the fast Rayleigh fading channel, the source-relay link becomes more vulnerable with the influence of the noise and fading than on the AWGN channel. We use the Chase algorithm with at least 128 test patterns (7 least reliable bits) for the soft decoding at the relay so as to reach the near-optimal ML performance. At the destination, in the proposed simulations, the turbo decoder always uses the 16 test patterns in the Chase algorithm. **The simulated FER curves are superposed with the theoretical results until a $FER = 10^{-4}$.**

As a conclusion, using Eq. 3.22, we can accurately predict the network error performance behavior for any ΔSNR value in the case of soft-decoding at the relay.

If we use a short-length BCH code at the sources, e.g. BCH (64, 51) code, the corresponding soft decoding complexity at the relay is not prohibitive and we can have more reliable transmission on the relay-destination channel in the case of poor SNR_{sr} , which will help the turbo decoding at the destination.

As has been explained for the hard detection / decoding at the relay, the decoded source codewords at the relay are not always valid source codewords. The error probability for the hard detection / decoding at the relay is more complicated to analytically

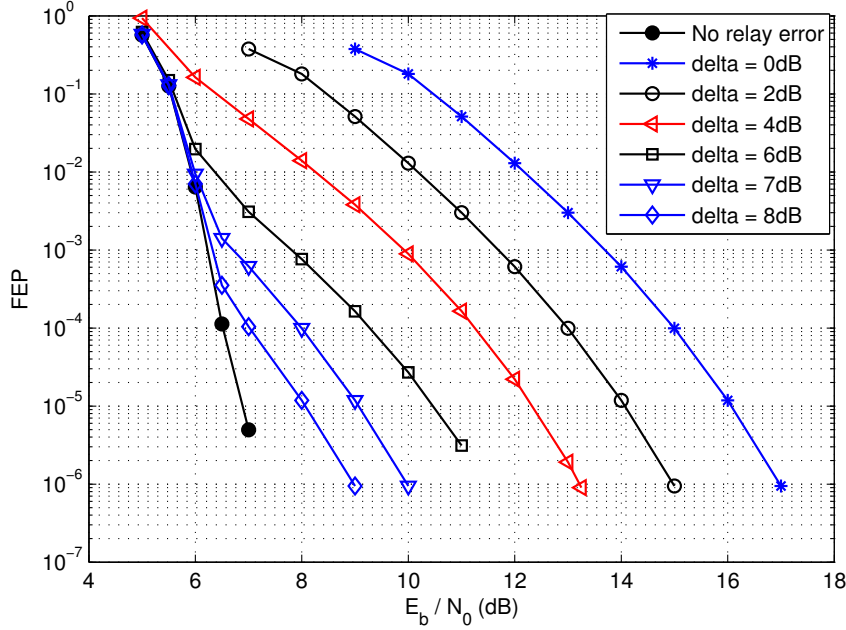


Figure 3.19 — Theoretical network frame error probability on the fast Rayleigh fading channel with the soft decoding at the relay. $(n_S, k_S, \delta_S) = (64, 51, 6)$, $(n_R, k_R, \delta_R) = (32, 26, 4)$, $SNR_{rd} = SNR_{sd}$, $SNR_{sr} = SNR_{sd} + \Delta SNR$.

derive than the one with soft decoding and remains an unsolved problem.

3.3.3 LLR limitation in the turbo decoding

We have proved that with residual errors at the relay, these errors are amplified after the relay encoding. The turbo decoder at the destination should take it into account in order to avoid the performance degradation. In the following, we will introduce a solution [PGA10] based on the limitation of the log-likelihood ratio (LLR) observed on the relay-destination channel.

We denote the i -th row of the product codeword generated at the relay without errors as $\mathbf{c}_i = (c_{i,1}, c_{i,2}, \dots, c_{i,n})$ where $i = 1, 2, \dots, n_R$. We use the antipodal modulation BPSK so $c_{ij} \in \{\pm 1\}$. The observation at the destination is given by :

$$r_{il} = \alpha_{il}\varepsilon_{il}c_{il} + b_{il}, \quad (3.23)$$

where α_{il} is the fading coefficient. b_{il} represents the additive white Gaussian noise (AWGN) with zero mean and variance σ^2 . $\varepsilon_{il} \in \{\pm 1\}$ is a random variable representing the binary error event at the output of the relay encoder with a corresponding bit error probability $\Pr\{\varepsilon_{il} = -1\} = p$, which equals p_{out} given in Eq. 3.7. Here, we suppose the destination has full knowledge of α_{il} , σ^2 and p .

For every transmitted bit c_{il} , the turbo decoder at the destination computes the input LLR as :

$$\lambda_{il} = \ln \frac{\Pr\{c_{il} = +1 | r_{il}, \alpha_{il}\}}{\Pr\{c_{il} = -1 | r_{il}, \alpha_{il}\}}. \quad (3.24)$$

For the source-destination channel, there is no error event at the sources so we have $\varepsilon_{il} = 1$ and $\lambda_{il} = \frac{2\alpha_{il}r_{il}}{\sigma^2}$. For the observations coming from the relay-destination channel, it has been proved in [PGA10] that if the errors at the output of the relay encoder are i.i.d, then :

$$\lambda_{il} = \ln \frac{\Pr \{c_{il} = +1 | r_{il}, \alpha_{il}\}}{\Pr \{c_{il} = -1 | r_{il}, \alpha_{il}\}} = \text{sgn}(r_{il}) \cdot \left[\frac{2\alpha_{il}|r_{il}|}{\sigma^2} + \ln \frac{1 + \frac{p}{1-p} \exp\left(\frac{-2\alpha_{il}|r_{il}|}{\sigma^2}\right)}{1 + \frac{p}{1-p} \exp\left(\frac{2\alpha_{il}|r_{il}|}{\sigma^2}\right)} \right]. \quad (3.25)$$

For large absolute values of the observation r_{il} , the LLR λ_{il} tends to $-\text{sgn}(r_{il}) \times \ln(p/(1-p))$, so we obtain the following approximation :

$$\begin{aligned} \lambda_{il} &\approx \text{sgn}(r_{il}) \times \min \left\{ \frac{2\alpha_{il}|r_{il}|}{\sigma^2}, -\ln\left(\frac{p}{1-p}\right) \right\} \\ &= \text{sgn}(r_{il}) \times \min \left\{ \frac{2\alpha_{il}|r_{il}|}{\sigma^2}, x \right\}, \end{aligned} \quad (3.26)$$

where $x = -\ln\left(\frac{p}{1-p}\right)$ is defined as a **LLR limiter** to be applied on the input LLR value for the observations coming from the relay.

In Fig. 3.20, the LLR λ_{il} given in Eq. 3.25 is plotted with different p on the AWGN channel. The relay-destination SNR is fixed to 3dB. In the figure, we can verify that the LLR is well limited by $-\text{sgn}(r_{il}) \times \ln(p/(1-p))$.

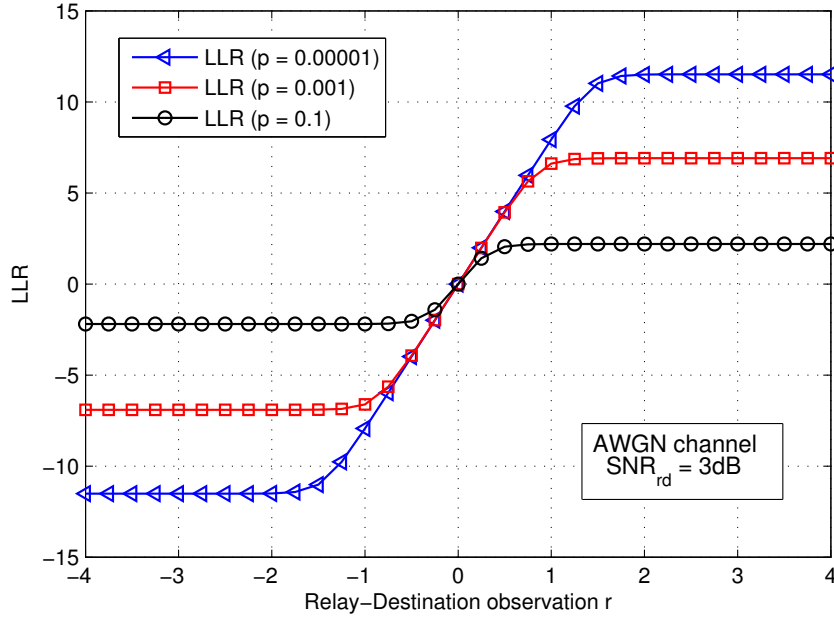


Figure 3.20 — Relay-destination channel output LLR at the input of turbo decoder, AWGN channel with $SNR_{rd} = 3\text{dB}$ [PGA10].

When the source-relay channel is noisy, we can use the LLR limitation combined with the turbo decoding algorithm [Pyn98]. At each iteration of the turbo decoding, a similar LLR limiter y will be applied to the extrinsic information associated with the

relay generated redundancy. The value of y can be optimized experimentally through simulations.

The overall system block diagram is depicted in Fig. 3.21.

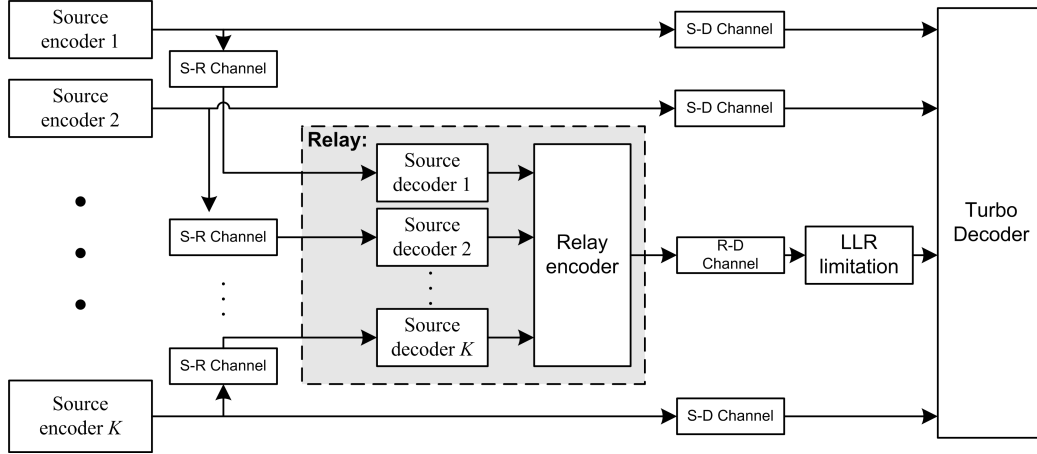


Figure 3.21 — System block diagram

3.3.4 LLR limiter for independent relay errors

In practice, the source-relay channel is not perfect and the relay needs to detect the noisy source codewords. As described previously, we can use three relay detection strategies : the hard detection, the hard decoding and the soft decoding. The error performance and the complexity of the soft decoding depend on the number of test patterns used in the Chase algorithm. In the following, we use 16 test patterns at both the relay (soft-decoding strategy) and the destination (turbo decoding) for simplicity.

We consider the BCH product code scheme of $(n_S, k_S) \times (n_R, k_R) = (64, 51) \times (32, 26)$ as the example. Based on Eq. 3.26, we plot the theoretical values of the LLR limiter $x = -\ln\left(\frac{p}{1-p}\right)$ for the three different relay strategies on the fast Rayleigh fading channel as shown in Fig. 3.22. Using this figure, we can easily find the theoretical LLR limiter value associated with a given $(E_b/N_0)_{sr}$ in the case of independent relay errors.

In the following, we study the optimality of the LLR limiter x defined in Eq. 3.26 when the binary errors are i.i.d. in the relay-generated redundancy.

For this purpose, we suppose that the source codewords are perfectly detected at the relay. After the column-wise relay encoding as shown in Fig. 3.2, we randomly generate i.i.d. errors with a binary error probability $p = 3.5 \times 10^{-2}$ in the relay-generated redundancy part. Then, we evaluate the network error probability through the BER on the Gaussian and the fast Rayleigh fading channels. The results are plotted in Fig. 3.23 and 3.24.

The theoretical value of LLR limiter $x = -\ln\left(\frac{p}{1-p}\right)$ equals 3.3 when $p = 3.5 \times 10^{-2}$. For the limiter y applied to the extrinsic information during the turbo decoding, we set it to a big enough value, 20 in the simulation, in order to focus on the contribution

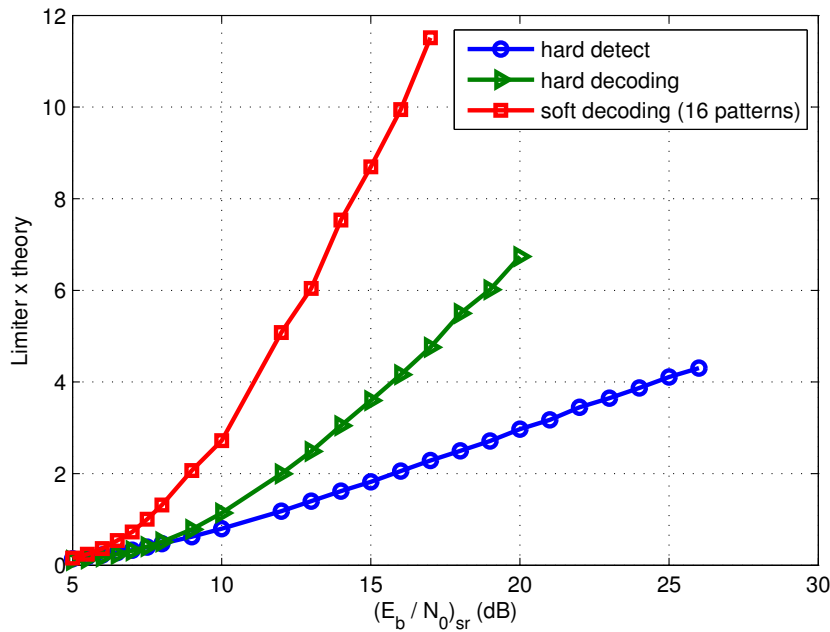


Figure 3.22 — Theoretic LLR-limiter x on the fast Rayleigh fading channel, independent relay errors; $(n_S, k_S, \delta_S) = (64, 51, 6)$, $(n_R, k_R, \delta_R) = (32, 26, 4)$; soft decoding uses 16 test patterns.

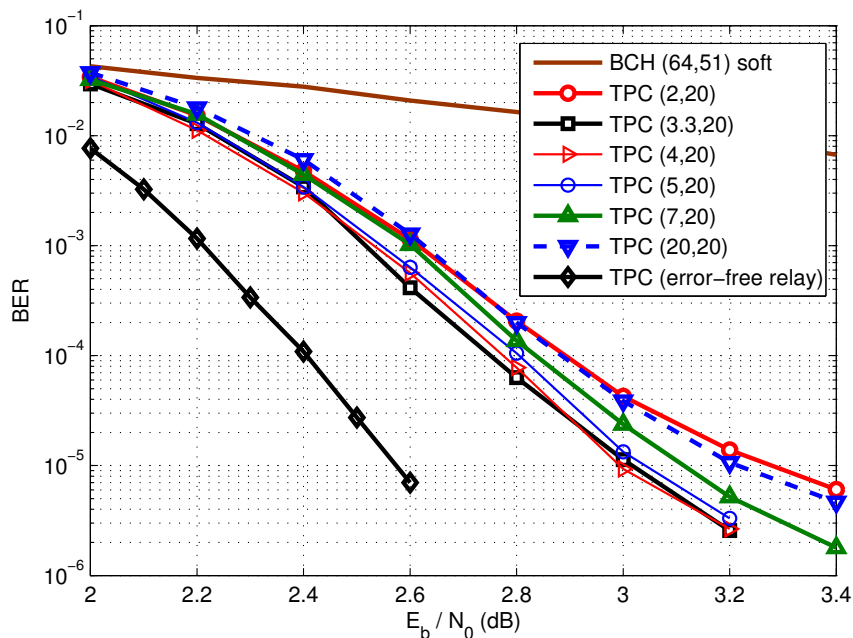


Figure 3.23 — Network BER of single-relay cooperation on the AWGN channel. $(n_S, k_S, \delta_S) = (64, 51, 6)$, $(n_R, k_R, \delta_R) = (32, 26, 4)$; i.i.d. errors at the relay encoder output ($p = 3.5 \times 10^{-2}$); theoretical limiter $x^* \approx 3.3$; TPC (x, y) : x is the limiter on relay-destination channel output LLR; y is the limiter on extrinsic information associated with the relay redundancy, TPC (error-free relay): $(x, y) = (-\infty, +\infty)$.

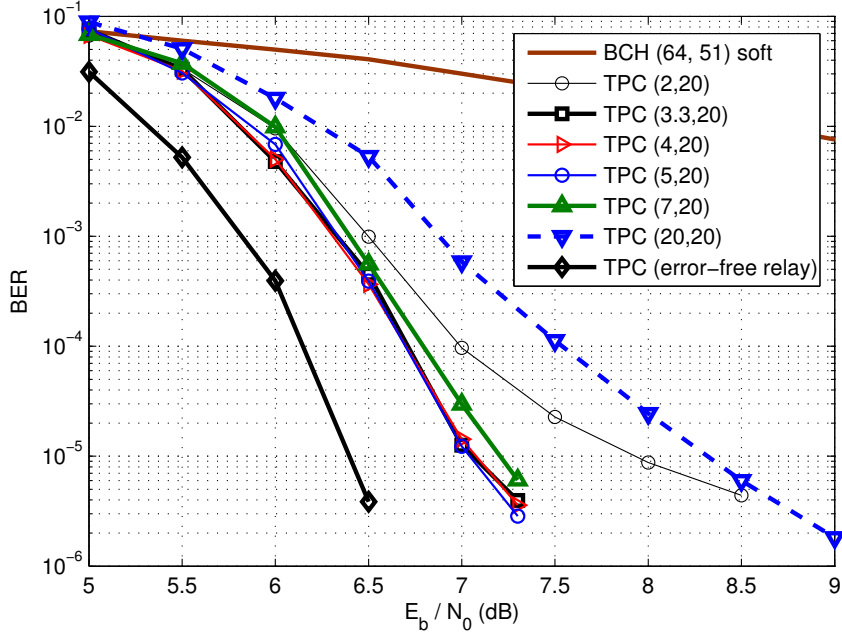


Figure 3.24 — Network BER of single-relay cooperation on the fast Rayleigh fading channel. $(n_S; k_S, \delta_S) = (64, 51, 6)$, $(n_R, k_R, \delta_R) = (32, 26, 4)$; i.i.d. errors at the relay encoder output ($p = 3.5 \times 10^{-2}$); theoretical limiter $x^* \approx 3.3$; TPC (x, y) : x is the limiter on relay-destination channel output LLR; y is the limiter on extrinsic information associated with the relay redundancy, TPC (error-free relay) : $(x, y) = (-\infty, +\infty)$.

of limiter x .

In the above figures, the curve marked with diamonds shows the BER of the perfect relay cooperation ($p = 0$), which is a lower bound of the network BER. The curve with legend ‘BCH (64, 51) soft’ is the soft-decoding BER of the direct transmission of source BCH codewords without relay cooperation. The curves labeled with ‘TPC (x, y) ’ correspond to the relay cooperation BER with the LLR limiters (x, y) in the case of i.i.d. relay errors whose $p = 3.5 \times 10^{-2}$. We can observe that the LLR limiter is quasi-optimal in both channel models because the corresponding BER curve ‘TPC (3.3, 20)’ has the best performance for almost all tested E_b/N_0 values.

3.3.5 Network error performance with different relay detection strategies

In this section, we study the network error performance when the source-relay channel is noisy. The relay uses three different detection strategies to detect the source codewords and the LLR limitation is applied during the turbo decoding. We take the example of BCH product code $(64, 51) \times (32, 26)$.

3.3.5.1 AWGN channel

We first consider the AWGN channel used in [PGA10]. The authors fixed $E_{sr}/N_0 = 6\text{dB}$ where E_{sr} is the average energy per codeword bit received on the source-relay channel. When E_{sr}/N_0 is fixed, SNR_{sr} doesn't change with the increase of SNR_{sd} , which is a pessimist configuration in practice but is considered for illustration purpose. The relay uses the bit-by-bit hard detection to estimate the source codewords, the bit error probability p at relay output, i.e. bit error probability in the relay-generated redundancy, is about 3.5×10^{-2} and the corresponding theoretical limiter x is about 3.3.

In Fig. 3.25 (resp. Fig. 3.26), we plot the BER (resp. FER) versus E_b/N_0 . The curve with diamonds is the BER of the perfect relay cooperation scheme (error-free relay), which serves as a lower bound of the network BER. The continuous curve with circles is the soft-decoding BER of the direct transmission using BCH (64, 51) code without relay cooperation.

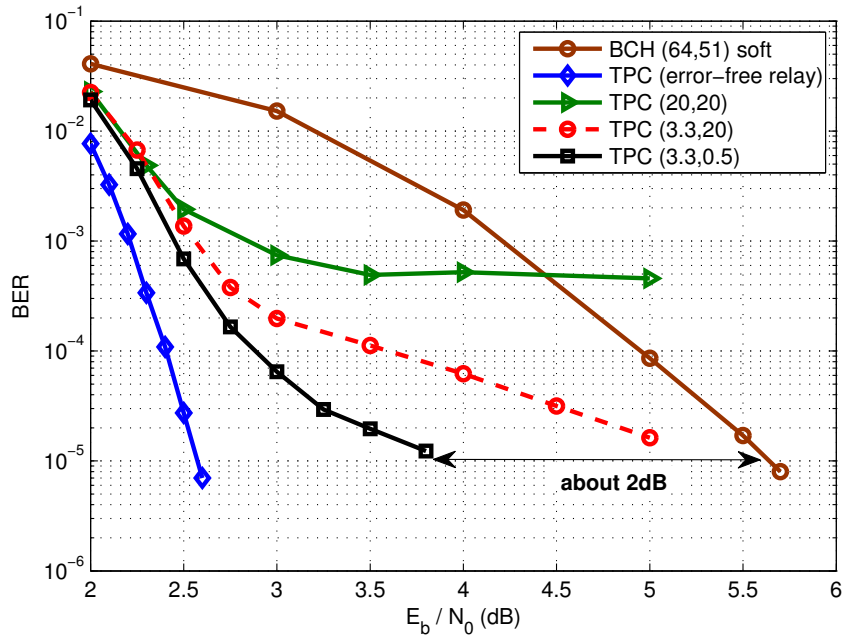


Figure 3.25 — BER of single-relay hard-detection cooperation, AWGN channel;

$$\frac{E_{sr}}{N_0} = 6\text{dB} \quad (n_S; k_S, \delta_S) = (64, 51, 6), \quad (n_R, k_R, \delta_R) = (32, 26, 4);$$

TPC (x, y) : x is the limiter on relay-destination channel output LLR;

y is the limiter on extrinsic information associated with the relay redundancy,

TPC (error-free relay) : $(x, y) = (-\infty, +\infty)$.

The curves labeled ‘TPC (x, y) ’ correspond to the noisy relay cooperation BER with the LLR limiters (x, y) . We can observe that without the LLR limitation, the BER curve with triangles suffers from a severe error floor. This floor can be significantly alleviated by applying the limiter $x = 3.3$ on the input LLRs of the turbo decoder, as shown by the dashed curve. By adding the second limiter $y = 0.5$ on the extrinsic information, the error floor is further reduced and the turbo decoder becomes more robust in the

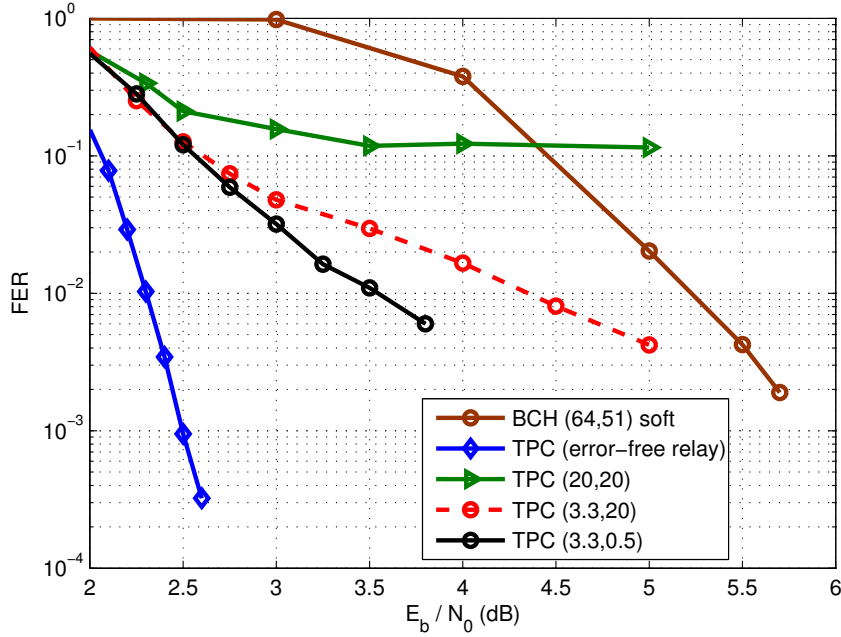


Figure 3.26 — FER of single-relay hard-detection cooperation, AWGN channel;
 $\frac{E_{sr}}{N_0} = 6\text{dB}$ ($n_S; k_S, \delta_S$) = (64, 51, 6), (n_R, k_R, δ_R) = (32, 26, 4);
 TPC (x, y): x is the limiter on relay-destination channel output LLR;
 y is the limiter on extrinsic information associated with the relay redundancy,
 TPC (error-free relay) : (x, y) = $(-\infty, +\infty)$.

presence of relay errors, which corresponds to the curve with squares. This curve offers a coding gain of about 2dB versus the direct transmission of BCH (64, 51) codewords at a BER of 10^{-5} for a relatively high BER at relay output (3.5×10^{-2}). The value of y is obtained through simulations and needs further investigation.

3.3.5.2 Fast Rayleigh fading channel

In the above simulation on the AWGN channel (subsection 3.3.5.1.), we considered the network error performance when the relay hard-detects the source codewords. In this subsection, we will show the results on the fast Rayleigh fading channel with different relay strategies such as the hard detection and hard / soft decoding.

Fig. 3.27 plots the network BER performance versus E_b/N_0 for these three relay strategies on the fast Rayleigh fading channel. To show the influence of relay residual errors, we set $\Delta SNR = SNR_{sr} - SNR_{sd} = 10\text{dB}$ for both the hard-detection and the hard-decoding strategies. For the soft-decoding strategy with very few residual errors when $\Delta SNR = 10\text{dB}$, we reduced ΔSNR to 8dB. Theoretically, the LLR limiter x changes with E_b/N_0 . To simplify the system, we used a predefined average value of x for all E_b/N_0 considered in Fig. 3.27 for each relay strategy, e.g. for the hard detection at the relay, we take $E_b/N_0 = 8\text{dB}$ as a reference, which is a middle value around which the BER exhibits the error floor. According to the corresponding bit error probability p at the relay output, we get the LLR limiter $x = 2.5$ defined in Eq. 3.26.

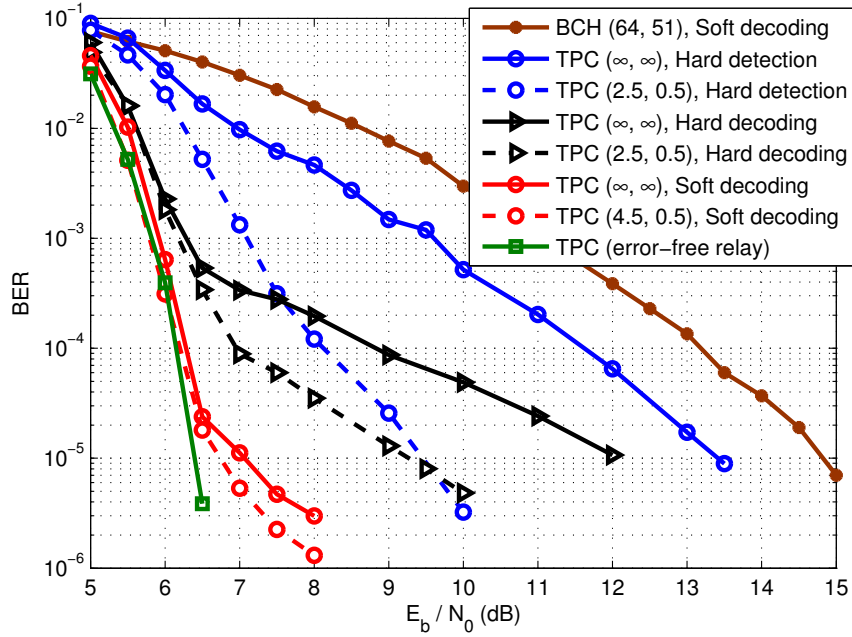


Figure 3.27 — BER of the single-relay cooperation, fast Rayleigh fading channel; $SNR_{sr} = SNR_{sd} + \Delta SNR$, $(n_S; k_S, \delta_S) = (64, 51, 6)$, $(n_R, k_R, \delta_R) = (32, 26, 4)$; TPC (x, y) : x is the limiter on relay-destination channel output LLR; y is the limiter on extrinsic information associated with the relay redundancy, TPC (error-free relay): $(x, y) = (-\infty, +\infty)$.

In Fig. 3.27, the curve with dots is the soft-decoding BER of the direct transmission using BCH (64, 51) code without relay. The curve with squares corresponds to the error-free source-relay channel (no residual error), which is a lower bound for this network BER. Using the perfect relay, the coding gain at $BER = 10^{-5}$ is of about 8.4dB. This gain can be exploited either to extend the transmission range or to reduce the transmission power by a factor of 7 for a path-loss coefficient $\alpha = 3.5$. The other curves correspond to the noisy relay cooperation. The legend indicates the corresponding relay strategy and the average LLR limiter threshold x being used. The limiter y is fixed to 0.5 for all cases. The two curves with circles correspond to the relay hard-detection case. With the LLR limitation, we get an improvement of about 4dB at $BER = 10^{-5}$. We can observe similar improvements for the other two relay strategies in the figure. The error performance of the soft-decoding strategy is the most robust one since it has the smallest number of residual error after the relay decoding.

In the case of independent relay errors as shown in Fig. 3.23 and 3.24, we notice that, there is only a slight error floor for a limiter $y = 20$. Here, we can observe that on both the AWGN and the fast Rayleigh fading channels, even with the LLR limitation on y , the network BER curve still exhibits a much more severe error floor effect than the BER curve associated with the independent relay errors presented in the previous subsection. In fact, for the three different relay detection strategies, the errors propagated to the relay-generated redundancy are correlated and contribute to this error floor. We will investigate it in the next section.

3.3.6 Correlated relay errors and multi-relay cooperation

3.3.6.1 Relay errors correlation

The LLR limitation in Eq. 3.26 considers independent errors at the output of the relay encoder. Actually, the errors generated at the relay output are more or less correlated according to the relay detection strategy. This correlation will influence the efficiency of the LLR limitation, causing the error floor effect as shown in Fig. 3.27. In this subsection, we will investigate the correlation and study a multi-relay solution to reduce the error floor.

In Fig. 3.28, we illustrate the error pattern examples at the relay for the hard-detection strategy (left part) and the soft-decoding strategy (right part). For the hard-detection strategy, the errors (represented by black dots) are independently distributed in the first k_R rows of the relay product encoding matrix. The relay encodes every column using the block code (n_R, k_R) . The relay-generated parity bits are contaminated by the errors at the relay input and these errors will be correlated column-wise since each column corresponds to a column codeword.

For the soft-decoding strategy, the decoded source codewords are valid source codewords even though they may contain errors. In this case the residual errors are correlated in the row direction. After the relay encoding in the column direction and according to the product code property, the residual errors are propagated to the relay redundancy and they are correlated both row-wise and column-wise.

The error pattern in the case of the hard-decoding strategy is more complicated.

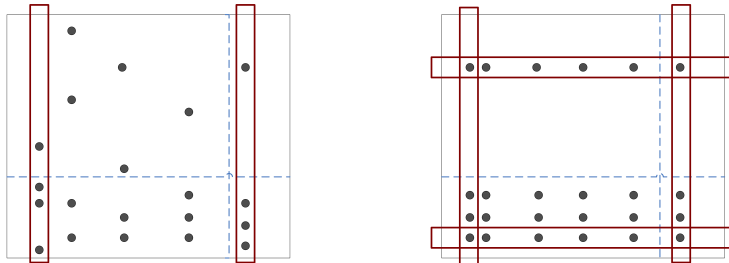


Figure 3.28 — Correlated errors in the case of hard detection and soft decoding at the relay.

The destination observes a binary matrix as shown in Fig. 3.2. The first k_R rows are the codewords coming from the sources and the last $(n_R - k_R)$ rows correspond to the redundancy associated with the correlated errors at the relay output. The turbo decoding at the destination is thus degraded and suffers from the error floor as shown in Fig. 3.27. If we can reduce this correlation, the network error performance should be improved.

3.3.6.2 Error decorrelation using multiple relays

In order to mitigate the influence of the correlated errors in the relay-generated redundancy, we investigate the use of multiple relays.

In Fig. 3.29, we show an example of a two-relay cooperation. Each block in the figure represents the relay-generated redundancy, i.e., the last $(n_R - k_R)$ rows of the observed matrix at the destination. The left block is horizontally divided into two parts and each part corresponds to the data forwarded by one of the relays. By such a *row-wise division*, the column-wise correlation is reduced, which is suitable for the hard-detection relay strategy where there is no row-wise error correlation.

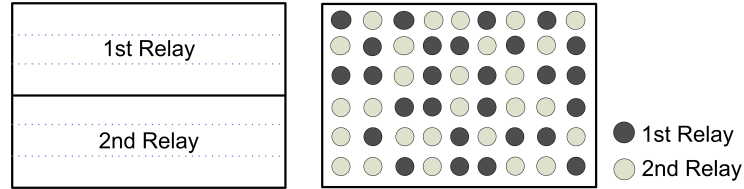


Figure 3.29 — Decorrelation by the row-wise division and the pseudo-random selection of the relay redundancy.

For hard / soft decoding relay strategies, the relay-generated redundancy contains both row-wise and column-wise error correlation. So we propose the *pseudo-random (PR) selection* of the relay redundancy (right block in Fig. 3.29) where every relay redundancy bit observed by the destination comes from either the first relay or the second relay in a pseudo-random manner. This reduces the error correlation in both directions.

Both methods are multi-relay extensible. Contrary to [OCC10], the above two methods allow each relay to forward only a fraction of the whole relay redundancy, so we preserve the turbo decoder complexity and the code rate. If we use more relays, the product codeword observed at the destination will contain less error correlation so that the error floor effect in Fig. 3.25-3.27 can be alleviated. For multi-relay cooperation where there is little error correlation, the LLR limiter threshold given in Eq. 3.26 can be directly applied to all relay strategies and we can easily calculate the error probability at the relay output by using Eq. 3.26 or Fig. 3.22.

The disadvantage of the multi-relay cooperation is the increased complexity and the requirement of additional energy. At each relay, we need to demodulate / re-modulate, decode / re-encode the signals, so the total energy consumption will increase with the number of relays. We should consider this shortcoming in the choice of the cooperation scheme including the number of relays and the relay detection strategy.

3.3.6.3 Performance of turbo Network Coding with multiple relays

In the following, we show the network error performance of the cooperative network according to different relay detection strategies on the fast Rayleigh fading channel.

(a) Hard detection at the relay

In Fig. 3.30, we plot the network BER performance versus E_b/N_0 with the hard detection at the relay(s). We test three cases of $\Delta SNR = SNR_{sr} - SNR_{sd} = 10\text{dB}, 15\text{dB}$ and 25dB . For each case of ΔSNR , we set the LLR limiter $x = 2.5$ and $y = 0.5$ for all E_b/N_0 , which is a simplified configuration for illustration purpose.

For the hard detection strategy at the relay, there is no major benefit in using the pseudo-random selection method since there is no row-wise error correlation. So we only consider the row-wise division decorrelation method for the multi-relay cooperation.

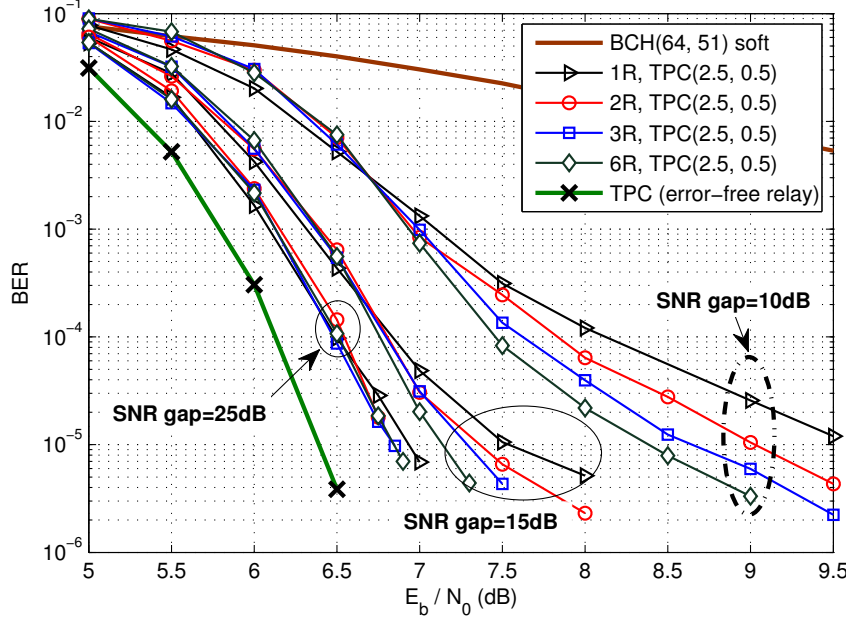


Figure 3.30 — BER performance with the hard detection at the relay(s), row-wise division of the relay redundancy, fast Rayleigh fading channel; $SNR_{sr} = SNR_{sd} + \Delta SNR$, $(n_S, k_S, \delta_S) = (64, 51, 6)$, $(n_R, k_R, \delta_R) = (32, 26, 4)$; TPC (x, y) : x is the limiter on relay-destination channel output LLR; y is the limiter on extrinsic information associated with the relay redundancy, TPC (error-free relay) : $(x, y) = (-\infty, +\infty)$.

The curve marked with ‘ \times ’ corresponds to the case with an error-free relay (without residual decoding errors), which is a lower bound for the BER. The curve labeled ‘BCH (64, 51) soft’ is the soft decoding BER performance of the direct transmission of source codewords without relay cooperation. All the other curves correspond to the noisy relay cooperation combined with the LLR limitation.

Here we can observe the improvements brought by the multi-relay cooperation. For each ΔSNR case, with the increasing number of cooperative relays, the error performance is improved and the error floor effect can be gradually reduced. This improvement is relatively small for a high ΔSNR value, e.g., $\Delta SNR = 25\text{dB}$, which corresponds to a relatively good source-relay channel condition where the number of erroneous bits is very small. There is a gap between the curve of best BER performance of $\Delta SNR = 25\text{dB}$ and that of the error-free relay case. This is mainly caused by the LLR limiter x .

(b) Hard decoding at the relay

In Fig. 3.31, we plot the network BER performance with hard decoding at the relay(s). We consider the cases of $\Delta SNR = 10\text{dB}$. Because there are both row-wise and column-wise error correlations in the relay-generated redundancy, we can use either

the row-wise division or the pseudo-random (PR) selection methods to de-correlate the errors.

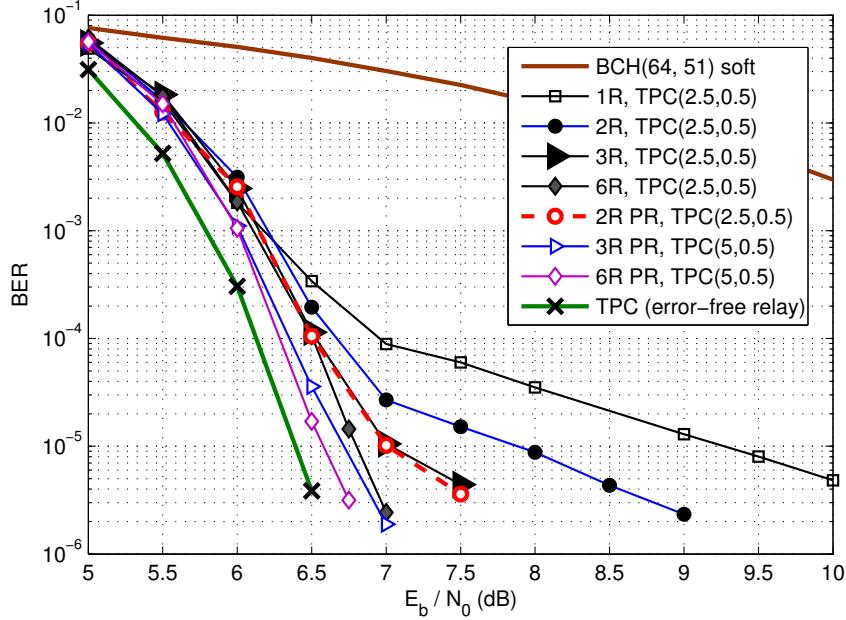


Figure 3.31 — BER performance with the hard decoding at the relay(s), row-wise division / pseudo-random (PR) selection of the relay redundancy, fast Rayleigh fading channel; $\Delta SNR = 10\text{dB}$, $(n_S; k_S, \delta_S) = (64, 51, 6)$, $(n_R, k_R, \delta_R) = (32, 26, 4)$; TPC (x, y) : x is the limiter on relay-destination channel output LLR; y is the limiter on extrinsic information associated with the relay redundancy, TPC (error-free relay) : $(x, y) = (-\infty, +\infty)$.

The curves whose labels including ‘TPC (x, y) ’ correspond to the BER of noisy relay cooperation. In multi-relay case, we indicate the relay number in the curve labels. For the pseudo-random selection case, the abbreviation ‘PR’ is added to the corresponding curve labels.

In the row-wise division case, we set the LLR limiter $x = 2.5$ and $y = 0.5$ for simplification purpose. Here we show the improvements brought by the multi-relay cooperation. The curve with squares is the single-relay case. Using the row-wise division of the relay-generated redundancy, the 2-relays (curve with filled circles), 3-relays (curve with filled triangles) and 6-relays (curve with filled diamonds) cooperation gradually improves the error performance and alleviates the error floor effect. With the pseudo-random selection of the relay redundancy, the performance of 2-relays (curve with hollow circles) outperforms the 3-relays cooperation using the row-wise division.

The difference between the row-wise division scheme and the pseudo-random selection scheme decreases with the number of relays. At a $BER = 1 \times 10^{-5}$, this difference is of about 1dB for 2 relays and it is less than 0.2dB for 6 relays. The 6-relay cooperation offers the near-best BER and the improvement brought by additional relays is negligible.

According to Fig. 3.22, the theoretical LLR limiter x is about 5 in this simulation.

It is the high error correlation in the relay-generated redundancy that turns the optimal value of x to 2.5. With enough cooperative relays (≥ 3) using hard decoding strategy, the error correlation can be reduced and the optimal value of x tends to its theoretical value. As a result, in the case of pseudo-random selection in Fig. 3.31, we have set the limiter values (2.5, 0.5) for the 2-relays cooperation and (5, 0.5) for the 3 or 6-relays cooperation.

(c) Soft decoding at relay

In Fig. 3.32, we plot the network BER performance with soft decoding at the relay(s). We set $\Delta SNR = 4\text{dB}$ for illustration purpose, which corresponds to a relatively unfavorable condition ($d_{sd} \approx 1.3d_{sr}$). In this case, for an $E_b/N_0 = 7\text{dB}$, the BER at relay output is as high as 2×10^{-2} .

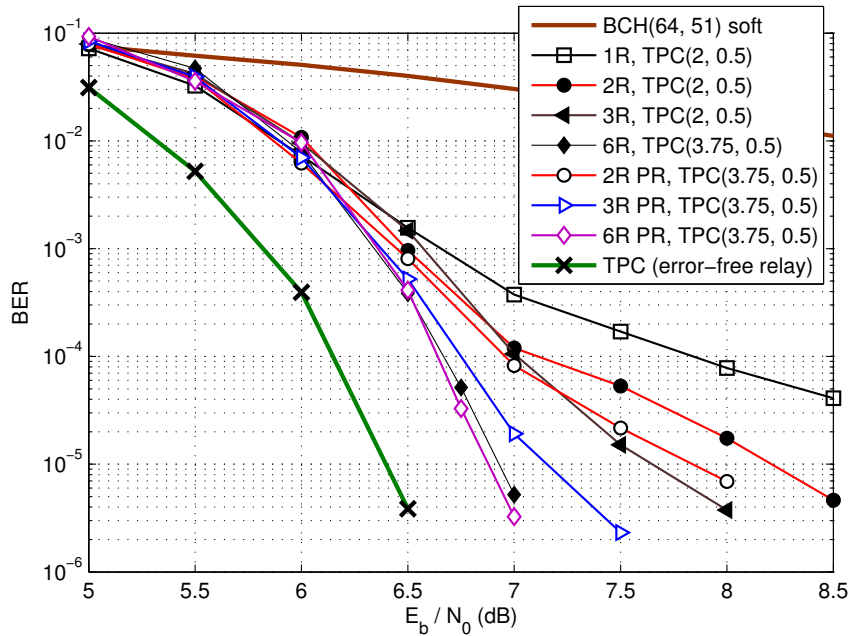


Figure 3.32 — BER performance with the soft decoding at the relay(s), row-wise division / pseudo-random (PR) selection of the relay redundancy, fast Rayleigh fading channel; $\Delta SNR = 4\text{dB}$,

$$(n_S; k_S, \delta_S) = (64, 51, 6), (n_R, k_R, \delta_R) = (32, 26, 4);$$

TPC (x, y) : x is the limiter on relay-destination channel output LLR ;

y is the limiter on extrinsic information associated with the relay redundancy,

TPC (error-free relay) : $(x, y) = (-\infty, +\infty)$.

As for the case of hard decoding at the relay(s), we can observe the improvements brought by the multi-relay cooperation with the soft decoding at the relay(s). The curve with squares is the single-relay case. Using the row-wise division of the relay-generated redundancy, the 2-relays (curve with filled circles), 3-relays (curve with filled triangles) and 6-relays (curve with filled diamonds) cooperation gradually improves the error performance and alleviates the error floor effect. With the pseudo-random selection of the relay redundancy, the 2-relays (curve with hollow circles) cooperation has a performance similar to the 3-relays cooperation using the row-wise division.

The high error correlation in the relay-generated redundancy turns the optimal value of x to 2. With enough cooperative relays (> 3) using soft decoding strategy, the error correlation can be reduced and the optimal value of x tends to its theoretical value 3.75. As a result, we have set the limiter values (2, 0.5) for the 1-3 relays cooperation in the case of row-wise division and (3.75, 0.5) for the rest simulations.

The difference between the row-wise division scheme and the pseudo-random selection scheme decreases with the number of relays. At a $BER = 10^{-5}$, this difference is of about 0.5dB for 2 relays and it is smaller than 0.1dB for 6 relays. The 6-relay cooperation offers the near-best BER and the improvement brought by additional relays is negligible.

There is a difference of about 0.5dB on E_b/N_0 between the near-best performance and the lower bound of error-free relay cooperation. There are two causes. This gap is firstly associated with the LLR limiter value x as we have explained in the case of hard-detection at the relay. Another source of degradation is the low $\Delta SNR = 4dB$. For example, at $E_b/N_0 = 7dB$, we have $(E_b/N_0)_{sr} = (E_b/N_0)_{sd} + \Delta SNR = 11dB$. The corresponding bit error probability at the output of the relay(s) is about 2×10^{-2} . This high error probability further degrades the performance.

3.3.7 Comparison of different cooperation strategies

For most practical applications in WSN, previous work usually considered $d_{sd} \geq 4d_{sr}$ ($\Delta SNR \geq 21dB$). Here we consider $d_{sd} < 4d_{sr}$ in order to establish the lower limit of the ΔSNR operating range. In Fig. 3.33, we compare the network performance for the three relay strategies. The abscissa represents the value of ΔSNR and the ordinate represents the value of E_b/N_0 necessary to reach a network $BER = 10^{-5}$.

The curves with triangles correspond to the hard-detection strategy. The dashed curves correspond to the hard-decoding strategy. The last three curves in the legend correspond to the soft-decoding strategy.

We only consider the row-wise division as the decorrelation method in the multi-relay cooperation using the hard-detection strategy because there is no column-wise error correlation. For the multi-relay cooperation using hard-decoding or soft-decoding strategy, we use the pseudo-random (PR) selection method, which offers better performance than the row-wise division for a given number of relays with a similar complexity.

We can observe three cases in the figure :

When ΔSNR is high enough ($\Delta SNR \geq 20dB$, $d_{sd} \geq 3.8d_{sr}$), the three relay strategies have similar performance. The single-relay cooperation with the hard-detection strategy is the best solution as it exhibits the lowest complexity.

For middle ΔSNR (8dB to 20dB, $1.7d_{sr} \leq d_{sd} < 3.8d_{sr}$), the single-relay scheme with soft decoding and the multi-relay scheme with hard decoding perform almost the same and there is only a minor degradation at $\Delta SNR = 8dB$ for the soft decoding case compared to the near-best performance. The multi-relay scheme implies multiple demodulation / decoding of source codewords (each relay receiver has to demodulate and decode them). The additional complexity compared to the single relay case is much

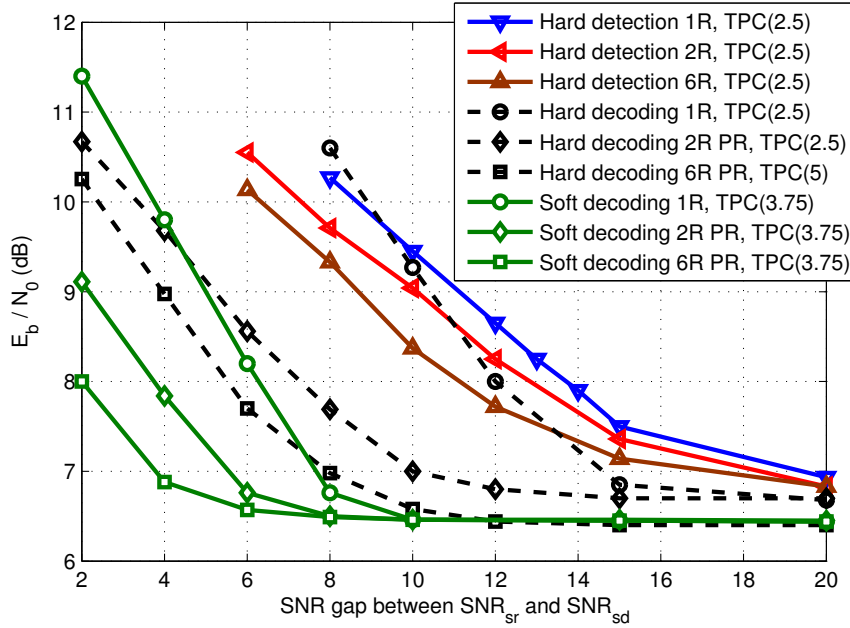


Figure 3.33 — Comparison of different schemes : E_b/N_0 needed for hard detection, hard / soft decoding at relay to reach a $BER = 10^{-5}$, on the fast Rayleigh fading channel ;
 $(n_S; k_S, \delta_S) = (64, 51, 6)$, $(n_R, k_R, \delta_R) = (32, 26, 4)$;
 TPC (x) : x is the limiter on relay-destination channel output LLR ;
 $y = 0.5$ is the limiter on extrinsic information associated with the relay redundancy.

higher than that brought by the soft decoding compared to the hard decoding. We thus recommend to use the single-relay scheme with soft-decoding strategy.

For very low ΔSNR (≤ 8 dB, $d_{sr} < d_{sd} < 1.7d_{sr}$), the multi-relay cooperation with soft decoding outperforms the other schemes. With 6 relays, the gain compared to the single-relay scheme with soft decoding increases as ΔSNR decreases (3.5dB at $\Delta SNR = 2$ dB). A high BER at relay output is the bottleneck of the cooperation scheme. We can reduce it by increasing the test pattern number used in the relay soft decoding Chase algorithm, and thus improve the performance of single-relay solution. If this improvement is not sufficient, we can increase the number of relays with respect to the energy constraints.

From the above analysis, we know that for all practical applications, **the single-relay cooperation using the soft-decoding strategy at the relay exhibits the most satisfying tradeoff** between the network error performance and the energy / complexity constraints.

3.3.8 Conclusions

In Section 3.3, we have studied the impact of relay-generated errors on the performance of the cooperative scheme proposed in [PGA10]. The relay-generated error correlation yields an error floor at the destination. To reduce this phenomenon, we have studied the use of multiple relays. When associated to a pseudo-random selection

of the redundancy sent to the destination, the scheme is efficient, all the more as the correlation degree is high, which is the case of poor source-relay channel conditions. For a fast fading channel with medium to high source-relay channel SNR, the single-relay cooperation scheme achieves the best trade-off between bit error rate and complexity. For very poor source-relay channel conditions, the relay soft-decoding performance can be improved by adding test patterns. If not sufficient, multiple relays can be used with respect to the system requirements. In the multi-relay case, the pseudo-random selection is privileged to the row-wise division for better decorrelation performance under similar complexity.

3.4 Capacity of the cooperative network

In Chapter 2, we have briefly introduced the classical point-to-point channel capacity of the AWGN and the Rayleigh fading channels in the infinite code-length regime.

For the proposed multi-source relay cooperative network, the results previously presented in this chapter show that the source-relay channel is actually the bottleneck of the network. The information loss on the source-relay link is unrecoverable and degrades the turbo decoding at the destination. Because the sources use a short-length channel code, the corresponding error probability is directly linked with the code length.

Contrary to the traditional capacity study of the cooperative network where only the infinite-length channel code is considered, we investigate the cooperative network capacity and take into account the finite length of the channel code on the source-relay link. Our analysis focuses on the optimal code rate associated with a finite code length recently studied in [PPV10].

3.4.1 Achievable rate using short-length FEC codes

In [PPV08, PPV09], Polyanskiy, Poor and Verdú have established an upper bound on the error probability which can be achieved by a code of length n . This bound has been established for the binary symmetric channel (BSC), binary erasure channel (BEC) and continuous-input continuous-output Gaussian channel. In order to simplify the analysis, the authors have also proposed an approximate expression of the bound based on the Gaussian approximation [PPV10]. In their approximation, the achievable channel transmission rate R^* is expressed as a function of the code length n and the channel error probability P_e :

$$R^*(n, P_e) = C - \sqrt{\frac{V}{n}} Q^{-1}(P_e) + \frac{\alpha \log_2 n}{n} + \frac{O(1)}{n}, \quad (3.27)$$

where $Q(x) = \frac{1}{\sqrt{2\pi}} \int_x^{+\infty} e^{-\frac{t^2}{2}} dt$ is the complementary Gaussian cumulative distribution function. The constant $\alpha = 0.5$ when all codewords have the same energy. The capacity C and the channel dispersion factor V depend on the channel model. For the continuous-input and continuous-output Gaussian channel, they are respectively given by :

$$C = C_{\text{shannon}} = 0.5 \log_2(1 + SNR) \text{ bits/channel use}. \quad (3.28)$$

$$V(SNR) = \frac{SNR}{2} \cdot \frac{SNR + 2}{(SNR + 1)^2} (\log_2 e)^2. \quad (3.29)$$

In our study, we are interested in the binary-input continuous-output Gaussian channel but the corresponding parameters C and V have not been addressed yet.

There are two properties that can help us to approximate the channel capacity of the binary-input continuous-output Gaussian channel. Firstly, the transmission rate of the binary-input channel is upper-bounded by that of the continuous-input channel. Secondly, the transmission rate of the binary-input Gaussian channel cannot exceed 1 for the BPSK modulation. By combining these two limitations and Eq. 3.27, we have an upper bound on the rate of the binary-input Gaussian channel in the finite code length regime :

$$R^*(n, P_e) \leq \min \left\{ C - \sqrt{\frac{V}{n}} Q^{-1}(P_e) + \frac{0.5 \log_2 n}{n}, 1 \right\}, \quad (3.30)$$

where the parameters C and V are defined in the continuous-input Gaussian channel as given in Eq. 3.28 and 3.29.

In Fig. 3.34, we plot the different code rates on the Gaussian channel. The capacity of continuous-input AWGN channel C_{shannon} (see Eq. 3.28) corresponds to the dashed curve. The continuous curve ‘Binary input : infinite length’ shows the optimal code rate on the binary-input channel without code length constraint. The curve with circles (resp. with triangles) corresponds to the maximum channel rate of continuous-input Gaussian channel with the finite code length $n = 2048$ (resp. $n = 64$) obtained by Eq. 3.27 with the error probability $P_e = 10^{-6}$.

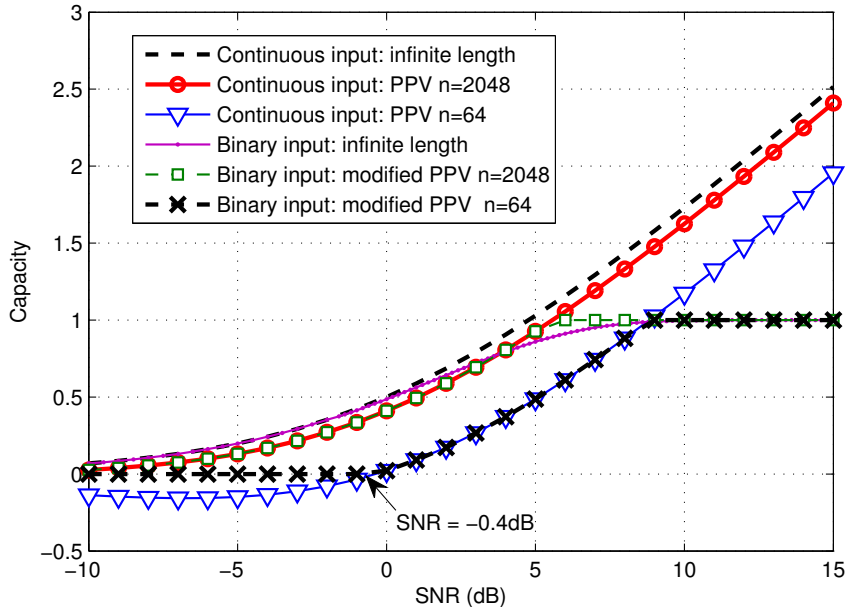


Figure 3.34 — Transmission rate bound of different code lengths, $P_e = 10^{-6}$, Binary / Continuous input Gaussian channel.

The rate approximation of the binary-input channel with code length $n = 64$ corresponds to the curve marked with crosses given by Eq. 3.30. For the code length $n = 64$,

the rate calculated by Eq. 3.30 is negative when $SNR < -0.4\text{dB}$. In this case, we set the corresponding rate to zero, since the rate should be always non-negative.

The BCH product code used in our simulation has a code length of 2048 (64×32). From Fig. 3.34, we can see that its corresponding achievable rate on the binary-input channel (curve with squares) is very similar to the channel rate in the infinite code-length regime (magenta curve with points). In practical simulations of the binary-input channel, we can further elaborate the achievable rate in the finite code-length regime by applying an upper bound corresponding to the capacity of the binary-input AWGN channel without code-length constraint, which can be obtained through numerical integrations.

The achievable rate with a code length of $n_S = 64$ is important in our study because it corresponds to the BCH (64, 51) code used at the sources. Different to the destination where the whole product code ($n_P = 2048$) can be constructed with the joint efforts of the sources and the relay, the relay observes only the short-length source code ($n_S = 64$). In Fig. 3.34, we can see the large gap between the rate bound of $n_S = 64$ and that of an infinite length code. So for the proposed cooperative WSN scheme, the traditional capacity analysis using the infinite-length rate bound on the source-relay link is too optimistic and not precise in practice. In the following, we give an example applying the rate bound for $n_S = 64$ in the evaluation of the cooperative network capacity.

3.4.2 Min-cut max-flow theorem and relay channel capacity bounds

In this subsection, we will first introduce the important min-cut max-flow theorem and the capacity bounds of the relay channel, especially for the relay network working in the time-division duplex (TDD) mode.

3.4.2.1 Min-cut max-flow theorem

The min-cut max-flow theorem was established by Ford-Fulkerson [FF56] and Elias-Feinstein-Shannon [EFS56] independently in 1956. It is the most fundamental theoretical tool to analyze the capacity of the cooperative network.

Theorem Min-cut max-flow theorem [FF56,EFS56] : the maximum possible flow, e.g., the transmission rate, from a source to a sink through a given network, is equal to the minimum capacity among all simple cut-sets.

The network mentioned in the theorem can be modeled as a directed graph with nodes and directed edges. Each edge has a limited transmission capacity. A *cut-set* of a two-terminal network is a set of edges such that when deleted from the network, the network falls into two or more unconnected parts with the two terminals in different parts. The *simple cut-set* is a cut-set satisfying that if any edge is removed from the set, it is no longer a cut-set.

3.4.2.2 Relay channel capacity bounds

The analytical relay network capacity is difficult to establish and still remains an unsolved problem. Based on the min-cut max-flow theorem, researchers have derived important and useful capacity bounds for basic relay networks. The capacity of the proposed multi-source cooperative network is an extension of these capacity bounds. Let us start with the simplest relay network containing only one source, one relay and a single destination as shown in Fig. 3.35.

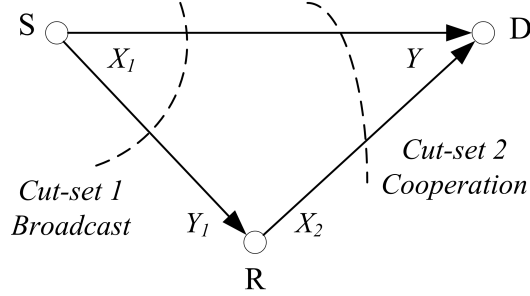


Figure 3.35 — 1-1-1 relay network.

We denote this network as the 1-1-1 relay network, where the three numbers indicate respectively the number of source, relay and destination nodes. The capacity of the 1-1-1 relay network was first studied by Cover and El. Gamal in [CG79, Theorem 4] where an upper bound can be found :

$$C^+ = \sup_{p(x_1, x_2)} \min \{I(X_1; Y, Y_1 | X_2), I(X_1, X_2; Y)\}, \quad (3.31)$$

where $I(X; Y)$ represents the average mutual information between the channel input X and the corresponding channel output Y . The first term (resp. second term) enclosed in the braces corresponds to the capacity of cut-set Broadcast (resp. cut-set Cooperation) in Fig. 3.35.

The authors in [CG79] also investigated the capacity of the degraded relay channel. Here ‘degraded’ means that $p(y | x_1, x_2, y_1) = p(y | x_2, y_1)$, i.e., $X_1 \rightarrow (X_2, Y_1) \rightarrow Y$ forms a Markov chain, so we have $I(X_1; Y, Y_1 | X_2) = I(X_1; Y_1 | X_2)$. The corresponding network capacity is given by [CG79, Theorem 1] :

$$C = \sup_{p(x_1, x_2)} \min \{I(X_1; Y_1 | X_2), I(X_1, X_2; Y)\}. \quad (3.32)$$

3.4.2.3 TDD relay channel capacity bounds

In many practical relay networks, the relay usually transmits and receives on the same frequency band using the time-division duplex (TDD) mode. This mode constrains the relay not to transmit and receive at the same time. TDD is widely used because it only needs cheap relay nodes without the expensive designs such as precise synchronization or refined antenna. The multi-source relay cooperative scheme studied in this chapter also considers the TDD mode.

With this background, the relay channel capacity bounds described in the last subsection are further elaborated in [KSA03a, KSA03b] for the TDD mode. In the following, we will first introduce the basic capacity bounds of the 1-1-1 and the 2-1-1 relay network and then extend the results to the multi-source relay cooperative scheme which corresponds to an M -1-1 network setup.

(1) 1-1-1 TDD relay network capacity

Using the TDD mode, the network transmission in Fig. 3.35 is divided into two time slots. In the first slot (broadcast), the source transmits information to both the relay and the destination. In the second slot (cooperation), the relay forwards the information. There are two cases depending on whether the source remains silent during the relay transmission. The multiple-access situation will be introduced in Chapter 4. Here, we assume that the source remains silent in the second time slot, so there is no multiple-access issue.

It has been proved in [KSA03b, Theorem 2] that any network rate smaller or equal to the capacity C in Eq. 3.32 is achievable whether the TDD relay channel is degraded or not. So we can take Eq. 3.32 as a lower bound on the capacity of the general 1-1-1 TDD relay channel :

$$C_{TDD}^- = \sup_{p(x_1, x_2)} \min \{I(X_1; Y_1 | X_2), I(X_1, X_2; Y)\}. \quad (3.33)$$

Let the whole network transmission time be normalized to 1. During the first time slot, the relay remains silent and we denote this time duration as θ , which is a normalized time allocation factor between 0 and 1. The second time slot has a duration of $1 - \theta$. Based on Eq. 3.31 and Eq. 3.33, we obtain the following upper and lower bounds :

$$\begin{aligned} C_{TDD}^+ &= \sup_{p(x_1, x_2)} \min \{ \theta I(X_1; Y, Y_1 | X_2 = 0, slot_1) + (1 - \theta) I(X_1 = 0; Y | X_2, slot_2), \\ &\quad \theta I(X_1, X_2 = 0; Y | slot_1) + (1 - \theta) I(X_1 = 0, X_2; Y | slot_2) \} \\ &= \sup_{p(x_1, x_2)} \min \{ \theta I(X_1; Y, Y_1 | slot_1), \theta I(X_1; Y | slot_1) + (1 - \theta) I(X_2; Y | slot_2) \}. \end{aligned} \quad (3.34)$$

$$C_{TDD}^- = \sup_{p(x_1, x_2)} \min \{ \theta I(X_1; Y_1 | slot_1), \theta I(X_1; Y | slot_1) + (1 - \theta) I(X_2; Y | slot_2) \}. \quad (3.35)$$

The detailed demonstration of the above bounds can be found in [HMZ05, Appendix A] and [CT06, Theorem 15.10.1].

(2) 2-1-1 TDD relay network capacity

The 2-1-1 relay network using TDD mode is illustrated in Fig. 3.36. The whole transmission time is divided into three time slots. The two sources transmit separately during the first two slots while the relay remains silent. The relay forwards information during the last time slot while the sources remain silent.

We suppose the source S_i ($i = 1, 2$) sends k_i information bits using the code of length n_i . The relay decodes the source information, generates N_r redundancy

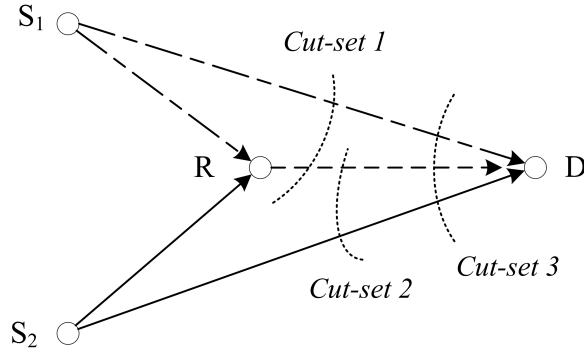


Figure 3.36 — 1-1-1 relay network.

bits and forwards them to the destination. The transmission rate of the i -th source is defined as $R_i = k_i/(n_1 + n_2 + N_r)$ and the network transmission rate $R = R_1 + R_2 = (k_1 + k_2)/(n_1 + n_2 + N_r)$. The time allocation factors are defined as $\theta_i = n_i/(n_1 + n_2 + N_r)$ for the i -th source and $\theta_r = N_r/(n_1 + n_2 + N_r)$ for the relay. The achievable rate of this network has been studied in [KSA03a, Hau08, YGiA10].

In [KSA03a], the authors consider a more general multi-terminal network of senders and receivers. The nodes in the network can shift their roles of sender or receiver as a function of time. The partition of the nodes into sets of sender / receiver is defined as the network state. The following theorem of the achievable transmission rate has been proved by [KSA03a, Theorem 2] :

Theorem [KSA03a, Theorem 2] Consider a general network with finite states, M , for which the sequence m_k of the states of the network is fixed and known to all nodes. For any cut-set which partitions all the network nodes into two disjoint sets S and S^c , if the information rates $\{R^{(ij)}\}$ (the rate at which the node i transmits information to node j) are achievable then there exist some joint probability distribution $p(x^{(1)}, x^{(2)}, \dots, x^{(N)} | m)$ such that the sum rate of information transfer from a node set S_1 (contains node i) to a disjoint node set S_2 (contains node j), $S_1, S_2 \subset \{1, 2, \dots, N\}$, is bounded by :

$$\sum_{i \in S_1, j \in S_2} R^{(ij)} \leq \min_S \sum_{m=1}^M t_m I(X_{(m)}^S; Y_{(m)}^{S^c} | X_{(m)}^{S^c}) \quad (3.36)$$

where the minimization is taken over all node set $S \subset \{1, 2, \dots, N\}$ subject to $S \cap S_1 = S_1$ and $S \cap S_2 = \phi$. t_m is defined as the portion of the time that network has been used in the state m .

The TDD relay network studied here can be treated as a special case of the above theorem such that the network state sequence is predefined and fixed for all network transmission use, e.g. in the 2-1-1 network, the network state sequence has three network states corresponding to the three time slots. t_m corresponds to the time allocation factor linked to the different time slots.

Besides the above theorem, there is an alternative approach as introduced in [Hau08] which renders similar result. For the 2-1-1 relay network, [Hau08, Chapter 6] listed the

following bounds :

$$\begin{aligned}
k_1 &\leq n_1 C(SNR_{s_1r}) \\
k_2 &\leq n_2 C(SNR_{s_2r}) \\
k_1 &\leq n_1 C(SNR_{s_1d}) + N_r C(SNR_{rd}) \\
k_2 &\leq n_2 C(SNR_{s_2d}) + N_r C(SNR_{rd}) \\
k_1 + k_2 &\leq n_1 C(SNR_{s_1d}) + n_2 C(SNR_{s_2d}) + N_r C(SNR_{rd})
\end{aligned} \tag{3.37}$$

The first two inequalities correspond to the rate constraint of the point-to-point transmission on the source-relay channel ensuring the relay decoding. The last three inequalities correspond respectively to the cut-set 1 to 3 in Fig. 3.36. The detailed derivation is given in [Hau08, Appendix A2].

We consider the case where both sources use the same code (n_S, k_S) and transmit in turns during equal-duration time slots $(\theta_1 = \theta_2)$. Suppose the relay (resp. the destination) is located at the same distance to each source and $SNR_{rd} = SNR_{sd}$, we get the following achievable rate for each source by dividing the inequalities in Eq. 3.37 by $2n_S + N_r$:

$$R_i \leq \min \left\{ \theta_i C(SNR_{sr}), \theta_i C(SNR_{sd}) + \theta_r C(SNR_{sd}), \theta_i C(SNR_{sd}) + \frac{\theta_r}{2} C(SNR_{sd}) \right\} \tag{3.38}$$

The network transmission rate (sum-rate of all sources) becomes :

$$R = 2R_i \leq \min \{ 2\theta_i C(SNR_{sr}), 2(\theta_i + \theta_r) C(SNR_{sd}), 2\theta_i C(SNR_{sd}) + \theta_r C(SNR_{sd}) \} \tag{3.39}$$

The result in Eq. 3.39 can also be obtained by applying directly Eq. 3.36, i.e., [KSA03a, Theorem 2], so both approaches confirm each other.

3.4.3 Achievable rate of the multi-source relay cooperative scheme

In the previous subsections, we have introduced the indispensable analytic tools to evaluate the achievable rate of the proposed multi-source relay cooperative network. These tools enable us to compute :

1. The point-to point achievable rate in the finite code-length regime (subsection 3.4.2.2).
2. Capacity bounds of the basic TDD relay cooperative network (subsection 3.4.2.3).

The proposed cooperative network corresponds to an M -1-1 TDD relay network setup. In this section, we investigate the achievable rate of this network where the channel code on the source-relay channel is subject to the code-length constraint.

3.4.3.1 Time allocation factor and network transmission rate

In the proposed cooperative scheme based on turbo product code, $K = k_R$ sources transmit data to the same destination with the help of one relay. The network uses

TDD mode and the relay is half-duplex. Each source uses the same block code (n_S, k_S) . The relay uses the block code (n_R, k_R) . The product code (n_P, k_P) is constructed in a distributed manner at the destination.

To simplify the analysis, we assume that the relay processes the detected source codewords symbol by symbol. The cooperation consists in applying the relay encoding to source symbols corresponding to the same position in their respective original source codewords. For every $K = k_R$ source symbols, the relay generates $r_R = n_R - k_R$ redundancy symbols, which is illustrated in Fig. 3.37.

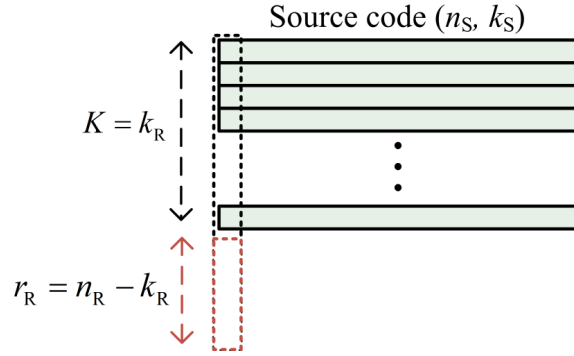


Figure 3.37 — Symbol-by symbol network encoding at the relay.

We define the *time allocation factor* $\theta_i = n_S/n_P$ for each source and $\theta_r = 1 - k_R\theta_i = r_R/n_R$ for the relay. We can verify that $\theta_r/\theta_i = r_R$. We define $R_i = k_S/n_P$ as the transmission rate for each source and $R_{sys} = k_R R_i$ as the **network transmission rate**.

Similar to [YGIA10] and following the same approach to obtain Eq. 3.39, we derive the network transmission rate of the M -1-1 relay network :

$$\begin{aligned}
 R_{sys} &= k_R R_i \\
 &= \min_{m=1,2,\dots,k_R} \left\{ k_R \theta_i \cdot C_{n_S} (SNR_{sr}), \right. \\
 &\quad \left. k_R \theta_i \cdot C_{(m+r_R) \cdot n_S} (SNR_{sd}) + \frac{k_R}{m} \theta_r \cdot C_{(m+r_R) \cdot n_S} (SNR_{rd}) \right\} \\
 &= \min_{m=1,2,\dots,k_R} \left\{ \frac{k_R}{k_R + r_R} \cdot C_{n_S} (SNR_{sr}), \right. \\
 &\quad \left. \frac{k_R}{k_R + r_R} \cdot C_{(m+r_R) \cdot n_S} (SNR_{sd}) + \frac{k_R}{m} \cdot \frac{r_R}{k_R + r_R} \cdot C_{(m+r_R) \cdot n_S} (SNR_{rd}) \right\}, \tag{3.40}
 \end{aligned}$$

where $m = 1, 2, \dots, k_R$ and C_n denotes the capacity (transmission rate) of the binary-input Gaussian channel with finite code length n , which can be evaluated by Eq. 3.30.

In Eq. 3.40, the first term corresponds to the broadcast cut-set as illustrated in Fig. 3.35. For this cut-set, the relay observes codewords of length n_S and the corresponding rate is C_{n_S} .

The second term in the minimization corresponds to the *cut-set isolating m sources and the relay from the rest of network*. In such a cut-set, the m sources broadcast $m \cdot n_S$ bits and the relay forwards $r_R \cdot n_S$ bits. The destination can thus obtain a codeword of length $(m + r_R) \cdot n_S$, so we use $C_{(m+r_R) \cdot n_S}$ to evaluate the corresponding transmission rate.

3.4.3.2 Evaluation of network transmission rate

In the following, we assume that $SNR_{rd} = SNR_{sd}$ and take an example with $K = k_R = 26$ and $n_S = 64$. These values are fixed here just for illustration purpose and can be changed in different network setup. According to Eq. 3.40, the network transmission rate R_{sys} is a function of parameters (r_R, SNR_{sd}) .

In Fig. 3.38, we set $\Delta SNR = SNR_{sr} - SNR_{sd} = 0$ dB and calculate the network rate for different number of relay-generated redundancy bits ($r_R = 0, 1, 3, 6, 10$ and 100). In the case of $r_R = 0$, the relay does not forward information and it corresponds to the non-cooperation case. We can find that the network rates using relay cooperation ($r_R \geq 1$) are smaller than in the case of non-cooperation ($r_R = 0$). So, there is no benefit in cooperation to increase the network rate when $\Delta SNR = 0$ dB. Besides that, in the case of relay cooperation ($r_R \geq 1$), the network rate is limited at high SNR_{sd} values by the relay code rate $R_R = k_R / (k_R + r_R)$. This value can be obtained through the minimization in Eq. 3.40 when the binary-input channel capacity approaches 1 in the high SNR region.

At low SNRs, the network rate is negative due to the rate approximation error of the length- n_S code on the binary-input / continuous-output Gaussian channel as shown in Fig. 3.34. Similar to Fig. 3.34, we set the negative network rate to zero if there is negative term in Eq. 3.40. We could ameliorate the result in this region with a more accurate approximation for the achievable rate of short-length code.

In Fig. 3.39, we set $\Delta SNR = 1$ dB and calculate the network transmission rates associated with different r_R values. Similarly, we can verify that the network rate is limited by the relay code rate R_R at high SNR_{sd} values. Different to the scenario of $\Delta SNR = 0$ dB (see Fig. 3.38), the relay cooperation ($r_R \geq 1$) outperforms the performance of the non-cooperation case ($r_R = 0$) when -1.4 dB $\leq SNR_{sd} \leq 8.5$ dB.

In Fig. 3.40, we increase ΔSNR to 6dB and calculate the network rates for $r_R = 0, 1, 3, 6, 10, 20, 50$ and 100 . At middle SNR_{sd} values, the network transmission rate is largely improved with relay cooperation ($r_R \geq 1$) versus the non-cooperation case ($r_R = 0$, blue curve with hollow circles). The cooperation with $r_R = 1$ (dashed black curve) has the near best performance for $SNR_{sd} > 4$ dB but degrades at low SNR_{sd} . $r_R = 1$ corresponds to a parity-check code applied at the relay, which is efficient at high SNRs (for its high code rate) but performs poorly in low SNR region (for its small Hamming distance). The cooperation with $r_R = 3, 6$ and 10 offers similar optimal network rates for -6.4 dB $\leq SNR_{sd} \leq 3.5$ dB and exhibits some degradation at high SNRs caused by the relay code rate limitation. If we continue to increase r_R , the network rate will degrade for all SNR values because the column code rate limitation becomes dominant.

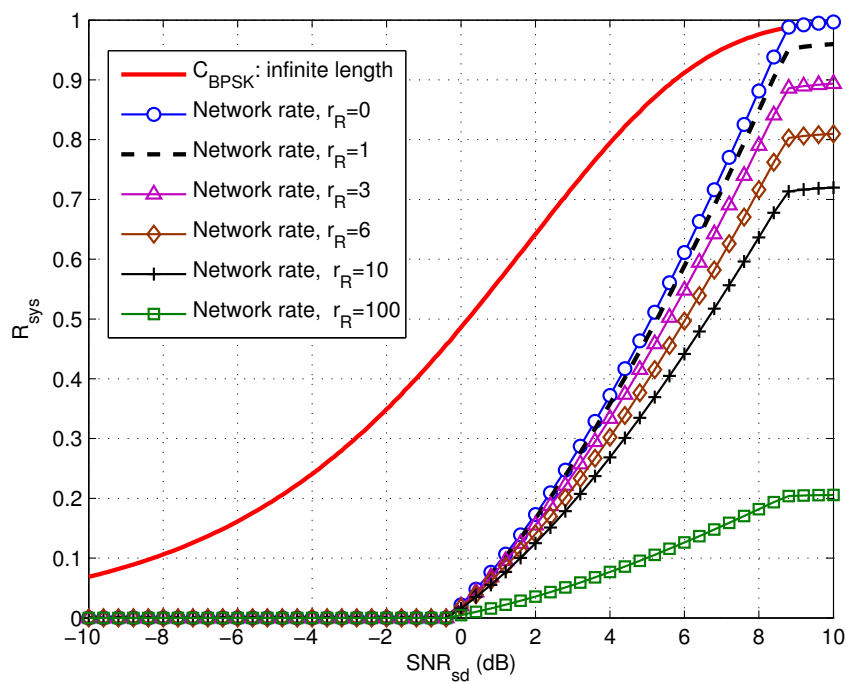


Figure 3.38 — Network achievable rate versus SNR_{sd} on the binary-input Gaussian channel, $SNR_{rd} = SNR_{sd}$, $\Delta SNR = 0\text{dB}$, $K = k_R = 26$, $n_S = 64$.

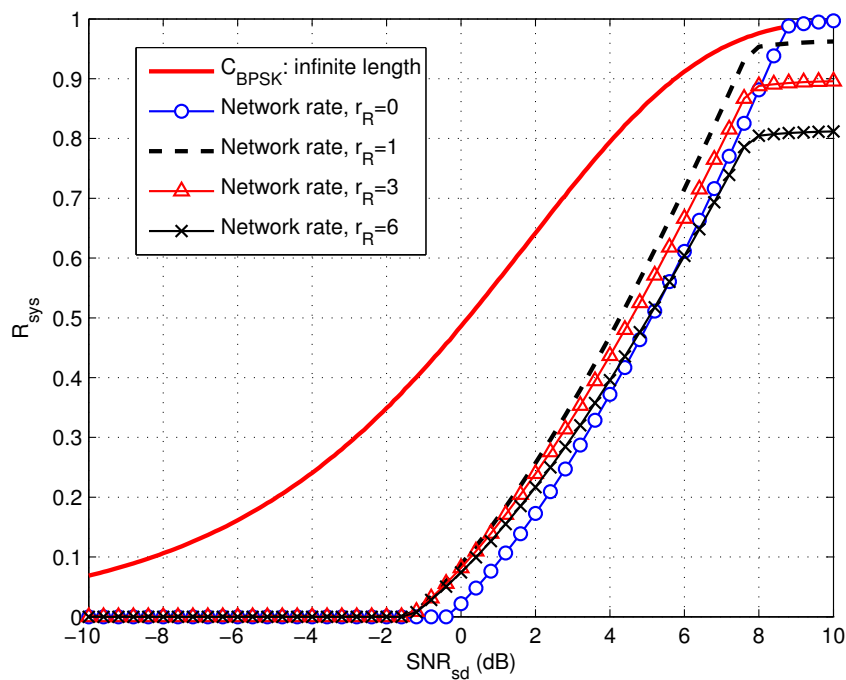


Figure 3.39 — Network achievable rate versus SNR_{sd} on the binary-input Gaussian channel, $SNR_{rd} = SNR_{sd}$, $\Delta SNR = 1\text{dB}$, $K = k_R = 26$, $n_S = 64$.

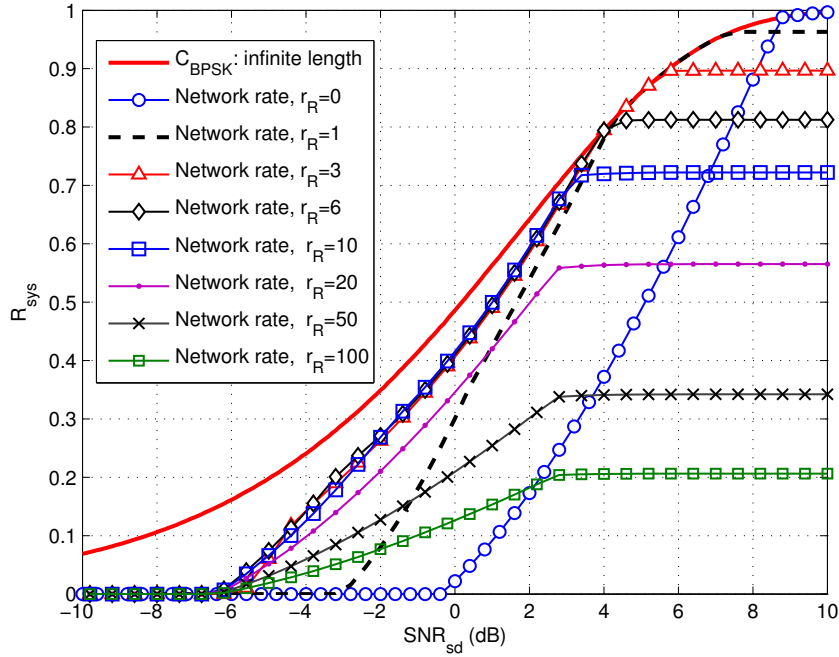


Figure 3.40 — Network achievable rate versus SNR_{sd} on the binary-input Gaussian channel, $SNR_{rd} = SNR_{sd}$, $\Delta SNR = 6\text{dB}$, $K = k_R = 26$, $n_S = 64$.

In Fig. 3.41, we evaluate the optimal value of the relay code redundancy length r_R maximizing the network rate under the condition of $SNR_{rd} = SNR_{sd}$. We consider different ΔSNR values corresponding to different source-relay channel conditions. r_R should be an integer and we take $0 \leq r_R \leq 20$ as the optimization searching range.

In the figure, when $\Delta SNR = 0\text{dB}$, the optimal $r_R \equiv 0$, which means there is no benefit using cooperation when the channel condition is not good enough. When ΔSNR becomes positive, we can improve the network rate with the cooperation for some given SNR_{sd} ranges. In the case of $\Delta SNR = 1\text{dB}$, we can improve the network rate using the optimal $r_R = 1$ in the range of $1.4\text{dB} \leq SNR_{sd} \leq 8.5\text{dB}$. With the improvement of the source-relay channel condition (increasing of ΔSNR), we need to use more relay redundancy r_R to improve the corresponding network rate. In all cases, $SNR_{sd} \geq 4\text{dB}$ is the region where the network rate is mainly dominated by the relay code rate R_R , so the cooperation with $r_R = 1$ or non-cooperation ($r_R = 0$) remains to be the best choice. When $SNR_{sd} > 8.5\text{dB}$, there is no need to do the cooperation for any ΔSNR values.

Fig. 3.41 provides an **information-theoretical reference to design the cooperative code scheme according to different channel conditions**. For the given parameters ($\Delta SNR, SNR_{sd}$), we can directly find the optimal r_R and thus fix the relay code. However, some useful information is not included in Fig. 3.41. For example, in the case of $\Delta SNR = 6\text{dB}$ (black dashed curve), the cooperation with $r_R = 3$ to 12 actually offers similar network rates for $-6.4\text{dB} \leq SNR_{sd} \leq 3.5\text{dB}$ (see Fig. 3.40). But only the r_R offering the best rates is given in Fig. 3.41.

In Fig. 3.42, we evaluate the network achievable rate R_{sys} versus SNR_{sd} for the

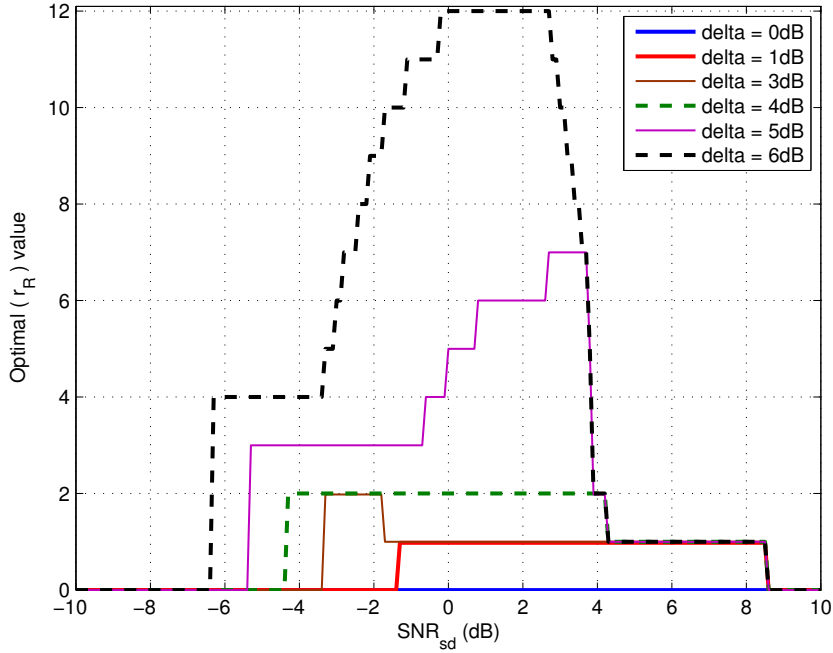


Figure 3.41 — Optimal r_R maximizaing the network rate on the binary-input Gaussian channel, r_R tested in the interval of $[0, 20]$
 $SNR_{rd} = SNR_{sd}$, $K = k_R = 26$, $n_S = 64$.

example cooperation scheme based on TPC : $(n_S, k_S) \times (n_R, k_R) = (64, 51) \times (32, 26)$. The corresponding $r_R = 6$ and the product code rate $R_P = \frac{26 \times 51}{32 \times 64} \approx 0.647$. Combining Fig. 3.40 and 3.41, we know that $r_R = 6$ is the near-optimal value for $\Delta SNR = 6\text{dB}$ when $-6.4\text{dB} \leq SNR_{sd} \leq 3.8\text{dB}$.

In the figure, the blue round point corresponds to a practical functional point of the cooperative scheme based on the BCH TPC in the case of $\Delta SNR = 6\text{dB}$. This point can obtained from Fig. 3.43 at a FEP = 10^{-6} . The detailed parameters of the functional point are given in Table 3.2.

| FEP = 10^{-6} | ΔSNR | E_b/N_0 | $SNR_{sd} = 2R_{sys}E_b/N_0$ |
|-----------------|--------------|-----------|------------------------------|
| Round Point | 6dB | 2.6dB | 3.72dB |

TABLE 3.2 — The practical functional point of the cooperative scheme based on BCH product code : $(n_S; k_S, \delta_S) = (64, 51, 6)$, $(n_R, k_R, \delta_R) = (32, 26, 4)$.

In Fig. 3.42, we find that the practical functional point is close to their corresponding theoretical achievable rate bounds. The gap is about 1.1dB. So the proposed cooperative scheme based on the BCH product code is quasi-optimal in the given channel conditions.

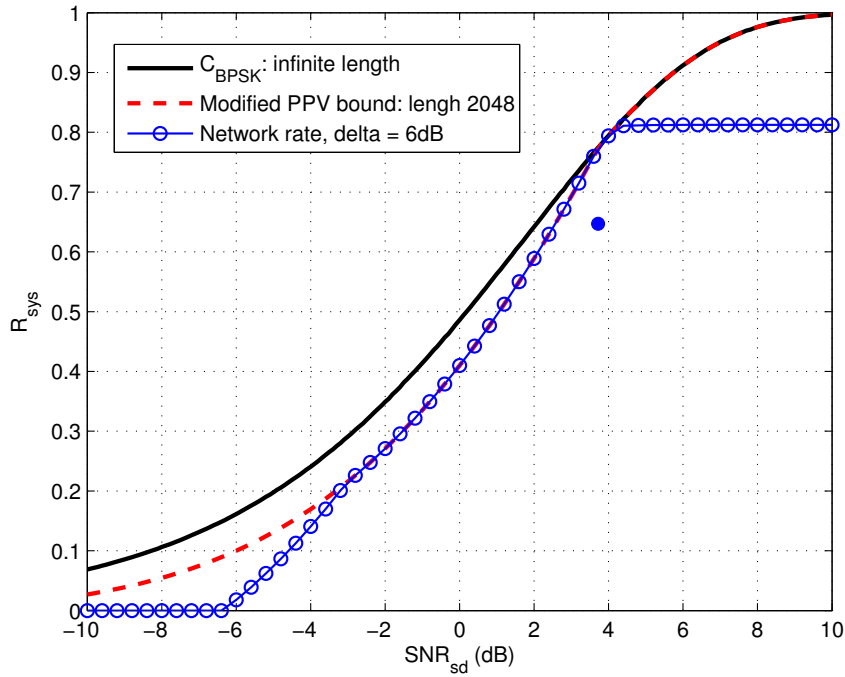


Figure 3.42 — Network achievable rate R_{sys} versus SNR_{sd} for the example cooperative scheme : $K = k_R = 26$, $n_S = 64$, on the binary-input Gaussian channel with $SNR_{rd} = SNR_{sd}$.

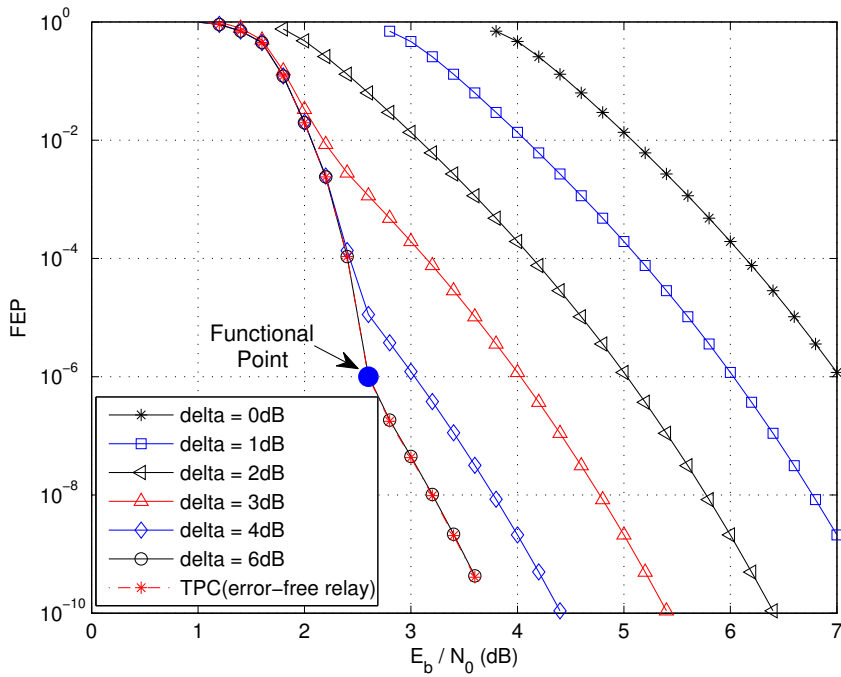


Figure 3.43 — The functional point given by the theoretical approximation of the network FEP on the AWGN channel with soft decoding at the relay, $SNR_{rd} = SNR_{sd}$ ($n_S; k_S, \delta_S$) = (64, 51, 6), (n_R, k_R, δ_R) = (32, 26, 4) ;

3.5 Conclusions

Based on the proposed cooperative scheme [PGA10], we have theoretically analyzed the bit error probability at the input and output of the relay encoder on the fast Rayleigh fading channel. Three relay detection strategies : the *bit-by-bit hard detection*, *hard decoding* and *soft decoding*, have been considered. After the relay encoding, we have proved that the bit error probability is amplified for different relay strategies. The amplification factor is independent of the relay strategy but depends on the relay code.

We have then established a theoretical frame error probability bound for the proposed cooperative network in the case of soft decoding at the relay. We have proved that the dominant error event at high SNR regime is caused by the error pattern at the relay associated with only one erroneous row in the detected source codewords matrix. Different bounds are derived as a function of source-relay channel conditions on both the AWGN and the fast Rayleigh fading channels. The theoretical results have been verified by simulations and can be used to predict the network error performance without using the time consuming simulations.

Thereafter, we have studied the mitigation of relay residual errors by using the LLR limitation in the turbo decoding. The theoretical LLR limiter derived in [PGA10] is optimal in the case of i.i.d relay errors. We have shown that, for the three different relay detection strategies, the relay-generated errors are correlated. The corresponding network BER performance exhibits an error floor. To reduce this phenomenon, we have considered multi-relay cooperation. Two decorrelation methods are proposed as the *row-wise division* and the *pseudo-random selection* of the redundancy sent to the destination. We have compared different cooperation strategies (single or multiple relays using different relay detection strategies) as a function of the source-relay link quality. By using the multi-relay cooperation with pseudo-random selection, the scheme is efficient especially for a high correlation degree, which corresponds to a poor source-relay configuration. The multiple relays involve multiple de-modulation / decoding of source codewords, which is more complex than the single-relay cooperation using soft decoding. We have concluded that for all practical applications, the single-relay cooperation using soft decoding at the relay achieves the best trade-off between bit error rate and complexity. For very poor source-relay link conditions, we can increase the test pattern number in the Chase soft decoding algorithm or use multi-relay cooperation. In the multi-relay case, the pseudo-random selection is privileged to the row-wise division for better decorrelation performance with similar additional complexity.

Through analyzing the cooperative scheme, we have found that the source-relay link is actually the network bottleneck. Since the sources use the short-length linear block code, we have thus evaluated the network capacity in the finite code-length regime. Based on [PPV10], we have proposed an upper bound on the rate of the binary-input Gaussian channel with finite code-length constraint. Using this result, we have derived the achievable rate for the proposed cooperative network based on the methods used in [KSA03b, YGiA10]. We have investigated the relation between the network rate and the relay redundancy bit number. An information-theoretical reference is derived to evaluate the optimal relay redundancy according to different channel conditions. By comparing the achievable rate bound and the operational point of the cooperative

scheme based on BCH product codes, we have shown that the proposed scheme is quasi-optimal in terms of information transmission if the relay uses the optimal code.

The main unsolved problem is the theoretical network error probability in the case of using hard detection or hard decoding at the relay. Besides that, the analysis of network capacity can be ameliorated if there is more accurate rate bound in the finite-length code regime especially for low SNRs.

In the next chapter, we will extend this cooperative scheme by introducing the CDMA technique such that the relay signal is superposed with the source signals. The main purpose is to better exploit the network resources under practical bandwidth constraints.

In the previous chapter, we have introduced the multi-source relay cooperation based on the turbo product codes using the time-division multiple-access (TDMA) technique. TDMA is simple to implement and is widely used in wireless applications. Using this mode, the sources and the relay transmit separately in different time slots. The column code used at the relay has a code rate close to 1, so the additional bandwidth used by the relay is a small portion of that used by the sources. If we apply the BCH (32, 26) code at the relay for the product code scheme, it is possible to approach the turbo code performance at the cost of 19% additional bandwidth.

In this chapter, we consider a different scenario where a wireless sensor network (WSN) has already been deployed in a given area. The objective is to enhance the transmission quality or to increase the network coverage without significantly modifying the existing network structure. More precisely, we cannot afford to modify the sensors, because the sensor number is high and the total cost would be expensive. Besides that, we do not expand the radio-frequency (RF) band compared to the original network.

As a solution, we investigate a relay cooperation scheme based on the turbo product codes where the relay transmission adopts a code-division multiple-access (CDMA) technique in the same RF band as the source-destination channel with a limited perturbation on the source-destination link. The sources can use either the TDMA or the frequency-division multiple-access (FDMA) mode as in the original network. We will analyze the interference on each link and present a turbo decoding procedure including an interference cancellation scheme. After that, we will evaluate the error performance of two kinds of cooperative networks where the CDMA-based relaying is superposed on either TDMA or FDMA source transmissions.

4.1 Problem statement

Suppose a WSN has already been deployed with K sensors transmitting to a same destination. All sensors use the same systematic linear block code (n_S, k_S) . We setup a relay without modifying the sensors or the existing network structure. The relay applies the Network Coding as described in the previous chapter through a systematic linear block code (n_R, k_R) . The source-relay channel is supposed error-free. The relay

transmission adopts the CDMA technique occupying the same RF band as the source-destination channel. The source and relay signals are superposed with each other at the destination. Fig. 4.1 shows the schema of the CDMA-based relay cooperation.

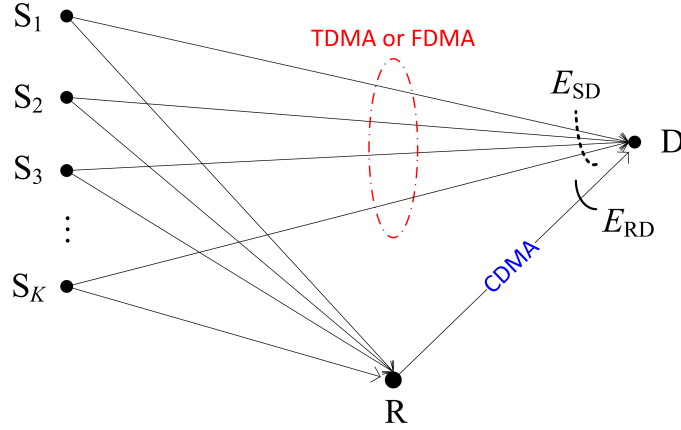


Figure 4.1 — Schema of superposed CDMA relay cooperation.

We introduce the following notations :

- E_{SD} is the average received energy on the source-destination link in a given duration of T_{SD} ;
- E_{RD} is the average received energy on the relay-destination link in a given duration of T_{RD} ;
- E_b is the average received energy per source information bit at the destination ;
- $x = \frac{E_{RD}}{E_{SD}}$ is the ratio between two kinds of average received energy at the destination coming from the relay and from the sources.

We consider the interference on each link and propose a turbo product code decoding procedure including the interference cancelation on the source-destination link. **Our objective is to optimize the value of $x = E_{RD}/E_{SD}$** according to the network error performance as a function of E_b/N_0 . We consider **two source multiple-access modes** : TDMA and FDMA. In each mode, we investigate **two energy scenarios** :

(1) The energy consumed by the relay is considered such that E_b is a function of both E_{SD} and E_{RD} :

$$E_b = f_1(E_{SD}, E_{RD}).$$

(2) The relay is autonomous in energy so that E_b depends only on E_{SD} :

$$E_b = f_2(E_{SD}).$$

4.2 CDMA-based relaying in the cooperative scheme

In Chapter 2, we have briefly introduced the basic notions and principles of direct spread spectrum CDMA and its synchronous transmission model. In this chapter,

we apply this technique in the multi-source relay cooperation. We first analyze the isolated relay-destination CDMA-based relaying without the interference coming from the source transmissions. The analysis of the complete cooperation scheme involving interference is addressed later.

4.2.1 CDMA-based relay-destination model

In the previous chapter, the problem was the transmission of independent data streams from different sources towards a common destination. In the proposed cooperative scheme, the relay encodes the received source codewords and forwards only the relay-generated redundancy to the destination. By appending the codewords coming from sources and relay, the destination observes a complete turbo product codeword and benefits from the turbo decoding. All transmissions are scheduled in the TDMA mode. In this case, the relay transmission needs an additional bandwidth which is a small portion of that occupied by the source transmissions.

In this chapter, we consider the same framework with some differences :

The purpose here is to enhance the transmission quality or to increase the network coverage without modifying the WSN already deployed and without consuming additional bandwidth resources. The source transmissions may be scheduled in either the TDMA or FDMA mode. We consider the error-free relay which is placed close enough to the sources and forwards the relay-generated redundancy using the CDMA mode. With well-chosen parameters, we can reuse the RF band of the source-destination channel. The corresponding CDMA model is illustrated in Fig. 4.2.

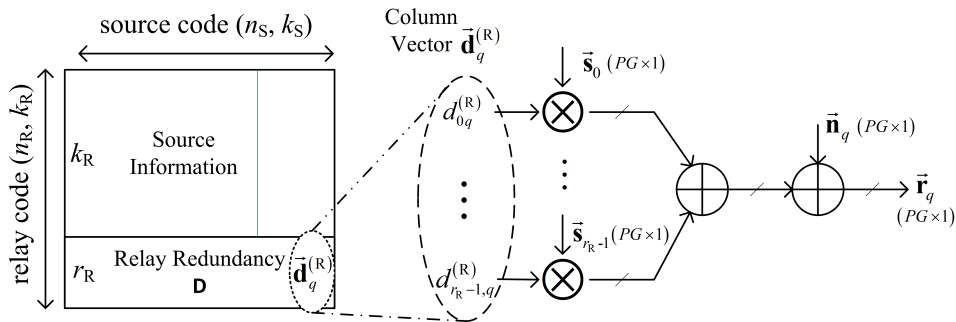


Figure 4.2 — CDMA-based relaying model.

The relay encodes its detected source codewords using the code (n_R, k_R) where $k_R = K$. We denote the relay code redundancy length $r_R = n_R - k_R$. The relay-generated codewords are stored in a matrix denoted \mathbf{D} whose q -th column is denoted $\vec{\mathbf{d}}_q^{(R)} = (d_{0q}^{(R)}, d_{1q}^{(R)}, \dots, d_{r_R-1,q}^{(R)})^T$ as shown in Fig. 4.2.

The relay has only one transmitter and uses a synchronous CDMA mode to transmit its codewords. During the q -th transmission interval the relay simultaneously transmits the r_R binary components of $\vec{\mathbf{d}}_q^{(R)}$ thanks to the spreading sequences of length PG . Defining $\mathbf{S} = (\vec{\mathbf{s}}_0, \vec{\mathbf{s}}_1, \dots, \vec{\mathbf{s}}_{r_R-1})$ the $PG \times r_R$ spreading sequence matrix, the received

vector at the destination is given by :

$$\vec{\mathbf{r}}_q = A_{Relay} \cdot \mathbf{S} \cdot \vec{\mathbf{d}}_q^{(R)} + \vec{\mathbf{n}}_q, \quad (4.1)$$

where A_{Relay} is the received amplitude. $\vec{\mathbf{n}}_q$ is the average white Gaussian noise vector. In the following, we suppose BPSK modulation and $d_{iq}^{(R)} \in \{\pm 1\}$ for $i = 0, 1, \dots, r_R - 1$.

4.2.2 Definition of the spreading sequences used at the relay

In our study, we wish to exploit the complete bandwidth of the original network to maximize the CDMA processing gain, so the relay CDMA transmission is designed to occupy the same RF band as the source transmission. Taking into account that there are K sources using either the TDMA or FDMA mode, it is necessary to find a set of spreading sequences having a processing gain equal to the source number. In a short-code CDMA system, it means that the sequence length $PG = K = k_R$.

There are r_R relay-generated codewords to be transmitted using CDMA. Each one requires a unique spreading sequence. In the literature, there are several conventional binary spreading sequences [Stu02], such as the m -sequences, Walsh-Hadamard sequences, Gold sequences, Barker sequences, etc. Each of them has specific properties appropriate for CDMA applications. If these sequences can be constructed with the given length PG , we can directly apply them in our application.

In this chapter, we consider the same BCH product code example as in the previous chapter. The source code is BCH (64, 51) and the relay code is BCH (32, 26). The corresponding source number is 26. We cannot generate the conventional spreading sequences satisfying $PG = 26$. As a consequence, we randomly generate the spreading sequence set.

The generation of spreading sequences must fulfill the constraints of good auto-correlation and cross-correlation properties, which is crucial for the CDMA transmission quality. Through exhaustive search, we have found a set of $r_R = 6$ optimized spreading sequences given in Appendix. 4.A. They are randomly generated PN sequences and have nearly balanced antipodal elements and good auto-correlation properties. They are not perfectly orthogonal but have good cross-correlation properties. Their normalized cross-correlation matrix is given in Eq. 4.2 :

$$\begin{aligned} \mathbf{C}_{(6 \times 6)} &= \mathbf{S}_{(6 \times PG)}^T \cdot \mathbf{S}_{(PG \times 6)} \\ &= \begin{pmatrix} 1 & 0.1538 & 0.1538 & 0.2308 & 0 & 0.1538 \\ 0.1538 & 1 & 0.2308 & 0 & -0.2308 & 0.0769 \\ 0.1538 & 0.2308 & 1 & 0 & -0.2308 & -0.0769 \\ 0.2308 & 0 & 0 & 1 & 0.1538 & 0 \\ 0 & -0.2308 & -0.2308 & 0.1538 & 1 & 0.2308 \\ -0.1538 & 0.0769 & -0.0769 & 0 & 0.2308 & 1 \end{pmatrix}. \end{aligned} \quad (4.2)$$

4.2.3 Maximum-likelihood multi-user detection

The optimal detector observes \vec{y} at the output of the matched filter bank and decides in favor of the transmitted vector $\vec{d}^{(R)}$ that maximizes the probability $\Pr(\vec{d}^{(R)} | \vec{y})$. This rule can be mathematically expressed as :

$$\vec{d}^{(R)} = \arg \max_{1 < i < M} \Pr(\vec{d}_i^{(R)} | \vec{y}). \quad (4.3)$$

$$\vec{d}^{(R)} = \arg \max_{1 < i < M} \Pr(\vec{y} | \vec{d}_i^{(R)}), \quad (4.4)$$

which is known as the maximum-likelihood (ML) detection [PS08, p.162].

ML detection minimizes the error probability by testing all possible transmitted vectors. This method has an exponential complexity with the number of CDMA users. In the practical CDMA system, there are usually a large number of users so that the ML complexity is prohibitive and one prefers to use the sub-optimal detection methods [Mos96], such as the linear detector or the successive interference cancelation detector. In our application, there are r_R virtual CDMA users corresponding to r_R relay redundancy rows. In general, r_R is a small integer because the relay code rate is close to 1. In the case of using the BCH (32, 26) code at the relay, $r_R = 6$. For every transmitted vector $\vec{d}^{(R)}$, there are $2^{r_R} = 64$ possible vectors to be tested so the complexity is affordable.

In the following, we formulate the CDMA ML detection on the relay-destination channel with no source interference. In the next sections, we shall extend the analysis by introducing the TDMA / FDMA source interference.

As introduced in section 2.4.2, the received signal \vec{r} in Eq. 4.1 is despread as :

$$\begin{aligned} \vec{y}_{(r_R \times 1)} &= \mathbf{S}^T \cdot \vec{r}_{(PG \times 1)} \\ &= A_{Relay} \cdot \mathbf{S}_{(r_R \times PG)}^T \cdot \mathbf{S}_{(PG \times r_R)} \cdot \vec{d}_{(r_R \times 1)}^{(R)} + \mathbf{S}_{(r_R \times PG)}^T \cdot \vec{n}_{(PG \times 1)} \\ &= A_{Relay} \cdot \mathbf{C}_{(r_R \times r_R)} \cdot \vec{d}_{(r_R \times 1)}^{(R)} + \vec{n}_{t(r_R \times 1)}. \end{aligned} \quad (4.5)$$

We apply the ML rule based on the log-likelihood ratio (LLR) so that the soft detection result can be directly provided to the turbo product decoder in a later step. The ML detector calculates the LLR of the k -th bit $d_k^{(R)}$ in the relay transmitted vector $\vec{d}^{(R)}$ as :

$$\Lambda(d_k^{(R)}) = \ln \frac{\Pr(d_k^{(R)} = 1 | \vec{y})}{\Pr(d_k^{(R)} = -1 | \vec{y})} = \ln \frac{\sum_{\vec{d}^i \in \text{set}\{\vec{d}_{+1}\}} p(\vec{y} | \vec{d}^{(R)} = \vec{d}^i)}{\sum_{\vec{d}^i \in \text{set}\{\vec{d}_{-1}\}} p(\vec{y} | \vec{d}^{(R)} = \vec{d}^i)}, \quad (4.6)$$

where the set \vec{d}_{+1} (resp. \vec{d}_{-1}) denotes the transmitted vector set satisfying that the k -th bit of the vector equals 1 (resp. -1). In our example of 6-user CDMA, the summation either in the numerator or denominator contains 32 terms of $p(\vec{y} | \vec{d}^{(R)} = \vec{d}^i)$ in Eq. 4.6.

Based on Eq. 4.5, we can model $\vec{y} - A_{Relay} \cdot \mathbf{C} \cdot \vec{d}^{(R)} = \vec{n}_{t(r_R \times 1)}$ as a zero-mean multivariate Gaussian variables [PS08, p.54] whose covariance matrix is :

$$\mathbf{COV} = Cov(\vec{n}_t) = E(\mathbf{S}^T \vec{n} \cdot \vec{n}^T \mathbf{S}) = \mathbf{S}^T \cdot E(\vec{n} \cdot \vec{n}^T) \cdot \mathbf{S} = \mathbf{S}^T \cdot \sigma_n^2 \mathbf{I} \cdot \mathbf{S} = \sigma_n^2 \cdot \mathbf{C}, \quad (4.7)$$

where σ_n^2 is the noise variance of $\vec{n}_{(PG \times 1)}$. So $p(\vec{y} | \vec{d}^{(R)} = \vec{d}^i)$ is given by :

$$\begin{aligned} p(\vec{y} | \vec{d}^{(R)} = \vec{d}^i) &= \frac{1}{(2\pi)^{\frac{r_R}{2}} |\mathbf{COV}|^{\frac{1}{2}}} \exp \left\{ -\frac{1}{2} (\vec{y} - A_{Relay} \cdot \mathbf{C} \vec{d}^{(R)})^T (\mathbf{COV})^{-1} (\vec{y} - A_{Relay} \cdot \mathbf{C} \vec{d}^{(R)}) \right\}. \end{aligned} \quad (4.8)$$

Canceling the common term in the numerator and denominator in Eq. 4.6, we get the following exponent part defining the metric to be computed for each possible $\vec{d}^{(R)}$:

$$\exp \left\{ -\frac{1}{2} (\vec{y} - A_{Relay} \cdot \mathbf{C} \vec{d}^{(R)})^T (\mathbf{COV})^{-1} (\vec{y} - A_{Relay} \cdot \mathbf{C} \vec{d}^{(R)}) \right\}. \quad (4.9)$$

From Eq. 4.7, we have $(\mathbf{COV})^{-1} = \frac{1}{\sigma_n^2} \mathbf{C}^{-1}$ and we know that $\mathbf{C}^T = \mathbf{C}$, so Eq. 4.9 simplifies to :

$$\exp \left\{ \frac{1}{2\sigma_n^2} \left(2A_{Relay} \cdot \vec{y}^T \cdot \vec{d}^{(R)} - A_{Relay}^2 \cdot (\vec{d}^{(R)})^T \mathbf{C} \vec{d}^{(R)} \right) \right\}. \quad (4.10)$$

In summary, for each CDMA channel observation \vec{r} , we first pass it through the matched filter bank to get the despread vector \vec{y} . Then using Eq. 4.10, we can calculate the ML metrics of all possible vectors $\vec{d}^{(R)}$. By substituting them into Eq. 4.6, we obtain the LLR $\Lambda(d_k^{(R)})$ of the k -th bit in the transmitted vector.

The value of $\Lambda(d_k^{(R)})$ can be directly used as the input of the turbo decoder. If hard detection is required, we make the following decisions on $\Lambda(d_k^{(R)})$:

$$\hat{d}_k^{(R)} = \begin{cases} +1, & \text{if } \Lambda(d_k^{(R)}) \geq 0 \\ -1, & \text{if } \Lambda(d_k^{(R)}) < 0 \end{cases}. \quad (4.11)$$

In Fig. 4.3, we show the BER performance of the ML detection of the 6-user CDMA transmission as an example. We do not consider the source interference and suppose that the CDMA user data are independent and uniformly distributed (i.i.d.) random binary digits.

In Fig. 4.3, we compare the BER of the conventional hard detection and that of the ML multi-user detection. The theoretical bit error probability of the BPSK modulation is given on the AWGN channel by :

$$P_{eb} = \frac{1}{2} \operatorname{erfc} \left(\sqrt{\frac{E_b}{N_0}} \right). \quad (4.12)$$

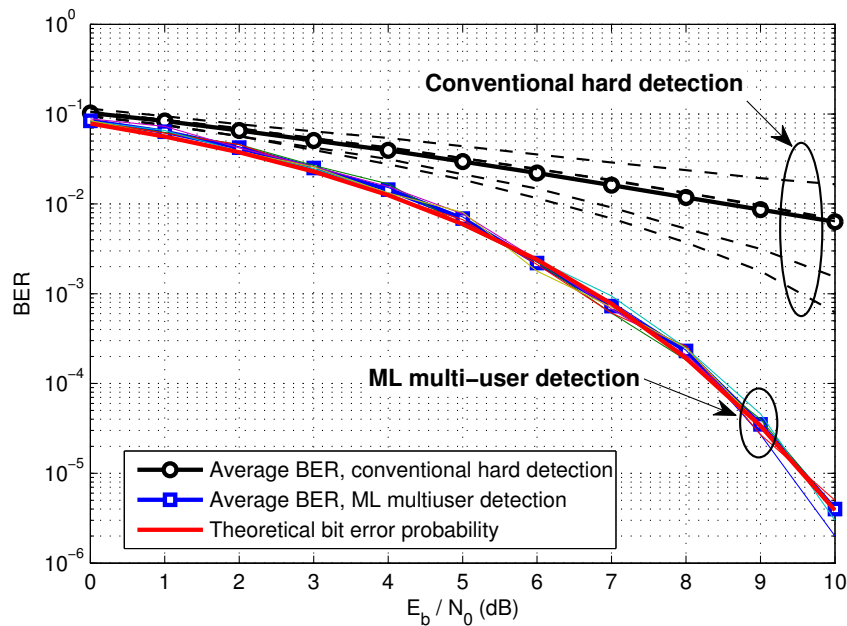


Figure 4.3 — BER of relay CDMA transmission (6-user) without source interference, BPSK modulation over the AWGN channel : Conventional hard detection (each source is detected separately and the MAI is considered as a Gaussian noise at each decorrelator output) & ML CDMA multi-user detection.

For the conventional hard detection, the destination applies the hard threshold decision on $\bar{\mathbf{y}}$ at the output of the matched filter bank, which is given in Eq. 4.5. The MAI is simply treated as an additional Gaussian noise so the BER performance is largely degraded. The individual BERs counted for each CDMA user are plotted using the discontinuous curves which are dispersive for high SNR. It is because the MAI associated with different spreading sequences are different in that case.

For the ML multi-user detection, we observe that the individual BER performance curves are practically superposed and their average BER curve coincides with the theoretical bit error probability curve. Simulations confirm its optimality in terms of error probability.

4.3 Iterative interference cancelation

In the previous section, we have introduced the isolated CDMA transmission on the relay-destination channel. In this section, we add the source transmissions in the framework of the multi-source relay cooperation based on the turbo product code. In this case, the source and the relay signals are superposed and interfere mutually.

4.3.1 Time-aligned transmission protocol

In our study, we carefully select the CDMA parameters including the processing gain, chip duration, carrier frequency etc., such that :

1. The relay CDMA signal occupies the same RF band as the source signals ;
2. The duration of one relay CDMA transmission, i.e., the time used to forward the relay-generated redundancy part, equals the duration of the whole source transmissions, i.e. the total time required by all sources to transmit their data. We denote this duration T_{BCH} .

For the multi-source relay cooperation, the source transmission is scheduled by either TDMA or FDMA. We consider time blocks of duration T_{BCH} . The K sources broadcast their data in one time block. The relay encodes the detected source codewords and forwards the relay-generated redundancy in the following time block, which is also used by the sources for the next-round of source transmission. In this way, the relay CDMA transmission associated with the current data generation is superposed with the source transmission of the next data generation.

We denote the source data part including K source codewords as $\mathbf{S}(m)$ where m is the block generation index. The relay redundancy part is denoted $\mathbf{R}(m)$, which is the column redundancy of $\mathbf{S}(m)$ in the TPC scheme. The time-aligned transmission scheme described above is illustrated in Fig. 4.4. The circled couple $[\mathbf{S}(m), \mathbf{R}(m)]$ corresponds to the same product codeword. In the figure, each column is transmitted in a same time block. If two parts belong to the same column, it means that their signals are superposed at the destination. Here we have supposed synchronous transmission with no relative transmission delay.

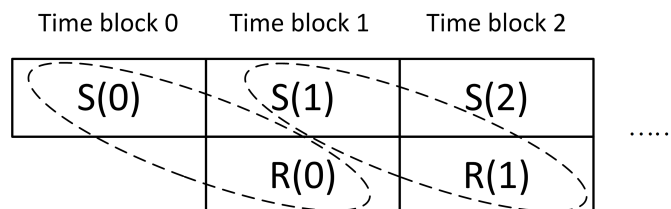


Figure 4.4 — Aligned time blocks at the destination.

4.3.2 Turbo decoding with interference cancelation

From Fig. 4.4, we consider that the source and relay signals are superposed at the destination and will interfere with one another. In this section, we propose an iterative decoding procedure to cancel a part of the interference.

There is an initialization step at the beginning (in time block 0) when the relay is silent and the sources transmit $\mathbf{S}(0)$. In this time block, the destination observes only the source BCH codewords and stores them. In time block 1, destination observes the source part $\mathbf{S}(1)$ of the second product codeword superposed with the CDMA relay redundancy part $\mathbf{R}(0)$ of the previous product codeword. Based on the ML multi-user detection described in section 4.2.3, the destination detects $\mathbf{R}(0)$ in the presence of

$\mathbf{S}(1)$. The detailed ML detection differs a little according to the source multiple-access mode and we will introduce it in the next sections. The destination thus observes the first product codeword by combining the observed interference-free $\mathbf{S}(0)$ and the detected LLR of $\mathbf{R}(0)$. After the turbo decoding, we get the decoded $\hat{\mathbf{S}}(0)$, which should contain less errors than the direct BCH decoding of $\mathbf{S}(0)$ at the initialization step.

Based on the decoded $\hat{\mathbf{S}}(0)$, we can regenerate the relay redundancy part $\hat{\mathbf{R}}(0)$ at the destination through product encoding. $\hat{\mathbf{R}}(0)$ will usually be more reliable than the ML-detected $\mathbf{R}(0)$ because of the turbo decoding gain. Once we get $\hat{\mathbf{R}}(0)$, we can regenerate the relay CDMA signal and cancel its interference on the source-destination transmission to get a ‘cleaned’ version of $\mathbf{S}(1)$.

The above procedure is then repeated. After the turbo decoding of the m -th time block at the destination, we can recover the source information of the $(m - 1)$ -th source transmission. The concise iterative decoding procedure is given below using the pseudo-code :

Time block 0 : Initialization

Destination (D) stores the noisy $\mathbf{S}(0)$ as $\tilde{\mathbf{S}}(0)$.

Time block 1 : D receives $\mathbf{S}(1) + [\text{CDMA } \mathbf{R}(0)] + \text{noise}$

(a) *D applies ML multi-user detection to detect $\mathbf{R}(0)$ in the presence of $\mathbf{S}(1)$.*

(b) *D turbo decodes the product codeword $[\mathbf{R}(0)^T, \tilde{\mathbf{S}}(0)^T]^T$ to decide $\hat{\mathbf{S}}(0)$.*

(c) *D recalculates the column redundancy part $\hat{\mathbf{R}}(0)$ from $\hat{\mathbf{S}}(0)$.*

(d) *D cancels the interference coming from the relay :*

$$\tilde{\mathbf{S}}(1) = \mathbf{S}(1) + [\text{CDMA } \mathbf{R}(0)] + \text{noise} - [\text{CDMA } \hat{\mathbf{R}}(0)]$$

Repeat the above procedures from (a) to (d) in the following time blocks with incremental indices for the corresponding variables.

4.4 Superposed TDMA-CDMA scheme

In this section, we focus on the superposed CDMA relay cooperation considering a TDMA mode for source transmissions. The cooperation is based on the BCH product code : $\text{BCH}(n_S, k_S) \times \text{BCH}(n_R, k_R)$, i.e., there are $K = k_R$ sources employing the source BCH code (n_S, k_S) and the relay applies the column BCH code (n_R, k_R) whose redundant bit number is denoted $r_R = n_R - k_R$.

4.4.1 Network configuration

The K sources transmit according to a TDMA mode and there are $K \times n_S$ coded symbols corresponding to K source codewords of length n_S . The source coded symbol duration is denoted $T_s^{(S)}$. We consider the BPSK modulation, so $T_s^{(S)}$ is the duration of source codeword bit.

The relay uses the single antenna CDMA transmission as described in Fig. 4.2. The relation between the symbol duration of the relay redundancy symbol $T_s^{(R)}$ and the chip duration $T_{chip}^{(R)}$ is :

$$T_s^{(R)} = PG \cdot T_{chip}^{(R)}, \quad (4.13)$$

where $PG = K$ as described in section 4.2.2.

To ensure that sources and relay transmit in the same time interval, it is necessary that :

$$K \cdot n_s T_s^{(S)} = PG \cdot n_s T_{chip}^{(R)}, \quad (4.14)$$

which means that the source-destination TDMA bit duration equals the relay-destination CDMA chip duration :

$$T_s^{(S)} = T_{chip}^{(R)} = T_s. \quad (4.15)$$

The TDMA-CDMA multiple-access scheme based on the TPC is summarized in Fig. 4.5. The PSD of the source signal and the relay signal is illustrated in Fig. 4.6.

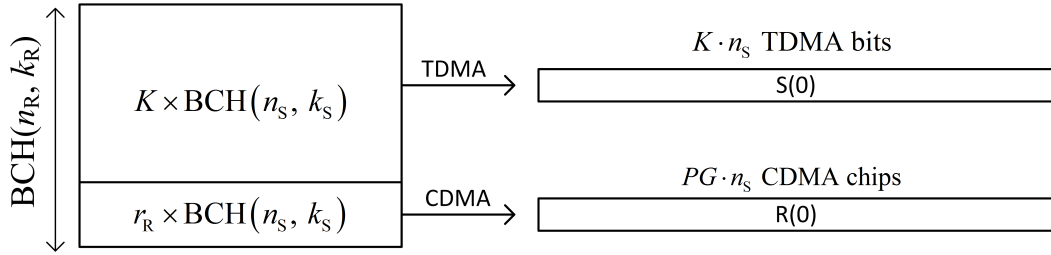


Figure 4.5 — Multiple access of the hybrid TDMA-CDMA scheme $K = PG$.

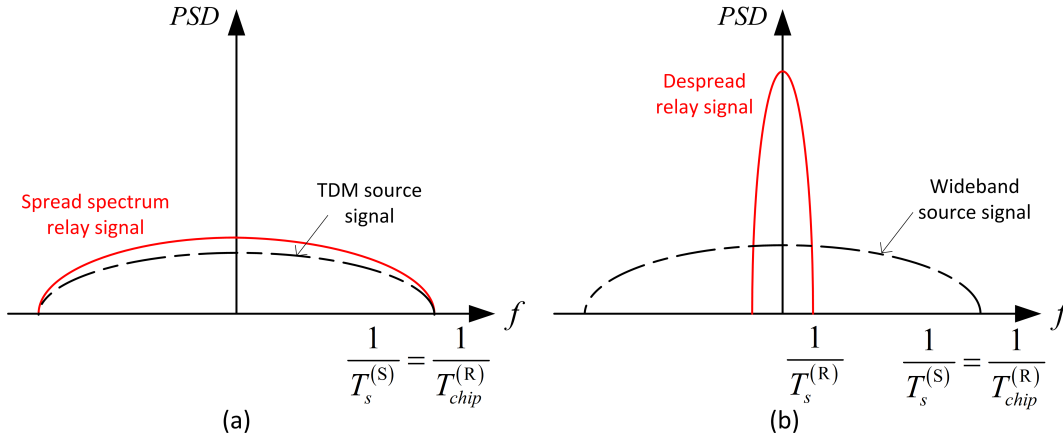


Figure 4.6 — Power spectral density of the source TDMA signal and the relay CDMA signal,
(a) before despreading; (b) after despreading.

4.4.2 Block diagrams of the receiver

We have the following hypotheses :

1. All transmissions are BPSK modulated.
2. The K sources transmit one after another in the TDMA mode using the same transmission power.
3. The relay uses completely the same transmission interval of the K sources.
4. The source-relay link is assumed error-free.

The noise-free received signals at the destination can be expressed by :

source-destination channel(TDMA) :

$$r_{SD}^{\text{TDM}}(t) = \sum_n A_{Source} d_n^{\text{TDM}} \cdot h_{Ts}(t - nT_s^{(S)}) \cdot \cos(2\pi f_0 t + \varphi_0). \quad (4.16)$$

relay-destination channel(CDMA) :

$$r_{RD}^{(R)}(t) = \sum_{i=0}^{r_R-1} A_{Relay} \sum_n d_{i,n}^{(R)} \sum_m s_{i,m} \cdot h_{Ts}(t - n \cdot PG \cdot T_s^{(S)} - mT_s^{(S)}) \cdot \cos(2\pi f_0 t + \varphi_0). \quad (4.17)$$

The sources and relay use the same root-raised-cosine pulse shaping function $h_{Ts}(t)$ as defined in Appendix 4.B. $d_n^{\text{TDM}} \in \{\pm 1\}$ is the source codeword bit in the time-divided multiplexed data stream. $d_{i,n}^{(R)} \in \{\pm 1\}$ is the relay codeword bit of the i -th CDMA user, i.e. i -th row of the relay redundancy. $s_{i,m} \in \{\pm 1/\sqrt{PG}\}$ is the m -th element of the i -th spreading sequence whose entries have been normalized for unit sequence energy. f_0 is the carrier frequency and φ_0 is the delay phase which will be compensated at the destination.

The superposed noisy signal received at the destination is thus given by :

$$\begin{aligned} r(t) &= r_{SD}^{\text{TDM}}(t) + r_{RD}^{(R)}(t) + n(t) \\ &= A_{Source} \sum_n d_n^{\text{TDM}} \cdot h_{Ts}(t - nT_s^{(S)}) \cdot \cos(2\pi f_0 t + \varphi_0) \\ &\quad + A_{Relay} \sum_{i=0}^{r_R-1} \sum_q d_{i,q}^{(R)} \sum_{m=0}^{PG-1} s_{i,m} \cdot h_{Ts}(t - q \cdot PG \cdot T_s^{(S)} - mT_s^{(S)}) \cdot \cos(2\pi f_0 t + \varphi_0) \\ &\quad + n(t), \end{aligned} \quad (4.18)$$

where $n(t)$ is an AWGN process whose double-side PSD is $N_0/2$.

Different parts of the receiver at the destination are illustrated by the block diagrams in Fig. 4.7 - 4.10.

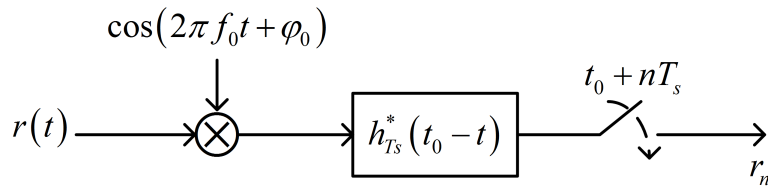


Figure 4.7 — Coherent detection of the superposed signal at the destination.

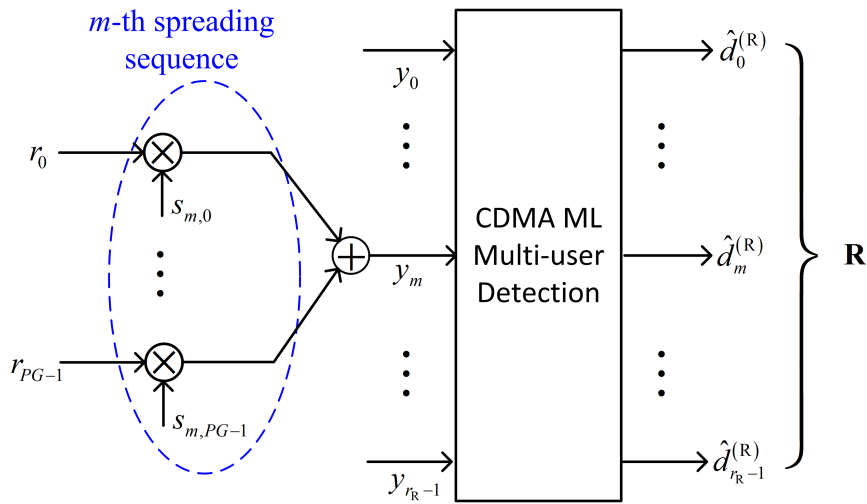


Figure 4.8 — Relay part detection : CDMA ML multi-user detection.

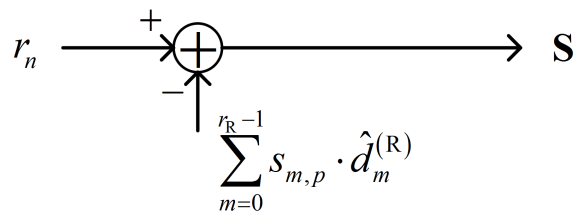


Figure 4.9 — Source part detection including the cancellation of relay interference.

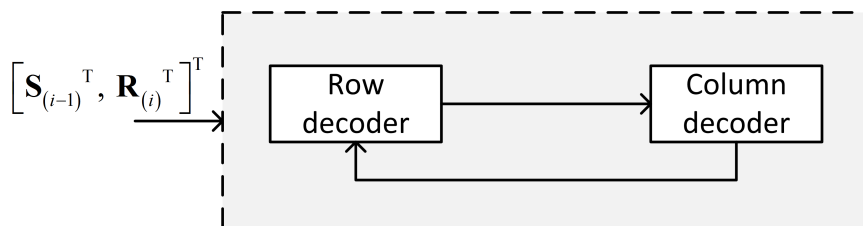


Figure 4.10 — Turbo product code decoding.

4.4.3 Relay-destination ML multi-user detection with TDMA interference

Following the same model to derive Eq. 4.1, we can express the received signal at the destination with the source TDMA interference as :

$$\vec{\mathbf{r}}_{(PG \times 1)}^{\text{TDM}} = A_{\text{Relay}} \cdot \mathbf{S}_{(PG \times r_R)} \cdot \vec{\mathbf{d}}_{(r_R \times 1)}^{(\text{R})} + A_{\text{Source}} \cdot \vec{\mathbf{d}}_{(PG \times 1)}^{\text{TDM}} + \vec{\mathbf{n}}_{(PG \times 1)}, \quad (4.19)$$

where A_{Source} is the received source signal amplitude. $\vec{\mathbf{d}}_{(PG \times 1)}^{\text{TDM}}$ corresponds to the TDMA source interference terms which are superposed with the relay signal. We denote their variance σ_I^2 . As shown in Fig. 4.5, these source interference terms are in fact the BPSK modulated source codeword bits. Their values belong to $\{\pm 1\}$, so we have $\sigma_I^2 = 1$.

At the destination, we despread the signal $\vec{\mathbf{r}}^{\text{TDM}}$ by the correlation with local spreading sequences :

$$\begin{aligned} \vec{\mathbf{y}}'_{(r_R \times 1)} &= \mathbf{S}^T \cdot \vec{\mathbf{r}}_{(PG \times 1)}^{\text{TDM}} \\ &= A_{\text{Relay}} \cdot \mathbf{S}^T_{(r_R \times PG)} \cdot \mathbf{S}_{(PG \times r_R)} \cdot \vec{\mathbf{d}}_{(r_R \times 1)}^{(\text{R})} \\ &\quad + A_{\text{Source}} \cdot \mathbf{S}^T_{(r_R \times PG)} \cdot \vec{\mathbf{d}}_{(PG \times 1)}^{\text{TDM}} + \mathbf{S}^T_{(r_R \times PG)} \cdot \vec{\mathbf{n}}_{(PG \times 1)} \\ &= A_{\text{Relay}} \cdot \mathbf{C}_{(r_R \times r_R)} \cdot \vec{\mathbf{d}}_{(r_R \times 1)}^{(\text{R})} + A_{\text{Source}} \cdot \vec{\mathbf{d}}_{\mathbf{t}(r_R \times 1)}^{\text{TDM}} + \vec{\mathbf{n}}_{\mathbf{t}(r_R \times 1)}, \end{aligned} \quad (4.20)$$

where $\mathbf{C}_{(r_R \times r_R)} = \mathbf{S}^T_{(r_R \times PG)} \cdot \mathbf{S}_{(PG \times r_R)}$ is the spreading sequences cross-correlation matrix.

Here we model $\vec{\mathbf{y}}' - A_{\text{Relay}} \cdot \mathbf{C} \cdot \vec{\mathbf{d}}^{(\text{R})} = A_{\text{Source}} \cdot \vec{\mathbf{d}}_{\mathbf{t}}^{\text{TDM}} + \vec{\mathbf{n}}_{\mathbf{t}}$ as a multivariate Gaussian variable and we further assume the PG elements of source interference $\vec{\mathbf{d}}_{(PG \times 1)}^{\text{TDM}}$ are i.i.d variables, so we get the following covariance :

$$\text{Cov}(\vec{\mathbf{n}}_{\mathbf{t}}) = E(\mathbf{S}^T \vec{\mathbf{n}} \cdot \vec{\mathbf{n}}^T \mathbf{S}) = \mathbf{S}^T \cdot E(\vec{\mathbf{n}} \cdot \vec{\mathbf{n}}^T) \cdot \mathbf{S} = \mathbf{S}^T \cdot \sigma_n^2 \mathbf{I} \cdot \mathbf{S} = \sigma_n^2 \cdot \mathbf{C}. \quad (4.21)$$

$$\begin{aligned} \text{Cov}(\vec{\mathbf{d}}_{\mathbf{t}}^{\text{TDM}}) &= A_{\text{Source}}^2 \cdot E(\mathbf{S}^T \cdot \vec{\mathbf{d}}^{\text{TDM}} \cdot \vec{\mathbf{d}}^{\text{TDM},T} \cdot \mathbf{S}) \\ &= A_{\text{Source}}^2 \cdot \mathbf{S}^T \cdot E(\vec{\mathbf{d}}^{\text{TDM}} \cdot \vec{\mathbf{d}}^{\text{TDM},T}) \cdot \mathbf{S}. \end{aligned} \quad (4.22)$$

The covariance matrix of $(\vec{\mathbf{y}}' - A_{\text{Relay}} \cdot \mathbf{C} \cdot \vec{\mathbf{d}}^{(\text{R})})$ can be calculated as :

$$\mathbf{COV} = \text{Cov}(\vec{\mathbf{y}}' - A_{\text{Relay}} \cdot \mathbf{C} \cdot \vec{\mathbf{d}}^{(\text{R})}) = \text{Cov}(\vec{\mathbf{d}}_{\mathbf{t}}^{\text{TDM}}) + \text{Cov}(\vec{\mathbf{n}}_{\mathbf{t}}) = (A_{\text{Source}}^2 \cdot \sigma_I^2 + \sigma_n^2) \mathbf{C}. \quad (4.23)$$

Using the same procedure as in section 4.2.3, the ML multi-user detector calculates

the LLR of each bit of the relay redundancy as :

$$\begin{aligned} \Lambda \left(d_k^{(R)} \right) &= \ln \frac{\Pr \left(d_k^{(R)} = 1 | \vec{y} \right)}{\Pr \left(d_k^{(R)} = -1 | \vec{y} \right)} = \ln \frac{\sum_{\vec{d}^i \in \text{set}\{\vec{d}_{+1}\}} p \left(\vec{y} | \vec{d}^{(R)} = \vec{d}^i \right)}{\sum_{\vec{d}^i \in \text{set}\{\vec{d}_{-1}\}} p \left(\vec{y} | \vec{d}^{(R)} = \vec{d}^i \right)} \\ &= \ln \frac{\sum_{\vec{d}^i \in \text{set}\{\vec{d}_{+1}\}} M_{\vec{d}^i}}{\sum_{\vec{d}^i \in \text{set}\{\vec{d}_{-1}\}} M_{\vec{d}^i}}, \end{aligned} \quad (4.24)$$

where the metric $M_{\vec{d}^i}$ is given by :

$$M_{\vec{d}^i} = \exp \left\{ \frac{1}{2(A_{Source}^2 \cdot \sigma_1^2 + \sigma_n^2)} \left(2A_{Relay} \cdot \vec{y}^T \cdot \vec{d}^i - A_{Relay}^2 \cdot \vec{d}^{i,T} \mathbf{C} \vec{d}^i \right) \right\}. \quad (4.25)$$

The only difference with the interference-free ML detection is in the definition of covariance matrix \mathbf{COV} .

4.4.4 Energy scenarios

We evaluate the cooperative network error performance as a function of the received energy at the destination. There are TDMA signals coming from the sources and also superposed CDMA signals forwarded by the relay. We study their contribution to the received energy in this section.

The destination receives the superposed signal $r(t)$ given in Eq.4.18. After the coherent filtering and sampling without ISI as shown in Fig. 4.7, we obtain the following discrete transmission equation :

$$y_n = \frac{A_{Source}}{2} d_n^{\text{TDM}} \varphi_{T_s}(t_0) + \frac{A_{Relay}}{2} \sum_{i=0}^{r_R-1} s_{i,m} d_{i,q}^{(R)} \varphi_{T_s}(t_0) + n_n, \quad (4.26)$$

where $\varphi_{T_s}(t_0) = \int_{-\infty}^{\infty} |H_{T_s}(f)|^2 df$. n_n is an AWGN random variable whose variance $\sigma_n^2 = \frac{N_0}{4} \varphi_{T_s}(t_0)$.

The average received energy on the source-destination link in a given duration of $T_s^{(S)}$ is :

$$E_{SD} = \frac{(A_{Source})^2}{2} \varphi_{T_s}(t_0). \quad (4.27)$$

The average received energy on the relay-destination link in a given duration of $T_{chip}^{(R)} = T_s^{(S)}$ is :

$$E_{RD} = \frac{(A_{Relay})^2}{2} \varphi_{T_s}(t_0) \cdot \frac{r_R}{PG}. \quad (4.28)$$

So we have :

$$x = \frac{E_{RD}}{E_{SD}} = \frac{r_R}{PG} \cdot \left(\frac{A_{Relay}}{A_{Source}} \right)^2. \quad (4.29)$$

Our main purpose here is to measure the cooperation network performance in terms of BER as a function of the energy-noise ratio E_b/N_0 . Using the root-raised-cosine pulse shaping function $h_{T_s}(t)$ defined in Appendix 4.B, we have $\varphi_{T_s}(t_0) = 1$ and $\sigma_n^2 = N_0/4$. We will distinguish two energy scenarios :

Case A : The energy consumed by the relay is considered such that E_b is a function of both E_{SD} and E_{RD} .

Based on the BCH product code scheme shown in Fig.4.2, we have the following relation :

$$(k_S \times k_R) E_b = (K \times n_S) E_{SD} + (PG \times n_S) E_{RD}, \quad (4.30)$$

where $k_R = K = PG$. Substituting $E_{RD} = xE_{SD}$ into Eq.4.30, we obtain that :

$$E_b = \frac{(K \times n_S) E_{SD} + (PG \times n_S) xE_{SD}}{k_S \times k_R} = \frac{1+x}{R_S} \cdot E_{SD}, \quad (4.31)$$

where $R_S = k_S/n_S$ corresponds to the source code rate. Substituting Eq.4.27 into Eq.4.31, we can express E_b/N_0 as :

$$\frac{E_b}{N_0} = \frac{(1+x) \cdot E_{SD}}{R_S \cdot 4\sigma_n^2} = \frac{(1+x) \cdot (A_{Source})^2 \varphi_{T_s}(t_0)}{8R_S \cdot \sigma_n^2}. \quad (4.32)$$

Based on this relation, we can express the noise variance in Eq.4.26 on the AWGN channel :

$$\sigma_n^2 = \frac{(A_{Source})^2}{8 \frac{R_S}{1+x} \cdot \frac{E_b}{N_0}}, \quad (4.33)$$

where $x = \frac{E_{RD}}{E_{SD}} = \frac{r_R}{PG} \cdot \left(\frac{A_{Relay}}{A_{Source}} \right)^2$, A_{Relay} and A_{Source} are respectively the received amplitude of the relay and the source signal.

Case B : The relay is autonomous in energy so that E_b depends only on E_{SD} .

We investigate this case because it corresponds to a ‘self-powered’ relay scenario in a WSN. A self-powered relay usually has abundant low-cost energy, for example, the relay is equipped with a solar panel. The relay energy consumption is subordinate to that of the sensors. The network energy consumption is then dominated by the source transmission energy.

In this case, we measure the network BER as a function of only the energy used at the sources to transmit the TDMA signal. The relay CDMA received energy is not considered. Then we have the following relation :

$$(k_S \times k_R) E_b = (K \times n_S) E_{SD}. \quad (4.34)$$

Following the same steps as in Case A, we obtain the corresponding noise variance :

$$\sigma_n^2 = \frac{(A_{Source})^2}{8R_S \cdot \frac{E_b}{N_0}}. \quad (4.35)$$

4.4.5 Simulation results

In this section, we evaluate the error performance of the proposed cooperative network. We take an example using the BCH product code : BCH(64, 51)×BCH(32, 26). All channels are modeled as an AWGN channel. We focus on the performance of CDMA relay cooperation and assume that the source-relay channel is error-free, i.e., at the relay, there is no error in the detected source codewords.

4.4.5.1 BER measured with E_b including the energy received from R-D channel

In Fig. 4.11 and Fig. 4.12, we plot the network BER performance versus E_b/N_0 where E_b includes the energy received from R-D channel. We have considered different energy allocations between sources and relay. For the sake of clarity, we use two figures and each one corresponds to a group of energy allocations.

The curve labeled ‘BCH turbo (Ref)’ corresponds to the BER of the error-free relay cooperation using TDMA to schedule both the sources and the relay transmissions, which is the cooperation scheme described in the previous chapter. This curve serves as a reference here although it needs a little larger bandwidth than the proposed CDMA relay cooperation scheme. Another reference curve labeled ‘BCH (64, 51) soft’ corresponds to the soft decoding BER performance of the direct source-destination transmission without relay cooperation.

The other curves show the BER performance of the proposed CDMA relay cooperation scheme where the source transmissions are scheduled by TDMA. The source transmission and the relay transmission are co-existent and mutually interfering. A high transmission power of one part favors its own data reception, but it degrades the data reception of the other part. So we need to find a balance point that offers the optimal error performance.

In order to find the optimal energy allocation between the sources and the relay, we fix the received amplitude of the source signal $A_{Source} = 2$ and vary the relay amplitude A_{Relay} . Recall the relation between the relay CDMA power and the source TDMA power : $E_{RD} = \frac{(A_{Relay})^2}{2} \cdot \frac{r_R}{P_G} = xE_{SD}$. For various values of A_{Relay} , different BER performance curves associated with different relay energy are given in the two figures. The corresponding relay-source energy relation is denoted as ‘ $E_{RD} = x \cdot E_{SD}$ ’ in the legend.

By comparing the curves in the two figures, we observe that $E_{RD} = 0.9E_{SD}$ ($A_{Relay} \approx 1.97A_{Source}$) is the optimal configuration in the case where the relay energy consumption is taken into account. This curve is shown in Fig. 4.12 with the legend ‘ $E_{RD} = 0.9E_{SD}$ ’. Compared to the reference TDMA relay cooperation curve, the penalty to maintain the same RF bandwidth is about 2dB at a BER = 10^{-5} .

If the relay transmission power is too small, e.g. the curve ‘ $E_{RD} = E_{SD}/26$ ’ in Fig. 4.11, the network BER reasonably reduces to that of the soft decoding of source BCH codewords with no cooperation.

In the above two figures, some configurations of the CDMA relay cooperation exhibit

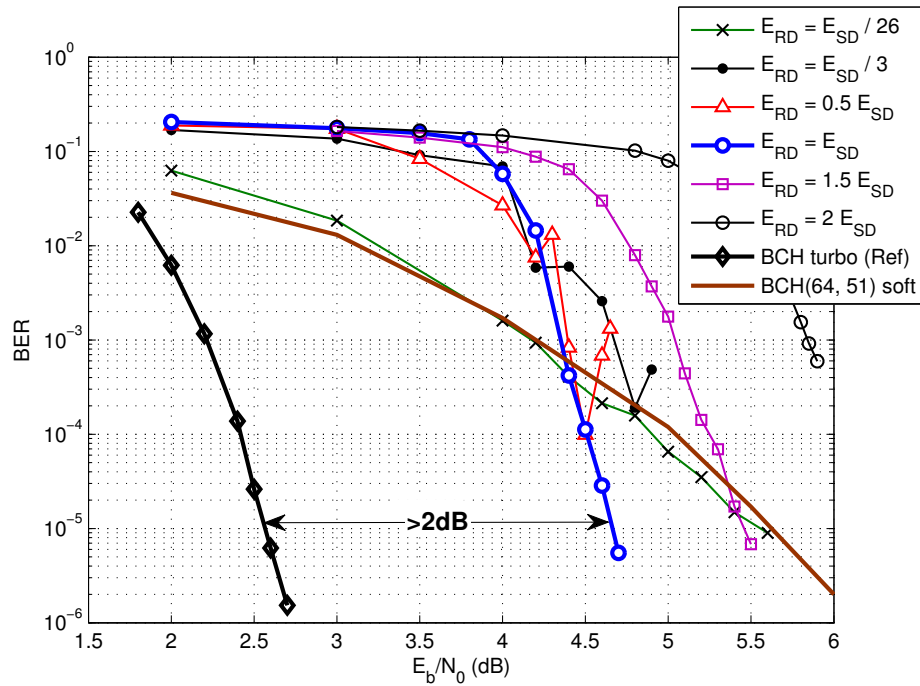


Figure 4.11 — BER versus E_b/N_0 of the CDMA-TDMA cooperation (part 1), BPSK, on the AWGN channel, E_b includes the energy from relay-destination channel.

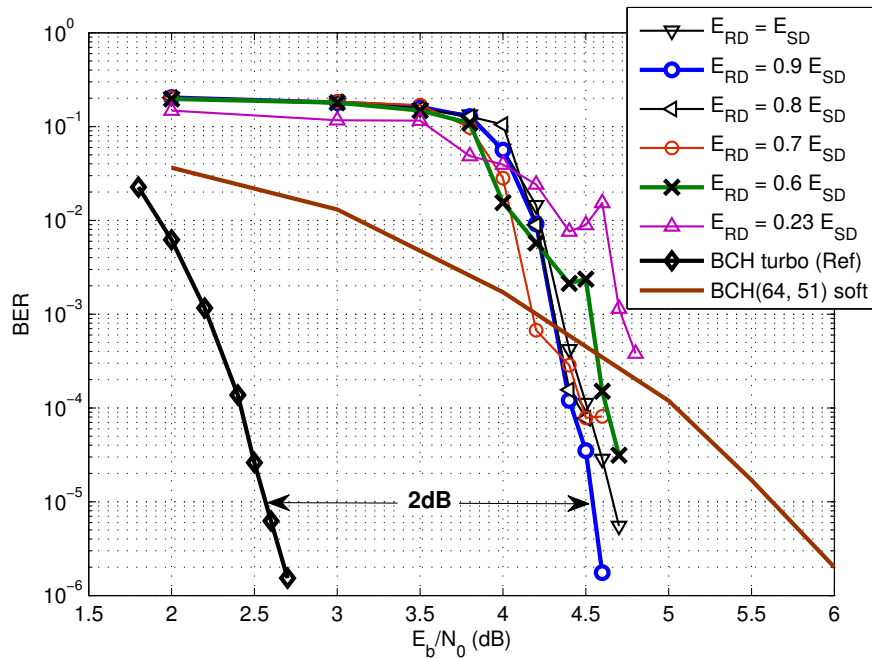


Figure 4.12 — BER versus E_b/N_0 of the CDMA-TDMA cooperation (part 2), BPSK, on the AWGN channel, E_b includes the energy from relay-destination channel.

an unstable BER performance, especially when $E_{RD} < 0.8E_{SD}$. It is caused by the high error probability ($> 1 \times 10^{-1}$) at the input of the turbo decoder in the detection of either the source TDMA data (26 source BCH codewords) or the relay CDMA data (6 relay codewords). We show the corresponding BER of the source and relay data parts in Fig. 4.13 for three configurations : $E_{RD} = E_{SD}/26$, $E_{RD} = E_{SD}/3$ and $E_{RD} = E_{SD}$.

In Fig. 4.13, only the configuration $E_{RD} = E_{SD}$ has both the source and relay parts BER less than 1×10^{-1} in the waterfall region of the turbo decoder. Each of the other two configurations has one part whose BER is too high to keep the turbo decoding stable.

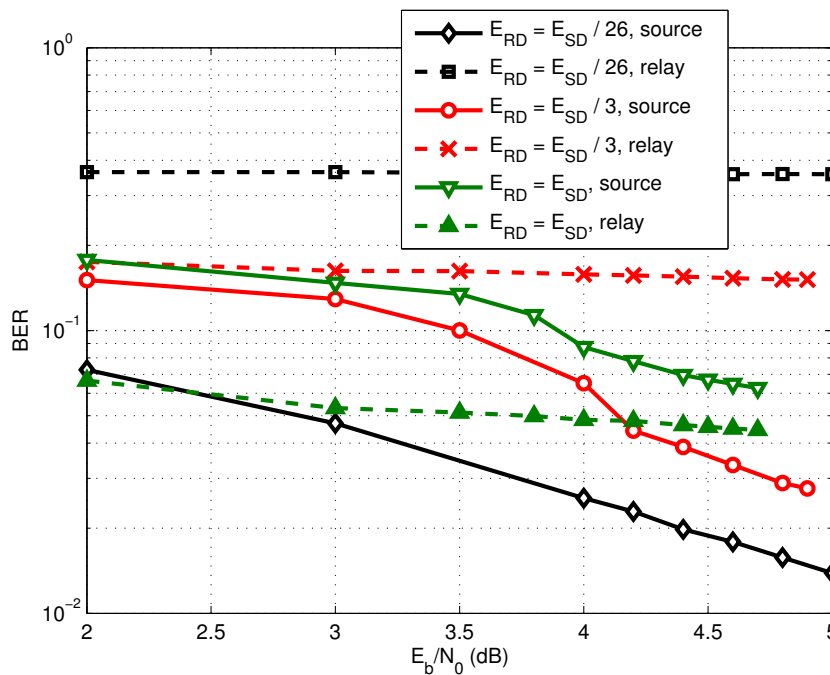


Figure 4.13 — High BER of the relay (CDMA) data part and of the source (TDMA) data part at the input of turbo decoder, BPSK, on the AWGN channel .

4.4.5.2 BER measured with the energy received from S-D channel

We consider this case if the relay has abundant low-cost energy, for example, the relay is equipped with a solar panel. The relay energy consumption is subordinate to that of the sensors. The network energy consumption is then restricted to the source transmission energy.

In Fig. 4.14, we show the network BER measured considering only the energy used by the sources. The noise variance is calculated using Eq. 4.35.

In the figure, we observe that $E_{RD} = 1.5E_{SD}$ ($A_{Relay} \approx 2.55A_{Source}$) is the optimized configuration if the relay energy consumption is neglected. This curve has a gain of about 4.1dB at $BER = 10^{-5}$ compared to the soft decoding BER of the source BCH codewords with no cooperation.

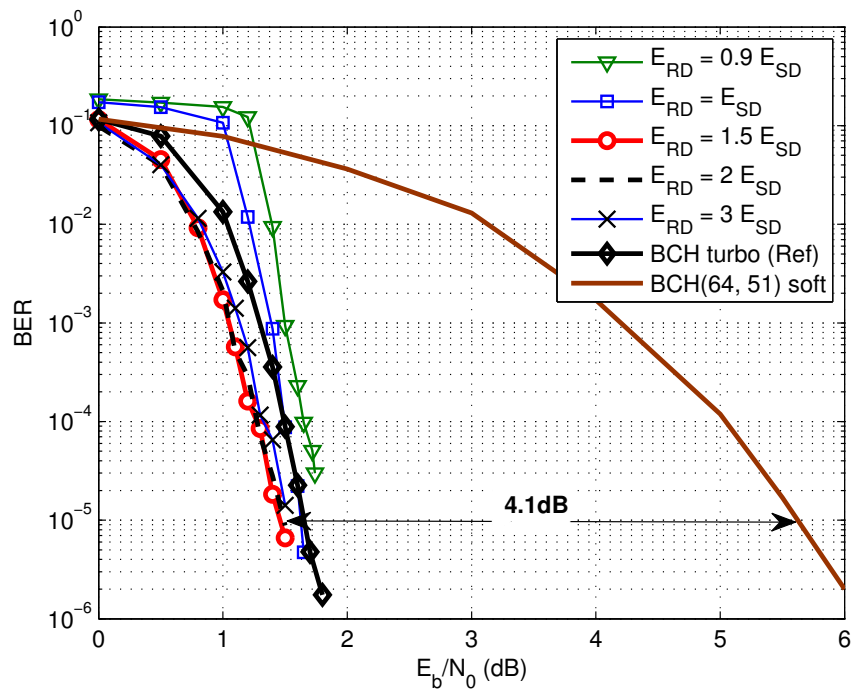


Figure 4.14 — BER versus E_b/N_0 of the CDMA-TDMA cooperation, BPSK, on the AWGN channel, E_b excludes the energy from relay-destination channel.

4.4.5.3 Data interleaving at the relay

We have introduced the iterative interference cancellation in Section 4.2. During the cancellation, i.e., the step (d) of the pseudo-code procedure, if there is one relay redundancy symbol in error in the decoded $\hat{\mathbf{R}}(0)$, the corresponding PG chips are also erroneous after the CDMA spreading. These PG errors are canceled from the source TDMA signals in an aggregated manner influencing PG successive TDMA bits, which may degrade the decoding performance. As a solution, we can use an interleaver at the relay to spread these errors. The interleaving is illustrated in Fig. 4.15.

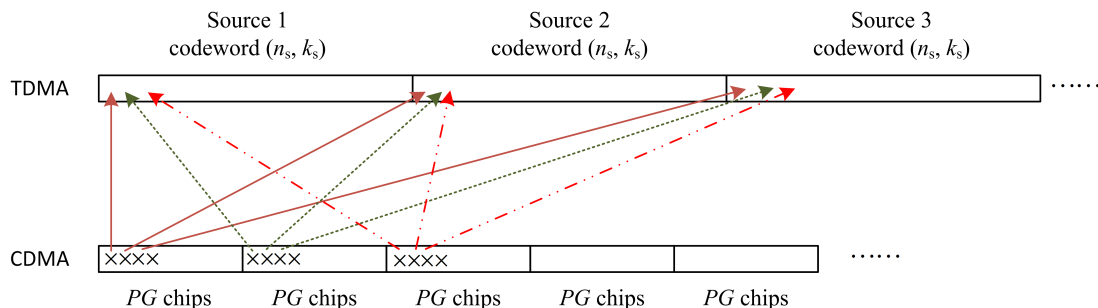


Figure 4.15 — Relay interleaving before the cancellation.

This interleaving is introduced before the relay CDMA transmission. Through such an interleaving, each one of the PG chips associated with the same column of the relay-generated redundancy is randomly distributed into one of the PG source TDMA

codewords. Since there is a whole frame delay for the relay transmission of the same data generation, no additional time delay is introduced by interleaving.

Using the proposed interleaving, we re-evaluate the simulated BER given in Fig. 4.16 and 4.17. In Fig. 4.16, we observe that the BER curve ‘ $E_{RD} = 0.5E_{SD}$ ’ becomes less unstable than in Fig. 4.11. In Fig. 4.17, there is no apparent improvement for $E_{RD} \geq 1.5E_{SD}$. When $E_{RD} \leq E_{SD}$, a minor improvement (0.2dB at BER = 6×10^{-2}) is observed at low / middle SNR region. The energy factor that leads to the optimal configuration remains unchanged.

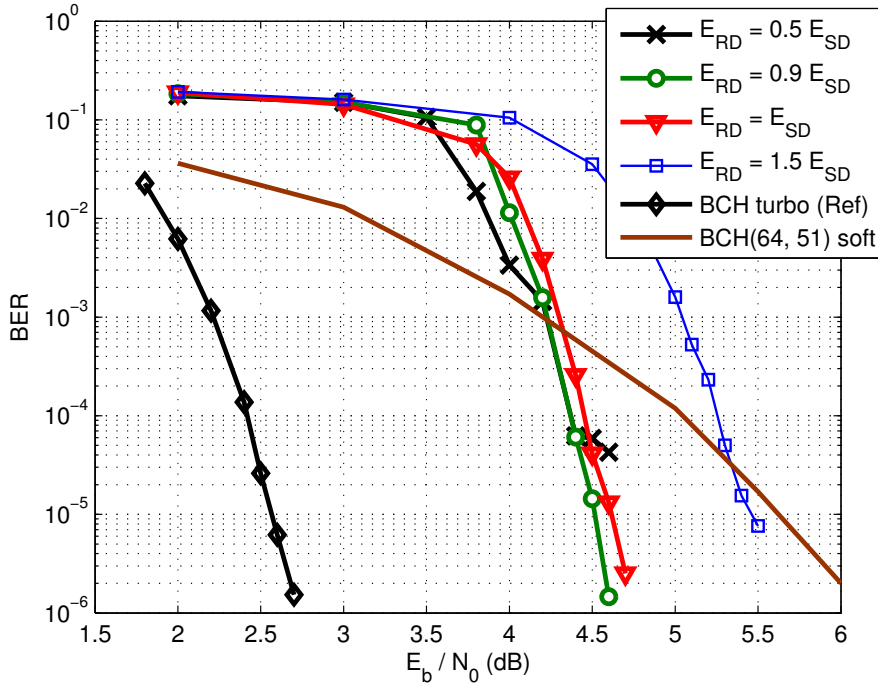


Figure 4.16 — BER versus E_b/N_0 of the CDMA-TDMA cooperation (relay-interleaved) BPSK, on the AWGN channel, E_b includes the energy from relay-destination channel.

4.4.5.4 Simulation results on the fast Rayleigh fading channel

In the case of fast Rayleigh fading, the received signal at the destination can be expressed by :

$$\vec{\mathbf{r}}_{(PG \times 1)}^{\text{TDM}} = A_{\text{Relay}} \cdot \mathbf{H}_{(PG \times PG)}^{(R)} \mathbf{S}_{(PG \times r_R)} \vec{\mathbf{d}}_{(r_R \times 1)}^{(R)} + A_{\text{Source}} \cdot \mathbf{H}_{(PG \times PG)}^{(S)} \vec{\mathbf{d}}_{(PG \times 1)}^{\text{TDM}} + \vec{\mathbf{n}}_{(PG \times 1)}, \quad (4.36)$$

where $\mathbf{H}^{(R)}$ (resp. $\mathbf{H}^{(S)}$) is the diagonal matrix of the fading coefficients on the R-D (resp. S-D) link. We assume all Rayleigh fading coefficients are normalized. After despreading, the matched filter output is given by :

$$\begin{aligned} \vec{\mathbf{y}}_{(r_R \times 1)} &= \mathbf{S}^T \cdot \vec{\mathbf{r}}_{(PG \times 1)}^{\text{TDM}} \\ &= A_{\text{Relay}} \cdot \mathbf{S}^T \mathbf{H}^{(R)} \mathbf{S} \cdot \vec{\mathbf{d}}^{(R)} + A_{\text{Source}} \cdot \mathbf{S}^T \mathbf{H}^{(S)} \cdot \vec{\mathbf{d}}^{\text{TDM}} + \mathbf{S}^T \cdot \vec{\mathbf{n}}. \end{aligned} \quad (4.37)$$

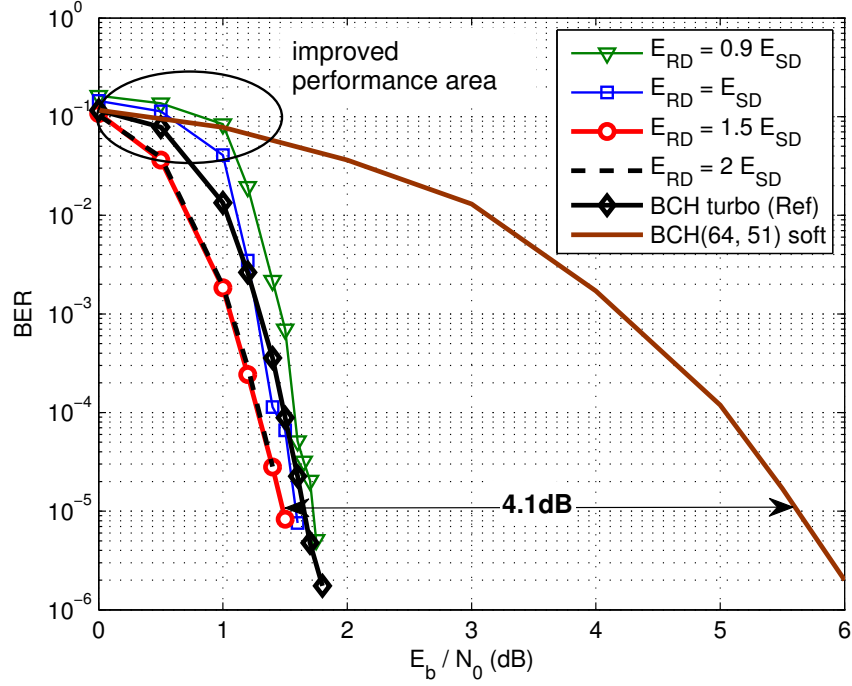


Figure 4.17 — BER versus E_b/N_0 of the CDMA-TDMA cooperation (relay-interleaved) BPSK, on the AWGN channel, E_b excludes the energy from relay-destination channel.

We model $\vec{y} - A_{Relay} \cdot \mathbf{S}^T \mathbf{H}^{(R)} \mathbf{S} \cdot \vec{d}^{(R)} = A_{Source} \cdot \mathbf{S}^T \mathbf{H}^{(S)} \cdot \vec{d}^{TDM} + \vec{n}_t$ as a zero-mean multivariate Gaussian variable. We can verify that :

$$\text{Cov}(\vec{n}_t) = \sigma_n^2 \cdot \mathbf{C}, \quad (4.38)$$

$$\begin{aligned} \text{Cov}\left(A_{Source} \cdot \mathbf{S}^T \mathbf{H}^{(S)} \cdot \vec{d}^{TDM}\right) &= A_{Source}^2 \cdot E\left(\mathbf{S}^T \mathbf{H}^{(S)} \cdot \vec{d}^{TDM} \cdot \vec{d}^{TDM, T} \cdot \mathbf{H}^{(S), T} \mathbf{S}\right) \\ &= A_{Source}^2 \cdot \mathbf{S}^T \cdot E(h^2) \cdot \sigma_1^2 \mathbf{I} \cdot \mathbf{S} = A_{Source}^2 \cdot \sigma_1^2 \mathbf{C}. \end{aligned} \quad (4.39)$$

So the covariance matrix of $\vec{y} - A_{Relay} \cdot \mathbf{S}^T \mathbf{H}^{(R)} \mathbf{S} \cdot \vec{d}^{(R)}$ is given by :

$$\mathbf{COV} = \text{Cov}\left(\vec{y}' - A_{Relay} \cdot \mathbf{C} \cdot \vec{d}^{(R)}\right) = (A_{Source}^2 \cdot \sigma_1^2 + \sigma_n^2) \mathbf{C}, \quad (4.40)$$

and the metric $M_{\vec{d}^i}$ (see Eq. 4.25) is given by :

$$\begin{aligned} M_{\vec{d}^i} &= \exp \left\{ \frac{2A_{Relay} \vec{y}'^T \mathbf{C}^{-1} (\mathbf{S}^T \mathbf{H}^{(R)} \mathbf{S}) \vec{d}^i - A_{Relay}^2 \vec{d}^{i, T} (\mathbf{S}^T \mathbf{H}^{(R)} \mathbf{S}) \mathbf{C}^{-1} (\mathbf{S}^T \mathbf{H}^{(R)} \mathbf{S}) \vec{d}^i}{2(A_{Source}^2 \sigma_1^2 + \sigma_n^2)} \right\}. \end{aligned} \quad (4.41)$$

Using the iterative interference cancelation and the data interleaving at the relay introduced previously, we obtain the network BER on the fast Rayleigh fading channels as shown in Fig. 4.18 and 4.19.

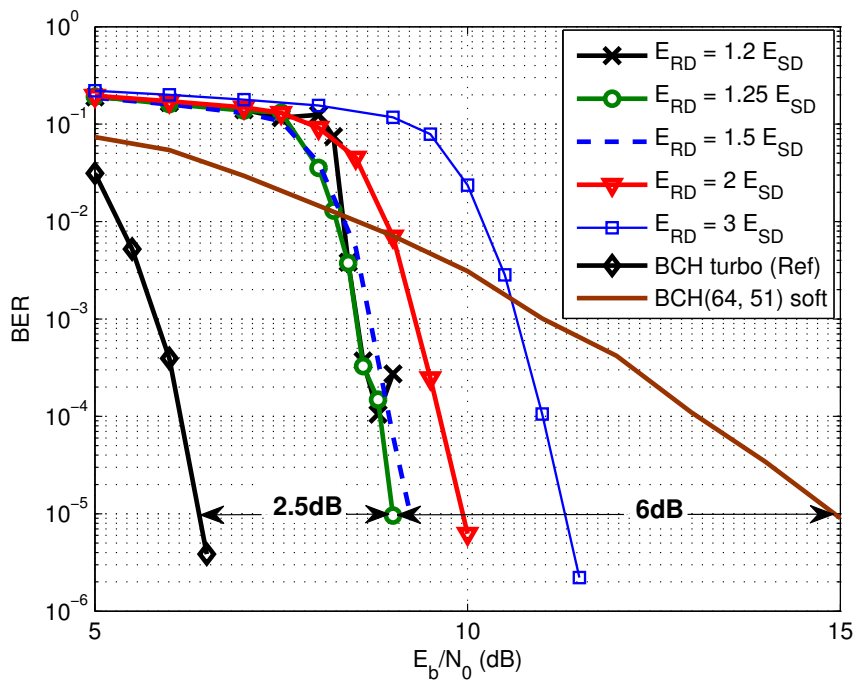


Figure 4.18 — BER versus E_b/N_0 of the CDMA-TDMA cooperation (relay-interleaved) BPSK, on the fast Rayleigh fading channel, E_b includes the energy from relay-destination channel.

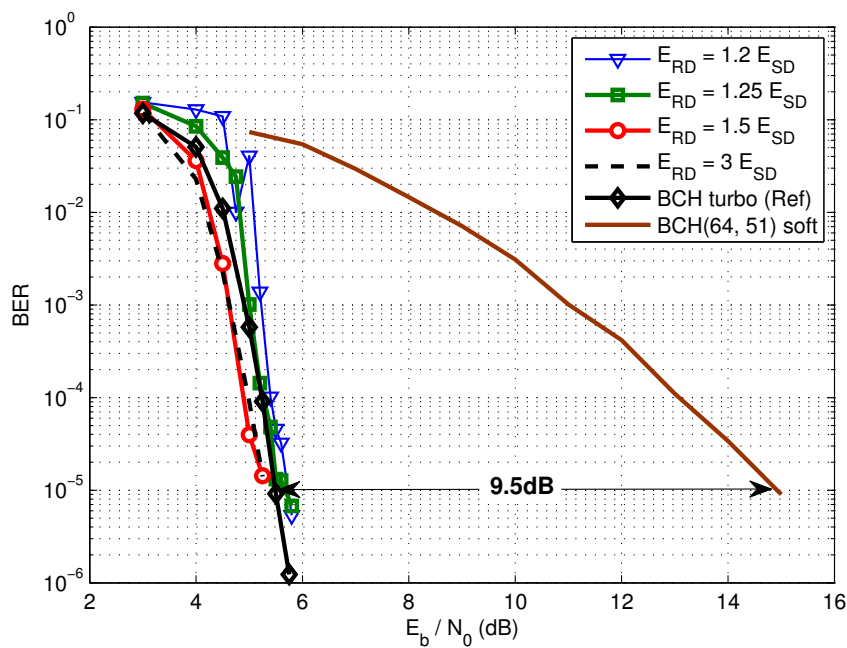


Figure 4.19 — BER versus E_b/N_0 of the CDMA-TDMA cooperation (relay-interleaved) BPSK, on the fast Rayleigh fading channel, E_b excludes the energy from relay-destination channel.

In Fig. 4.18, BER is measured with E_b including the energy received from R-D channel. ‘ $E_{RD} \leq 1.2E_{SD}$ ’ are non-stable configurations. ‘ $E_{RD} = 1.25E_{SD}$ ’ is the optimal energy allocation offering a coding gain of 6dB at $BER = 10^{-5}$.

In Fig. 4.19, BER is only measured with the energy received from S-D channel. ‘ $E_{RD} = 1.5E_{SD}$ ’ is the optimal energy allocation offering a coding gain of 9.5dB at $BER = 10^{-5}$.

4.5 Superposed FDMA-CDMA scheme

In this section, we study the superposed CDMA relay cooperation scheme with the sources operating in the FDMA mode.

4.5.1 Network configuration

The K sources transmit simultaneously on the K FDMA carrier frequencies. The source coded symbol duration is denoted $T_s^{(S)}$. The relay uses the single antenna CDMA transmission as described in Fig. 4.2. The relation between the duration of the relay redundancy symbol $T_s^{(R)}$ and the chip duration $T_{chip}^{(R)}$ is :

$$T_s^{(R)} = PG \cdot T_{chip}^{(R)}, \quad (4.42)$$

with the CDMA processing gain $PG = K$.

To align in time both the source and the relay transmissions, the symbol durations should satisfy the following relation :

$$T_s^{(S)} = T_s^{(R)} = PG \cdot T_{chip}^{(R)}. \quad (4.43)$$

Under this condition, the FDMA-CDMA multiple-access scheme associated with a product codeword is shown in Fig. 4.20 where the relay CDMA transmission is detailed in Fig. 4.2. The PSD of the source signal and the relay signal are shown in Fig. 4.21.

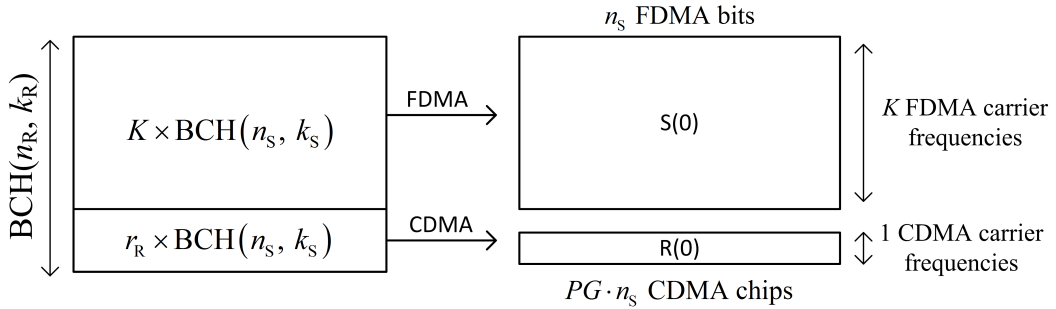


Figure 4.20 — Multiple access of the hybrid FDMA-CDMA scheme.

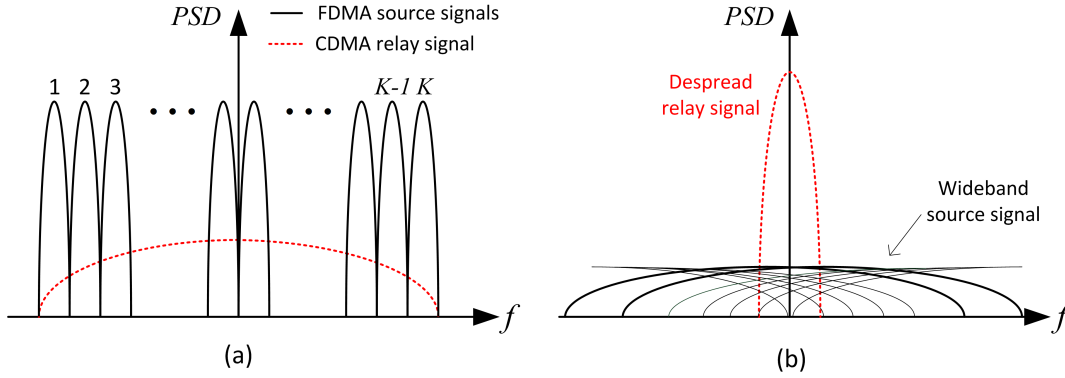


Figure 4.21 — Power spectral density of the source FDMA signal and the relay CDMA signal,
 (a) before despreading; (b) after despreading.

4.5.2 Block diagrams of the receiver

Besides the notations commonly used in this chapter, we introduce :

- $d_n^{(k)}$ is the n -th codeword symbol of the k -th source codeword, $d_n^{(k)} \in \{\pm 1\}$;
- $d_{i,n}^{(R)}$ is the n -th codeword symbol of the i -th relay-generated redundancy row in the product codeword, $d_{i,n}^{(R)} \in \{\pm 1\}$;
- $h_{T_c}(t)$ and $h_{T_s}(t)$ are the root-raised-cosine pulse shaping functions used in the modulation of the relay CDMA and source TDMA signals respectively. $T_c = T_{chip}^{(R)}$ and $T_s = T_s^{(S)}$. Their definition is given in Appendix 4.B.
- $\sum_m s_{i,m} h_{T_c}(t - mT_c)$ is the i -th full period ($(PG = K)$) spreading pulse shaping of the duration. $T_s^{(S)} = T_s^{(R)}$, $s_{i,m} \in \{\pm 1/\sqrt{PG}\}$;
- f_k is the k -th FDMA carrier frequency and f_c is the CDMA carrier frequency;

The received FDMA-CDMA signal at the destination is thus given by :

$$\begin{aligned}
 r(t) = & A_{Source} \sum_{k=0}^{K-1} \sum_n d_n^{(k)} h_{T_s}(t - nT_s^{(S)}) \cdot \cos(2\pi f_k t + \varphi_0) \\
 & \quad \text{(Source FDMA part)} \\
 & + A_{Relay} \sum_{i=0}^{r_R-1} \sum_n d_{i,n}^{(R)} \sum_{m=0}^{PG-1} s_{i,m} h_{T_c}(t - nT_s^{(R)} - mT_{chip}^{(R)}) \cdot \cos(2\pi f_c t + \varphi_0) \\
 & \quad \text{(Relay CDMA part)} \\
 & + n(t).
 \end{aligned} \tag{4.44}$$

The receiver at the destination is illustrated by the block diagrams in Fig. 4.22.

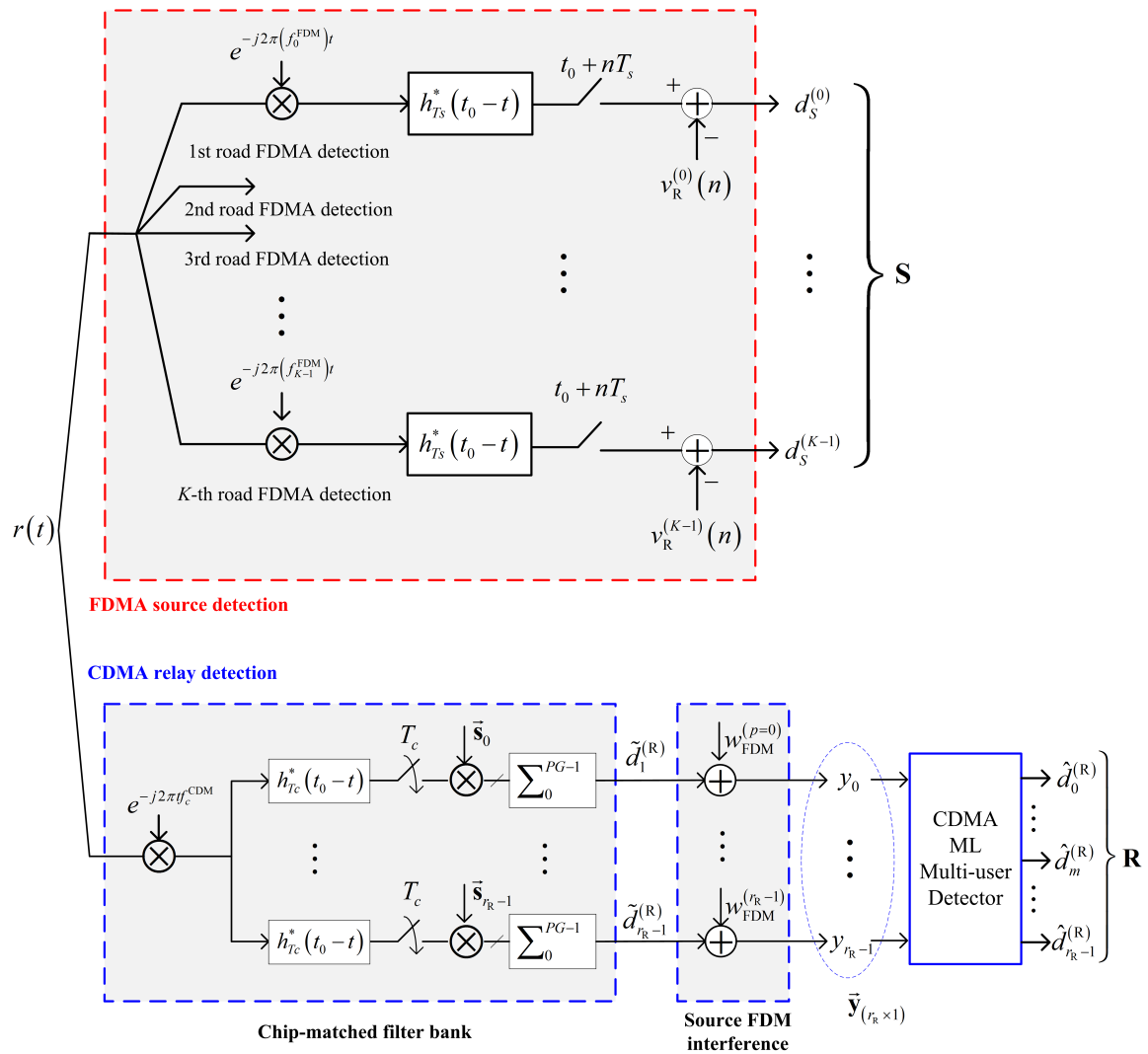


Figure 4.22 — Source and relay data detection at the destination.

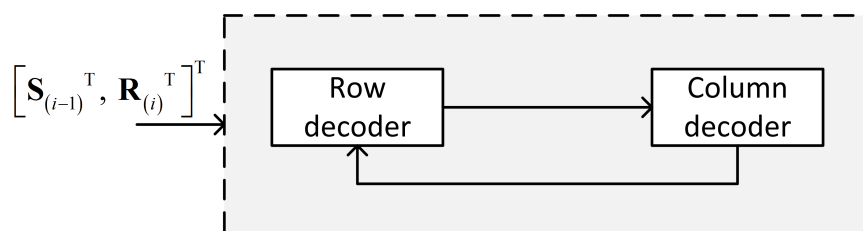


Figure 4.23 — Turbo decoding of the product codeword at the destination.

4.5.3 Relay-destination ML multi-user detection with FDMA interference

In the FDMA-CDMA network, although it is more difficult to model the interference than in the case of TDMA-CDMA network, the structure of the ML multi-user detection remains the same. In the following, we continue our analysis on the AWGN channel with BPSK modulation.

Contrary to the TDMA-CDMA network whose discrete vector-matrix model is simple and immediate to use, the FDMA-CDMA network needs a continuous-discrete analysis before getting the equivalent discrete baseband model. The continuous-discrete front-end of the ML multi-user detection is illustrated in Fig. 4.24.

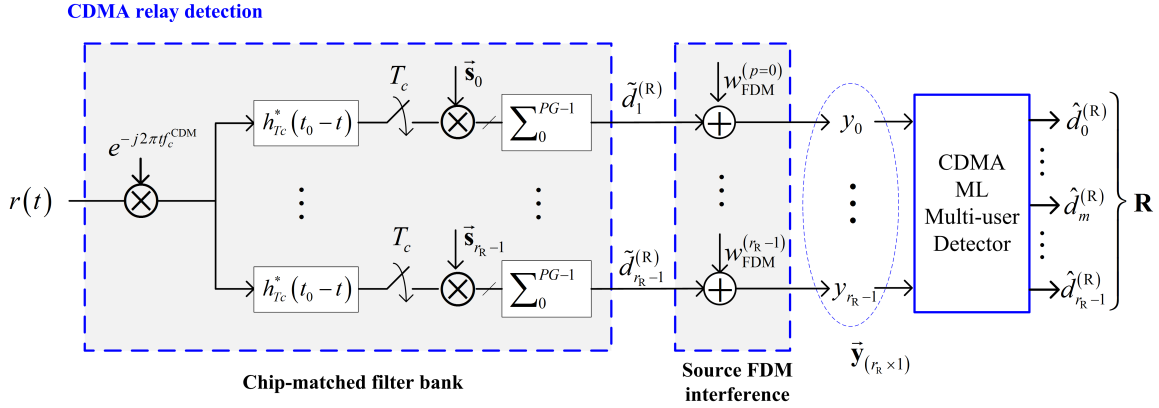


Figure 4.24 — Continuous-discrete front-end of the CDMA ML detection for the R-D transmitted symbols.

For the sake of concision, in the following we only use the main conclusion formulae. Their detailed derivation is given in Appendix 4.C.

We can formulate the symbol-level discrete variable at the output of the chip-matched filter bank (right after the despreading and summation of PG samples in Fig. 4.24) as (see Eq. 4.C.14 in Appendix 4.C) :

$$\tilde{d}_p^{(R)}(n') = \frac{A_{\text{Relay}}}{2} \cdot \left[d_{p,n'}^{(R)} + \sum_{\substack{i=0 \\ i \neq p}}^{r_R-1} d_{j,n'}^{(R)} \left(\sum_{m'=0}^{PG-1} s_{i,m'} s_{p,m'} \right) \right] \cdot \varphi_{T_c}(t_0). \quad (4.45)$$

In Fig. 4.24, the source FDMA interference on the p -th CDMA detection branch is denoted $w_{\text{FDM}}^{(p)}$, with $p = 0, 1, \dots, r_R - 1$. Its value is given by (see Eq. 4.C.17 in Appendix 4.C) :

$$w_{\text{FDM}}^{(p)} = \sqrt{T_c} \frac{A_{\text{Source}}}{2} \sum_{m'=0}^{PG-1} s_{p,m'} \sum_{k=0}^{K-1} \sum_n d_n^{(k)} h_{T_s}((n' - n)T_s + m'T_c) \cdot e^{j2\pi(f_k^{\text{FDM}} - f_c^{\text{CDM}})(n'T_s + m'T_c)}, \quad (4.46)$$

whose variance (see Eq. 4.C.18 in Appendix 4.C) is :

$$\begin{aligned} Var \left(w_{\text{FDM}}^{(p)} \right) &= E \left(\left| w_{\text{FDM}}^{(p)} \right|^2 \right) \\ &= \frac{T_c}{PG} \cdot \frac{(A_{\text{Source}})^2}{4} \cdot \sum_{k=0}^{PG-1} \sum_{m'=0}^{PG-1} \sum_{n=0}^{N-1} [h_{T_s} ((n' - n) T_s + (m' + 1) T_c)]^2. \end{aligned} \quad (4.47)$$

In the case of BPSK, we only use the real part of the FDMA interference with half of the above variance.

Similar to Eq. 4.18 in the TDMA-CDMA network, we can model the discrete received signal with FDMA interference as :

$$\mathbf{r}_{(PG \times 1)}^{\text{FDM}} = A_{\text{Relay}} \cdot \mathbf{S}_{(PG \times r_R)} \cdot \mathbf{d}_{(r_R \times 1)}^{(\text{R})} + A_{\text{Source}} \cdot \mathbf{w}_{(PG \times 1)}^{\text{FDM}} + \mathbf{n}_{(PG \times 1)}, \quad (4.48)$$

where we suppose the PG elements of source interference $\mathbf{w}_{(PG \times 1)}^{\text{FDM}}$ are i.i.d.

The destination de-spreads the signal \mathbf{r}^{FDM} by correlation with local spreading sequences yielding the vector $\mathbf{y}'_{(r_R \times 1)}$:

$$\begin{aligned} \mathbf{y}'_{(r_R \times 1)} &= \mathbf{S}^T \cdot \mathbf{r}_{(PG \times 1)}^{\text{FDM}} \\ &= A_{\text{Relay}} \cdot \mathbf{S}_{(r_R \times PG)}^T \cdot \mathbf{S}_{(PG \times r_R)} \cdot \mathbf{d}_{(r_R \times 1)}^{(\text{R})} \\ &\quad + A_{\text{Source}} \cdot \mathbf{S}_{(r_R \times PG)}^T \cdot \mathbf{w}_{(PG \times 1)}^{\text{FDM}} + \mathbf{S}_{(r_R \times PG)}^T \cdot \mathbf{n}_{(PG \times 1)} \\ &= A_{\text{Relay}} \cdot \mathbf{C}_{(r_R \times r_R)} \cdot \mathbf{d}_{(r_R \times 1)}^{(\text{R})} + A_{\text{Source}} \cdot \mathbf{w}_{\mathbf{t}(r_R \times 1)}^{\text{FDM}} + \mathbf{n}_{\mathbf{t}(r_R \times 1)}. \end{aligned} \quad (4.49)$$

The p -th element of vector $\mathbf{w}_{\mathbf{t}}^{\text{FDM}}$ is the $w_{\text{FDM}}^{(p)}$ given in Eq. 4.46 hence we get the corresponding covariance matrix :

$$Cov \left(\mathbf{w}_{\mathbf{t}}^{\text{FDM}} \right) = E \left(\mathbf{w}_{\mathbf{t}}^{\text{FDM}} \cdot \left(\mathbf{w}_{\mathbf{t}}^{\text{FDM}} \right)^T \right) = \sigma_W^2 \cdot \mathbf{I}_{(r_R \times r_R)}, \quad (4.50)$$

where $\mathbf{I}_{(r_R \times r_R)}$ is the identity matrix and $\sigma_W^2 = Var \left(w_{\text{FDM}}^{(p)} \right)$ is given in Eq. 4.47.

We can verify that $\mathbf{w}_{\mathbf{t}}^{\text{FDM}}$ follows a zero-mean Gaussian distribution (see Appendix 4.D). We model $\mathbf{y}' - A_{\text{Relay}} \cdot \mathbf{C} \cdot \mathbf{d}^{(\text{R})} = A_{\text{Source}} \cdot \mathbf{w}_{\mathbf{t}(r_R \times 1)}^{\text{FDM}} + \mathbf{n}_{\mathbf{t}(r_R \times 1)}$ as a multivariate Gaussian variable. Its covariance matrix is :

$$\mathbf{COV} = Cov \left(\mathbf{y}' - A_{\text{Relay}} \cdot \mathbf{C} \cdot \mathbf{d}^{(\text{R})} \right) = Cov \left(\mathbf{w}_{\mathbf{t}}^{\text{FDM}} \right) + Cov \left(\mathbf{n}_{\mathbf{t}} \right) = \sigma_W^2 \cdot \mathbf{I}_{(r_R \times r_R)} + \sigma_n^2 \cdot \mathbf{C}. \quad (4.51)$$

The ML detector calculates the soft decision LLR of the relay transmitted symbols in $\mathbf{d}^{(\text{R})}$ as :

$$\Lambda \left(d_k^{(\text{R})} \right) = \ln \frac{\sum_{\mathbf{d}^i \in \text{set}\{+1\}} p \left(\mathbf{y}' \mid \mathbf{d}^{(\text{R})} = \mathbf{d}^i \right)}{\sum_{\mathbf{d}^i \in \text{set}\{-1\}} p \left(\mathbf{y}' \mid \mathbf{d}^{(\text{R})} = \mathbf{d}^i \right)} = \ln \frac{\sum_{\mathbf{d}^i \in \text{set}\{+1\}} M_{\mathbf{d}^i}}{\sum_{\mathbf{d}^i \in \text{set}\{-1\}} M_{\mathbf{d}^i}}, \quad (4.52)$$

where the metric $M_{\mathbf{d}^i}$ is given by :

$$M_{\mathbf{d}^i} = \exp \left\{ -\frac{1}{2} \left(\mathbf{y}' - A_{\text{Relay}} \cdot \mathbf{C} \mathbf{d}^{(\text{R})} \right)^T \left(\mathbf{COV} \right)^{-1} \left(\mathbf{y}' - A_{\text{Relay}} \cdot \mathbf{C} \mathbf{d}^{(\text{R})} \right) \right\}. \quad (4.53)$$

4.5.4 Discrete FDMA source detection model with CDMA interference

The discrete FDMA source detection model will be useful in the cancelation step in the iterative decoding procedure where the CDMA interference should be subtracted from the received signal. We can derive the discrete model as :

$$\begin{aligned}
 d_S^{(k)}(n') &= \frac{A_{Source}}{2} d_{n'}^{(k)} \\
 &+ \sqrt{T_c} \frac{A_{Relay}}{2} \sum_{i=0}^{r_R-1} \sum_n d_{i,n}^{(R)} \sum_{m=0}^{PG-1} s_{i,m} h_{T_s}((n' - n) T_s - m T_c) e^{-j2\pi(f_c^{CDM} - f_k^{FDM})n' T_s} \\
 &+ n_\eta,
 \end{aligned} \tag{4.54}$$

where $d_S^{(k)}(n')$ is the source symbol-level decision variable of the received signal and $d_{n'}^{(k)}$ is the n' -th symbol of the k -th FDMA source transmission. The second term in the equation corresponds to the CDMA interference coming from the CDMA relay transmission. The detailed derivation of Eq. 4.54 is given in Eq. 4.C.3, 4.C.9 and 4.C.11 in Appendix 4.C.

We cancel the interference coming from the relay in Eq. 4.54 by subtracting the recovered CDMA interference term based on the regenerated $\hat{d}_{i,n}^{(R)}$, i.e. elements of \hat{R} (0) in the step (c) of the iterative decoding procedure. Note that $\hat{d}_{i,n}^{(R)}$ may be erroneous.

4.5.5 Energy scenarios

In the FDMA-CDMA cooperative network, the average received energy on the source-destination link in the duration of $T_s^{(S)}$ is defined as E_{SD} . The average received energy on the relay-destination link in the duration of $T_s^{(R)} = T_s^{(S)} = PG \cdot T_{chip}^{(R)}$ is defined as E_{RD} .

We can derive (see Appendix 4.E) that :

$$E_{SD} = \frac{(A_{Source})^2}{2} \cdot K \cdot \varphi_{T_s^{(S)}}(t_0). \tag{4.55}$$

$$E_{RD} = P_{RD}^{(R)} \cdot T_s^{(R)} = \frac{(A_{Relay})^2}{2} \cdot r_R \cdot \varphi_{T_c}(t_0). \tag{4.56}$$

The energy ratio x of E_{RD} to E_{SD} is :

$$x = \frac{E_{RD}}{E_{SD}} = \frac{r_R}{K} \cdot \left(\frac{A_{Relay}}{A_{Source}} \right)^2. \tag{4.57}$$

We distinguish two energy configurations as in the case of FDMA-CDMA cooperative network :

Case A : The energy consumed by the relay is considered such that E_b is a function of both E_{SD} and E_{RD} .

Based on the BCH product code scheme shown in Fig. 4.2, we have the following relation :

$$(k_S \times k_R) E_b = n_S E_{SD} + n_S E_{RD}, \quad (4.58)$$

where $k_R = K = PG$. Substituting $E_{RD} = x E_{SD}$ into Eq. 4.58, we obtain that :

$$E_b = \frac{n_S E_{SD} + n_S x E_{SD}}{k_S \times k_R} = \frac{1+x}{R_S \cdot k_R} \cdot E_{SD}, \quad (4.59)$$

where $R_S = k_S/n_S$ corresponds to the source code rate. So we can express E_b/N_0 as :

$$\frac{E_b}{N_0} = \frac{(1+x) \cdot E_{SD}}{R_S \cdot k_R \cdot 4\sigma_n^2} = \frac{(1+x) \cdot (A_{Source})^2 \cdot \varphi_{Ts}(t_0)}{8R_S \cdot \sigma_n^2}. \quad (4.60)$$

Based on this relation, we can express the noise variance in Eq. 4.60 on the AWGN channel :

$$\sigma_n^2 = \frac{(A_{Source})^2}{8 \frac{R_S}{1+x} \cdot \frac{E_b}{N_0}}, \quad (4.61)$$

where $x = \frac{E_{RD}}{E_{SD}} = \frac{r_R}{K} \left(\frac{A_{Relay}}{A_{Source}} \right)^2$, A_{Relay} and A_{Source} are respectively the received amplitude of the relay and the source signal.

Case B : The relay is autonomous on energy so that E_b depends only on E_{SD} .

In this case, we measure the network BER as a function of only the energy used at the sources to transmit the TDMA signal. The relay CDMA received energy is not considered. Then we have the following relation :

$$(k_S \times k_R) E_b = n_S E_{SD}. \quad (4.62)$$

Following the same steps as in Case A, we obtain the corresponding noise variance :

$$\sigma_n^2 = \frac{(A_{Source})^2}{8R_S \cdot \frac{E_b}{N_0}}. \quad (4.63)$$

σ_n^2 is used to generate the noise variable in the source-destination treatment (n_η in Eq. 4.54) and in relay-destination treatment (elements of $\vec{\mathbf{n}}_{\mathbf{t}(6 \times 1)}$ in Eq. 4.49). These two kinds of noise variables have equal variance because we have two normalizations : the normalized root-raised cosine filter and the normalized spreading sequence. The detailed explanation is given in Appendix 4.C after Eq. 4.C.19.

4.5.6 Simulation results

In the simulation of FDMA-CDMA cooperative network, we use the same BCH product code scheme example as in the case of TDMA-CDMA. The source code is BCH (64, 51) and the relay code is BCH (32, 26). All channels are modeled as an AWGN channel. We focus on the performance of CDMA relay cooperation and assume that the source-relay channel is error-free.

4.5.6.1 BER measured with E_b including the energy received from R-D channel

In Fig. 4.25, we plot the network BER performance versus E_b/N_0 where E_b includes the energy received from the R-D channel.

The purpose here is to find an optimum source to relay energy ratio for optimal network error performance. With the fixed source transmission power, we plot different BER curves associated with different relay powers.

We find that the configuration $E_{RD} = (6/13) E_{SD}$ ($A_{Relay} \approx 1.4A_{Source}$) is the optimum value if the relay energy consumption is considered. It corresponds to the curve marked with circles. The coding gain is of about 1.9dB at $BER = 10^{-5}$ versus the soft decoding performance of source codewords.

In the figure, there are some unstable curves, e.g., when $E_{RD} < (6/13) E_{SD}$. It is caused by the high error rates ($> 1 \times 10^{-1}$) either in the FDMA part ($K = 26$ source BCH codewords) or in the CDMA part ($r_R = 6$ relay codewords) at the input of the turbo decoder.

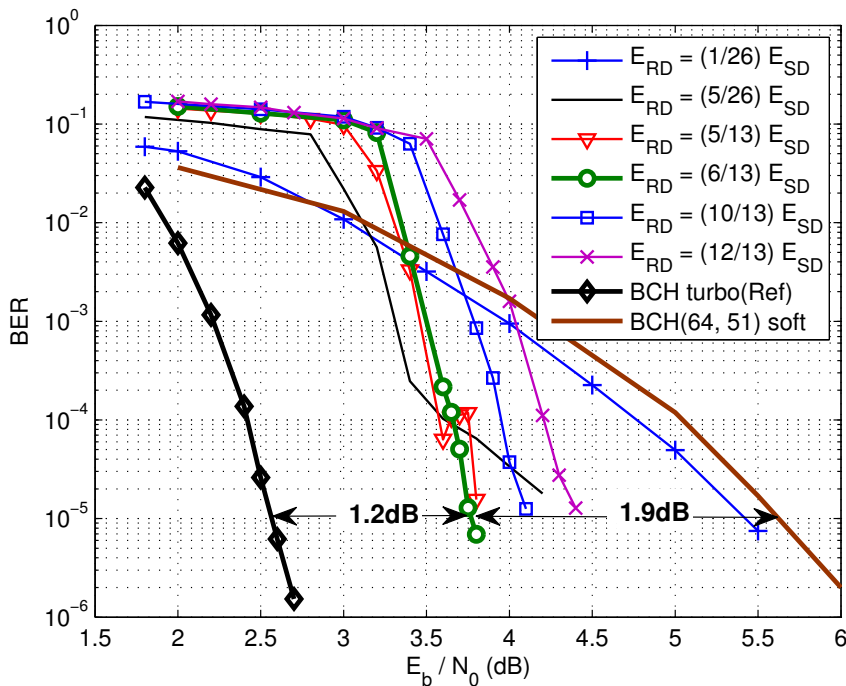


Figure 4.25 — BER versus E_b/N_0 of the FDMA-CDMA cooperation, BPSK modulation on the AWGN channel, E_b includes the energy from relay-destination channel.

4.5.6.2 BER measured with the energy received from S-D channel

In Fig. 4.26, we show the network BER measured with only the energy used at the sources to transmit the FDMA signal.

We observe that the configuration $E_{RD} = (17/13)E_{SD}$ ($A_r \approx 2.4A_s$) is the best

value if the relay energy consumption is not considered. The corresponding BER curve marked with hollow circles has a gain of about 4dB at $\text{BER} = 10^{-5}$.

At high SNR, the value of E_{RD} between $(10/13)E_{\text{SD}}$ and $(48/13)E_{\text{SD}}$ has similar BER performance, so we can choose the smallest $E_{\text{RD}} = (10/13)E_{\text{SD}}$ ($A_r \approx 1.8A_s$) as the optimized solution.

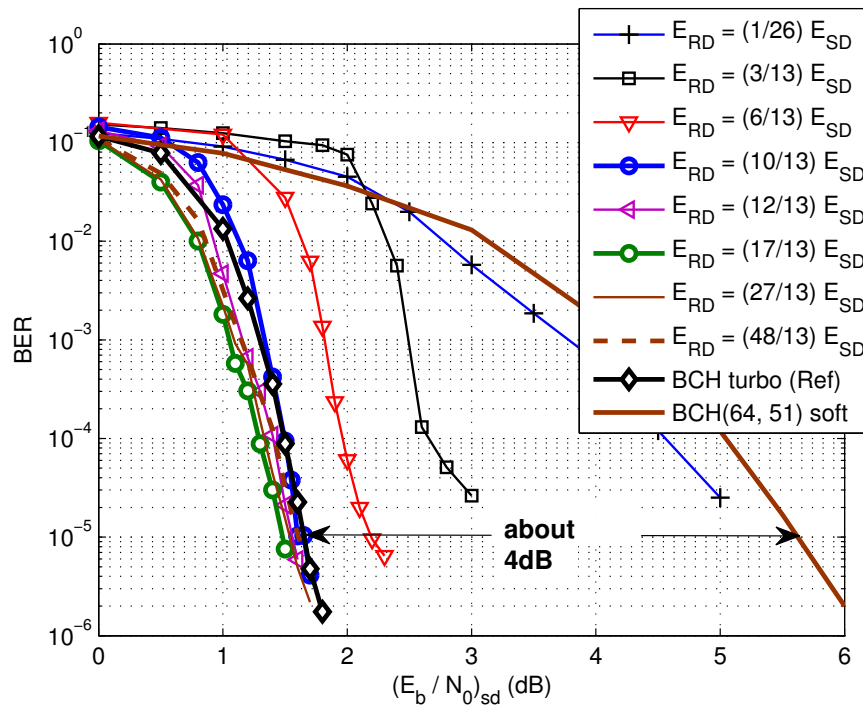


Figure 4.26 — BER versus E_b/N_0 of the FDMA-CDMA cooperation, BPSK modulation on the AWGN channel, E_b excludes the energy from relay-destination channel.

4.5.7 Comparison of TDMA-CDMA and FDMA-CDMA schemes

The value of E_{SD} and E_{RD} depends on the observation time durations. In order to simplify the analysis, we have chosen different time durations in TDMA-CDMA and FDMA-CDMA cooperative schemes. In this section, we need to compare the performance of TDMA-CDMA and FDMA-CDMA cooperative networks under comparable conditions. So we introduce two unified energy notations :

$E_s^{(k)}$: Average received energy per codeword bit on the source-destination link contributed by the k -th source ;

$E_s^{(\text{RG})}$: Average received energy per *relay-generated* codeword bit on the relay-destination link ;

These two notations are pertinent energy measurements for both TDMA-CDMA and FDMA-CDMA cooperative networks.

In the TDMA-CDMA scheme, we can verify that :

$$E_s^{(k)} = E_{SD}. \quad (4.64)$$

$$E_s^{(RG)} = E_{RD}. \quad (4.65)$$

In the FDMA-CDMA scheme :

$$E_s^{(k)} = \frac{E_{SD}}{K}. \quad (4.66)$$

$$E_s^{(RG)} = \frac{E_{RD}}{r_R}. \quad (4.67)$$

Based on these relations, we establish the following tables according to two different energy configurations.

| | $E_b = f_1(E_{SD}, E_{RD})$ | Coding gain at BER = 10^{-5} |
|-----------|-----------------------------|--------------------------------|
| TDMA-CDMA | $E_s^{(RG)} = 3.9E_s^{(k)}$ | 1.2 dB |
| FDMA-CDMA | $E_s^{(RG)} = 2E_s^{(k)}$ | 1.9 dB |

TABLE 4.1 — Comparison of two cooperative schemes in the case of E_b including the energy from relay-destination channel, BPSK on AWGN channel

| | $E_b = f_2(E_{SD})$ | Coding gain at BER = 10^{-5} |
|-----------|-----------------------------|--------------------------------|
| TDMA-CDMA | $E_s^{(RG)} = 6.5E_s^{(k)}$ | 4 dB |
| FDMA-CDMA | $E_s^{(RG)} = 5.6E_s^{(k)}$ | 4 dB |

TABLE 4.2 — Comparison of two cooperative schemes in the case of E_b excluding the energy from relay-destination channel, BPSK on AWGN channel

In the case of E_b including the energy coming from relay-destination channel, both cooperative schemes offer a limited coding gain less than 2dB at BER = 10^{-5} . The FDMA-CDMA scheme offers a higher coding gain with a lower relay energy consumption than the TDMA-CDMA scheme.

In the case of E_b excluding the energy from relay-destination channel, we obtain the same coding gain in both cooperative schemes. This coding gain is as high as 4dB. The relay consumption of FDMA-CDMA scheme has a small advantage over the TDMA-CDMA scheme.

The short-coming of the FDMA-CDMA scheme is a more complex receiver at the destination, but it is not a big problem in WSN applications where the complexity and energy constraints are usually limited to the sensor side.

4.6 Conclusion and perspectives

In this chapter, we have analyzed two relay cooperation schemes using the CDMA technique. It is an extension of the TDMA multi-source relay cooperation based on turbo product code in the previous chapter.

In an already deployed wireless sensor network, if additional bandwidth is available, the relay cooperation using the TDMA technique offers good error probability performance at the cost of a small portion of band expansion but we have to modify the existing sensors. If there is no additional bandwidth available or the modification of sensors is prohibitive, then we can choose to reuse the source-destination band for the relay transmission, which is the case of the CDMA relay cooperation.

Compared with the TDMA relay cooperation with bandwidth expansion, we find that the CDMA relay cooperation proposed here only offers a limited coding gain at the high SNR region when the network error performance is measured with the received energy including that coming from the relay. In practical situations where the relay energy is not limited, the CDMA relay cooperation offers a coding gain similar to that in the TDMA relay cooperation case. So it is a valuable solution without using additional bandwidth or modifying the sensors.

For the choice between TDMA-CDMA and FDMA-CDMA cooperative scheme, it depends on the deployed WSN applications. The FDMA-CDMA scheme offers a little better performance in terms of error probability and the consumption of relay energy.

To conclude this chapter, we give some perspectives on the extension of our study :

1. Derivation of the theoretical optimal energy allocation ratio $x = \frac{E_{RD}}{E_{SD}}$;
2. Extension the theoretical and simulation results to the Rayleigh fading channel ;
3. Multi-antenna transmission and reception at the relay and destination.

Conclusion

In this thesis, we studied the performance of the multi-source relay cooperative networks where linear algebraic Network Coding is applied at the relay.

At first, we have introduced the basic notions of Network Coding, especially for its potential benefits and known difficulties in the case of error-prone wireless applications. After a brief recall of the fundamental knowledge about wireless communications and the information theory, we introduced the base of our study : the multi-source relay cooperative scheme proposed in [PGA10] in the WSN configuration. This scheme functions in the TDMA or FDMA mode. The sources are sensors with limited energy and use the same short-length systematic linear block code. The linear algebraic Network Coding is applied to the detected source codewords through the use of a systematic linear block code at the relay. The destination observes a product codeword by combining the source codewords and the relay-generated redundancy. The turbo decoding at the destination considers the residual errors in the relay detection. High coding gain has been obtained without introducing excessive transmission delays which is usually associated with the long-code turbo encoding at the sources.

The main contributions of this thesis are presented as follows :

Based on the proposed cooperative scheme [PGA10], we have theoretically analyzed the bit error probability at the input and output of the relay encoder on the fast Rayleigh fading channel. Three relay detection strategies : the bit-by-bit hard detection, hard decoding and soft decoding, have been considered. After the relay encoding, we have proved that the bit error probability is amplified for the different relay strategies. The amplification factor is independent of the relay receiver strategy and depends on the relay code.

We have also established a theoretical frame error probability bound for the proposed cooperative network in the case of using soft decoding at the relay. We have proved that the dominant error event at high SNR regime is caused by the error pattern at the relay associated with only one erroneous row in the detected source codewords matrix. Different bounds are derived as a function of source-relay channel conditions on both the AWGN and the fast Rayleigh fading channels. The theoretical results have been verified by simulations and can be used to predict the network error performance without using the time consuming simulations.

Thereafter, we have studied the mitigation of relay residual errors by using the LLR limitation in the turbo decoding. The theoretical LLR limiter derived in [PGA10] is

optimal in the case of i.i.d relay errors. We have shown that, for the three different relay detection strategies, the relay-generated errors are correlated. The corresponding network BER performance exhibits an error floor. To reduce this phenomenon, we have considered the use of multiple relays. Two de-correlation methods are proposed as the row-wise division and the pseudo-random selection of the redundancy sent by the relays to the destination. We have compared different cooperation strategies (single or multiple relays using different relay detection strategies) as a function of the source-relay link quality. By using the multi-relay cooperation with pseudo-random selection, the scheme is efficient especially for a high correlation degree, which corresponds to a poor source-relay configuration. The multiple relays involve multiple de-modulation / decoding of source codewords, which is more complex than the single-relay cooperation using soft decoding. We have concluded that for all practical applications, the single-relay cooperation using soft decoding at the relay achieves the best trade-off between bit error rate and complexity. For very poor source-relay link conditions, we can increase the test pattern number in the Chase soft decoding algorithm or use multi-relay cooperation. In the multi-relay case, the pseudo-random selection yields better decorrelation performance.

Through analyzing the cooperative scheme, we have found that the source-relay link is actually the network bottleneck. Since the sources use the short-length linear block code, we have thus evaluated the network capacity in the finite code-length regime. Based on [PPV10], we have proposed an upper bound on the rate of the binary-input Gaussian channel with finite code-length constraint. Using this result, we have derived the achievable rate for the proposed cooperative network based on the methods proposed in [KSA03b, YGiA10]. By comparing the achievable rate bound and the operational points of the cooperative scheme based on BCH product codes, we have shown that the proposed scheme is quasi-optimal in terms of information transmission.

As an extension of the TDMA-scheduled multi-source cooperative scheme, we have further studied the CDMA-based relay cooperation. We have considered that the relay transmission occupies the same RF band as the source transmissions. The relay-generated redundancy is transmitted to the destination in the synchronous CDMA mode by using a set of near-orthogonal spreading sequences. The sources can use either the TDMA or the FDMA transmission mode. The signals coming from the sources and from the relay are superposed at the destination and are mutually interfering. We have presented a turbo decoding procedure including the interference cancelation. We have evaluated the error performance of two kinds of CDMA-based relay cooperation : the TDMA-CDMA and FDMA-CDMA cooperation. The optimal energy allocation ratio between sources and relay has been found through simulations in both cases.

Compared with the TDMA-scheduled relay cooperation, we have shown that the CDMA-based relay cooperation only offers a limited coding gain in the high SNR region when the network error performance is measured with the received energy including that coming from the relay. In practical situations if the relay energy is not limited, the CDMA-based relay cooperation offers a coding gain similar to that in the TDMA relay cooperation case and turns to be a valuable solution.

The TDMA-scheduled relay cooperation offers good error performance at the cost of a small portion of band expansion and we should setup the relay during the deployment

of WSN. In an already deployed WSN, if there is no additional bandwidth available or the modification of sensors is not allowed, then we can choose the CDMA-based relay cooperation.

To conclude, we give some perspectives of our study :

For the TDMA-scheduled relay cooperation, we can extend the network capacity analysis to the Rayleigh fading channel if the corresponding bound of the achievable transmission rate is available in the finite-length code regime.

For the CDMA-based relay cooperation, we need to derive a theoretical optimal energy allocation ratio $x = E_{RD}/E_{SD}$ between the sources and the relay on the gaussian channel. Then, the theoretical and simulation results can be extended to the Rayleigh fading channel. Multi-antenna transmission and reception can also be envisioned at the relay and destination in order to provide diversity gain and thus improve the network performance.

Appendix

Appendix 3.A

Derivation of the pair-wise error probability of $\Pr\{\hat{\mathbf{C}}|\mathbf{E}, \mathbf{C}\}$ given the error pattern \mathbf{E} in the case of soft decoding at the relay.

We consider the cooperative scheme based on product code with the soft decoding at the relay. The sources use the systematic linear block code (n_S, k_S) and the relay uses a block code (n_R, k_R) . The destination observes a product codeword of $(n_S, k_S) \times (n_R, k_R)$ whose minimum distance $\delta_P = \delta_S \delta_R$ and code rate is denoted R_P . We suppose that the source-destination and the relay-destination channels have the same SNR ($SNR_{sd} = SNR_{rd}$).

We define the following notations :

- \mathbf{C} denotes the product codeword without errors at the relay ;
- \mathbf{E} denotes the error pattern in the first k_R rows of the product code matrix after the soft decoding at the relay ;
- $\hat{\mathbf{C}}$ is the product codeword associated with the error pattern \mathbf{E} ;
- \mathbf{E}^{Col} is the error pattern in the column redundancy (the last $n_R - k_R$ rows) of $\hat{\mathbf{C}}$;
- w is the weight of \mathbf{E}^{Col} ;
- d is the Hamming distance between codewords \mathbf{C} and $\hat{\mathbf{C}}$;
- \mathbf{R} denotes the observation of the whole product codeword at destination ;
- \mathbf{B} denotes the channel AWGN noise whose variance is σ^2 .

In the proposed cooperative network, the destination observes one part of the product codeword coming from the direct source transmissions. This part is not influenced by the relay errors. The other part of observation corresponds to the column redundancy forwarded by the relay, which is associated with the relay errors. The elements of \mathbf{R} can be expressed as :

$$r_{ql} = \begin{cases} (2c_{ql} - 1) + b_{ql}, & 1 \leq q \leq k_R, 1 \leq l \leq n_S \\ (2\hat{c}_{ql} - 1) + b_{ql} = [2(c_{ql} \oplus e_{ql}^{\text{Col}}) - 1] + b_{ql}, & k_R + 1 \leq q \leq n_R, 1 \leq l \leq n_S \end{cases} \quad (3.A.1)$$

where $c_{ql} \in \{0, 1\}$ (resp. \hat{c}_{ql}) is the binary element of product codeword \mathbf{C} (resp. $\hat{\mathbf{C}}$). b_{ql} is the element of \mathbf{B} . $e_{ql}^{\text{Col}} \in \{0, 1\}$ is the binary element of the error pattern \mathbf{E}^{Col} in

the column redundancy of $\hat{\mathbf{C}}$.

The ML decoding rule minimizes the Euclidian distance between \mathbf{R} and the decoded product codeword. The minimization of Euclidian distance equals the maximization of corresponding inner product. If $\hat{\mathbf{C}}$ is the decoding result whose entries belong to $\{0, 1\}$, then :

$$\begin{aligned}\hat{\mathbf{C}} &= \arg \max_{1 \leq i \leq 2^{k_S k_R}} \{p(\mathbf{R} | 2\mathbf{C}_i - 1)\} \\ &= \arg \min_{1 \leq i \leq 2^{k_S k_R}} \{d_E(\mathbf{R}, 2\mathbf{C}_i - 1)\} \\ &= \arg \max_{1 \leq i \leq 2^{k_S k_R}} \{\langle \mathbf{R}, 2\mathbf{C}_i - 1 \rangle\},\end{aligned}\tag{3.A.2}$$

where $\langle \cdot \rangle$ calculates the inner product of two vectors.

The pair-wise error probability that the destination decides on $\hat{\mathbf{C}}$ instead of \mathbf{C} given the error pattern \mathbf{E} at the relay can thus be calculated by :

$$\begin{aligned}\Pr \left\{ \hat{\mathbf{C}} | \mathbf{E}, \mathbf{C} \right\} &\leq \Pr \left\{ \langle \mathbf{R}, 2\hat{\mathbf{C}} - 1 \rangle \geq \langle \mathbf{R}, 2\mathbf{C} - 1 \rangle \right\} \\ &= \Pr \left\{ \langle \mathbf{R}, \hat{\mathbf{C}} - \mathbf{C} \rangle \geq 0 \right\}.\end{aligned}\tag{3.A.3}$$

Introducing the channel AWGN noise \mathbf{B} and considering the relation between \mathbf{R} and \mathbf{B} in Eq. 3.A.1, we can further express the above equation as :

$$\begin{aligned}\Pr \left\{ \hat{\mathbf{C}} | \mathbf{E}, \mathbf{C} \right\} &\leq \Pr \left\{ \langle \mathbf{R}, \hat{\mathbf{C}} - \mathbf{C} \rangle \geq 0 \right\} \\ &= \Pr \left\{ \langle \mathbf{B}, \hat{\mathbf{C}} - \mathbf{C} \rangle \geq A \right\}.\end{aligned}\tag{3.A.4}$$

where A is a constant depending on the error pattern \mathbf{E} . We denote $d^{(S)} = \sum_{q=1}^{k_R} \sum_{l=1}^{n_S} (c_{ql} \oplus \hat{c}_{ql})$ as the Hamming distance between the first k_R rows of \mathbf{C} and $\hat{\mathbf{C}}$. $d^{(R)} = \sum_{q=k_R+1}^{n_R} \sum_{l=1}^{n_S} (c_{ql} \oplus \hat{c}_{ql})$ is the Hamming distance between the $(n_R - k_R)$ rows of relay-generated redundancy in \mathbf{C} and $\hat{\mathbf{C}}$. The Hamming distance between \mathbf{C} and $\hat{\mathbf{C}}$ equals $d^{(S)} + d^{(R)}$, then A can be calculated as :

$$A = \sum_{q=1}^{k_R} \sum_{l=1}^{n_S} (2c_{ql} - 1) \cdot (c_{ql} - \hat{c}_{ql}) + \sum_{q=k_R+1}^{n_R} \sum_{l=1}^{n_S} [2(c_{ql} \oplus e_{ql}^{\text{Col}}) - 1] \cdot (c_{ql} - \hat{c}_{ql}).\tag{3.A.5}$$

Since

$$(2c_{ql} - 1) \cdot (c_{ql} - \hat{c}_{ql}) = \begin{cases} 0, & \text{if } c_{ql} = \hat{c}_{ql} \\ 1, & \text{if } c_{ql} \neq \hat{c}_{ql} \end{cases},\tag{3.A.6}$$

we have :

$$A = d^{(S)} + (d^{(R)} - 2w) = d - 2w.\tag{3.A.7}$$

In Eq. 3.A.4, let $z = \langle \mathbf{B}, \hat{\mathbf{C}} - \mathbf{C} \rangle$ and we have :

$$\Pr \left\{ \hat{\mathbf{C}} | \mathbf{E}, \mathbf{C} \right\} \leq \Pr \left\{ \langle \mathbf{B}, \hat{\mathbf{C}} - \mathbf{C} \rangle \geq A \right\} = \Pr \{z \geq A\}.\tag{3.A.8}$$

z is the summation of d i.i.d. zero-mean Gaussian variables, so it is also a zero-mean Gaussian variable whose variance $\sigma_z^2 = d\sigma^2$.

(1) If $d \geq 2w$, then $A = d - 2w \geq 0$:

$$\begin{aligned}
\Pr \left\{ \hat{\mathbf{C}} | \mathbf{E}, \mathbf{C} \right\} &\leq \Pr \{ z \geq d - 2w \} = \Pr \{ z \leq 2w - d \} \\
&= \int_{-\infty}^{2w-d} \frac{1}{\sqrt{2\pi\sigma_z^2}} \cdot \exp \left(-\frac{z^2}{2\sigma_z^2} \right) dz \\
&= \frac{1}{\sqrt{\pi}} \int_{\frac{d-2w}{\sqrt{2\sigma_z^2}}}^{+\infty} \exp(z^2) dz \\
&= \frac{1}{2} \operatorname{erfc} \sqrt{\frac{(d-2w)^2}{2\sigma_z^2}} = \frac{1}{2} \operatorname{erfc} \sqrt{\frac{(d-2w)^2}{2d\sigma^2}} \\
&= \frac{1}{2} \operatorname{erfc} \sqrt{\frac{(d-2w)^2}{d} \cdot \frac{R_P E_b}{N_0}}.
\end{aligned} \tag{3.A.9}$$

(2) If $d < 2w$, then $A = d - 2w < 0$:

$$\begin{aligned}
\Pr \left\{ \hat{\mathbf{C}} | \mathbf{E}, \mathbf{C} \right\} &\leq \Pr \{ z \geq d - 2w \} = 1 - \Pr \{ z \geq 2w - d \} \\
&= 1 - \frac{1}{2} \operatorname{erfc} \sqrt{\frac{(d-2w)^2}{d} \cdot \frac{R_P E_b}{N_0}}.
\end{aligned} \tag{3.A.10}$$

Substituting Eq. 3.A.9 and 3.A.10 into Eq. 3.A.3, we obtain that :

$$\begin{aligned}
\Pr \left\{ \hat{\mathbf{C}} | \mathbf{E}, \mathbf{C} \right\} &\leq \Pr \left\{ \left\langle \mathbf{R}, 2\hat{\mathbf{C}} - 1 \right\rangle \geq \left\langle \mathbf{R}, 2\mathbf{C} - 1 \right\rangle \right\} \\
&= \Pr \{ z \geq d - 2w \} \\
&= \begin{cases} \frac{1}{2} \operatorname{erfc} \sqrt{\frac{(d-2w)^2}{d} \cdot \frac{R_P E_b}{N_0}}, & \text{if } d \geq 2w \\ 1 - \frac{1}{2} \operatorname{erfc} \sqrt{\frac{(d-2w)^2}{d} \cdot \frac{R_P E_b}{N_0}}, & \text{if } d < 2w \end{cases}
\end{aligned} \tag{3.A.11}$$

Appendix 4.A

Non-orthogonal spreading sequence set (6 users).

$\{0, 0, 0, 1, 1, 1, 1, 0, 1, 1, 0, 1, 1, 0, 1, 1, 0, 0, 0, 1, 1, 0, 1, 1, 1, 1\}$
 $\{0, 0, 0, 1, 0, 1, 1, 1, 0, 0, 0, 1, 1, 0, 0, 1, 1, 0, 1, 1, 0, 1, 0, 0, 1, 1\}$
 $\{0, 0, 1, 0, 1, 0, 1, 1, 0, 1, 0, 1, 1, 0, 1, 1, 0, 1, 0, 1, 0, 1, 0, 0, 1, 0\}$
 $\{1, 0, 0, 0, 1, 0, 0, 0, 0, 1, 0, 1, 0, 0, 1, 1, 1, 0, 1, 0, 1, 1, 1, 1, 1, 1\}$
 $\{0, 0, 1, 0, 1, 0, 1, 0, 1, 0, 1, 0, 0, 0, 1, 0, 1, 0, 1, 0, 1, 0, 1, 0, 0, 1\}$
 $\{0, 1, 1, 1, 1, 1, 0, 0, 0, 0, 0, 0, 0, 0, 1, 1, 1, 1, 1, 0, 0, 0, 0, 0, 0, 1\}$

This spreading sequence set contains 6 spreading sequences of length $PG = 26$. In the DSSS CDMA application, the sequence elements are antipodal modulated such that $(0, 1) \rightarrow (-1, +1)$. Besides that, we normalize the spreading sequence by multiplying each element with a constant $1/\sqrt{PG}$ so that the sequence has the unit energy. Their normalized cross-correlation matrix is :

$$\begin{pmatrix} 1 & 0.1538 & 0.1538 & 0.2308 & 0 & 0.1538 \\ 0.1538 & 1 & 0.2308 & 0 & -0.2308 & 0.0769 \\ 0.1538 & 0.2308 & 1 & 0 & -0.2308 & -0.0769 \\ 0.2308 & 0 & 0 & 1 & 0.1538 & 0 \\ 0 & -0.2308 & -0.2308 & 0.1538 & 1 & 0.2308 \\ -0.1538 & 0.0769 & -0.0769 & 0 & 0.2308 & 1 \end{pmatrix}_{(6 \times 6)}$$

Appendix 4.B

Root-raised-cosine pulse shaping function.

Frequency response function :

$$H_T(f) = \begin{cases} \sqrt{T}, & \text{if } |f| \leq \frac{1-\alpha}{2T} \\ \sqrt{\frac{T}{2}} \cdot \sqrt{1 + \cos \left[\frac{\pi T}{\alpha} \left(|f| - \frac{1-\alpha}{2T} \right) \right]}, & \text{if } \frac{1-\alpha}{2T} \leq |f| \leq \frac{1+\alpha}{2T} \\ 0, & \text{otherwise} \end{cases} \quad (4.B.1)$$

where α is the roll-off coefficient. Here we set $\alpha = 0.22$.

The corresponding root-raised-cosine impulse function :

$$h_T(t) = \frac{4\alpha}{\pi\sqrt{T}} \cdot \frac{\cos \frac{(1+\alpha)\pi t}{T} + \frac{(1-\alpha)\pi}{4\alpha} \cdot \text{sinc} \frac{(1-\alpha)t}{T}}{1 - \left(\frac{4\alpha t}{T} \right)^2}. \quad (4.B.2)$$

The pulse energy is normalized to unit with the above definition :

$$\varphi_T(t_0) = \|H_T\|^2 = \int_{-\infty}^{\infty} |H_T(f)|^2 df = 1. \quad (4.B.3)$$

Appendix 4.C

Discrete reception model of the superposed FDMA-CDMA scheme.

Recall some notations :

- $d_n^{(k)}$ is the n -th codeword symbol of the k -th source codeword, $d_n^{(k)} \in \{\pm 1\}$;
- $d_{i,n}^{(R)}$ is the n -th codeword symbol of the i -th relay-generated redundancy row in the product codeword, $d_{i,n}^{(R)} \in \{\pm 1\}$;
- $h_{T_c}(t)$ and $h_{T_s}(t)$ are the root-raised-cosine pulse shaping functions used in the modulation of the relay CDMA and source TDMA signals respectively. Their definition is given in Appendix 4.B.;
- $\sum_{m=0}^{PG-1} s_{i,m} h_{T_c}(t - mT_c)$ is the i -th full period (PG=K) spreading pulse shaping of the duration $T_s^{(R)} = T_s^{(S)}$, $s_{i,m} \in \{\pm 1/\sqrt{PG}\}$;
- f_k^{FDMA} is the k -th FDMA carrier frequency and f_c^{CDM} is the CDMA carrier frequency.

In the following, we denote :

$$T_s = T_s^{(S)} = T_s^{(R)} = PG \cdot T_{chip}^{(R)}.$$

$$T_c = T_{chip}^{(R)}.$$

The superposed signal (FDMA + CDMA) received at the destination is :

$$r(t) = A_{Source} \sum_{k=0}^{K-1} \sum_n d_n^{(k)} h_{T_s}(t - nT_s^{(S)}) \cdot \cos(2\pi f_k t + \varphi_0)$$

(Source FDMA part)

$$+ A_{Relay} \sum_{i=0}^{r_R-1} \sum_n d_{i,n}^{(R)} \sum_{m=0}^{PG-1} s_{i,m} h_{T_c}(t - nT_s^{(R)} - mT_{chip}^{(R)}) \cdot \cos(2\pi f_c t + \varphi_0)$$

(Relay CDMA part)

$$+ n(t).$$

(4.C.1)

As show in Fig. 4.C.1, the destination applies two parallel treatments on the received signal $r(t)$ to detect respectively the source and the relay data parts. The detection results are in the form of LLR and will be turbo-decoded.

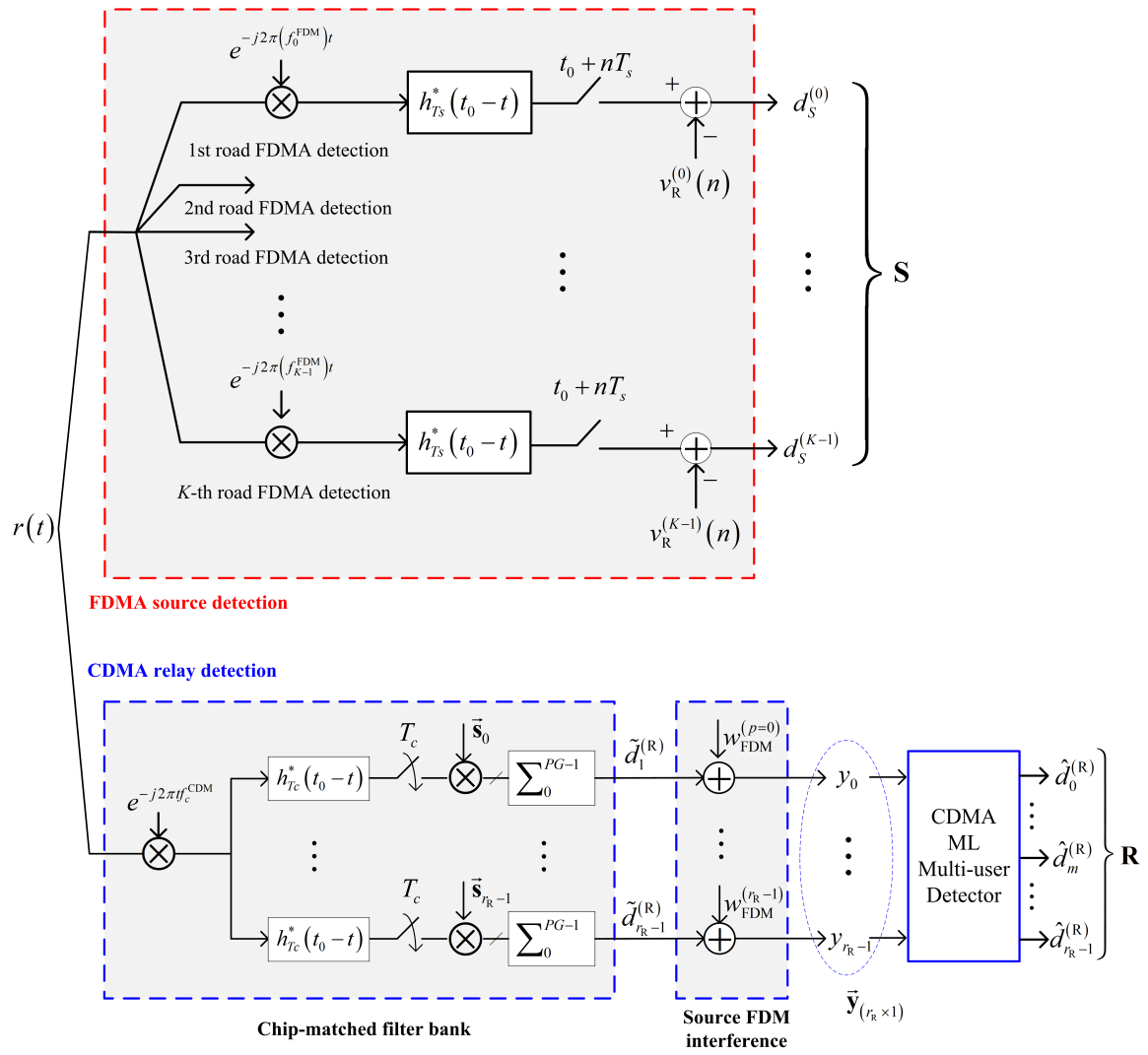


Figure 4.C.1 — Source and relay data detection at the destination.

(1) FDMA source detection treatment

- For the source part term in $r(t)$:

There are K branches in the FDMA source detection of Fig. 4.C.1. The l -th branch is dedicated to detect the l -th source codeword whose transmission is centered at f_l^{FDM} . Here we focus on the l -th FDMA detection branch. We process the received source FDMA term in $r(t)$ as :

$$\begin{aligned}
& \left\{ A_{\text{Source}} \cdot \sum_{k=0}^{K-1} \text{Re} \left[\sum_n d_n^{(k)} h_{T_s}(t - nT_s) \cdot e^{j2\pi t f_k^{\text{FDM}}} \right] \cdot e^{j2\pi t f_l^{\text{FDM}}} \right\} \otimes g_{T_s}(t) \\
&= \frac{A_{\text{Source}}}{2} \left\{ \sum_{k=0}^{K-1} \sum_n d_n^{(k)} h_{T_s}(t - nT_s) \cdot \left[e^{j2\pi(f_k^{\text{FDM}} - f_l^{\text{FDM}})t} + e^{j2\pi(f_k^{\text{FDM}} + f_l^{\text{FDM}})t} \right] \right\} \otimes g_{T_s}(t) \\
&= \frac{A_{\text{Source}}}{2} \left\{ \sum_{k=0}^{K-1} \sum_n d_n^{(k)} h_{T_s}(t - nT_s) \cdot e^{j2\pi(f_k^{\text{FDM}} - f_l^{\text{FDM}})t} \right\} \otimes g_{T_s}(t) \\
&= \frac{A_{\text{Source}}}{2} \sum_n d_n^{(k=l)} h_{T_s}(t - nT_s) \otimes g_{T_s}(t) \\
&= \frac{A_{\text{Source}}}{2} \sum_n d_n^{(k=l)} \int_{-\infty}^{+\infty} h_{T_s}(\tau - nT_s) \cdot h_{T_s}(T_s + \tau - t) d\tau,
\end{aligned} \tag{4.C.2}$$

where $g_{T_s}(t) = h_{T_s}^*(t_0 - t)$ is the band-pass filter centered at the l -th source FDM carrier frequency f_l^{FDM} . Its bandwidth is just adequate to reserve the l -th source FDMA signal and to attenuate the other FDMA signals.

Sample the above signal at $t = (n' + 1)T_s$, we obtain the detected FDM symbol of the l -th source :

$$d_S^{(k=l)}(n') = \frac{A_{\text{Source}}}{2} d_{n'}^{(k=l)} \cdot \int_{-\infty}^{\infty} |H_{T_s}(t)|^2 dt = \frac{A_{\text{Source}}}{2} d_{n'}^{(k=l)} \cdot \varphi_{T_s}(t_0). \blacksquare \tag{4.C.3}$$

- For the relay part term in $r(t)$:

During the source part detection, the relay CDMA part is treated as interference. The received relay CDMA term in $r(t)$ after the processing of the l -th FDMA detection branch becomes :

$$\begin{aligned}
& \left\{ A_{Relay} \cdot \text{Re} \left[\sum_{i=0}^{r_R-1} \sum_n d_{i,n}^{(R)} \sum_{m=0}^{PG-1} s_{i,m} h_{T_c}(t - nT_s - mT_c) \cdot e^{j2\pi t f_c^{\text{CDM}}} \right] \cdot e^{j2\pi t f_l^{\text{FDM}}} \right\} \otimes g_{T_s}(t) \\
&= \frac{A_{Relay}}{2} \cdot \left\{ \sum_{i=0}^{r_R-1} \sum_n d_{i,n}^{(R)} \sum_{m=0}^{PG-1} s_{i,m} h_{T_c}(t - nT_s - mT_c) \right. \\
&\quad \left. \cdot \left[e^{j2\pi(f_c^{\text{CDM}} - f_l^{\text{FDM}})t} + e^{j2\pi(f_c^{\text{CDM}} + f_l^{\text{FDM}})t} \right] \right\} \otimes g_{T_s}(t) \\
&= \frac{A_{Relay}}{2} \cdot \left[\sum_{i=0}^{r_R-1} \sum_n d_{i,n}^{(R)} \sum_{m=0}^{PG-1} s_{i,m} h_{T_c}(t - nT_s - mT_c) \cdot e^{j2\pi(f_c^{\text{CDM}} - f_l^{\text{FDM}})t} \right] \otimes g_{T_s}(t)
\end{aligned} \tag{4.C.4}$$

The Fourier transform (FT) of the above signal is :

$$\begin{aligned}
& \text{FT} \rightarrow \\
& \frac{A_{Relay}}{2} \cdot \left[\sum_{i=0}^{r_R-1} \sum_n d_{i,n}^{(R)} \sum_{m=0}^{PG-1} s_{i,m} H_{T_c}(f) \cdot e^{-j2\pi f(nT_s + mT_c)} \otimes \delta(f - f_c^{\text{CDM}} + f_l^{\text{FDM}}) \right] \\
& \quad \cdot H_{T_s}^*(f) e^{-j2\pi f T_s}.
\end{aligned} \tag{4.C.5}$$

Remark : with the normalized root-raised cosine filter we have :

$$H_{T_c}(f) \cdot H_{T_s}(f) \approx \sqrt{T_c} \cdot H_{T_s}(f). \tag{4.C.6}$$

Substitute Eq. 4.C.6 into Eq. 4.C.5 :

$$\sqrt{T_c} \frac{A_{Relay}}{2} \left[\sum_{i=0}^{r_R-1} \sum_n d_{i,n}^{(R)} \sum_{m=0}^{PG-1} s_{i,m} H_{T_s}(f) e^{-j2\pi f(nT_s + mT_c)} \otimes \delta(f - f_c^{\text{CDM}} + f_l^{\text{FDM}}) \right] e^{-j2\pi f T_s}. \tag{4.C.7}$$

The inverse FT of this signal is :

$$\begin{aligned}
& \text{FT}^{-1} \rightarrow \\
& \sqrt{T_c} \frac{A_{Relay}}{2} \left[\sum_{i=0}^{r_R-1} \sum_n d_{i,n}^{(R)} \sum_{m=0}^{PG-1} s_{i,m} h_{T_s}(t - nT_s - mT_c) e^{-j2\pi(f_c^{\text{CDM}} - f_l^{\text{FDM}})t} \right] \otimes \delta(t - T_s) \\
&= \sqrt{T_c} \frac{A_{Relay}}{2} \sum_{i=0}^{r_R-1} \sum_n d_{i,n}^{(R)} \sum_{m=0}^{PG-1} s_{i,m} h_{T_s}(t - (n+1)T_s - mT_c) e^{-j2\pi(f_c^{\text{CDM}} - f_l^{\text{FDM}})(t - T_s)}
\end{aligned} \tag{4.C.8}$$

Sample the above signal at $t = (n' + 1)T_s$, we get the relay CDMA interference term $v_R^{(l)}(n')$ on the l -th FDMA source detection branch :

$$v_R^{(l)}(n') = \sqrt{T_c} \frac{A_{Relay}}{2} \sum_{i=0}^{r_R-1} \sum_n d_{i,n}^{(R)} \sum_{m=0}^{PG-1} s_{i,m} h_{T_s}((n' - n)T_s - mT_c) e^{-j2\pi(f_c^{CDM} - f_i^{FDM})n'T_s}. \blacksquare \quad (4.C.9)$$

Remark : Eq.4.C.9 is used in the discrete S-D transmission model to simulate the CDMA interference and the corresponding $d_{i,n}^{(R)}$ is error-free in this case. During the cancelation step, $d_{i,n}^{(R)}$ is replaced by the turbo decoding results, which contains decoding errors.

- For the noise term in $r(t)$:

$$\eta(t) = [n(t) \cdot e^{-j2\pi f_0 t}] \otimes g_{T_s}(t) = \frac{1}{2} n_{\text{envelop}}^{\text{complex}}(t) \otimes g_{T_s}(t). \quad (4.C.10)$$

Its PSD : $\gamma_\eta(f) = \frac{1}{4} \cdot 2N_0 \cdot |H_{T_s}(f)|^2$ and its variance $\sigma_\eta^2 = \int \gamma_\eta(f) df = \frac{N_0}{2} \varphi_{T_s}(t_0)$. So for the one dimensional symbol-level noise variance :

$$\sigma_\eta^2 = \frac{N_0}{4} \cdot \varphi_{T_s}(t_0). \blacksquare \quad (4.C.11)$$

All FDMA source detection branches are influenced by the noise of the same variance as given in Eq.4.C.11.

(2) CDMA relay detection treatment

- For the relay part term in $r(t)$:

$$\begin{aligned} & \left\{ A_{Relay} \text{Re} \left[\sum_{i=0}^{r_R-1} \sum_n d_{i,n}^{(R)} \sum_{m=0}^{PG-1} s_{i,m} h_{T_c}(t - nT_s - mT_c) e^{j2\pi t f_c^{CDM}} \right] \cdot e^{-j2\pi t f_c^{CDM}} \right\} \otimes g_{T_c}(t) \\ &= \frac{A_{Relay}}{2} \sum_{i=0}^{r_R-1} \sum_n d_{i,n}^{(R)} \sum_{m=0}^{PG-1} s_{i,m} h_{T_c}(t - nT_s - mT_c) \otimes g_{T_c}(t) \\ &= \frac{A_{Relay}}{2} \sum_{i=0}^{r_R-1} \sum_n d_{i,n}^{(R)} \sum_{m=0}^{PG-1} s_{i,m} \int_{-\infty}^{+\infty} h_{T_c}(\tau - nT_s - mT_c) \cdot h_{T_c}(\tau + T_c - t) d\tau. \end{aligned} \quad (4.C.12)$$

Sample the above signal at $t = n'T_s + (m' + 1)T_c$, we obtain :

$$d_R^{(i)}(n', m') = \frac{A_{Relay}}{2} \sum_{i=0}^{r_R-1} s_{i,m'} d_{i,n'}^{(R)} \cdot \varphi_{T_c}(t_0). \quad (4.C.13)$$

After de-spreading (using the p -th spreading sequence) and the summation of PG chip-level discrete variables in the same symbol duration :

$$\begin{aligned}
\tilde{d}_p^{(R)}(n') &= \sum_{m'=0}^{PG-1} s_{p,m'} \left[\frac{A_{Relay}}{2} \cdot \sum_{i=0}^{r_R-1} s_{i,m'} \cdot d_{i,n'}^{(R)} \cdot \varphi_{T_c}(t_0) \right] \\
&= \frac{A_{Relay}}{2} \left[d_{p=n'}^{(R)} \left(\sum_{m'=0}^{PG-1} (s_{p,m'})^2 \right) + \sum_{\substack{i=0 \\ i \neq p}}^{r_R-1} d_{j,n'}^{(R)} \left(\sum_{m'=0}^{PG-1} s_{i,m'} s_{p,m'} \right) \right] \cdot \varphi_{T_c}(t_0) \\
&= \frac{A_{Relay}}{2} \left[d_{p,n'}^{(R)} + \sum_{\substack{i=0 \\ i \neq p}}^{r_R-1} d_{j,n'}^{(R)} \left(\sum_{m'=0}^{PG-1} s_{i,m'} s_{p,m'} \right) \right] \cdot \varphi_{T_c}(t_0) . \blacksquare
\end{aligned} \tag{4.C.14}$$

- For source part term in $r(t)$:

$$\begin{aligned}
&\left\{ A_{Source} \cdot \sum_{k=0}^{K-1} \text{Re} \left[\sum_n d_n^{(k)} h_{T_s}(t - nT_s) \cdot e^{j2\pi t f_k^{\text{FDM}}} \right] \cdot e^{-j2\pi t f_c^{\text{CDM}}} \right\} \otimes g_{T_c}(t) \\
&= \frac{A_{Source}}{2} \cdot \sum_{k=0}^{K-1} \sum_n d_n^{(k)} h_{T_s}(t - nT_s) \cdot e^{j2\pi (f_k^{\text{FDM}} - f_c^{\text{CDM}})t} \otimes g_{T_c}(t) .
\end{aligned}$$

FT \rightarrow

$$\begin{aligned}
&\frac{A_{Source}}{2} \cdot \left[\sum_{k=0}^{K-1} \sum_n d_n^{(k)} H_{T_s}(f) \cdot e^{-j2\pi f n T_s} \otimes \delta(f - f_k^{\text{FDM}} + f_c^{\text{CDM}}) \right] \cdot H_{T_c}(f) \cdot e^{-j2\pi f n T_c} \\
&= \sqrt{T_c} \frac{A_{Source}}{2} \left[\sum_{k=0}^{K-1} \sum_n d_n^{(k)} H_{T_s}(f) e^{-j2\pi f n T_s} \otimes \delta(f - f_k^{\text{FDM}} + f_c^{\text{CDM}}) \right] e^{-j2\pi f n T_c}
\end{aligned}$$

FT $^{-1} \rightarrow$

$$\sqrt{T_c} \frac{A_{Source}}{2} \sum_{k=0}^{K-1} \sum_n d_n^{(k)} h_{T_s}(t - nT_s - T_c) e^{j2\pi (f_k^{\text{FDM}} - f_c^{\text{CDM}})(t - T_c)} .$$

(4.C.15)

Sample the above signal at $t = n'T_s + (m' + 1)T_c$, we obtain :

$$d_S(n', m') = \sqrt{T_c} \frac{A_{Source}}{2} \sum_{k=0}^{K-1} \sum_n d_n^{(k)} h_{T_s}((n' - n)T_s + m'T_c) e^{j2\pi (f_k^{\text{FDM}} - f_c^{\text{CDM}})(n'T_s + m'T_c)} .$$

(4.C.16)

After despreading (using the p -th spreading sequence) and the summation of PG chip-level discrete variables in the same symbol duration, we get the symbol-level

FDMA source interference term :

$$\begin{aligned}
w_{\text{FDM}}^{(p)} &= d_S^{(p)}(n') \\
&= \sqrt{T_c} \frac{A_{\text{Source}}}{2} \sum_{m'=0}^{PG-1} s_{p,m'} \sum_{k=0}^{K-1} \sum_n d_n^{(k)} h_{T_s}((n' - n)T_s + m'T_c) e^{j2\pi(f_k^{\text{FDM}} - f_c^{\text{CDM}})(n'T_s + m'T_c)}. \blacksquare
\end{aligned} \tag{4.C.17}$$

According to the FDMA-CDMA RF band allocation shown in Fig. 4.21.a, we can verify that : $f_k^{\text{FDM}} - f_c^{\text{CDM}} = (2k + 1) \frac{1+\alpha}{2T_s} - \frac{1+\alpha}{2T_c} = \frac{1+\alpha}{2T_c} \left(\frac{2k+1}{PG} - 1 \right)$.

The variance of the symbol-level FDMA source interference $w_{\text{FDM}}^{(p)}$:

$$E \left(\left| w_{\text{FDM}}^{(p)} \right|^2 \right) = \frac{T_c}{PG} \cdot \frac{(A_{\text{Source}})^2}{4} \sum_{k=0}^{PG-1} \sum_{m'=0}^{PG-1} \sum_{n=0}^{N-1} [h_{T_s}((n' - n)T_s + (m' + 1)T_c)]^2, \blacksquare \tag{4.C.18}$$

where the coefficient $\frac{T_c}{PG}$ is associated with the normalization of both the root-raised-cosine function and the spreading sequence.

- For the noise term in $r(t)$:

$$\eta^{\text{R}}(t) = [n(t) \cdot e^{-j2\pi f_c t}] \otimes g_{T_c}(t) = \frac{1}{2} n_{\text{envelop}}^{\text{Complex}}(t) \otimes g_{T_c}(t). \tag{4.C.19}$$

Its PSD : $\gamma_n^{\text{R}}(f) = \frac{1}{4} \cdot 2N_0 |H_{T_c}(f)|^2$ and its variance $(\sigma_n^{\text{R}})^2 = \int \gamma_n^{\text{R}}(f) df = \frac{N_0}{2} \cdot \varphi_{T_c}(t_0)$. So for the one dimensional symbol-level noise variance :

$$(\sigma_n^{\text{R}})_{\text{chip}}^2 = \frac{N_0}{4} \cdot \varphi_{T_c}(t_0). \tag{4.C.20}$$

After despreading (with the p -th spreading sequence) and the summation of PG chip-level discrete variables in the same symbol duration, we have the symbol-level noise variance :

$$(\sigma_n^{\text{R}})^2 = \frac{N_0}{4} \cdot \varphi_{T_c}(t_0), \blacksquare \tag{4.C.21}$$

which is the same of that in chip level thanks to the normalization the spreading sequence.

Remark : with the normalized root-raised-cosine filter and the normalized spreading sequence, Eq. 4.C.21 has the same value of Eq. 4.C.11. So in the simulation, we can use the same noise variance (symbol-level) for the symbol-level noise terms in the S-D and R-D transmission equations.

Appendix 4.D

Distribution of the FDMA source interference in the FDMA-CDMA scheme.

In the CDMA relay detection at the destination, there is a FDMA source interference term :

$$\begin{aligned}
 w_{\text{FDM}}^{(p)} &= d_S^{(p)}(n') \\
 &= \sqrt{T_c} \frac{A_{\text{Source}}}{2} \sum_{m'=0}^{PG-1} s_{p,m'} \sum_{k=0}^{K-1} \sum_n d_n^{(k)} h_{T_s}((n'-n)T_s + m'T_c) e^{j2\pi(f_k^{\text{FDM}} - f_c^{\text{CDM}})(n'T_s + m'T_c)}.
 \end{aligned}
 \tag{4.D.1}$$

This interference term is derived in Eq. 4.C.17. Here we study its distribution in the case of BPSK modulation. We take an example with following parameters : $PG = 26$, $A_{\text{Source}} = 2$, $T_s = 260$, $T_c = 10$, $d_n^{(k)} \in \{\pm 1\}$ and $s_{i,m'} \in \{\pm 1/\sqrt{PG}\}$. $h_{T_s}(\cdot)$ is the normalized root-raised-cosine filter defined in Appendix 4.B.

In Fig. 4.D.1, we show the simulated PDF of this interference and also the theoretical PDF of zero-mean Gaussian distribution whose variance equals to 0.5. The simulation result agrees with the theoretical curve. So we can statistically verify that the FDMA source interference has a Gaussian distribution in the CDMA relay detection.

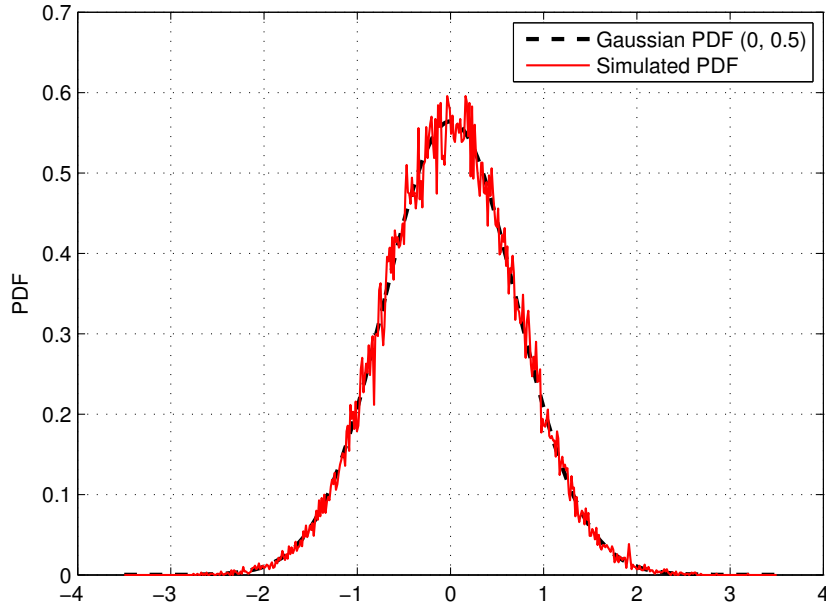


Figure 4.D.1 — Gaussian PDF verification using 50000 samples counted in 500 slots in the interval of $[-3.5, 3.5]$.

Appendix 4.E

Received energy ratio in the FDMA-CDMA network.

(1) k -th FDMA source signal (complex envelop) :

$$A_{Source} \cdot \sum_n d_n^{(k)} h_{T_s^{(S)}}(t - nT_s^{(S)}). \quad (4.E.1)$$

Its power :

$$P_{SD}^{(k)} = \frac{(A_{Source})^2}{T_s} \int_{-\infty}^{\infty} |H_{T_s^{(S)}}(f)|^2 df = \frac{(A_{Source})^2}{T_s^{(S)}} \varphi_{T_s^{(S)}}(t_0). \quad (4.E.2)$$

The average received energy of the k -th FDMA source signal in the duration of $T_s^{(S)}$ is denoted $E_{SD}^{(k)}$, i.e., the average received energy per symbol of the k -th source codeword, can be calculated as :

$$E_{SD}^{(k)} = P_{SD}^{(k)} \cdot T_s^{(S)}. \quad (4.E.3)$$

So for K FDMA sources, the overall average received energy in the duration of $T_s^{(S)}$ is :

$$E_{SD} = K \cdot E_{SD}^{(k)} = K \cdot P_{SD}^{(k)} \cdot T_s^{(S)} = K(A_{Source})^2 \varphi_{T_s^{(S)}}(t_0). \quad (4.E.4)$$

(2) CDMA relay signal(complex envelop) :

$$A_{Relay} \cdot \sum_{i=0}^{r_R-1} \sum_n d_{i,n}^{(R)} \sum_{m=0}^{PG-1} s_{i,m} h_{T_c}(t - nT_s - mT_c). \quad (4.E.5)$$

We denote $s_i(t) = \sum_{m=0}^{PG-1} s_{i,m} \cdot h_{T_c}(t - mT_c)$. The Fourier transform of $s_i(t)$:

$$S_i(f) = H_{T_c}(f) \sum_{m=0}^{PG-1} s_{i,m} \cdot e^{-j2\pi f m T_c}. \quad (4.E.6)$$

The PSD of the CDMA signal in Eq. 4.E.5 :

$$\begin{aligned}
D_{r_R}^{(R)}(f) &= \sum_{i=0}^{r_R-1} \frac{(A_{Relay})^2}{T_s} \sigma_d^2 |S_i(f)|^2 \\
&= \sum_{i=0}^{r_R-1} \frac{(A_{Relay})^2}{T_s} |H_{T_c}(f)|^2 \cdot \sum_{p=0}^{PG-1} \sum_{q=0}^{PG-1} s_{i,p} s_{i,q} e^{-j2\pi f(p-q)T_c} \\
&= \sum_{i=0}^{r_R-1} \frac{(A_{Relay})^2}{T_s} |H_{T_c}(f)|^2 \cdot \sum_{n=-PG+1}^{PG-1} \sum_{p=0}^{PG-1} s_{i,p} s_{i,p+n} e^{-j2\pi f n T_c} \quad (4.E.7) \\
&= \sum_{i=0}^{r_R-1} \frac{(A_{Relay})^2}{T_s} |H_{T_c}(f)|^2 \cdot \sum_{n=-PG+1}^{PG-1} \sum_{p=0}^{PG-1} s_{i,p} s_{i,p+n} e^{-j2\pi f n T_c} \\
&= r_R \cdot \frac{(A_{Relay})^2}{T_s} |H_{T_c}(f)|^2 \cdot \sum_{n=-PG+1}^{PG-1} \phi^a(n) e^{-j2\pi f n T_c},
\end{aligned}$$

where $\phi^a(n)$ is the aperiodic autocorrelation function of the spreading sequence defined in Eq. 2.53. We assume that this autocorrelation function is ideal :

$$\phi^a(n) = \sum_{p=0}^{PG-1} s_{i,p} s_{i,p+n} = \begin{cases} 1, & \text{if } n = 0 \\ 0, & \text{if } n \neq 0 \end{cases} \quad (4.E.8)$$

So we can approximate the PSD of the CDMA signal by :

$$D_{r_R}^{(R)}(f) \approx r_R \frac{A_r^2}{T_s} |H_{T_c}(f)|^2. \quad (4.E.9)$$

Its power is :

$$P_{RD}^{(R)} = \int_{-\infty}^{+\infty} D_{r_R}^{(R)}(f) df = \frac{r_R (A_{Relay})^2}{T_s} \cdot \varphi_{T_c}(t_0). \quad (4.E.10)$$

The average received energy on the relay-destination link in a given duration of $T_s^{(R)} = T_s^{(S)} = PG \cdot T_{chip}^{(R)}$ is thus given by :

$$E_{RD} = P_{RD}^{(R)} \cdot T_s^{(R)} = r_R (A_{Relay})^2 \varphi_{T_c}(t_0). \quad (4.E.11)$$

(3) Energy ratio :

Based on E_{SD} and E_{RD} derived in Eq. 4.E.4 and 4.E.11, we obtain the average received energy ratio :

$$x = \frac{E_{RD}}{E_{SD}} = \frac{r_R (A_{Relay})^2}{K (A_{Source})^2} \cdot \frac{\varphi_{T_c}(t_0)}{\varphi_{T_s}(t_0)} = \frac{r_R}{K} \left(\frac{A_{Relay}}{A_{Source}} \right)^2. \blacksquare \quad (4.E.12)$$

Bibliography

- [ABS10] T.u.R. Ahsin and S. Ben Slimane. Network coding based on product codes in cooperative relaying. In *IEEE Wireless Communications and Networking Conference (WCNC)*, pages 1 –6, april 2010.
- [ACLY00] R. Ahlswede, Ning Cai, S.-Y.R. Li, and R.W. Yeung. Network information flow. *IEEE Transactions on Information Theory*, 46(4) :1204 –1216, jul 2000.
- [Ber68] E. Berlekamp. Nonbinary bch decoding (abstr.). *IEEE Transactions on Information Theory*, 14(2) :242, march 1968.
- [BGT93] C. Berrou, A. Glavieux, and P. Thitimajshima. Near shannon limit error-correcting coding and decoding : Turbo-codes. 1. In *IEEE International Conference on Communications, (ICC)*, volume 2, pages 1064 –1070, may 1993.
- [BRC60] R.C. Bose and D.K. Ray-Chaudhuri. On a class of error correcting binary group codes. *Information and Control*, 3(1) :68 – 79, 1960.
- [CG79] T. Cover and A.E. Gamal. Capacity theorems for the relay channel. *IEEE Transactions on Information Theory*, 25(5) :572 – 584, sep 1979.
- [Cha72] D. Chase. A class of algorithms for decoding block codes with channel measurement information. *IEEE Transactions on Information Theory*, 18(1) :170 – 182, jan 1972.
- [CKL06] Yingda Chen, S. Kishore, and Jing Li. Wireless diversity through network coding. In *IEEE Wireless Communications and Networking Conference (WCNC)*, volume 3, pages 1681 –1686, april 2006.
- [CT06] Thomas M. Cover and Joy A. Thomas. *Elements of Information Theory 2nd Edition*. Wiley-Interscience, July 2006.
- [CY06] N. Cai and R. W. Yeung. Network error correction, part II : lower bounds. *Communications in Information and Systems*, 6(1) :37 – 54, 2006.
- [DJB⁺95] Catherine Douillard, Michel Jezequel, Claude Berrou, Pierre Didier, and Annie Picart. Iterative correction of intersymbol interference : turbo-equalization. *European transactions on telecommunications*, 6(5) :507 – 512, september 1995.
- [dM71] E.C. Van der Meulen. Three-terminal communication channels. *Advances in Applied Probability*, 3(1), 1971.

- [EFS56] P. Elias, A. Feinstein, and C. Shannon. A note on the maximum flow through a network. *IRE Transactions on Information Theory*, 2(4) :117–119, december 1956.
- [Eli54] P. Elias. Error-free coding. *IRE Professional Group on Information Theory*, 4(4) :29–37, sept. 1954.
- [FF56] L.R. Ford and D.R. Fulkerson. Maximal flow through a network. *Canadian Journal of Mathematics*, (8) :399–404, 1956.
- [Fri46] H.T. Friis. A note on a simple transmission formula. *Proceedings of the IRE*, 34(5) :254–256, may 1946.
- [Gal63] R.G. Gallager. *Low-density parity-check codes*. MIT press, 1963.
- [Gal68] R.G. Gallager. *Information theory and reliable communication*. Wiley, 1968.
- [GiAL10] A. Graell i Amat and I. Land. Bounds of the probability of error for decode-and-forward relaying with two sources. In *6th International Symposium on Turbo Codes and Iterative Information Processing (ISTC)*, pages 196–200, sept. 2010.
- [Gil52] E. N. Gilbert. A comparison of signaling alphabets. *Bell System Technical Journal*, 31 :504–522, 1952.
- [GLL97] A. Glavieux, C. Loat, and J. Labat. Turbo equalization over a frequency selective channel. In *International Symposium on Turbo Codes and related Topics*, pages 96–102, sept. 1997.
- [Hau08] Christoph Hausl. *Joint Network-Channel Coding for Wireless Relay Networks, thesis*. 2008.
- [HD06] C. Hausl and P. Dupraz. Joint network-channel coding for the multiple-access relay channel. In *3rd Annual IEEE Communications Society on Sensor and Ad Hoc Communications and Networks (SECON)*, volume 3, pages 817–822, sept. 2006.
- [HKM⁺03] T. Ho, R. Koetter, M. Medard, D.R. Karger, and M. Effros. The benefits of coding over routing in a randomized setting. In *IEEE International Symposium on Information Theory Proceedings.*, page 442, june-4 july 2003.
- [HL08] T. Ho and D. Lun. *Network Coding : An Introduction*. Network Coding : An Introduction. Cambridge University Press, 2008.
- [HMK⁺06] T. Ho, M. Medard, R. Koetter, D.R. Karger, M. Effros, Jun Shi, and B. Leong. A random linear network coding approach to multicast. *IEEE Transactions on Information Theory*, 52(10) :4413–4430, oct. 2006.
- [HMZ05] A. Host-Madsen and J. Zhang. Capacity bounds and power allocation for wireless relay channels. *IEEE Transactions on Information Theory*, 51(6) :2020–2040, june 2005.
- [Hoc59] A.J. Hocquenghem. *Codes correcteurs d’erreurs*, volume 2. Chiffre, 1959.
- [HSOB05] C. Hausl, F. Schreckenbach, I. Oikonomidis, and G. Bauch. Iterative network and channel decoding on a tanner graph. In *Allerton Conference on Communication, Control and Computing*, sept. 2005.

- [JHHN04] M. Janani, A. Hedayat, T.E. Hunter, and A. Nosratinia. Coded cooperation in wireless communications : space-time transmission and iterative decoding. *IEEE Transactions on Signal Processing*, 52(2) :362 – 371, feb. 2004.
- [JSC⁺05] S. Jaggi, P. Sanders, P.A. Chou, M. Effros, S. Egner, K. Jain, and L.M.G.M. Tolhuizen. Polynomial time algorithms for multicast network code construction. *IEEE Transactions on Information Theory*, 51(6) :1973 – 1982, june 2005.
- [KM03] R. Koetter and M. Medard. An algebraic approach to network coding. *IEEE/ACM Transactions on Networking*, 11(5) :782 – 795, oct. 2003.
- [KO10] Yusuke Kumano and Tomoaki Ohtsuki. Half-duplex relaying with serially-concatenated low-density generator matrix (sclldgm) codes. In *IEEE 71st Vehicular Technology Conference (VTC)*, pages 1 –5, may 2010.
- [Kri05] Bhaskar Krishnamachari. *Networking Wireless Sensors*. Cambridge University Press, New York, NY, USA, 2005.
- [KSA03a] M.A. Khojastepour, A. Sabharwal, and B. Aazhang. Bounds on achievable rates for general multi-terminal networks with practical constraints. In *Proc. of 2nd International Workshop on Information Processing (IPSN)*, pages 146–161, 2003.
- [KSA03b] M.A. Khojastepour, A. Sabharwal, and B. Aazhang. On capacity of gaussian ‘cheap’ relay channel. In *IEEE Global Telecommunications Conference (GLOBECOM)*, volume 3, pages 1776 – 1780 vol.3, dec. 2003.
- [LAMY10] Jun Li, M.H. Azmi, R. Malaney, and Jinhong Yuan. Design of network-coding based multi-edge type ldpc codes for a multi-source relaying system. In *6th International Symposium on Turbo Codes and Iterative Information Processing (ISTC)*, pages 414 –418, sept. 2010.
- [Lin70] S. Lin. *An introduction to error-correcting codes*. Prentice-Hall Press, 1970.
- [LVWD06] Yonghui Li, B. Vucetic, T.F. Wong, and M. Dohler. Distributed turbo coding with soft information relaying in multihop relay networks. *IEEE Journal on Selected Areas in Communications*, 24(11) :2040 –2050, nov. 2006.
- [LYC03] S.-Y.R. Li, R.W. Yeung, and Ning Cai. Linear network coding. *IEEE Transactions on Information Theory*, 49(2) :371 –381, feb. 2003.
- [Mas69] J. Massey. Shift-register synthesis and bch decoding. *IEEE Transactions on Information Theory*, 15(1) :122 – 127, jan 1969.
- [Mos96] S. Moshavi. Multi-user detection for ds-cdma communications. *IEEE Communications Magazine*, 34(10) :124 –136, oct 1996.
- [MS77] F.J. Macwilliams and N.J.A. Sloane. *The theory of error-correcting codes*. North-Holland Press, 1977.
- [NHH04] A. Nosratinia, T.E. Hunter, and A. Hedayat. Cooperative communication in wireless networks. *IEEE Communications Magazine*, 42(10) :74 – 80, oct. 2004.

- [OCC10] E.A. Obiedat, Guotai Chen, and Lei Cao. Distributed turbo product codes over multiple relays. In *7th IEEE Consumer Communications and Networking Conference (CCNC)*, pages 1–5, jan. 2010.
- [Pet60] W. Peterson. Encoding and error-correction procedures for the bose-chaudhuri codes. *IRE Transactions on Information Theory*, 6(4) :459–470, sept. 1960.
- [PGA10] R.M. Pyndiah, F. Guilloud, and K. Amis. Multiple source cooperative coding using turbo product codes with a noisy relay. In *6th International Symposium on Turbo Codes and Iterative Information Processing (ISTC)*, pages 98–102, sept. 2010.
- [PGPJ94] R.M. Pyndiah, A. Glavieux, A. Picart, and S. Jacq. Near optimum decoding of product codes. In *IEEE Global Telecommunications Conference, (GLOBECOM)*, volume 1, pages 339–343, nov- 2 dec 1994.
- [PPV08] Y. Polyanskiy, H.V. Poor, and S. Verdu. New channel coding achievability bounds. In *IEEE International Symposium on Information Theory (ISIT)*, pages 1763–1767, july 2008.
- [PPV09] Y. Polyanskiy, H.V. Poor, and S. Verdu. Dispersion of gaussian channels. In *IEEE International Symposium on Information Theory (ISIT)*, pages 2204–2208, 28 2009-july 3 2009.
- [PPV10] Y. Polyanskiy, H.V. Poor, and S. Verdu. Channel coding rate in the finite blocklength regime. *IEEE Transactions on Information Theory*, 56(5) :2307–2359, may 2010.
- [PS08] J.G. Proakis and M. Salehi. *Digital Communications*. McGraw-Hill higher education, 5th edition. McGraw-Hill, 2008.
- [PTVF92] W.H. Press, S.A. Teukolsky, W.T. Vetterling, and B.P. Flannery. *Numerical Recipes in C, the art of scientific computing*. Cambridge University Press, 1992.
- [Pyn98] R.M. Pyndiah. Near-optimum decoding of product codes : block turbo codes. *IEEE Transactions on Communications*, 46(8) :1003–1010, aug 1998.
- [RL09] W. E. Ryan and S. Lin. *Channel codes : classical and modern*. Cambridge University Press, 2009.
- [RY07] P. Razaghi and Wei Yu. Bilayer low-density parity-check codes for decode-and-forward in relay channels. *IEEE Transactions on Information Theory*, 53(10) :3723–3739, oct. 2007.
- [Sha48] Claude E. Shannon. A mathematical theory of communication. *Bell System Technical Journal*, 27 :379–423, 1948.
- [Stu02] G. L. Stuber. *Principles of Mobile Communication*. 2nd Edition, Kluwer Academic Publishers, 2002.
- [SV06] M.R. Souryal and B.R. Vojcic. Performance of amplify-and-forward and decode-and-forward relaying in rayleigh fading with turbo codes. In *2006 IEEE International Conference on Acoustics, Speech and Signal Processing (ICASSP) Proceedings*, volume 4, page IV, may 2006.

- [Var57] R. R. Varshamov. Estimate of the number of signals in error correcting codes. *Dokl. Acad. Nauk SSSR*, 117 :739 –741, 1957.
- [Ver98] Serge Verdu. *Multiuser Detection*. Cambridge University Press, 1998.
- [XFKC07] Lei Xiao, T. Fuja, J. Kliewer, and D. Costello. A network coding approach to cooperative diversity. *IEEE Transactions on Information Theory*, 53(10) :3714 –3722, oct. 2007.
- [XQYX09] Zhisheng Xia, Yun Qu, Hui Yu, and Youyun Xu. A distributed cooperative product code for multi-source multi-relay single-destination wireless network. In *15th Asia-Pacific Conference on Communications (APCC)*, pages 736 –739, oct. 2009.
- [YC06] R. W. Yeung and N. Cai. Network error correction, part i : basic concepts and upper bounds. *Communications in Information and Systems*, 6(1) :19 – 36, 2006.
- [YGiA10] R. Youssef and A. Graell i Amat. Distributed turbo-like codes for multi-user cooperative relay networks. In *IEEE International Conference on Communications (ICC)*, pages 1 –5, may 2010.
- [YK07] Sichao Yang and Ralf Koetter. Network coding over a noisy relay : a belief propagation approach. In *IEEE International Symposium on Information Theory (ISIT)*, pages 801 –804, june 2007.
- [YPA10] Y. Yin, R.M. Pyndiah, and K. Amis. Performance of random linear network codes concatenated with reed-solomon codes using turbo decoding. In *6th International Symposium on Turbo Codes and Iterative Information Processing (ISTC)*, pages 132 –136, sept. 2010.
- [YPA11] Y. Yin, R.M. Pyndiah, and K. Amis. Multi-source cooperative communications using low-density parity-check product codes. In *14th International Symposium on Wireless Personal Multimedia Communications (WPMC)*, pages 1 –5, oct. 2011.
- [YPA12] Y. Yin, R.M. Pyndiah, and K. Amis. Performance of turbo product codes on the multiple-access relay channel with relatively poor source-relay links. In *13th IEEE International Workshop on Signal Processing Advances in Wireless Communications (SPAWC)*, june 2012.
- [Zha11] Zhen Zhang. Theory and applications of network error correction coding. *Proceedings of the IEEE*, 99(3) :406 –420, march 2011.
- [ZKBW08] G. Zeitler, R. Koetter, G. Bauch, and J. Widmer. Design of network coding functions in multihop relay networks. In *5th International Symposium on Turbo Codes and Related Topics (ISTC)*, pages 249 –254, sept. 2008.